1

High-Resolution ^{1}H-Nuclear Magnetic Resonance Spectroscopy of Oligosaccharide-Alditols Released from Mucin-Type *O*-Glycoproteins

Johannis P. Kamerling and Johannes F. G. Vliegenthart

1. INTRODUCTION

1.1. General

In nature, complex carbohydrates form an enormous class of biologically important compounds, comprising polysaccharides, glycoproteins, proteoglycans, and glycolipids. Comprehensive reviews concerning the biochemistry, biology, immunology, and chemistry of these substances have been published (Aspinall, 1982, 1983, 1985; Berger *et al.*, 1982; Dwek *et al.*, 1988; Feizi and Childs, 1987; Ginsburg, 1978, 1982, 1987; Ginsburg and Robbins, 1981, 1984; Gottschalk, 1972; Horowitz, 1982a,b; Horowitz and Pigman, 1977, 1978; Hounsell, 1987; Lemieux, 1978; Lennarz, 1980; Montreuil, 1980, 1982; Sharon and Lis, 1981, 1982). The glycoproteins, being biopolymers consisting of a polypeptide backbone bearing one or more covalently linked carbohydrate chains, can be divided into two main groups, namely, *N*-glycoproteins and *O*-glycoproteins, depending on the atom involved in the linkage between carbohydrate and protein. In each carbohy-

Johannis P. Kamerling and Johannes F. G. Vliegenthart • Bijvoet Center, Department of Bio-Organic Chemistry, Utrecht University, Utrecht, The Netherlands.

drate-amino acid linkage the anomeric center of the involved monosaccharide and a functional group in the side chain of the involved amino acid are connected. For *N*-glycoproteins the carbohydrate-amino acid linkage consists of *N*-acetyl-β-D-glucosamine coupled to the amide function of L-asparagine. The *O*-glycoproteins can be subdivided into five main classes based on the type of carbohydrate-amino acid bond. The class of the mucin type is characterized by the occurrence of a carbohydrate-amino acid bridge between *N*-acetyl-α-D-galactosamine and the hydroxyl function of L-serine or L-threonine. The other four classes show carbohydrate-amino acid bonds between β-D-xylose and the hydroxyl group of L-serine; α-D-mannose and the hydroxyl group of L-serine; β-D-galactose and the δ-hydroxyl function of L-hydroxylysine; and β-L-arabinose and the hydroxyl function of 3-hydroxy-L-proline.

Mucin-type *O*-glycoproteins occur as high-molecular-weight gel-forming glycoproteins (mucins), soluble glycoproteins like plasma, milk and urinary glycoproteins, and membrane glycoproteins. The carbohydrate content of the mucins can vary from 50 to 80% or even more. The polypeptide backbone can bear several hundreds of carbohydrate chains. The numerous oligosaccharide chains may vary in size from a single up to 20 monosaccharide units. The carbohydrate content of the soluble and membrane glycoproteins can also be high. Frequently, these glycoproteins contain, in addition to the *O*-linked carbohydrate chains, *N*-linked oligosaccharides. For a comprehensive review of biological sources of *O*-glycoproteins, see Schachter and Brockhausen (1992).

Structural information on the mucin-type *O*-linked carbohydrate chains is important for understanding their biological role. Furthermore, knowledge of the structures is a prerequisite to start-up biosynthetic studies (Schachter and Brockhausen, 1992). In general, the carbohydrate chains are built up from the monosaccharides *N*-acetyl-D-galactosamine, *N*-acetyl-D-glucosamine, D-galactose, L-fucose, *N*-acetyl-D-neuraminic acid/*N*-glycolyl-D-neuraminic acid (Scheme 1). In addition, inorganic sulfate has been found as a substituent of *N*-acetyl-D-glucosamine and D-galactose, contributing together with *N*,*O*-acyl-D-neuraminic acids (generally called sialic acids) to the acidic properties of the chains. Roughly, in the mucin-type *O*-linked carbohydrate chains three structural domains can be distinguished: the core structure, the backbone structure, and the peripheral structure. Especially, the peripheral elements may express a variety of antigenic activities.

In general, it is not possible to analyze the structures of the carbohydrate chains directly in intact glycoproteins. One of the reasons is the possible occurrence of more than one carbohydrate chain attached to separate amino acids in the polypeptide backbone. Furthermore, the chains for definite amino acids frequently show heterogeneity. The isolation of glycopeptides

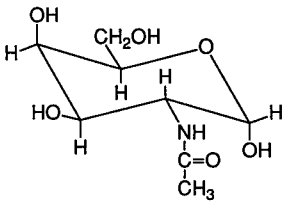

N-acetyl-α-D-galactosamine

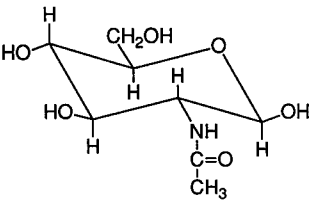

N-acetyl-β-D-glucosamine

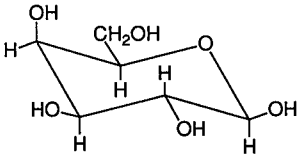

β-D-galactose

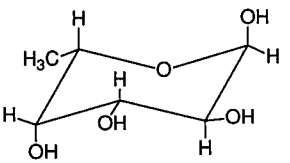

α-L-fucose

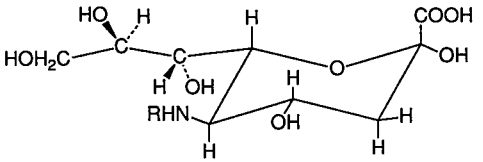

R=CH_3CO, N-acetyl-α-D-neuraminic acid
R=CH_2OHCO, N-glycolyl-α-D-neuraminic acid

Scheme 1. Chemical structures of relevant monosaccharides.

consisting of *O*-linked carbohydrate chains and only one or two amino acids is rather cumbersome. However, these carbohydrate chains can easily be released from the *O*-glycoproteins, as their corresponding oligosaccharide-alditols via alkaline borohydride treatment. These alditols are excellent alternatives for glycopeptides, although information on the carbohydrate–amino acid linkage is lost. Released mixtures of oligosaccharide-alditols have to be separated and purified, in which conventional gel-permeation chromatography and low- and high-pressure liquid chromatography, using a variety of column materials based on different separation principles, play a main role. The structural analysis of carbohydrates is highly complicated, because the primary structure of carbohydrate chains is defined by several parameters: (1) nature and number of the constituting monosaccharides; (2) sequence and ring size of the monosac-

charides; (3) type and anomeric configuration of the glycosidic linkages; (4) type of the carbohydrate–amino acid linkage and the nature and position in the polypeptide backbone of the amino acids involved (Scheme 2). For

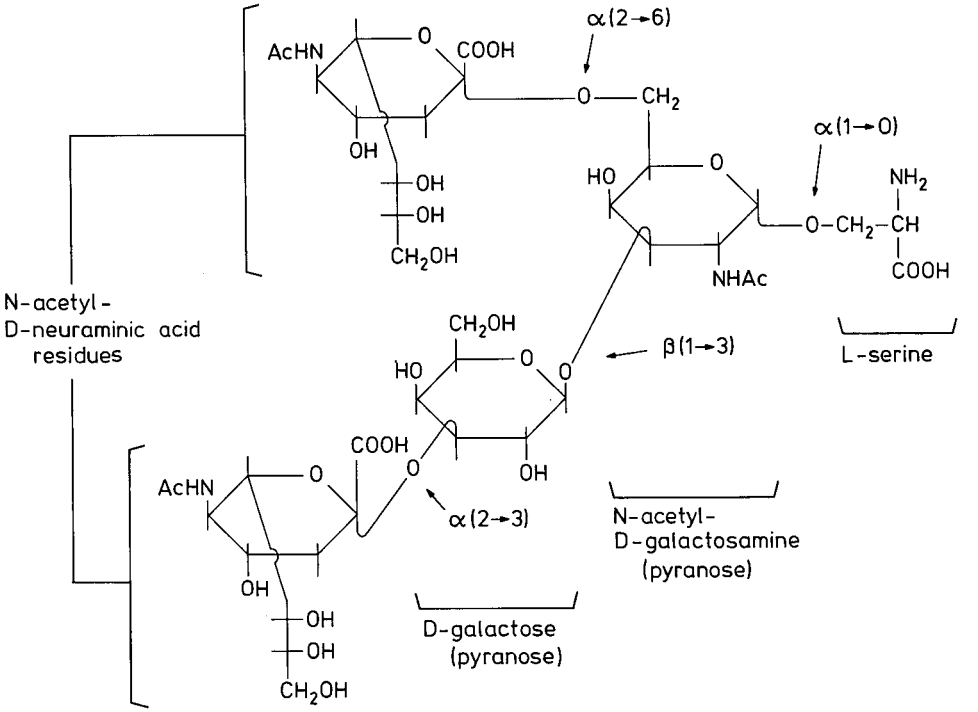

Scheme 2. Structural parameters defining a carbohydrate chain.

the determination of these parameters, gas–liquid chromatography, various modes of mass spectrometry (for recent reviews, see Egge and Peter-Katalinic, 1987; Dell, 1987; Kamerling and Vliegenthart, 1989), enzymatic methods, and, last but not least, NMR spectroscopy (Carver and Brisson, 1984; Carver and Cumming, 1987; Dill *et al.*, 1985; Koerner *et al.*, 1987; Vliegenthart *et al.*, 1980, 1981, 1982, 1983) play key roles.

High-resolution ^{1}H-NMR spectroscopy has shown to be an extremely powerful method for the primary structural characterization of carbohydrate chains in general. Because the NMR method is nondestructive, additional chemical, enzymatic, and/or immunological studies can be carried out later on. The suitability of high-resolution 1D ^{1}H-NMR spectroscopy in the primary structural analysis of *N*-linked carbohydrate chains using *N*-glycopeptides, prepared from *N*-glycoproteins, and related oligosaccharides obtained from patients with lysosomal storage diseases, has been extensively

reviewed by Vliegenthart *et al.* (1980, 1981, 1982, 1983). In principle, the ^{1}H-NMR spectra recorded in ^2H_2O solutions can be used as identity cards. The spectral patterns contain so many details and are that characteristic that a spectrum is unique. Comparison of the spectra of carbohydrate chains allows us to conclude whether or not compounds are identical. But the ^{1}H-NMR spectra can also be interpreted in terms of primary structure of carbohydrate chains. In fact, they may be considered to be composed of subspectra of the constituting monosaccharides. Usually, a spectrum is far too complex to be interpreted completely by a first-order approach. In particular, the interpretation of the so-called "bulk signal" in the spectral region between $\delta \sim 3{\cdot}5$ and $3{\cdot}9$ ppm, stemming from the majority of the nonanomeric protons, makes the application of 2D NMR techniques necessary. Fortunately, the signals of a number of protons, the so-called structural-reporter groups, resonate at clearly distinguishable spectral positions outside the bulk signal. The chemical shifts of these individually resonating protons, together with the coupling constants and the linewidths of their signals, furnish the essential structural information to carry out primary structural analyses. The structural reporters can be summarized as follows: (1) anomeric protons; (2) protons attached to carbon atoms in the direct vicinity of a substitution position in a monosaccharide residue; (3) protons attached to deoxy-carbon atoms; (4) *N*-acetyl methyl and *N*-glycolyl methylene group protons. The concept of structural-reporter-group signals could be developed due to the availability of carbohydrate chains with increasing complexity of primary structure. Each extension, starting from small oligomers, comes to expression in its own structural-reporter-group signals, as well as in its specific influences on the signals of other monosaccharide residues. Since the appearance of the NMR review of Vliegenthart *et al.* (1983), dealing with the ^{1}H-NMR data of *N*-glycopeptides and related oligosaccharides isolated from urine of patients with lysosomal storage diseases, a great number of research papers on the ^{1}H-NMR spectroscopy of oligosaccharide-alditols, obtained via the hydrazinolysis procedure from *N*-glycoproteins (including reduction), and oligosaccharides released via the same chemical procedure (without reduction) or via enzymatic cleavage using peptide-N^4-(*N*-acetyl-β-glucosaminyl)asparagine amidase, eventually reductively aminated with 2-aminopyridine, have been published. It turned out that the library of NMR data collected in the review by Vliegenthart *et al.* (1983) could be applied directly for the analysis of these *N*-glycoprotein-derived oligosaccharides, oligosaccharide-alditols, and oligosaccharides reductively aminated with 2-aminopyridine.

In this chapter a similar procedure will be summarized, showing that it has also been possible to formulate a concept of NMR structural-reporter groups for the primary structural analysis of oligosaccharide-alditols released from mucin-type *O*-glycoproteins.

1.2. Explanation of Code Systems Used in This Chapter

In Scheme 3 a list of abbreviations for the involved monosaccharide units, used in the presentation of the carbohydrate structures in this chapter,

Fuc	L-Fucose; 6-deoxy-L-galactose
dAlt	6-Deoxy-D-altrose
Gal	D-Galactose
Man	D-Mannose
GalNAc	*N*-Acetyl-D-galactosamine; 2-acetamido-2-deoxy-D-galactose
GlcNAc	*N*-Acetyl-D-glucosamine; 2-acetamido-2-deoxy-D-glucose
NeuAc	*N*-Acetyl-D-neuraminic acid; 5-acetamido-3,5-dideoxy-D-*glycero*-D-*galacto*-nonulosonic acid
NeuGc	*N*-Glycolyl-D-neuraminic acid; 5-hydroxyacetamido-3,5-dideoxy-D-*glycero*-D-*galacto*-nonulosonic acid
Kdn	3-Deoxy-D-*glycero*-D-*galacto*-nonulosonic acid
S	Sulfate

Scheme 3. List of abbreviations of relevant monosaccharides.

is given. For reasons of convenience a shorthand symbolic notation for the various structures is used in the tables. This notation is explained in Scheme 4. For each monosaccharide the presented symbol also includes the configur-

●	β-GlcNAc	◐	α-GlcNAc
◆	β-GalNAc	◇	α-GalNAc
■	β-Gal	◧	α-Gal
◆	β-Man	◈	α-Man
◒	β-Glc	○	α-Glc
△	α-NeuAc	▽	α-NeuGc
□	α-Fuc	⊙	α-KDN
◇–ol	GalNAc-ol	⊡	β-dAlt

Scheme 4. Information about the shorthand symbolic notation used for oligosaccharide-alditols.

ation at the anomeric center. The position of linkage in this notation is specified by the angle of the connecting bar as follows:

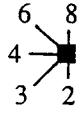

In the tables the first superscript after the abbreviated name of a monosaccharide residue indicates to which position of the adjacent monosaccharide

it is glycosidically linked (e.g., Gal^4 in the case of Galβ1 → 4GlcNAcβ1 →). Frequently, a second superscript is used to discriminate between identically linked residues, by indicating the type of the next linkage in the sequence (e.g., $Gal^{4,6}$ in the case of Galβ1 → 4GlcNAcβ1 → 6 and $Gal^{4,3}$ in the case of Galβ1 → 4GlcNAcβ1 → 3), etc.

1.3. General NMR Features

Prior to ^{1}H-NMR spectroscopic analysis the desalted samples are repeatedly treated with ^2H_2O, finally using 99.96 atom% ^2H_2O at p^{2}H 7 and room temperature. Except for those cases specifically indicated in the text, the included ^{1}H-NMR data have been obtained by recording resolution-enhanced 500-MHz ^{1}H-NMR spectra. If not further mentioned, the spectra have been recorded at 27 °C, but no great variation in chemical shifts has been observed between spectra recorded at 27 °C and 22 °C. Chemical shifts are expressed in ppm downfield from internal sodium 4,4-dimethyl-4-silapentane-1-sulfonate, but were actually measured by reference to internal acetone (δ = 2.225 ppm) with an accuracy of 0.002 ppm (Vliegenthart *et al.*, 1983).

2. CORE STRUCTURES

The GalNAc-ol residue **1** is the only structural element that all mucin-type oligosaccharide-alditols have in common. This alditol may be obtained after isolation as such, or substituted at C-3 and/or C-6. Up to now, five different monosubstitutions have been observed for GalNAc-ol. At the C-3 position, β-Gal, β-GlcNAc, or α-GalNAc can be attached, whereas the C-6 position can be substituted by β-GlcNAc or α-sialic acid (α-NeuAc/α-NeuGc). Taking into account non-, mono-, and disubstitutions, this affords theoretically 12 different types of core structures. At the moment, 11 of them have been characterized by ^{1}H-NMR spectroscopy, and the relevant ^{1}H-NMR data are compiled in Table 1. The presence of α-GalNAc at C-3 together with β-GlcNAc at C-6 of GalNAc-ol has not yet been observed. The objective of this section is to summarize the various ^{1}H-NMR structural-reporter-group signals that are highly useful to distinguish between the 11 core structures. In the additional sections of this chapter, it will be shown that the discrimination rules are of great value for the analysis of more complex structures. It should be noted that the "core-structure system" used throughout this chapter differs from the "core-class system" used in biosynthesis (see below; Schachter and Brockhausen, 1992).

TABLE 1

^{1}H Chemical Shifts of Structural-Reporter Groups of Constituent Monosaccharides for Oligosaccharide-Alditols Representing the Various Core Structures of Mucin-Type Carbohydrate Chains (1–11)

Residue	Reporter group	1 	2 	3 	4[a] 	5[a] 	6 	6A 	7 	8 	9 	9A 	10 	11 	11A 
GalNAc-ol	H-2	4.252	4.395	4.287	4.395	4.242	4.245	4.253	4.395	4.280	4.378	4.380	4.260	4.393	4.400
	H-3	3.850	4.065	3.996	3.888	3.841	3.842	3.842	4.061	3.984	4.055	4.061	3.985	3.874	n.d.
	H-4	3.390	3.507	3.546	3.680	3.379	3.413	3.416	3.468	3.519	3.534	3.541	n.d.	3.583	n.d.
	H-5	3.928	4.196	4.141	3.749	4.021	4.024	4.025	4.281	4.230	4.244	4.249	4.185	n.d.	n.d.
	H-6	3.668	3.69	3.65	3.647	3.933	3.846	3.842	3.931	3.905	3.85	3.860	n.d.	n.d.	n.d.
	H-6′	3.647	3.628	n.d.[b]	3.647	n.d.	3.528	3.536	n.d.	n.d.	3.486	3.497	3.487	n.d.	n.d.
	NAc	2.055	2.050	2.037	2.049	2.046	2.056	2.057	2.066	2.044	2.047	2.049	2.035[c]	2.041	2.042
Gal[3]	H-1	—	4.478	—	—	—	—	—	4.468	—	4.474	4.477	—	—	—
	H-2	—	3.564	—	—	—	—	—	3.542	—	3.57	3.574	—	—	—
	H-3	—	3.671	—	—	—	—	—	n.d.	—	n.d.	3.669	—	—	—
	H-4	—	3.901	—	—	—	—	—	3.901	—	3.894	3.899	—	—	—

GlcNAc[3]	H-1	—	—	4.604	—	—	—	—	—	4.600	—	—	4.608	—	—
	H-3	—	—	3.584	—	—	—	—	—	n.d.	—	—	n.d.	—	—
	H-6	—	—	3.950	—	—	—	—	—	3.949	—	—	3.939	—	—
	NAc	—	—	2.085	—	—	—	—	—	2.081	—	—	2.079	—	—
GalNAc[3]	H-1	—	—	—	5.103	—	—	—	—	—	—	—	—	5.086	5.087
	H-2	—	—	—	4.235	—	—	—	—	—	—	—	—	4.220	4.220
	H-3	—	—	—	3.921	—	—	—	—	—	—	—	—	3.916	n.d.
	H-4	—	—	—	4.043	—	—	—	—	—	—	—	—	4.042	4.042
	H-5	—	—	—	4.073	—	—	—	—	—	—	—	—	4.073	4.077
	NAc	—	—	—	2.060	—	—	—	—	—	—	—	—	2.087	2.090
GlcNAc[6]	H-1	—	—	—	—	4.553	—	—	4.538	4.543	—	—	—	—	—
	H-6	—	—	—	—	3.928	—	—	3.932	3.931	—	—	—	—	—
	NAc	—	—	—	—	2.059	—	—	2.066	2.063	—	—	—	—	—
NeuAc[6]	H-3a	—	—	—	—	—	1.700	—	—	—	1.692	—	1.697	1.704	—
	H-3e	—	—	—	—	—	2.728	—	—	—	2.726	—	2.733	2.731	—
	NAc	—	—	—	—	—	2.033	—	—	—	2.033	—	2.031[c]	2.034	—
NeuGc[6]	H-3a	—	—	—	—	—	—	1.721	—	—	—	1.711	—	—	1.720
	H-3e	—	—	—	—	—	—	2.746	—	—	—	2.746	—	—	2.750
	NGc	—	—	—	—	—	—	4.124	—	—	—	4.123	—	—	4.122

[a] Spectrum recorded at 22 °C.
[b] n.d. means value could not be determined merely by inspection of the spectrum.
[c] Assignments may have to be interchanged.

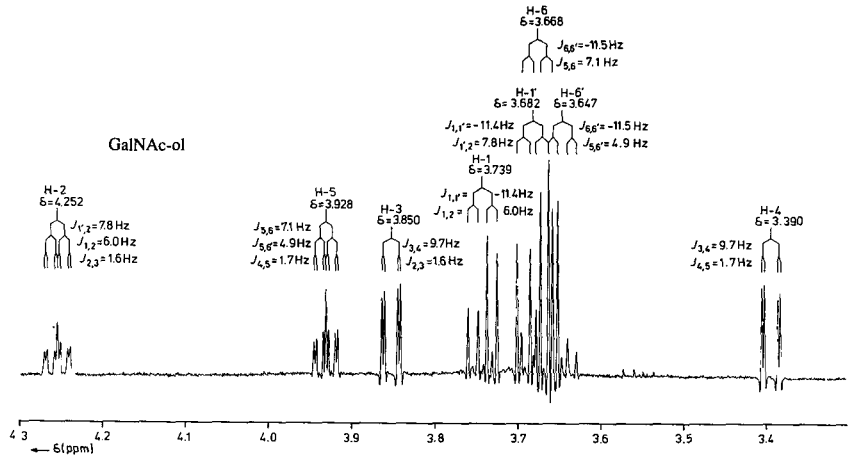

Figure 1. Resolution-enhanced ^{1}H-NMR spectrum of **1**. The GalNAc-ol NAc singlet at $\delta = 2.055$ ppm is not included in the spectrum.

The ^{1}H-NMR spectrum of **1** is presented in Figure 1. For references, see Dua *et al.* (1984, 1986) and Van Halbeek *et al.* (1980, 1981a, 1985b).

GalNAc-ol (1)

The chemical shifts and coupling constants represent the characteristics of the GalNAc-ol proton signals. The typical signal at $\delta = 4.252$ ppm was assigned to H-2, by comparing the spectrum of GalNAc-ol with that of its deuterated analog [1-^{2}H]-GalNAc-ol. In the following the ^{1}H-NMR spectrum of GalNAc-ol will serve as a starting point for the recognition of the different types of core structures, because the signals of some protons appeared to be excellent markers for the substitution of GalNAc-ol.

In Figure 2 the ^{1}H-NMR spectrum of **2** is shown (Van Halbeek *et al.*, 1982b). For additional references, see Dua *et al.* (1984, 1985, 1986), Fiat *et*

GalNAc-ol
Galβ1 → 3 (2)

al. (1988), Gleeson *et al.* (1984), Hounsell *et al.* (1985), Klein *et al.* (1988), Lamblin *et al.* (1984b), Mutsaers *et al.* (1986), Van Halbeek *et al.* (1980, 1981a,b, 1985b), and Vliegenthart *et al.* (1980). In the anomeric region the presence of a β-Gal residue (Gal^3) is reflected by the doublet for H-1 at $\delta = 4.478$ ppm ($J_{1,2} = 7.8$ Hz). Besides this resonance also the Gal^3 H-2 and H-4 signals appear outside the bulk of skeleton protons. The Gal^3 H-2 signal is observed at $\delta = 3.564$ ppm ($J_{2,3} = 10.0$ Hz), upfield from the bulk signal, and the characteristic Gal^3 H-4 signal at $\delta = 3.901$ ppm ($J_{3,4} = 3.5$ Hz; $J_{4,5} = 1.0$ Hz), downfield from the bulk signal. Comparison of the chemical

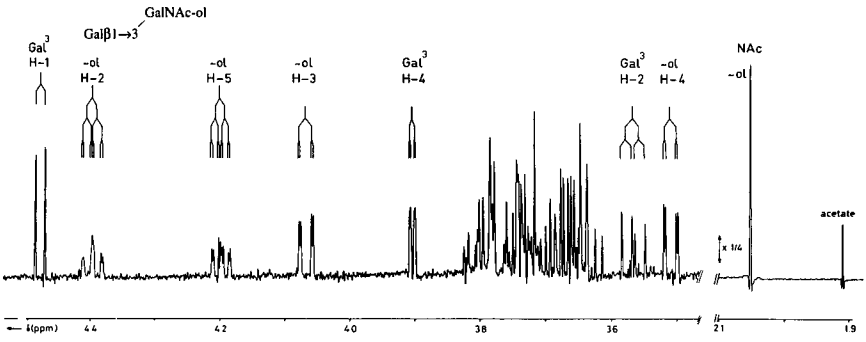

Figure 2. Resolution-enhanced ^{1}H-NMR spectrum of **2**. The relative-intensity scale of the *N*-acetyl methyl proton region of the spectrum differs from that of the other parts, as indicated. Contaminating acetate gives rise to a signal at $\delta = 1.908$ ppm.

shift values of the GalNAc-ol proton signals in **2** (Table 1) with those of **1**, shows shifts for all protons. The attachment of Gal^3 gives rise to a downfield shift of $\Delta\delta = +0.215$ ppm for GalNAc-ol H-3. Also the typical triplet-like-shaped GalNAc-ol H-2 signal undergoes a downfield shift ($\delta = 4.395$ ppm; $\Delta\delta = +0.143$ ppm). The latter resonance owes its typical symmetric pattern to the combination of the coupling constants $J_{1,2}$ (7.0 Hz), $J_{1',2}$ (7.8 Hz), and $J_{2,3}$ (1.4 Hz). The similarly shaped H-5 signal ($J_{5,6'} = 5.2$ Hz; $J_{5,6} = 7.5$ Hz; $J_{4,5} = 1.5$ Hz) is observed at $\delta = 4.196$ ppm. The relatively large shift increment of H-5 ($\Delta\delta = +0.268$ ppm), as compared to **1**, is noteworthy. Finally, GalNAc-ol H-4 resonates at $\delta = 3.507$ ppm ($\Delta\delta = +0.117$ ppm), clearly upfield from the bulk resonance. The GalNAc-ol NAc singlet is found at $\delta = 2.050$ ppm. Compound **2** has been referred to as core class 1 (Schachter and Brockhausen, 1992). For ^{1}H-NMR data of corresponding synthetic glycopeptides, see Paulsen and Paal (1984) and Paulsen *et al.* (1985).

The ^{1}H-NMR spectrum of **3** is depicted in Figure 3 (Van Halbeek *et al.*, 1982b). For additional references, see Breg *et al.* (1988b), Brockhausen

$$\text{GlcNAc}\beta 1 \rightarrow 3 \begin{matrix} \diagup \text{GalNAc-ol} \\ \diagdown \end{matrix} \qquad (3)$$

et al. (1985), Dua *et al.* (1984), Hounsell *et al.* (1985), and Lamblin *et al.* (1984b). The β configuration of the 1 → 3-linked GlcNAc residue is evident from the chemical shift of GlcNAc^3 H-1 ($\delta = 4.604$ ppm) in conjunction with its $J_{1,2}$ value (8.4 Hz). The GlcNAc^3 H-3, H-4, H-5, H-6, and H-6′ signals have been assigned by comparison with those of terminal GlcNAc in GlcNAcβ1 → N(Asn) (Vliegenthart *et al.*, 1983): H-3, $\delta = 3.584$ ppm; H-4, $\delta = 3.445$ ppm; H-5, $\delta = 3.475$ ppm; H-6, $\delta = 3.950$ ppm ($J_{6,6'} = -12.7$ Hz; $J_{5,6} = 2.2$ Hz); H-6′, $\delta = 3.752$ ppm. The NAc signal at $\delta =$

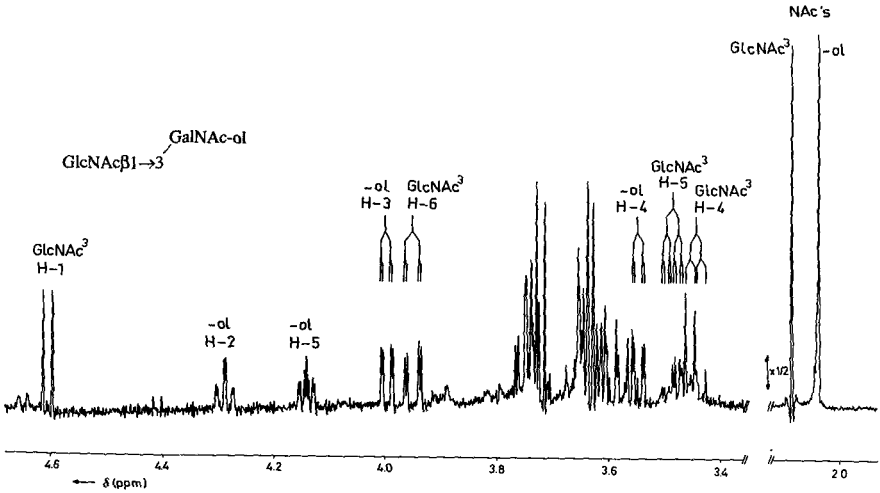

Figure 3. Resolution-enhanced ^{1}H-NMR spectrum of **3**. For comments, see Figure 2.

2.085 ppm has been ascribed to GlcNAc^3. Compared to **1**, shifts in δ values are observed for the skeleton protons of GalNAc-ol in **3**. The GalNAc-ol H-3 signal undergoes a downfield shift ($\Delta\delta = +0.146$ ppm) due to the introduction of the GlcNAc^3 residue. The highly diagnostic GalNAc-ol H-2 "triplet" is present at $\delta = 4.287$ ppm ($\Delta\delta = +0.035$ ppm). Close inspection of the "triplet" pattern reveals that it differs from that of GalNAc-ol H-2 in **2**. In the spectrum of **3** it is a well-resolved doublet of triplets ($J_{1,2} = J_{1',2} = 7.3$ Hz; $J_{2,3} = 1.5$ Hz). The typical GalNAc-ol H-5 signal is detected at $\delta = 4.141$ ppm ($\Delta\delta = +0.213$ ppm). A similarly large downfield shift for H-5 was also observed in **2**. The GalNAc-ol H-4 signal appears at $\delta = 3.546$ ppm ($\Delta\delta = +0.156$ ppm). Compound **3** has been referred to as core class 3 (Schachter and Brockhausen, 1992).

In Figure 4 the ^{1}H-NMR spectrum of **4** is shown (Feeney *et al.*, 1986; Hounsell *et al.*, 1985), and complete assignments have been made using a

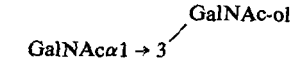

(4)

combination of 1D and 2D NMR techniques (COSY, RELAYED-COSY, and F_1-decoupled COSY). The presence of the α-GalNAc residue comes to expression by the doublet of H-1 at $\delta = 5.103$ ppm with a coupling constant of 4.1 Hz. Other GalNAc^3 proton signals resonating outside the bulk are those for H-2 at $\delta = 4.235$ ppm, for H-3 at $\delta = 3.921$ ppm, for H-4 at $\delta = 4.043$ ppm, and for H-5 at $\delta = 4.073$ ppm. As compared to **1**, the attachment of α-GalNAc at C-3 gives rise to a relatively small downfield

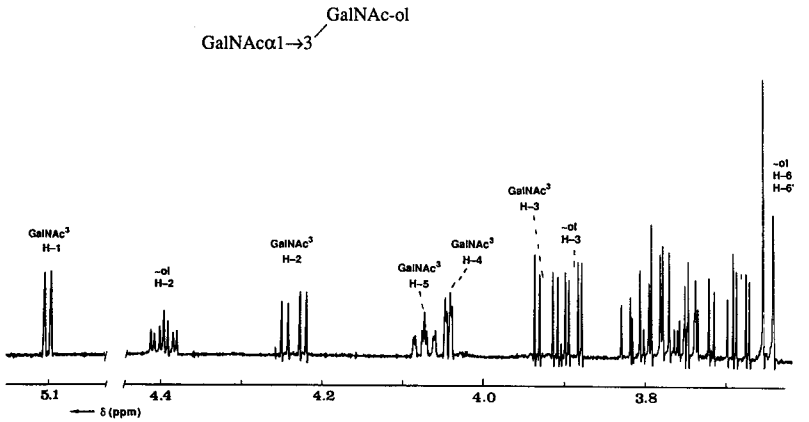

Figure 4. Resolution-enhanced ^{1}H-NMR spectrum of **4** at 22 °C. The NAc singlets for GalNAc-ol at $\delta = 2.049$ ppm and for GalNAc at $\delta = 2.060$ ppm are not included in the spectrum.

shift for GalNAc-ol H-3 ($\delta = 3.888$ ppm; $\Delta\delta = +0.038$ ppm); see also the δ values of the GalNAc-ol H-3 signals in **2** and **3**. However, the GalNAc-ol H-4 signal is observed at a much more downfield position that the corresponding H-4 signals in **2** and **3** ($\Delta\delta = +0.290$ ppm, as compared to **1**). The typical GalNAc-ol H-2 signal arises at $\delta = 4.395$ ppm ($J_{1,2} = 5.6$ Hz; $J_{1',2} = 8.2$ Hz; $J_{2,3} = 2.3$ Hz), the same value as observed for GalNAc-ol H-2 in **2**. Finally, the GalNAc-ol H-5 structural-reporter resonance is found at $\delta = 3.749$ ppm ($\Delta\delta = -0.179$ ppm). This substitution effect is quite different from the effects observed in **2** and **3**. The NAc resonances of GalNAc^3 ($\delta = 2.060$ ppm) and GalNAc-ol ($\delta = 2.049$ ppm) were assigned by comparison with the GalNAc-ol NAc signals in **2** and **3**. Compound **4** has been referred to as core class 5 (Schachter and Brockhausen, 1992).

The ^{1}H-NMR spectrum of **5** is depicted in Figure 5 (Mutsaers *et al.*, 1986; Van Halbeek *et al.*, 1985b). The β configuration of the linkage between

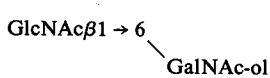

(5)

GlcNAc and GalNAc-ol follows from the chemical shift of GlcNAc^6 H-1 ($\delta = 4.553$ ppm), in conjunction with its coupling constant ($J_{1,2} = 8.1$ Hz). In addition, the following GlcNAc^6 proton signals have been indicated in Figure 5: H-3, $\delta = 3.542$ ppm; H-4, $\delta = 3.450$ ppm; H-5, $\delta = 3.462$ ppm; H-6, $\delta = 3.928$ ppm. The NAc signal at $\delta = 2.059$ ppm was assigned to GlcNAc^6 NAc (compare with **2**-**4**). The attachment of β-GlcNAc at C-6 of GalNAc-ol results in a specific downfield shift for GalNAc-ol H-6 to

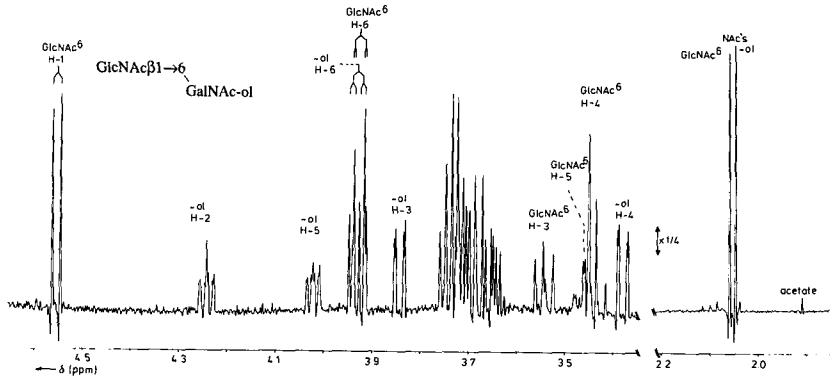

Figure 5. Resolution-enhanced ^{1}H-NMR spectrum of **5** at 22 °C. For comments, see Figure 2.

outside the bulk,* as compared to **1** (δ = 3.933 ppm; $J_{5,6}$ = 5.1 Hz and $J_{6,6'}$ = −10.4 Hz). Furthermore, the GalNAc-ol H-5 signal shows a downfield shift (δ = 4.021 ppm; $\Delta\delta$ = +0.093 ppm), but the increment is evidently smaller than that observed for GalNAc-ol H-5 in **2** and **3** (see Table 1). Finally, the chemical shift values of the GalNAc-ol H-2 (δ = 4.242 ppm; $J_{1,2}$ = 6.0 Hz; $J_{1',2}$ = 7.8 Hz; $J_{2,3}$ = 1.5 Hz), H-3, and H-4 signals are influenced to a small extent only, as compared to **1**.

The ^{1}H-NMR spectrum of **6** is presented in Figure 6 (Vliegenthart *et al.*, 1981). For additional references, see Nasir-Ud-Din *et al.* (1986), Savage

NeuAcα2 → 6
GalNAc-ol (**6**)

et al. (1987), and Van Halbeek *et al.* (1980, 1988). The presence of the NeuAc residue is reflected by the chemical shift values of the H-3a, H-3e, and NAc protons, being 1.700, 2.728, and 2.033 ppm, respectively. As compared to sets of structural-reporter groups of NeuAc in *N*-linked oligosaccharides (Vliegenthart *et al.*, 1983), the latter one is indicative of a NeuAc residue in α2 → 6 linkage to GalNAc-ol. The attachment of NeuAc at C-6 of GalNAc-ol causes a downfield shift for GalNAc-ol H-6 (δ = 3.846 ppm), as compared to **1**. On the other hand, the GalNAc-ol H-6′ is found at an upfield position clearly outside the bulk (δ = 3.528 ppm). Moreover, the geminal coupling constant $J_{6,6'}$ changes from −11.5 Hz to −10.0 Hz (cf. **1**). For GalNAc-ol H-5 a downfield shift was observed similar

* For reasons of convenience, it is defined that when one of the protons, attached to GalNAc-ol C-6, appears at a downfield position of the bulk signal, it is called GalNAc-ol H-6, and when it appears at an upfield position, GalNAc-ol H-6′. These rules are applied irrespective of the values of $J_{5,6}$ and $J_{5,6'}$.

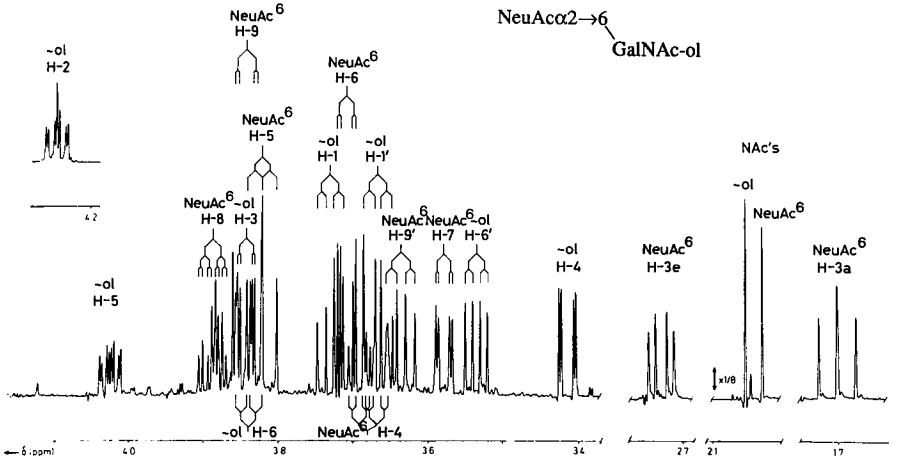

Figure 6. Resolution-enhanced ^{1}H-NMR spectrum of **6**. For comments, see Figure 2.

to that in **5** (see Table 1). The chemical shift values of the GalNAc-ol H-2, H-3, and H-4 signals are influenced to a small extent only (GalNAc-ol H-2, $\delta = 4.245$ ppm). Finally, Figure 6 includes specific NeuAc assignments, which are based on literature data on NeuAc derivatives (Vliegenthart *et al.*, 1982). In the case when NeuAc is replaced by NeuGc (**6A**), similar

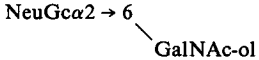

(6A)

^{1}H-NMR parameters are found (Savage *et al.*, 1987; Van Halbeek *et al.*, 1981a) (Figure 7). The diagnostic set of structural-reporter groups for NeuGc is as follows: H-3a, $\delta = 1.721$ ppm; H-3e, $\delta = 2.746$ ppm; NGc, $\delta = 4.124$ ppm (360-MHz ^{1}H-NMR data). The NeuGc H-3 signals are observed 0.02 ppm downfield from those of NeuAc in **6**. A similar observation has been made comparing NeuGcα2 → 3Galβ1 → 4Glc to NeuAcα2 → 3Galβ1 → 4Glc (Vliegenthart *et al.*, 1982).

The ^{1}H-NMR spectrum of **7** is depicted in Figure 8 (Van Halbeek *et al.*, 1982b). For additional references, see Brockhausen *et al.* (1984), Dua

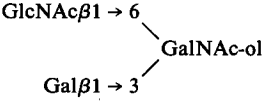

(7)

et al. (1986), Fiat *et al.* (1988), Klein *et al.* (1988), Lamblin *et al.* (1984b), Hounsell *et al.* (1985), Van Halbeek (1984), and Van Halbeek *et al.* (1985b). Based on comparison with the ^{1}H-NMR data of **2** and **5**, the doublets at $\delta = 4.468$ ppm ($J_{1,2} = 7.8$ Hz) and $\delta = 4.538$ ppm ($J_{1,2} = 8.4$ Hz) are

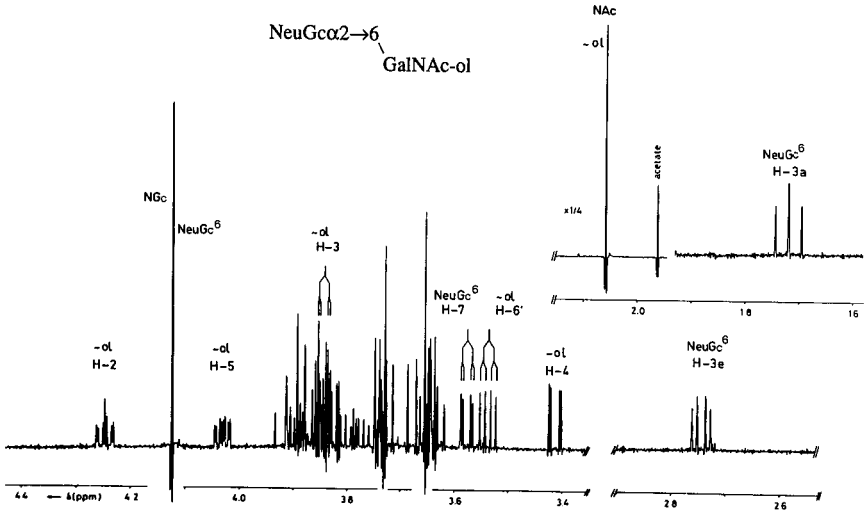

Figure 7. Resolution-enhanced ^{1}H-NMR spectrum of **6A**. For comments, see Figure 2.

attributed to the β-linked Gal^3 and GlcNAc^6 residues, respectively. Additional Gal^3 and GlcNAc^6 proton signals have been included in Table 1. The Gal^3 H-4 and GlcNAc^6 H-6 signals are found outside the bulk of skeleton protons, at similar positions as in the disaccharide building blocks **2** and **5**, respectively. The attachment of β-Gal at C-3 of GalNAc-ol in **7** gives rise to δ values for GalNAc-ol H-2 and H-3 similar to those in **2**

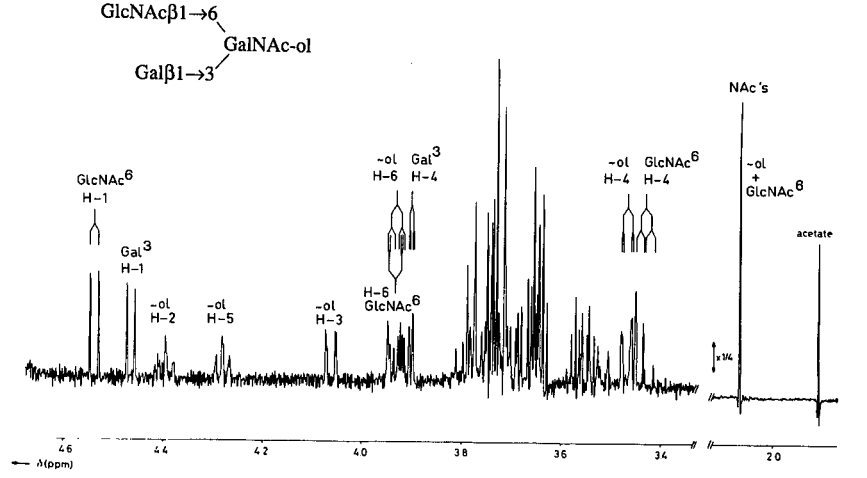

Figure 8. Resolution-enhanced ^{1}H-NMR spectrum of **7**. For comments, see Figure 2.

(H-2, δ = 4.395 ppm; H-3, δ = 4.061 ppm). The presence of β-GlcNAc at C-6 of GalNAc-ol in the trisaccharide-alditol **7** is expressed by a relatively strong downfield chemical shift value for GalNAc-ol H-5 (δ = 4.281 ppm), as compared to **1** ($\Delta\delta$ = +0.353 ppm). Evidently, the substitution effects observed for GalNAc-ol H-5 in the C-3-monosubstituted GalNAc-ol derivative **2** ($\Delta\delta$ = +0.268 ppm) and in the C-6-monosubstituted GalNAc-ol derivative **5** ($\Delta\delta$ = +0.093 ppm), reinforce each other in the C-3,6-disubstituted GalNAc-ol derivative **7**. The GalNAc-ol H-6 signal occurs at a similar position as in **5** (δ = 3.931 ppm; $J_{5,6}$ = 6.0 Hz; $J_{6,6'}$ = −10.5 Hz). Going from **2** to **7** a typical decrease in absolute value of the geminal coupling constant $J_{6,6'}$ is observed (**2**, $J_{6,6'}$ = −11.5 Hz), which is similar to the observations made for **5** and **6**. It has to be noted that going from **2** to **7** the introduction of GlcNAc^6 does not influence the chemical shift of H-2 of GalNAc-ol (compare also **1** and **5**). Compound **7** has been referred to as core class 2 (Schachter and Brockhausen *et al.*, 1992).

The ^{1}H-NMR spectrum of **8** is shown in Figure 9 (unpublished results from the authors' laboratory; Brockhausen *et al.*, 1985). In the anomeric

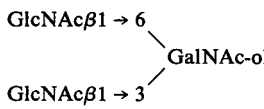

(8)

region two doublets (each $J_{1,2}$ = 8.4 Hz) are observable, belonging to the β-linked GlcNAc residues. For their assignments, use has been made of the ^{1}H-NMR data of **3** and **5**, respectively, whereby the signal at δ = 4.600 ppm is attributed to H-1 of GlcNAc^3, and that at δ = 4.543 ppm to H-1 of GlcNAc^6. The H-6 and NAc signals of GlcNAc^3 and the H-6 and

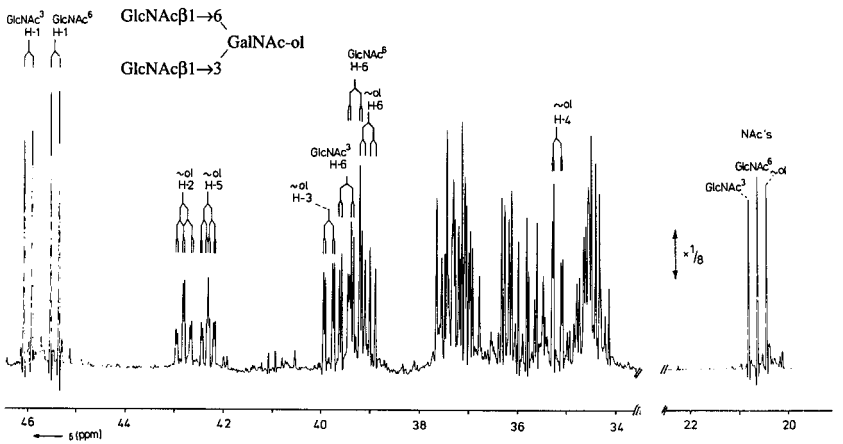

Figure 9. Resolution-enhanced ^{1}H-NMR spectrum of **8**. For comments, see Figure 2.

NAc signals of GlcNAc[6] are found at similar positions as reported for the disaccharide-alditol elements **3** and **5**. The influence of the attachment of β-GlcNAc at C-3 of GalNAc-ol on the H-2 and H-3 δ values of GalNAc-ol in **8**, is comparable to the effects observed in **3** (H-2, $\delta = 4.280$ ppm; H-3, $\delta =$ 3.984 ppm). The presence of the β-GlcNAc residue at C-6 of GalNAc-ol leads to a relatively strong downfield shift for GalNAc-ol H-5 ($\delta =$ 4.230 ppm, $\Delta\delta = +0.302$ ppm as compared to **1**; see also **7**). The shift increment is the sum of the increments for GalNAc-ol H-5 in **3** ($\Delta\delta =$ +0.213 ppm) and **5** ($\Delta\delta = +0.093$ ppm). The GalNAc-ol H-6 signal is found at $\delta = 3.905$ ppm ($J_{5,6} = 5.6$ Hz; $J_{6,6'} = -10.6$ Hz). Compared to the corresponding signal in **7**, the downfield shift effect is lower when **1** is taken as reference. In view of the δ values of the GalNAc-ol H-6 signals in **1**, **2**, and **3**, this difference in effect is due to the replacement of a Galβ1 → 3 by a GlcNAcβ1 → 3 unit. Compound **8** has been referred to as core class 4 (Schachter and Brockhausen, 1992).

In Figure 10 the ^{1}H-NMR spectrum of **9** is depicted (Van Halbeek *et al.*, 1988). For additional references, see Capon *et al.* (1989), Nasir-Ud-Din

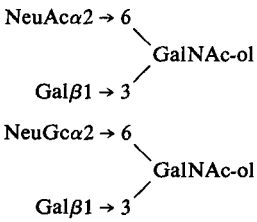

(9)

(9A)

et al. (1986), Savage *et al.* (1986, 1987, 1990a), and Van Halbeek *et al.* (1980). The presence of the β-Gal residue is evident from the doublet of

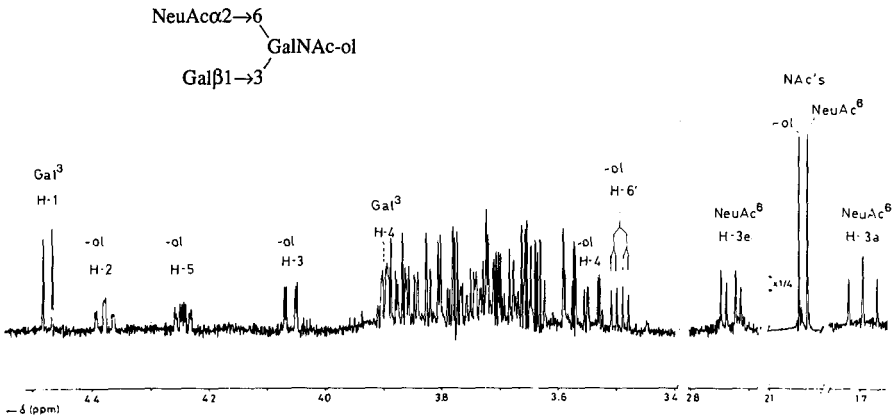

Figure 10. Resolution-enhanced ^{1}H-NMR spectrum of **9**. For comments, see Figure 2.

Gal[3] H-1 at $\delta = 4.474$ ppm ($J_{1,2} = 7.9$ Hz). Also the Gal[3] H-4 signal resonates at a characteristic position ($\delta = 3.894$ ppm). The presence of the α-NeuAc residue is indicated by the following set of structural-reporter groups: H-3a, $\delta = 1.692$ ppm; H-3e, $\delta = 2.726$ ppm; and NAc, $\delta = 2.033$ ppm. These chemical shifts are similar to those observed for α-NeuAc in **6**. The β-Gal substitution at C-3 of GalNAc-ol is reflected by the chemical shift value of GalNAc-ol H-2, being $\delta = 4.378$ ppm (compare to **2** and **7**). In the same way as reported for **6**, the attachment of NeuAc at C-6 of GalNAc-ol causes oppositely directed changes in the chemical shifts of GalNAc-ol H-6 and H-6′, as compared to **1** (GalNAc-ol H-6′, $\delta = 3.486$ ppm, $J_{5,6'} = 4.7$ Hz). The geminal coupling constant $J_{6,6'}$ changes from -11.5 Hz to -10.0 Hz. The GalNAc-ol H-5 signal is found at $\delta = 4.244$ ppm. Compared to **1**, the shift increment ($\Delta\delta = +0.316$ ppm) is built up from the specific increments found for C-3 and C-6 monosubstituted GalNAc-ol (**2**, $\Delta\delta = +0.268$ ppm; **6**, $\Delta\delta = +0.096$ ppm). The structural reporters established for the NeuGc analog (**9A**) (Savage *et al.*, 1986, 1987; Van Halbeek *et al.*, 1981a; Vliegenthart *et al.*, 1981) are almost identical to those discussed for **9** (see Table 1 and Figure 11). The specific set of chemical shifts for NeuGc comprises H-3a at $\delta = 1.711$ ppm, H-3e at $\delta = 2.746$ ppm, and NGc at $\delta = 4.123$ ppm. In a similar way as mentioned for **6A** and **6**, the NeuGc H-3 signals in **9A** are observed 0.02 ppm downfield from those of NeuAc in **9**.

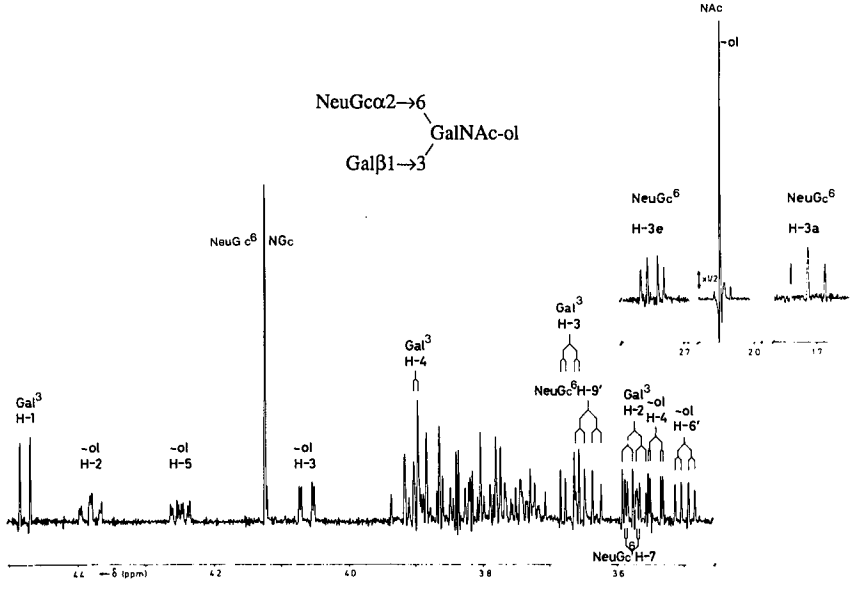

Figure 11. Resolution-enhanced ^{1}H-NMR spectrum of **9A**. For comments, see Figure 2.

The ^{1}H-NMR spectrum of **10** is shown in Figure 12 (Capon *et al.*, 1989; Savage *et al.*, 1987, 1990a; Van Halbeek *et al.*, 1988). The β-GlcNAc H-1

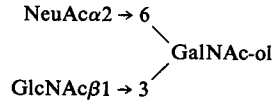

(10)

signal is found at $\delta = 4.608$ ppm ($J_{1,2} = 8.3$ Hz). The structural reporters observed for α-NeuAc (H-3a, $\delta = 1.697$ ppm; H-3e, $\delta = 2.733$ ppm; NAc, $\delta = 2.031$ ppm) are similar to those found in **6** and **9**. The attachment of GlcNAc[3] to GalNAc-ol gives rise to a typical GalNAc-ol H-2 signal at $\delta = 4.260$ ppm ($\Delta\delta = +0.008$ ppm). The GalNAc-ol H-5 signal resonates at $\delta = 4.185$ ppm, representing a shift increment of $\Delta\delta = +0.257$ ppm, as compared to **1**. The individual shift increments for this proton in **3** and **6** are $\Delta\delta = +0.213$ and $+0.096$ ppm, respectively, indicating the trend of the larger downfield shift in **10**. The attachment of α-NeuAc at C-6 of GalNAc-ol leads to a comparable δ value for GalNAc-ol H-6′ ($\delta = 3.487$ ppm; $J_{5,6'} = 4.8$ Hz; $J_{6,6'} = -10.0$ Hz) as discussed for that proton in **9**. Also in this case the coupling constant $J_{6,6'}$ changes from -11.5 Hz to -10.0 Hz, as compared to **1**. For NeuGc analog **10A**, see the Addendum.

The 400-MHz ^{1}H-NMR spectrum of **11** is depicted in Figure 13 (Capon *et al.*, 1989; Savage *et al.*, 1988, 1990a). The α1 → 3-linked GalNAc residue is reflected by the H-1 signal at $\delta = 5.086$ ppm, having a small coupling constant ($J_{1,2} = 4.0$ Hz). The GalNAc NAc signal in **11** ($\delta = 2.087$ ppm) strongly deviates from that in **4** ($\delta = 2.060$ ppm). The attachment of α-GalNAc at C-3 of GalNAc-ol gives rise to a GalNAc-ol H-2 signal at

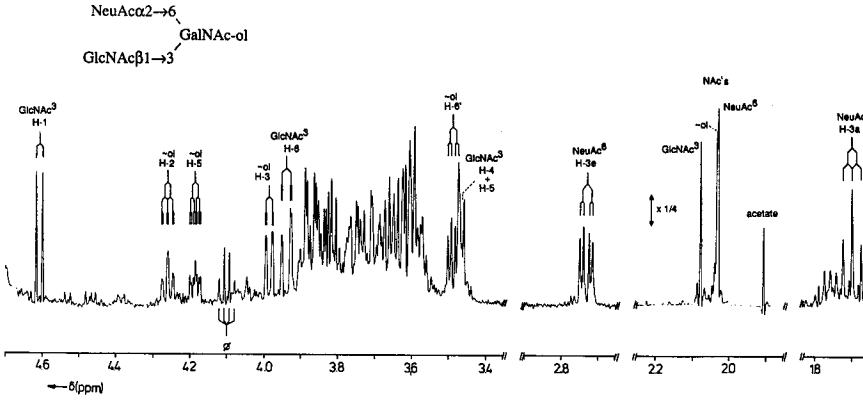

Figure 12. Resolution-enhanced ^{1}H-NMR spectrum of **10**. For comments, see Figure 2. The signal(s) marked by ϕ stem(s) from (a) frequently occurring, nonprotein noncarbohydrate contaminant(s).

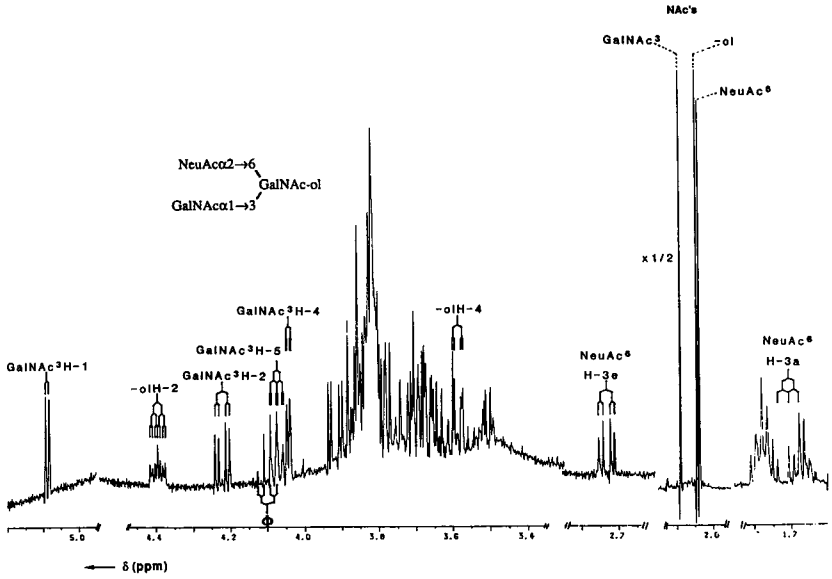

Figure 13. Resolution-enhanced 400-MHz ^{1}H-NMR spectrum of **11**. For comments, see Figures 2 and 12.

$\delta = 4.393$ ppm (**4**, $\delta = 4.395$ ppm). The positions of the characteristic H-3 and NAc signals of NeuAc fit the data reported for **6**, **9**, and **10**. The structural reporters established for the NeuGc analog (**11A**) (Savage *et al.*, 1988, 1990a) are almost identical to those discussed for **11** (see Table 1; 270-MHz ^{1}H-NMR data), except that the NeuAc^6 set has been replaced by the typical NeuGc^6 set (compare with **6A** and **9A**).

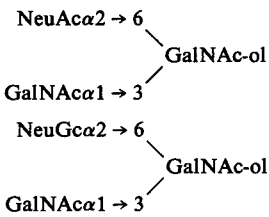

(11)

(11A)

Summarizing the ^{1}H-NMR data of **1–11**, the 11 core regions, discussed above individually, are distinguishable from each other on the basis of the positions of the GalNAc-ol structural-reporter-group resonances (Table 1, Figs. 1–13).

For $\beta 1 \rightarrow 3$-linked Gal the typical triplet-like-shaped GalNAc-ol H-2 signal is found at $\delta = 4.38$–4.40 ppm, irrespective of the presence or absence

of GlcNAc^6 or NeuAc^6/NeuGc^6 (compare **2**, **7**, **9**, and **9A**). Although the $\alpha 1 \rightarrow 3$-linked GalNAc residue also gives rise to a GalNAc-ol H-2 signal at $\delta = 4.39$–4.40 ppm, a discrimination between **2**, **7**, **9**, and **9A** on the one hand and **4**, **11**, and **11A** on the other, is possible by taking into account the chemical shifts of GalNAc-ol H-3 ($\delta = 4.05$–4.07 ppm [$\delta > 4.0$ ppm] versus $\delta = 3.87$–3.89 ppm [$\delta < 4.0$ ppm]) and H-5 (see below). If GalNAc-ol bears GlcNAc in $\beta 1 \rightarrow 3$ linkage, the GalNAc-ol H-2 signal is found at $\delta = 4.26$–4.29 ppm, irrespective of the presence or absence of GlcNAc^6 or NeuAc^6/NeuGc^6 (compare **3**, **8**, and **10**). In the case of a nonsubstituted C-3 position, but a substituted one at C-6 of GalNAc-ol (**5**, **6**, and **6A**), the GalNAc-ol H-2 signal is observed at $\delta = 4.24$–4.25 ppm, like for GalNAc-ol itself (**1**). It may be concluded that the chemical shift of GalNAc-ol H-2 (in combination with that of GalNAc-ol H-3) is highly diagnostic for the presence or absence of a substituent monosaccharide at GalNAc-ol C-3, and, if present, for the nature of that substituent.

Similarly, the chemical shift of GalNAc-ol H-5, in conjunction with the values of H-6 and/or H-6′, have proved to be discriminative in defining the type of substitution at GalNAc-ol C-6. If GalNAc-ol is monosubstituted at C-3 by β-Gal, β-GlcNAc, or α-GalNAc, the chemical shifts of the various H-5 signals have different δ values, namely, $\delta = 4.196$ ppm (**2**), $\delta = 4.141$ ppm (**3**), $\delta = 3.749$ ppm (**4**), respectively. However, if β-GlcNAc or α-NeuAc/α-NeuGc are present as substituent at GalNAc-ol C-6, the H-5 signal is found between $\delta = 4.02$–4.03 ppm (**5**, **6**, and **6A**). The disubstitution gives rise to typical more downfield shifts: **7**, $\delta = 4.281$ ppm; **8**, $\delta = 4.230$ ppm; **9**/**9A**, $\delta = 4.244/4.249$ ppm; **10**, $\delta = 4.185$ ppm. In the case of a GlcNAc^6 substitution at GalNAc-ol, the GalNAc-ol H-6 signal appears outside the bulk resonance at the downfield position of $\delta = 3.90$–3.93 ppm (**5**, **7**, and **8**). The attachment of NeuAc^6/NeuGc^6 at GalNAc-ol results in the appearance of the GalNAc-ol H-6′ signal outside the bulk resonance at the upfield position of $\delta = 3.48$–3.54 ppm (**6**, **6A**, **9**, and **9A**). As far as the H-5, H-6, and H-6′ signals are concerned, no information is available for **11** and **11A**. It is evident that the precise values of the chemical shifts of GalNAc-ol H-5, H-6, and H-6′ are modulated by the substituent at GalNAc-ol C-3.

As will be shown in Sections 3–10, especially the resonance positions of H-2 and H-5 of GalNAc-ol are used as starting points for the structural analysis of oligosaccharide-alditols, regardless of the extensions of the different sugar substituents at GalNAc-ol. However, when analyzing more complex and larger structures, the H-2 and H-5 signals may be obscured by other carbohydrate resonances. As will be shown for several examples, the complete structure is then in fact built up from separately recognizable peripheral structural elements. For a summary and evaluation of the general features of the core structures, see Section 11.

3. BACKBONE STRUCTURES

The backbone structures of many mucin-type oligosaccharide-alditols are constituted of alternating β-linked Gal and β-linked GlcNAc residues. For the series of backbone structures to be discussed in Sections 3.1–3.5, the H-1 signal of the β-Gal unit is found in the region $\delta = 4.40$–4.50 ppm. For the H-1 signal of the β-GlcNAc unit a different region can be established, namely, $\delta = 4.50$–4.80 ppm. For more complex oligosaccharide-alditols than discussed in Section 3, having different peripheral monosaccharide units attached to the backbone structures, some overlap between both regions can occur. In general, the average $J_{1,2}$ values for backbone Gal and GlcNAc seem to differ slightly but significantly ($J_{1,2} \approx 7.8$ and 8.2 Hz, respectively). Although not discussed in detail below, the various ^{1}H-NMR spectra give direct evidence for the molar ratio of the constituting monosaccharides. In this section the discrimination between backbone type-1 (Galβ1 → 3GlcNAc) and backbone type-2 (Galβ1 → 4GlcNAc; *N*-acetyllactosamine) structural elements will also get attention.

3.1. Extensions of the Galβ1 → 3GalNAc-ol Core Structure

In this section, extensions with β-Gal and β-GlcNAc residues at the β-Gal unit of Galβ1 → 3GalNAc-ol (**2**) will be discussed (**12–16**). The ^{1}H-NMR parameters of the structural reporters of these compounds have been summarized in Table 2. For comparison, the data of Galβ1 → 3GalNAc-ol (**2**) have been included. The ^{1}H-NMR data of **12–16**, having the Galβ1 → 3GalNAc-ol core in common, show the H-2 and H-5 signal of GalNAc-ol at $\delta = 4.38$–4.40 and 4.14–4.20 ppm, respectively (see Section 11). Extension of the core by substitutions on the Gal[3] residue determine the exact positions of H-2 and H-5 of GalNAc-ol. The GalNAc-ol H-3 signal arises at $\delta =$ 4.0–4.1 ppm. The position of the NAc signal of GalNAc-ol is found at $\delta = 2.046$–2.050 ppm.

The ^{1}H-NMR spectrum of **12** (Klein *et al.*, 1988; Lamblin *et al.*, 1984b; Van Halbeek *et al.*, 1982b) (Figure 14) shows two NAc signals and three doublets in the β-anomeric region. Two of the latter doublets resonate in

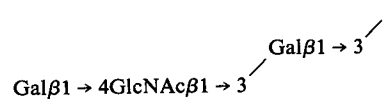

(12)

the specific β-Gal region ($\delta = 4.480$ ppm, $J_{1,2} = 8.0$ Hz; $\delta = 4.463$ ppm, $J_{1,2} = 8.0$ Hz); the third one is found in the specific β-GlcNAc region ($\delta = 4.688$ ppm, $J_{1,2} = 8.2$ Hz). GalNAc-ol is monosubstituted at C-3 by β-Gal, as can be inferred from the H-2 and H-5 signal of GalNAc-ol at

TABLE 2

^{1}H Chemical Shifts of Structural-Reporter Groups of Constituent Monosaccharides for Oligosaccharide-Alditols Representing Extensions with β-Gal and β-GlcNAc Residues at the β-Gal Unit of 2 (12–16)

Residue	Reporter group	2 	12 	13[a] 	14[a] 	15[a] 	16[b] 
GalNAc-ol	H-2	4.395	4.396	4.401	4.401	4.389	4.400
	H-3	4.065	4.051	4.050	4.052	4.020	4.050
	H-4	3.507	3.497	3.493	3.497	3.503	3.5
	H-5	4.196	4.184	4.184	4.188	4.142	4.191
	NAc	2.050	2.048	2.046	2.048	2.046	2.046
Gal^3	H-1	4.478	4.463	4.465	4.463	4.468	4.461
	H-4	3.901	4.126	4.128	4.128	4.118	4.124
GlcNAc^3	H-1	—	4.688	4.701	4.696	4.701	4.68
	H-3	—	3.7	3.909	3.91	3.949	n.d.[c]
	H-6	—	3.953	3.900	3.899	3.903	n.d.
	NAc	—	2.042	2.034	2.039	2.032	2.044
Gal^4	H-1	—	4.480	—	—	4.468	—
	H-4	—	3.928	—	—	3.922	—
Gal^{3,3}	H-1	—	—	4.449	4.441	4.451	—
	H-4	—	—	3.912	4.143	3.912	—
GlcNAc^6	H-1	—	—	—	—	4.607	—
	H-6	—	—	—	—	3.995	—
	NAc	—	—	—	—	2.053	—
GlcNAc^{3,3}	H-1	—	—	—	4.742	—	—
	H-3	—	—	—	3.91	—	—
	H-6	—	—	—	3.899	—	—
	NAc	—	—	—	2.024	—	—
Gal^{3,3,3}	H-1	—	—	—	4.448	—	—
	H-4	—	—	—	3.910	—	—

[a] Spectrum recorded at 22 °C.
[b] Spectrum recorded at 19 °C.
[c] n.d. means value could not be determined merely by inspection of the spectrum.

$\delta = 4.396$ and 4.184 ppm, respectively. The core Gal^3 residue (H-1, $\delta =$ 4.463 ppm) is substituted at C-3 by a β-GlcNAc residue. This conclusion is based on the chemical shift of the Gal^3 H-4 signal at $\delta = 4.126$ ppm ($\Delta\delta = +0.225$ ppm as compared to **2**), having coupling constants $J_{3,4} =$ 3.5 Hz and $J_{4,5} \approx 1.0$ Hz. Such a Gal H-4 signal is characteristic of the →GlcNAcβ1 → 3Galβ1 → sequence. See for example: NeuAcα2 → 3Galβ1 → 4GlcNAcβ1 → 3Galβ1 → 4GlcNAcβ1 → N(Asn), wherein Gal^{4,N} H-1: $\delta = 4.468$ ppm and Gal^{4,N} H-4: $\delta = 4.154$ ppm (Vliegenthart *et al.*,

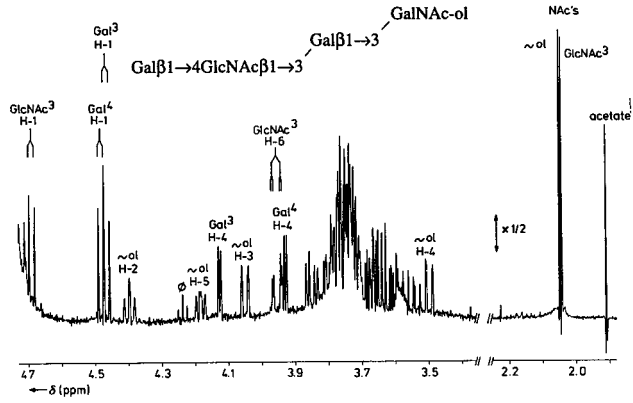

Figure 14. Resolution-enhanced ^{1}H-NMR spectrum of **12**. For comments, see Figures 2 and 12.

1983); Galβ1 → 4GlcNAcβ1 → 3Galβ1 → 4Glc, wherein Gal^4 H-1: δ = 4.436 ppm and Gal^4 H-4: δ = 4.153 ppm (unpublished results; Dua and Bush, 1983; Strecker *et al.*, 1989b); Galβ1 → 3GlcNAcβ1 → 3Galβ1 → 4Glc, wherein Gal^4 H-1: δ = 4.439 ppm and Gal^4 H-4: δ = 4.150 ppm (Bernard *et al.*, 1984; Dua and Bush, 1983; Rao *et al.*, 1985; Strecker *et al.*, 1989b); Galβ1 → 4GlcNAcβ1 → 3Gal, wherein Gal H-4: δ = 4.148 ppm (Herlant-Peers *et al.*, 1981); Galβ1 → 3GlcNAcβ1 → 3Gal, wherein Gal H-4: δ = 4.139 ppm (Herlant-Peers *et al.*, 1981). (Note that for the latter two compounds the data have been interchanged with respect to the original paper, due to an error in the coding system earlier; see Bernard *et al.*, 1984). The assignments of the additional Gal^4 and GlcNAc^3 structural reporters to a terminal Galβ1 → 4GlcNAcβ1 → 3 unit in **12** fit the ^{1}H-NMR data described for similar terminal *N*-acetyllactosamine sequences from other sources: Galβ1 → 4GlcNAcβ1 → N(Asn), wherein Gal H-1: δ = 4.481 ppm and Gal H-4: δ = 3.927 ppm (Vliegenthart *et al.*, 1983); Galβ1 → 4GlcNAcβ1 → 3Galβ1 → 4Glc, wherein Gal^{4,3} H-1: δ = 4.477 ppm, Gal^{4,3} H-4: δ = 3.925 ppm, and GlcNAc H-1: δ = 4.703 ppm (unpublished results; Dua and Bush, 1983).

The ^{1}H-NMR spectrum of **13** (Mutsaers *et al.*, 1986) (Figure 15) shows, like that of **12**, two NAc singlets and three doublets in the β-anomeric region, of which two are in the β-Gal region (δ = 4.449 ppm, $J_{1,2}$ = 7.8 Hz;

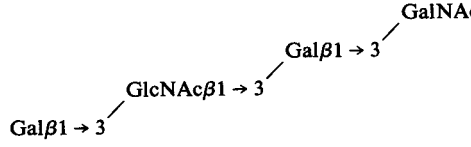

(13)

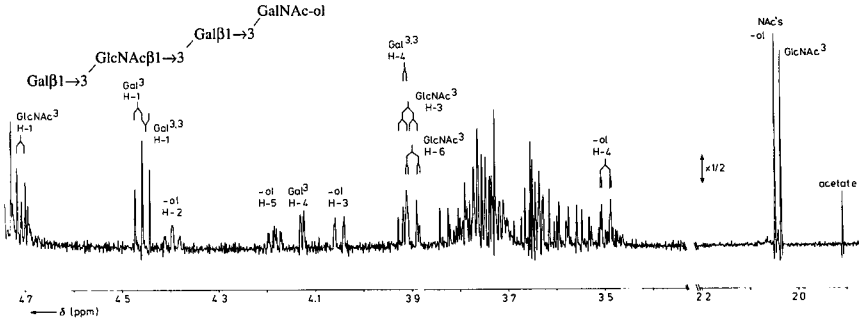

Figure 15. Resolution-enhanced ^{1}H-NMR spectrum of **13** at 22 °C. For comments, see Figure 2.

$\delta = 4.465$ ppm, $J_{1,2} = 7.5$ Hz) and one in the β-GlcNAc region ($\delta = 4.701$ ppm, $J_{1,2} = 8.4$ Hz). GalNAc-ol is monosubstituted at C-3 by β-Gal, as can be inferred from the H-2 and H-5 signal of GalNAc-ol at $\delta = 4.401$ and 4.184 ppm, respectively. The core Gal^3 residue (H-1, $\delta = 4.465$ ppm) is bearing a β-linked GlcNAc (H-1, $\delta = 4.701$ ppm) at C-3, as can be deduced from the diagnostic chemical shift of Gal^3 H-4 ($\delta = 4.128$ ppm) (Bernard *et al.*, 1984; Dua and Bush, 1983; Vliegenthart *et al.*, 1983). In contrast to **12**, in **13** the second β-Gal residue (Gal^{3,3}) (H-1, $\delta = 4.449$ ppm) is attached at C-3 of GlcNAc^3. Going from **12** to **13** a similar trend of chemical shift alteration (Table 2) for GlcNAc H-1 and Gal H-1 has been observed going from lacto-*N*-neotetraose (Galβ1 → 4GlcNAcβ1 → 3Galβ1 → 4Glc) to lacto-*N*-tetraose (Galβ1 → 3GlcNAcβ1 → 3Galβ1 → 4Glc) (Bernard *et al.*, 1984; Dua and Bush, 1983). Furthermore, for **13** the H-3 signal of GlcNAc^3 is found at $\delta = 3.909$ ppm, being more downfield than for **12** ($\delta \approx 3.7$ ppm). The latter finding makes GlcNAc H-3 a suitable structural-reporter group for the β1 → 3 linkage in this category of compounds.

In Table 3 a survey is presented of chemical shift values for pertinent reporter groups going from a Galβ1 → 4GlcNAcβ1 → (backbone type-2 chain) to a Galβ1 → 3GlcNAcβ1 → (backbone type-1 chain) sequence in several mucin-derived oligosaccharide-alditols together with a number of reference compounds from other sources. In general, it is possible to discriminate between these two sequences for a given oligosaccharide-alditol on the basis of the positions of the GlcNAc H-1, H-3, H-6, and NAc signals. Comparison of both types of chains shows that in each case for the backbone type-1 chain GlcNAc H-1 is found at lower field, while GlcNAc NAc is observed at higher field, as compared to the backbone type-2 chain. The precise values of the chemical shifts are dependent on the location of the backbone type-1 or type-2 unit in the carbohydrate chain, especially on the type of linkage in which GlcNAc is involved, and on the presence of

TABLE 3

^{1}H Chemical Shifts of Structural-Reporter Groups Going from a Galβ1 → 4GlcNAcβ1 → to a Galβ1 → 3GlcNAcβ1 → Sequence

Residue	Reporter group	*a* 	*b* 	*b* 	*b* 	*c*	*c* 	*d* 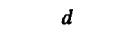	*d* 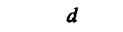
GlcNAc	H-1	4.725 (β)	4.746 (β)	4.718 (β)	4.740 (β)	4.703 (β)	4.730 (β)	4.582	4.600
	H-3	n.d.[e]	n.d.	n.d.	n.d.	n.d.	n.d.	n.d.	n.d.
	H-6	n.d.	n.d.	n.d.	n.d.	n.d.	n.d.	n.d.	n.d.
	NAc	2.042 (β)	2.032 (β)	n.d.	n.d.	2.034	2.027	2.050	2.045
Gal	H-1	4.474 (β)	4.423 (β)	4.482	4.438	4.477	4.439	4.467	4.445
	H-4	3.929	n.d.	3.920	n.d.	3.925	3.912	n.d.	n.d.
		12 	**13** 	**17** 	**18** 	**22** 	**23** 	**90** 	**94** 
GlcNAc	H-1	4.688	4.701	4.631	4.654	4.624	4.648	4.635	4.660
	H-3	3.7	3.909	3.6–3.7	3.911	3.6–3.7	n.d.	n.d.	n.d.
	H-6	3.953	3.900	4.021	3.954	4.021	3.955	4.009	3.970
	NAc	2.042	2.034	2.083	2.073	2.079	2.069	2.076	2.067
Gal	H-1	4.480	4.449	4.455	4.461	4.456	4.453	4.464	4.455
	H-4	3.928	3.912	3.926	3.919	3.927	3.92	3.927	3.918

[a] Van Halbeek *et al.* (1983b).
[b] Herlant-Peers *et al.* (1981).
[c] Unpublished results.
[d] Bernard *et al.* (1984).
[e] n.d. means value could not be determined merely by inspection of the spectrum.

additional substituents at GlcNAc and/or Gal (see below). The position of H-1 of Gal is not always sensitive to $\beta 1 \rightarrow 3$ or $\beta 1 \rightarrow 4$ linkage. The Gal H-4 signal seems to resonate at a somewhat lower field in the backbone type-2 chain, as compared to the backbone type-1 chain. Most decisive for the $\beta 1 \rightarrow 3$ linkage is the relatively downfield position of GlcNAc H-3 ($\delta = 3.91$ versus ≈ 3.7 ppm), whereas the relatively downfield position of GlcNAc H-6 is useful for substantiating the $\beta 1 \rightarrow 4$ type of backbone. For larger oligosaccharide-alditols, measurements of NOE effects may be needed to differentiate between a backbone type-1 and type-2 chain.

In the ^{1}H-NMR spectrum of **14** (Mutsaers *et al.*, 1986) (Figure 16), three NAc signals, three doublets in the β-Gal anomeric region, and two

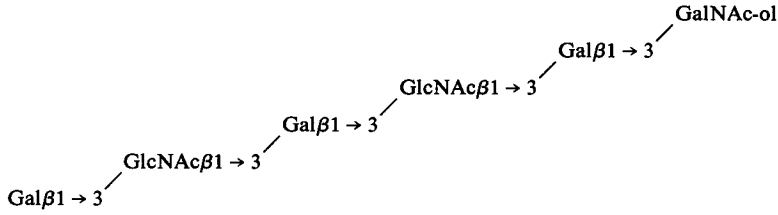

(14)

doublets in the β-GlcNAc anomeric region can be observed. The monosubstitution at C-3 of GalNAc-ol by β-Gal is evident from the positions of the GalNAc-ol H-2 and H-5 signals at $\delta = 4.401$ and 4.188 ppm, respectively. Comparison of the structural-reporter groups of **14** with those of **13** makes clear that **14** is an extension of **13** with an additional Gal-GlcNAc unit, being reflected by signals at $\delta = 4.143$ ppm for Gal^{3,3} H-4, at $\delta =$ 4.742 ppm for GlcNAc^{3,3} H-1, and at $\delta = 2.024$ ppm for GlcNAc^{3,3} NAc.

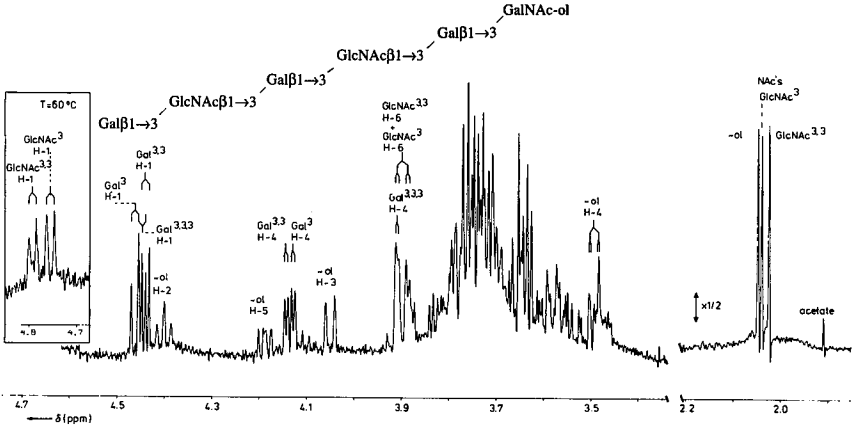

Figure 16. Resolution-enhanced ^{1}H-NMR spectrum of **14** at 22 °C. The inset shows the GlcNAc H-1 signals at 60 °C. For comments, see Figure 2.

The presence of two downfield Gal H-4 signals at $\delta = 4.128$ ppm (Gal^3 H-4) and $\delta = 4.143$ ppm are indicative of the occurrence of two →GlcNAcβ1 → 3Galβ1 → segments in the structure. This means that the additional Gal-GlcNAc unit is attached via a β1 → 3 linkage to $Gal^{3,3}$. The structural reporters of the constituting Gal and GlcNAc residues of the latter unit show that the terminal Gal is β1 → 3-linked to $GlcNAc^{3,3}$ (see discussion for **12** and **13** and the data in Table 3). In **13** as well as in **14** the terminal Galβ1 → 3GlcNAcβ1 → 3Gal segment is reflected by the same set of structural reporters for the terminal Gal residue (H-1, $\delta = 4.448$ ppm; H-4, $\delta = 3.910$ ppm).

The ^{1}H-NMR spectrum of a further extension of **13**, namely **15** (Mutsaers *et al.*, 1986), is presented in Figure 17. In the NAc region, three singlets

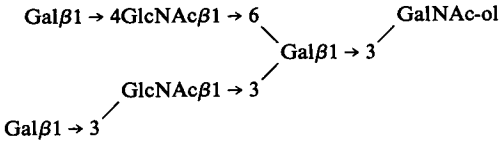

(15)

are observable, whereas the β-anomeric region shows the occurrence of two β-GlcNAc and three β-Gal residues. The monosubstitution at C-3 of GalNAc-ol by β-Gal is evident from the positions of the GalNAc-ol H-2 and H-5 signals at $\delta = 4.389$ and 4.142 ppm, respectively. The presence of the Galβ1 → 3GlcNAcβ1 → 3Galβ1 → element is supported by the signal at $\delta = 4.118$ ppm (Gal^3 H-4) and the various structural-reporter groups of $GlcNAc^3$ and $Gal^{3,3}$ (compare **15** with **13**, see Table 2). The structural-reporter groups of the remaining Gal and GlcNAc residues demonstrate

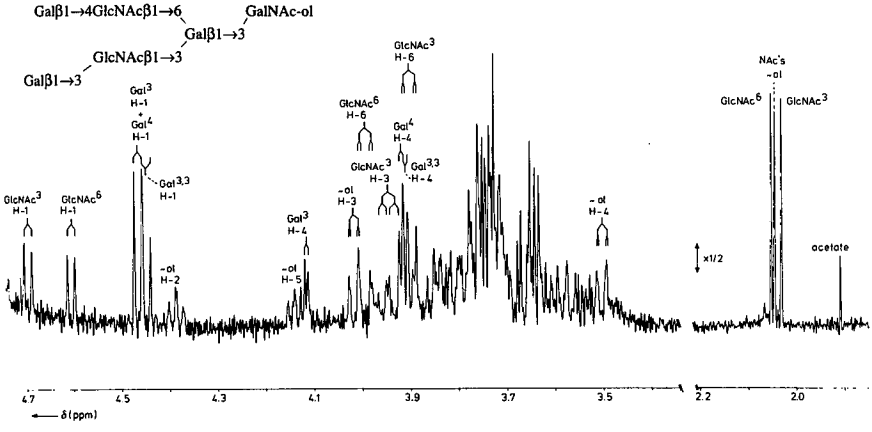

Figure 17. Resolution-enhanced ^{1}H-NMR spectrum of **15** at 22 °C. For comments, see Figure 2.

the occurrence of a Galβ1 → 4GlcNAcβ1 → 6Galβ1→ sequence. Comparable chemical shift values were observed for the model compound Galβ1 → 4GlcNAcβ1 → 6(Galβ1 → 4GlcNAcβ1 → 3)Gal (β-form), wherein $Gal^{4,6}$ H-1: $\delta = 4.468$ ppm, $Gal^{4,6}$ H-4: $\delta = 3.923$ ppm, $GlcNAc^{6}$ H-1: $\delta = 4.581$ ppm, and Gal H-4: $\delta = 4.112$ ppm (Van Halbeek *et al.*, 1982c). The Gal H-4 signals at $\delta = 3.922$ ppm (Gal^{4}) and $\delta = 3.912$ ppm ($Gal^{3,3}$) point to the presence of a terminal backbone type-2 and type-1 chain, respectively (see Table 3). In **15** Gal^{3} serves as a 3,6-branching point. In the case of disubstitution the H-4 signal of Gal^{3} shows a small upfield shift ($\Delta\delta \approx -0.01$ ppm), as compared to **12–14**. Finally, the presence of the Galβ1 → 4GlcNAcβ1→ sequence linked to C-6 of Gal^{3} has typical chemical shift effects on the H-3 and H-5 signals of GalNAc-ol (compare **15** with **12–14**).

The 360-MHz ^{1}H-NMR spectrum of **16** (Brockhausen *et al.*, 1984), being an extension of **2** with a β1 → 3-linked GlcNAc at Gal^{3}, shows two

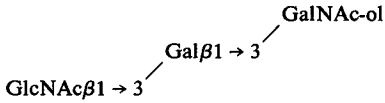

(16)

NAc signals and two doublets in the β-anomeric region. One of the doublets resonates in the β-Gal region ($\delta = 4.461$ ppm), the other in the β-GlcNAc region ($\delta = 4.68$ ppm). GalNAc-ol is monosubstituted at C-3 by β-Gal, indicated by the H-2 and H-5 signals of GalNAc-ol at $\delta = 4.400$ and 4.191 ppm, respectively. The structural-reporter-group signals of GalNAc-ol and Gal^{3} do not differ from those presented for **12** and **13** (Table 2). The reported H-1 and NAc δ values of $GlcNAc^{3}$ are identical to those of **12**.

3.2. Extensions of the GlcNAcβ1 → 3GalNAc-ol Core Structure

This section describes simple extensions with a β-Gal residue at the β-GlcNAc unit of GlcNAcβ1 → 3GalNAc-ol (**3**), namely, **17** and **18**. The

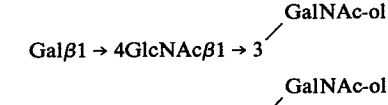

(17)

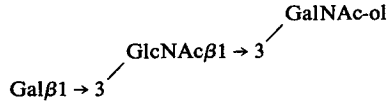

(18)

relevant ^{1}H-NMR parameters of these compounds have been summarized in Table 4. For comparison, the data of **3** (GlcNAcβ1 → 3GalNAc-ol) have been included. The ^{1}H-NMR spectra of **17** and **18** are depicted in Figures 18 and 19, respectively. The common GlcNAcβ1 → 3GalNAc-ol core follows from the characteristic GalNAc-ol H-2 and H-5 signals at $\delta = 4.27$–4.29

TABLE 4
^{1}H Chemical Shifts of Structural-Reporter Groups of Constituent Monosaccharides for Oligosaccharide-Alditols Representing Extensions with β-Gal Residues at the β-GlcNAc Unit of 3 (17–18)

Residue	Reporter group	3 	17 	18 
GalNAc-ol	H-2	4.287	4.290	4.289
	H-3	3.996	4.002	4.012
	H-4	3.546	3.552	3.560
	H-5	4.141	4.143	4.138
	NAc	2.037	2.038	2.034
GlcNAc^3	H-1	4.604	4.631	4.654
	H-3	3.584	3.6–3.7	3.911
	H-6	3.950	4.021	3.954
	NAc	2.085	2.083	2.073
Gal^4	H-1	—	4.455	—
	H-4	—	3.926	—
Gal^3	H-1	—	—	4.461
	H-4	—	—	3.919

and 4.11–4.14 ppm, respectively (see Section 11). The NAc signal resonates at $\delta = 2.034$–2.038 ppm. As will be seen later, the precise values of these structural reporters, as well as the chemical shifts of GlcNAc^3, are dependent on substitutions at the GlcNAc^3 residue.

Comparison of the ^{1}H-NMR spectra of **17** (Breg *et al.*, 1988b; Capon *et al.*, 1989; Van Halbeek, 1984; Van Halbeek *et al.*, 1982b) (Figure 18) and

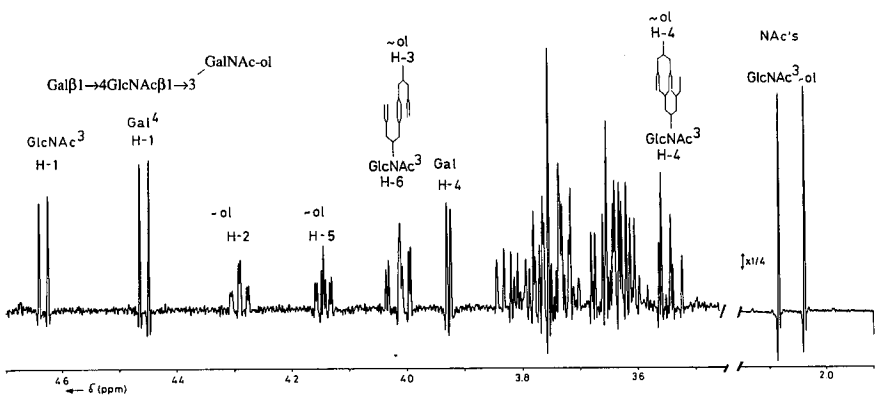

Figure 18. Resolution-enhanced ^{1}H-NMR spectrum of **17**. For comments, see Figure 2.

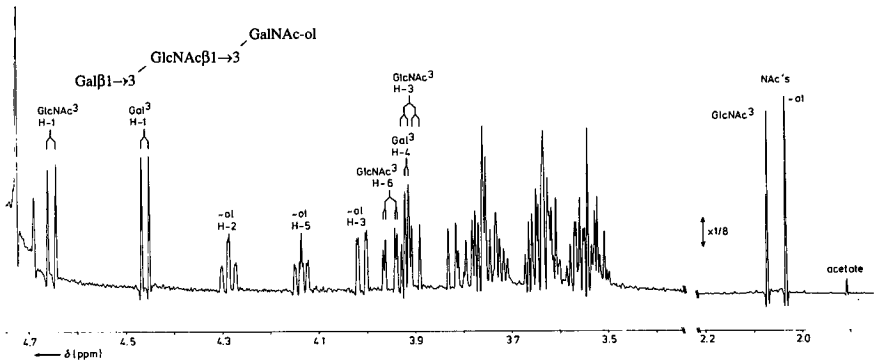

Figure 19. Resolution-enhanced ^{1}H-NMR spectrum of **18**. For comments, see Figure 2.

18 (Breg *et al.*, 1988b; Capon *et al.*, 1989; Mutsaers *et al.*, 1986; Van Halbeek, 1984; Van Halbeek *et al.*, 1982b) (Figure 19) reveals that in both cases two NAc signals and two doublets in the β-anomeric region occur. One of the two doublets resonates in the specific β-GlcNAc region (**17**: GlcNAc H-1, $\delta = 4.631$ ppm, $J_{1,2} = 8.0$ Hz; **18**: GlcNAc H-1, $\delta = 4.654$ ppm, $J_{1,2} = 8.4$ Hz). The second doublet occurs in the specific β-Gal region (**17**: Gal^4 H-1, $\delta = 4.455$ ppm, $J_{1,2} = 7.9$ Hz; **18**: Gal^3 H-1, $\delta = 4.461$ ppm, $J_{1,2} = 7.7$ Hz). The NAc singlets were assigned by comparison with the ^{1}H-NMR data of **3**. The terminal β-Gal residue in **17** and **18** is evident from the typical H-4 signals at $\delta = 3.926$ and 3.919 ppm, respectively. The shift effect for H-1 of GlcNAc ($\Delta\delta = +0.027$ ppm), introduced by the attachment of Gal to GlcNAc in **17** as compared to **3**, is in accordance with that described for the attachment of Gal in $\beta 1 \rightarrow 4$ linkage to GlcNAc, completing an *N*-acetyllactosamine unit in an *N*-glycoprotein carbohydrate chain (Vliegenthart *et al.*, 1983). A concomitant downfield shift is observed for GlcNAc H-6 ($\delta = 4.021$ ppm, $\Delta\delta = +0.071$ ppm, $J_{5,6} = 2.3$ Hz, $J_{6,6'} = -12.0$ Hz). A predominant difference between the spectra of **17** and **18** is the appearance of the GlcNAc H-3 signal outside the bulk of skeleton protons at $\delta = 3.911$ ppm ($J_{2,3} = 10.4$ Hz, $J_{3,4} = 8.5$ Hz) in **18**, reflecting the $1 \rightarrow 3$ linkage between Gal and GlcNAc ($\Delta\delta \approx +0.33$ ppm). The GlcNAc^3 H-1 signal in **18** is found more downfield than in **17**, whereas for the GlcNAc^3 NAc signal the reverse holds. For a general discussion concerning the differentiation between Gal$\beta 1 \rightarrow$ 4GlcNAc$\beta 1 \rightarrow$ (backbone type-2 chain) and Gal$\beta 1 \rightarrow$ 3GlcNAc$\beta 1 \rightarrow$ (backbone type-1 chain), see Section 3.1 and Table 3. Additional reference data are found in Gleeson *et al.* (1984), Hounsell *et al.* (1985), and Lamblin *et al.* (1984*b*) for **17**, and in Hounsell *et al.* (1985) and Lamblin *et al.* (1984b) for **18**.

3.3. Extensions of the GlcNAcβ1 → 6GalNAc-ol Core Structure

In this section, extensions with β-Gal and β-GlcNAc residues at the β-GlcNAc unit of GlcNAcβ1 → 6GalNAc-ol (**5**), namely, **19** and **20**, will be presented. The relevant ^{1}H-NMR parameters of these compounds have been compiled in Table 5, together with the data of **5** (GlcNAcβ1 → 6GalNAc-ol). Both ^{1}H-NMR spectra (Figures 20 and 21) indicate the occurrence of a GlcNAcβ1 → 6GalNAc-ol core type. The presence of the GalNAc-ol H-2 at $\delta = 4.24$–4.25 ppm ($J_{1,2} = 6.1$ Hz, $J_{1',2} = 7.9$ Hz, $J_{2,3} = 1.5$ Hz) indicates the absence of a substituent monosaccharide at GalNAc-ol C-3. Substitution at C-6 is supported by the detection of GalNAc-ol H-5 at $\delta = 4.02$–4.03 ppm ($J_{4,5} = 1.4$ Hz, $J_{5,6} = 5.0$ Hz, $J_{5,6'} = 7.5$ Hz). The appearance of the GalNAc-ol H-6 signal outside the bulk resonance at $\delta = 3.93$ ppm ($J_{6,6'} = -10.7$ Hz) suggests the presence of a GlcNAc^6 substitution at GalNAc-ol. Comparison of the ^{1}H-NMR parameters of GalNAc-ol for **5**, **19**, and **20** shows nearly identical chemical shift values.

TABLE 5
^{1}H Chemical Shifts of Structural-Reporter Groups of Constituent Monosaccharides for Oligosaccharide-Alditols Representing Extensions with β-Gal and β-GlcNAc Residues at the β-GlcNAc Unit of 5 (19–20)

Residue	Reporter group	5 	19[a] 	20[a] 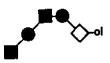
GalNAc-ol	H-2	4.242	4.243	4.242
	H-3	3.841	3.843	3.841
	H-4	3.379	3.379	3.379
	H-5	4.021	4.026	4.021
	H-6	3.933	3.932	3.932
	NAc	2.046	2.045	2.042
GlcNAc^6	H-1	4.553	4.577	4.573
	H-6	3.928	3.993	3.990
	NAc	2.059	2.061	2.060
Gal^4	H-1	—	4.471	4.440
	H-4	—	3.925	4.153
GlcNAc^3	H-1	—	—	4.722
	H-6	—	—	3.898
	NAc	—	—	2.028
Gal^3	H-1	—	—	4.460
	H-4	—	—	3.911

[a] Spectrum recorded at 22 °C. In order to ensure complete visualization of the H-1 signals in the spectral region $4.4 < \delta < 4.8$ ppm (δ HO^{2}H = 4.81 ppm).

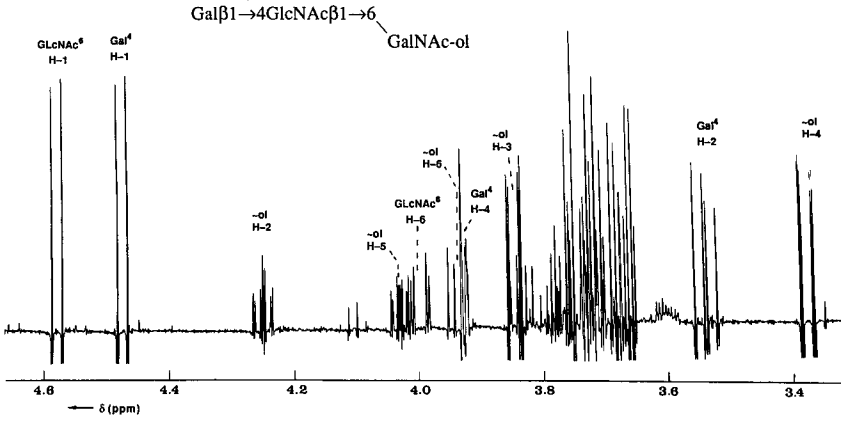

Figure 20. Resolution-enhanced ^{1}H-NMR spectrum of **19** at 22 °C. The NAc singlets for GalNAc-ol at $\delta = 2.045$ ppm and for GlcNAc at $\delta = 2.061$ ppm are not included in the spectrum.

The ^{1}H-NMR spectrum of **19** (Feeney *et al.*, 1986; Hounsell *et al.*, 1985; Mutsaers *et al.*, 1986; Van Halbeek *et al.*, 1985b) (Figure 20) shows

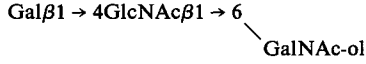

(19)

the presence of two NAc singlets and two doublets in the β-anomeric region, one in the β-GlcNAc region ($\delta = 4.577$ ppm, $J_{1,2} = 8.2$ Hz) and one in the β-Gal region ($\delta = 4.471$ ppm, $J_{1,2} = 7.8$ Hz). The structural-reporter groups

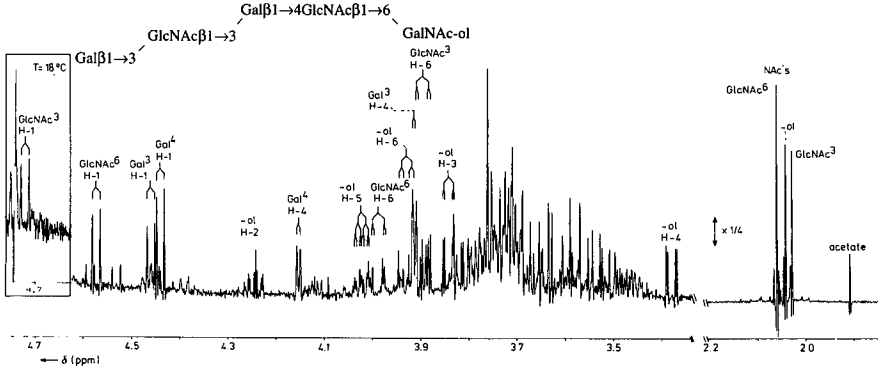

Figure 21. Resolution-enhanced ^{1}H-NMR spectrum of **20** at 22 °C. The inset shows the GlcNAc^3 H-1 signal at 18 °C. For comments, see Figure 2.

of Gal[4] (H-1, δ = 4.471 ppm; H-4, δ = 3.925 ppm/$J_{3,4}$ = 3.4 Hz, $J_{4,5}$ = 0.9 Hz) and GlcNAc[6] (H-6, δ = 3.993 ppm, $\Delta\delta$ = +0.065 ppm as compared to **5**; H-1, δ = 4.577 ppm, $\Delta\delta$ = +0.024 ppm) are in favor of a terminal Galβ1 → 4GlcNAcβ1→ sequence (see also the step **3** to **17**). For a full discussion of backbone type-1 and type-2 chains, see Section 3.1 (Table 3). The complete ^{1}H-NMR assignments have been obtained using a combination of 1D and 2D ^{1}H-NMR techniques (COSY, RELAYED-COSY, and F_1-decoupled COSY) (Feeney *et al.*, 1986).

In the ^{1}H-NMR spectrum of **20** (Mutsaers *et al.*, 1986) (Figure 21), three NAc signals, two doublets in the β-GlcNAc H-1 region (δ = 4.573

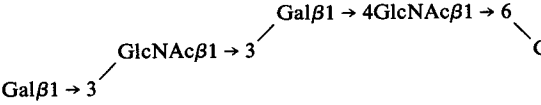

(20)

and 4.722 ppm; $J_{1,2}$ = 8.3 Hz) and two doublets in the β-Gal H-1 region (δ = 4.460 and 4.440 ppm; $J_{1,2}$ = 7.9 Hz) are observed. The structural reporters of **20** indicate that it is an extension of **19** with another Gal-GlcNAc element. Typical new signals in the spectrum of **20** are those at δ = 4.153 ppm (Gal[4] H-4), δ = 4.722 ppm (GlcNAc[3] H-1), and δ = 2.028 ppm (GlcNAc[3] NAc). The H-4 signal of Gal[4] at δ = 4.153 ppm indicates that the additional GlcNAc is β1 → 3 linked to Gal[4] (see also **12–14**). The set of chemical shifts of H-1, H-6, and NAc of GlcNAc[3] and of H-1 and H-4 of terminal Gal (see Table 5) point to the terminal Galβ1 → 3GlcNAcβ1→ sequence (compare with **12–14**; see Table 3). It has to be noted that in Table 5 the assignments of Gal[3] H-1 and Gal[4] H-1 have been interchanged, as compared to Mutsaers *et al.* (1986).

3.4. Extensions of the GlcNAcβ1 → 6(GlcNAcβ1 → 3)GalNAc-ol Core Structure

This section describes a series of extensions with β-Gal residues at the β-GlcNAc units of GlcNAcβ1 → 6(GlcNAcβ1 → 3)GalNAc-ol (**8**), leading to **21–23**. The relevant ^{1}H-NMR parameters of these oligosaccharide-alditols have been collected in Table 6, together with those of **8** [GlcNAcβ1 → 6(GlcNAcβ1 → 3)GalNAc-ol]. The ^{1}H-NMR spectra (Figures 22–24) show in each case the presence of a GlcNAcβ1 → 6(GlcNAcβ1 → 3)GalNAc-ol core type. Constant elements in the structural-reporter-group chemical shifts of this series are H-2, H-5, and NAc of GalNAc-ol at δ = 4.26–4.29, 4.20–4.24, and 2.043–2.045 ppm, respectively (see Section 11). The GlcNAc[6] substitution of GalNAc-ol leads to the appearance of the GalNAc-ol H-6 resonance at δ = 3.90–3.91 ppm.

TABLE 6
^{1}H Chemical Shifts of Structural-Reporter Groups of Constituent Monosaccharides for Oligosaccharide-Alditols Representing Extensions with β-Gal Residues at the β-GlcNAc Units of 8 (21–23)

Residue	Reporter group	8 	21 	22 	23 
GalNAc-ol	H-2	4.280	4.282	4.283	4.287
	H-3	3.984	3.986	3.991	n.d.[a]
	H-4	3.519	3.515	3.521	n.d.
	H-5	4.230	4.239	4.240	4.233
	H-6	3.905	3.906	3.91	n.d.
	NAc	2.044	2.045	2.045	2.043
GlcNAc^3	H-1	4.600	4.599	4.624	4.648
	H-3	n.d.	3.576	3.6–3.7	n.d.
	H-6	3.949	3.951	4.021	3.955
	NAc	2.081	2.081	2.079	2.069
Gal^{4,3}	H-1	—	—	4.456	—
	H-4	—	—	3.927	—
GlcNAc^6	H-1	4.543	4.564	4.565	4.559
	H-6	3.931	3.998	3.998	n.d.
	NAc	2.063	2.061	2.062	2.062
Gal^{4,6}	H-1	—	4.473	4.474	4.472
	H-4	—	3.927	3.927	3.92
Gal^{3,3}	H-1	—	—	—	4.453
	H-4	—	—	—	3.92

[a] n.d. means value could not be determined merely by inspection of the spectrum.

The ^{1}H-NMR spectrum of **21** (Breg *et al.*, 1988b; Lamblin *et al.*, 1984b; Van Halbeek *et al.*, 1982b) (Figure 22) contains three NAc singlets, two

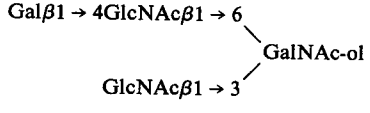

(21)

doublets in the β-GlcNAc anomeric region (δ = 4.599 ppm, $J_{1,2}$ = 8.5 Hz; δ = 4.564 ppm, $J_{1,2}$ = 8.2 Hz), and one doublet in the β-Gal anomeric region (δ = 4.473 ppm, $J_{1,2}$ = 7.8 Hz). The core type is evident from the chemical shifts of the GalNAc-ol H-2 (δ = 4.282 ppm) and H-5 (δ = 4.239 ppm) signals. In accordance with this assignment, the GalNAc-ol H-6 resonance is found at δ = 3.906 ppm ($J_{5,6}$ = 5.9 Hz; $J_{6,6'}$ = −10.9 Hz). By comparison with **8**, the H-1 doublet at δ = 4.599 ppm is attributed to GlcNAc in β1 → 3 linkage to GalNAc-ol. This implies that GlcNAc^3 is present in terminal position. The chemical shifts of the anomeric protons of GlcNAc^6 (δ =

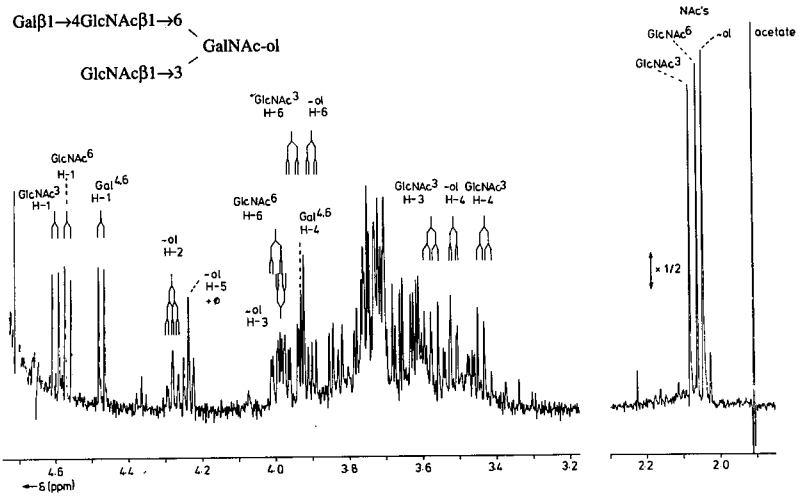

Figure 22. Resolution-enhanced ^{1}H-NMR spectrum of **21**. For comments, see Figures 2 and 12.

4.564 ppm; $\Delta\delta = +0.021$ ppm as compared to **8**) and of the terminal Gal residue point to the occurrence of a Galβ1 → 4GlcNAc sequence (Vliegenthart *et al.*, 1983). A concomitant downfield shift is observed for GlcNAc^6 H-6 ($\delta = 3.998$ ppm; $\Delta\delta = +0.067$ ppm, as compared to **8**). A β1 → 3 linkage between Gal and GlcNAc is excluded by missing the GlcNAc^6 H-3 signal in the region $3.9 < \delta < 4.1$ ppm. The chemical shift value of Gal^{4,6} H-4 at $\delta = 3.927$ ppm supports the terminal position of Gal. See also the discussion for backbone type-1 and type-2 chains in Section 3.1 (Table 3) and the ^{1}H-NMR data of **19**.

The ^{1}H-NMR spectrum of **22** (Breg *et al.*, 1988b; Lamblin *et al.*, 1984b; Van Halbeek *et al.*, 1982b; Hounsell *et al.*, 1989) (Figure 23) shows the

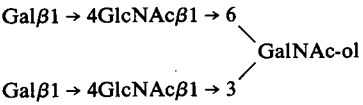

(22)

presence of three NAc signals, two doublets in the β-GlcNAc anomeric region ($\delta = 4.624$ ppm, $J_{1,2} = 8.1$ Hz; $\delta = 4.565$ ppm, $J_{1,2} = 8.2$ Hz), and two in the β-Gal anomeric region ($\delta = 4.474$ ppm, $J_{1,2} = 7.8$ Hz; $\delta = 4.456$ ppm, $J_{1,2} = 7.8$ Hz). The core type structure is indicated by the characteristic chemical shift values for GalNAc-ol H-2 ($\delta = 4.283$ ppm) and H-5 ($\delta = 4.240$ ppm). The GalNAc-ol H-6 signal is found at $\delta = 3.91$ ppm, downfield from the bulk of skeleton protons. Comparison of the ^{1}H-NMR data of **21** and **22** shows identical chemical shift values for one set of GlcNAc and

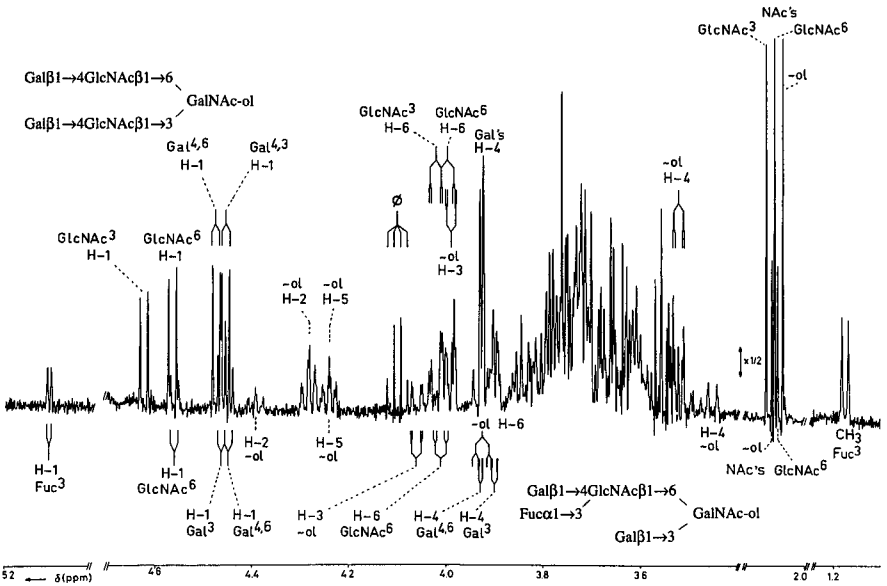

Figure 23. Resolution-enhanced ^{1}H-NMR spectrum of a mixture of **22** (upper) and **41** (lower) (see also Figure 39). For comments, see Figures 2 and 12.

one set of Gal structural reporters, namely, those of GlcNAc^6 and Gal^{4,6}, respectively. This finding proves the occurrence of a terminal Galβ1 → 4GlcNAc moiety β1 → 6 linked to GalNAc-ol in **22**. The remaining sets of structural-reporter groups of the additional GlcNAc and Gal residues fit a second terminal Galβ1 → 4GlcNAc moiety, β1 → 3 linked to GalNAc-ol. The GlcNAc^3 H-1 signal in **22** is shifted downfield (δ = 4.624 ppm; $\Delta\delta$ = +0.025 ppm), with respect to **21**. Similar downfield shifts were observed in the case of Galβ1 → 4GlcNAcβ1 → to GalNAc-ol C-6 in **8** → **21** and to GalNAc-ol C-3 in **3** → **17**. The structural-reporter groups of GlcNAc^3 H-6 (δ = 4.021 ppm; $\Delta\delta$ = +0.072 ppm, as compared to **8**) and of Gal^{4,3} H-1 and H-4 are also in accordance with the presence of a second *N*-acetyllactosamine unit (see **17** for the same structural element).

The ^{1}H-NMR spectral features of **23** (Lamblin *et al.*, 1984b) have been observed only in a mixture of compounds **23** and **40** (see below; see also Hounsell *et al.*, 1989). The spectrum of **23** (Figure 24) shows three NAc

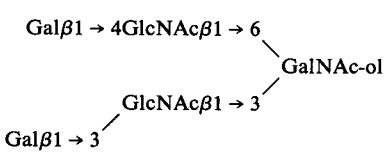

(23)

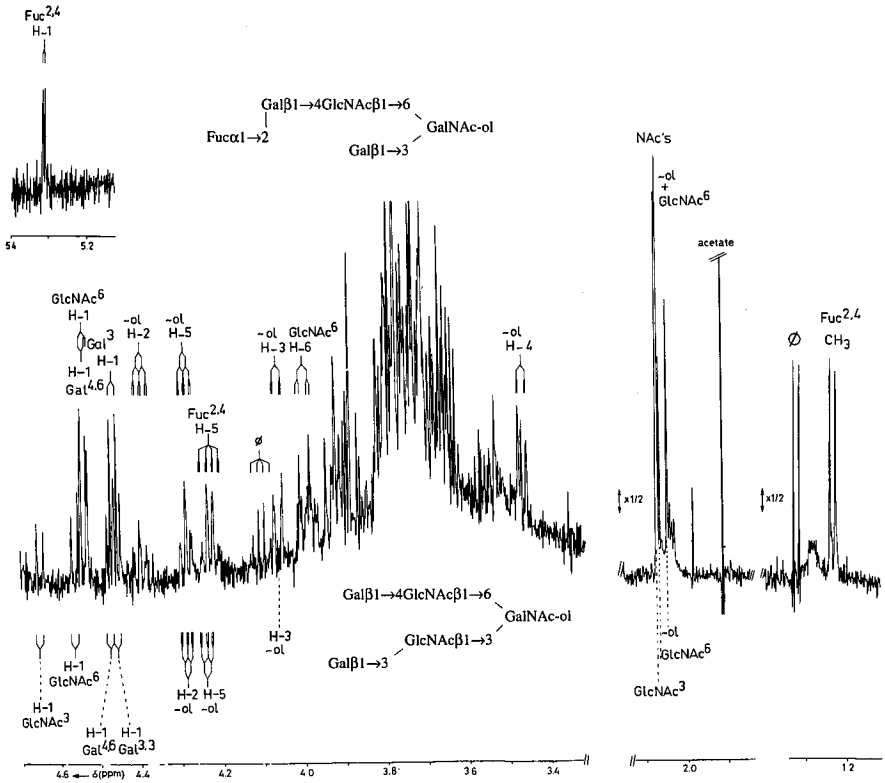

Figure 24. Resolution-enhanced ^{1}H-NMR spectrum of a mixture of **23** (lower) and **40** (upper) (see also Figure 38). The relative-intensity scale of the *N*-acetyl and Fuc methyl proton regions of the spectrum differ from that of the other parts, as indicated. Contaminating acetate gives rise to a signal at $\delta = 1.908$ ppm. The signal(s) marked by ϕ stem(s) from (a) frequently occurring, nonprotein noncarbohydrate contaminant(s).

signals and four doublets in the β-anomeric region, namely, the anomeric signals of two Gal residues ($\delta = 4.472$ ppm/$J_{1,2} = 7.9$ Hz; $\delta = 4.453$ ppm/$J_{1,2} = 7.9$ Hz) and those of the two GlcNAc residues ($\delta = 4.648$ ppm/$J_{1,2} = 8.9$ Hz; $\delta = 4.559$ ppm/$J_{1,2} = 8.3$ Hz) of the GlcNAcβ1 → 6(GlcNAcβ1 → 3)GalNAc-ol element (GalNAc-ol: H-2, $\delta = 4.287$ ppm; H-5, $\delta = 4.233$ ppm). In **23** a terminal Galβ1 → 4GlcNAcβ1→ element is present at C-6 of GalNAc-ol; similar sets of structural reporters can be detected in **21** and **22**. By consequence, a Gal residue is attached to GlcNAc^3. The presence of a 1 → 3 linkage between the latter residues can be inferred by comparing the ^{1}H-NMR data of **23** with those of **18**. The Galβ1 → 3GlcNAcβ1→ structural element causes a more downfield shift for GlcNAc^3 H-1 than the Galβ1 → 4GlcNAcβ1→ element does in **22** ($\delta = 4.648$ ppm;

$\Delta\delta$ = +0.049 ppm as compared to **21**). The GlcNAc^3 NAc singlet at δ = 2.069 ppm is shifted upfield for $\Delta\delta$ = −0.012 ppm, as compared to **21**. An identical shift was observed going from **3** to **18**. See also Table 3 for typical differences of ^{1}H-NMR parameters of backbone type-1 and type-2 chains.

3.5. Extensions of the GlcNAcβ1 → 6(Galβ1 → 3)GalNAc-ol Core Structure

This section summarizes a series of extensions with β-Gal and β-GlcNAc residues at β1 → 6-linked GlcNAc and/or β1 → 3-linked Gal of GlcNAcβ1 → 6(Galβ1 → 3)GalNAc-ol (**7**), namely, **24–28**. The relevant ^{1}H-

TABLE 7

^{1}H Chemical Shifts of Structural-Reporter Groups of Constituent Monosaccharides for Oligosaccharide-Alditols Representing Extensions with β-Gal and β-GlcNAc Residues at the β1 → 6-Linked GlcNAc and/or β1 → 3-Linked Gal Unit of 7 (24–28)

Residue	Reporter group	7 	24[a] 	25 	26 	27 	28[c] 
GalNAc-ol	H-2	4.395	4.403	4.394	4.397	4.406	4.392
	H-3	4.061	4.049	4.060	4.048	4.056	4.059
	H-4	3.468	n.d.[b]	3.465	3.50	3.443	3.464
	H-5	4.281	4.267	4.282	4.266	4.275	4.277
	H-6	3.931	n.d.	3.931	n.d.	n.d.	n.d.
	NAc	2.066	2.064	2.067	2.066	2.067	2.066
Gal^3	H-1	4.468	4.449	4.465	4.449	4.453	4.463
	H-4	3.901	4.124	3.900	4.125	4.133	3.901
GlcNAc^6	H-1	4.538	4.530	4.560	4.554	4.556	4.555
	H-6	3.932	n.d.	3.998	3.993	3.998	3.995
	NAc	2.066	2.064	2.064	2.058	2.059	2.061
Gal^{4,6}	H-1	—	—	4.470	4.468	4.472	4.441
	H-4	—	—	3.925	3.925	3.926	4.151
GlcNAc^3	H-1	—	4.657	—	4.684	4.700	4.740
	H-6	—	n.d.	—	3.952	3.901	n.d.
	NAc	—	2.042	—	2.039	2.032	2.029
Gal^{4,3}	H-1	—	—	—	4.481	—	—
	H-4	—	—	—	3.925	—	—
Gal^{3,3}	H-1	—	—	—	—	4.453	4.459
	H-4	—	—	—	—	3.916	3.918

[a] Spectrum recorded at 19 °C.

[b] n.d. means value could not be determined merely by inspection of the spectrum.

[c] See also Hounsell *et al.* (1989); GlcNAc^3 H-1: δ = 4.719 ppm; Gal^{4,6} H-1 and Gal^{3,3} H-1 have been interchanged.

NMR parameters of these compounds are presented in Table 7. For comparison, the data of **7** [GlcNAcβ1 → 6(Galβ1 → 3)GalNAc-ol] have been included. The ^{1}H-NMR spectra of **25–27** are given in Figures 25–27, respectively. The characterization of compounds with the GlcNAcβ1 → 6(Galβ1 → 3)GalNAc-ol core type elements is based on the following. The occurrence of the H-2 signal of GalNAc-ol at $\delta = 4.38$–4.41 ppm, together with the occurrence of the GalNAc-ol H-3 signal at $\delta = 4.0$–4.1 ppm suggests a β1 → 3-linked Gal residue at GalNAc-ol. On the other hand, the attachment of a GlcNAcβ1 → 6 residue at GalNAc-ol is supported by the appearance of the GalNAc-ol H-5 signal at $\delta = 4.22$–4.29 ppm, the GalNAc-ol NAc signal at $\delta = 2.064$–2.067 ppm, and the GalNAc-ol H-6 signal outside the bulk resonance at the downfield position of $\delta = 3.93$ ppm (see Section 11).

The 360-MHz ^{1}H-NMR spectrum of an extension of **7** with a β1 → 3-linked GlcNAc at Gal^3, namely **24** (Brockhausen *et al.*, 1984), shows three

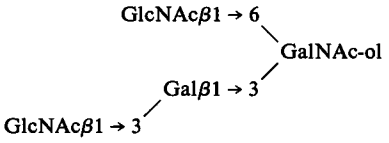

(24)

NAc singlets and three doublets in the β-anomeric region. One of the H-1 signals resonates in the β-Gal region ($\delta = 4.449$ ppm), the other two H-1 signals in the β-GlcNAc region ($\delta = 4.657$ ppm; $\delta = 4.530$ ppm). The disubstitution of GalNAc-ol is evident from the H-2 and H-5 signals of GalNAc-ol at $\delta = 4.403$ and 4.267 ppm, respectively. The structural-reporter-group signals of the GlcNAcβ1 → 3Galβ1 → 3 element match those of the same element in **16**. The Gal^3 H-4 signal resonates at $\delta = 4.124$ ppm, indicating a 3-substituted Gal residue. The structural reporters of the GlcNAcβ1 → 6 unit are similar to those of the same unit in **7**.

The ^{1}H-NMR spectrum of **25** (Pierce-Cretel *et al.*, 1989; Van Halbeek *et al.*, 1982b) (Figure 25) demonstrates the occurrence of two NAc singlets,

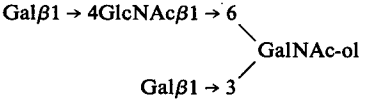

(25)

two doublets in the β-Gal H-1 region ($\delta = 4.465$ ppm, $J_{1,2} = 7.8$ Hz; $\delta = 4.470$ ppm, $J_{1,2} = 7.8$ Hz) and one in the β-GlcNAc H-1 region ($\delta = 4.560$ ppm, $J_{1,2} = 8.2$ Hz). The GalNAc-ol H-2, H-5, and H-6 signals resonate at $\delta = 4.394$, 4.282, and 3.931 ppm ($J_{5,6} = 6.5$ Hz), respectively. Comparison of the ^{1}H-NMR data of **25** and **7** indicates that the Gal^3 structural reporters do not change going from **7** to **25**, but downfield shifts are observed for GlcNAc^6 H-1 ($\delta = 4.560$ ppm; $\Delta\delta = +0.022$ ppm) and H-6 ($\delta = 3.998$ ppm;

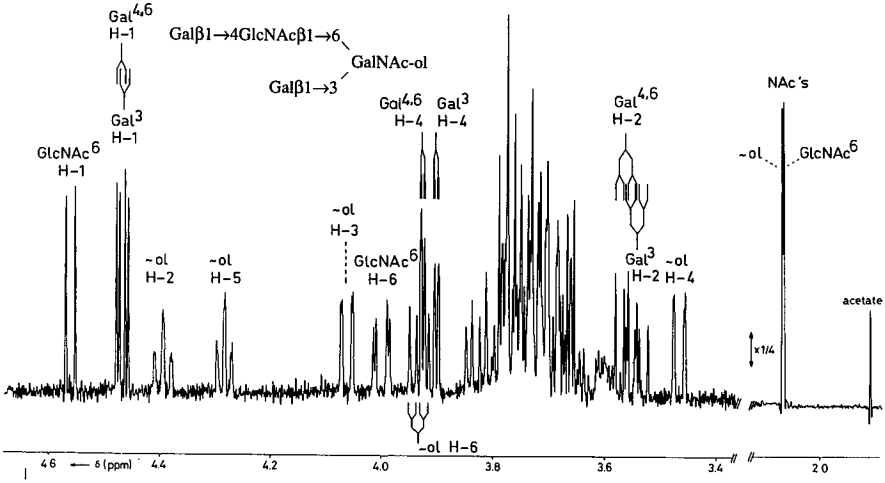

Figure 25. Resolution-enhanced ^{1}H-NMR spectrum of **25**. For comments, see Figure 2.

$\Delta\delta$ = +0.066 ppm). The latter chemical shifts and those of the Gal^{4,6} residue (H-1, δ = 4.470 ppm; H-4, δ = 3.925 ppm) fit well the presence of a terminal Galβ1 → 4GlcNAcβ1 → unit at C-6 of GalNAc-ol [compare for instance with the steps going from **5** to **19** (Table 5), and from **8** to **21**, **22**, or **23** (Table 6)]. It has to be noted that the assignment of the Gal H-1 doublets is based upon comparison with extensions of **25**, e.g., **41**. For additional

TABLE 8
Effect of Temperature on the Chemical Shifts[a] of 25 [Galβ1 → 4GlcNAcβ1 → 6(Galβ1 → 3)GalNAc-ol] (Dua *et al.*, 1985)

Residue	Reporter group	5 °C	25 °C	45 °C	60 °C	75 °C
GlcNAc^6	H-1	4.553	4.560	4.565	4.577	4.582
Gal^3	H-1	4.465	4.465	4.470	4.477	4.480
Gal^4	H-1	4.465	4.465	4.470	4.477	4.480
GalNAc-ol	H-2	4.411	4.393	4.380	4.375	4.367
	H-3	4.067	4.059	4.055	4.057	4.057
	H-4	3.448	3.468	3.492	3.500	3.510
	H-5	4.299	4.283	4.267	4.257	4.248
GlcNAc^6	H-1	4.010	4.000	4.000	4.000	4.000
	NAc	2.069	2.064	2.063	2.063	2.063

[a] δ values were obtained at 300 MHz.

references, see Breg *et al.* (1987), Capon *et al.* (1989), Dua *et al.* (1984, 1985), Fiat *et al.* (1988), Hanisch *et al.* (1989), Hounsell *et al.* (1985), Klein *et al.* (1988), Lamblin *et al.* (1984b), Strecker *et al.* (1987, 1989a), and Van Halbeek *et al.* (1981b, 1985b). As is evident from Table 8 (Dua *et al.*, 1985) a marked temperature dependence of many of the resonances of the tetrasaccharide-alditol occurs. The chemical shifts of H-2 and H-5 of GalNAc-ol move upfield with increasing temperature, while those of H-1 of β-Gal and β-GlcNAc and that of H-4 of GalNAc-ol move downfield (300-MHz ^{1}H-NMR data).

The ^{1}H-NMR spectrum of **26** (Klein *et al.*, 1988; Pierce-Cretel *et al.*, 1989; see also Hounsell *et al.*, 1989) (Figure 26) shows three NAc signals,

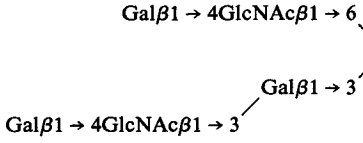

(26)

three doublets in the β-Gal anomeric region ($\delta = 4.481$ ppm; $\delta = 4.468$ ppm; $\delta = 4.449$ ppm), and two doublets in the β-GlcNAc anomeric region ($\delta = 4.684$ ppm; $\delta = 4.554$ ppm). The core type of the oligosaccharide-alditol is supported by the chemical shifts of GalNAc-ol H-2 at $\delta = 4.397$ ppm and H-5 at $\delta = 4.266$ ppm. The GlcNAc^6 residue is substituted by Gal in β1 → 4 linkage, as is evident from the chemical shifts of

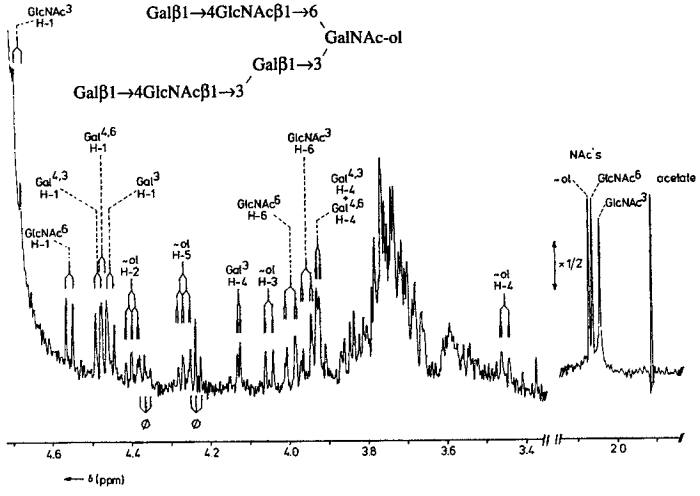

Figure 26. Resolution-enhanced ^{1}H-NMR spectrum of **26**. For comments, see Figures 2 and 12.

H-1 and H-6 of GlcNAc^6 (δ = 4.554 and 3.993 ppm, respectively), while the terminal position of Gal^{4,6} can be inferred from its H-1 signal at δ = 4.468 ppm and its H-4 signal at δ = 3.925 ppm (compare **26** with **25**, showing similar structural-reporter-group signals). The chemical shift of Gal^3 H-4 at δ = 4.125 ppm is characteristic for the →GlcNAcβ1 → 3Galβ1→ sequence, as was shown for compounds like **12** and **13** (Table 2). The structural reporters of Gal^{4,3} and GlcNAc^3 of the Galβ1 → 4GlcNAcβ1 → 3Galβ1 → 3 structural element match the ^{1}H-NMR data of this sequence in **12** (Table 2).

The ^{1}H-NMR spectrum of **27** (Mutsaers *et al.*, 1986; Pierce-Cretel *et al.*, 1989) (Figure 27) demonstrates the occurrence of three NAc singlets

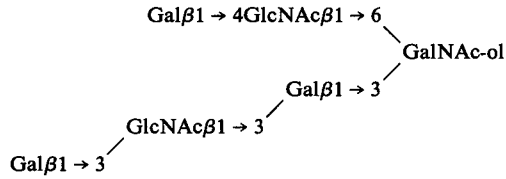

(27)

and five β-anomeric signals. Three of these signals resonate in the β-Gal region [δ = 4.472 ppm, $J_{1,2}$ = 8.0 Hz; δ = 4.453 ppm, $J_{1,2}$ = 8.0 Hz (two coinciding doublets)] and two in the β-GlcNAc region (δ = 4.700 ppm, $J_{1,2}$ = 8.4 Hz; δ = 4.556 ppm, $J_{1,2}$ = 8.4 Hz). Based on the chemical shifts for GalNAc-ol H-2 at δ = 4.406 ppm and H-5 at δ = 4.275 ppm, the GlcNAcβ1 → 6(Galβ1 → 3)GalNAc-ol core structure is assigned. As may become clear from a comparison of the ^{1}H-NMR data of the positional isomers **26** and **27**, a terminal Galβ1 → 4GlcNAcβ1 → unit at C-6 of GalNAc-ol is also present in **27** (see the specific GlcNAc^6 and Gal^{4,6}

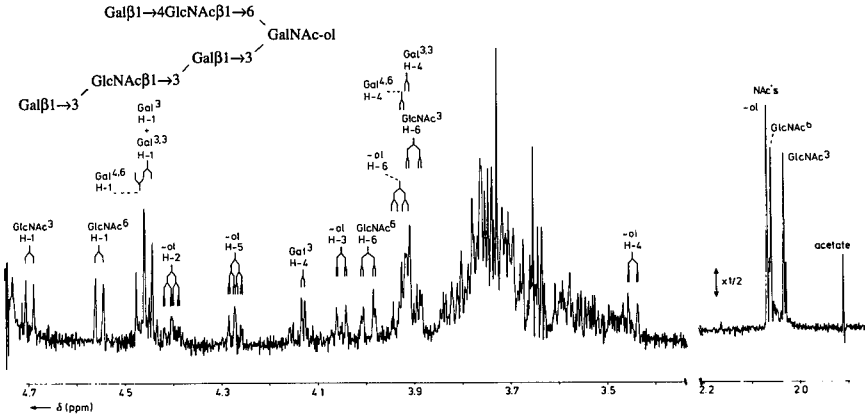

Figure 27. Resolution-enhanced ^{1}H-NMR spectrum of **27**. For comments, see Figure 2.

structural-reporter-group signals). Furthermore, the spectrum exhibits the typical changes in structural reporters when a Galβ1 → 4GlcNAcβ1 → 3Galβ1 → 3 structural element (see **26**) is replaced by a Galβ1 → 3GlcNAcβ1 → 3Galβ1 → 3 sequence [compare the step going from **12** (GlcNAc^3/Gal^{4,3}) to **13** (GlcNAc^3/Gal^{3,3}) (Table 2) with the step going from **26** to **27**]. (See also Hounsell *et al.*, 1989.)

The 400-MHz ^{1}H-NMR spectrum of **28** (Dua *et al.*, 1985; Pierce-Cretel *et al.*, 1989) shows three NAc resonances, three doublets in the β-Gal

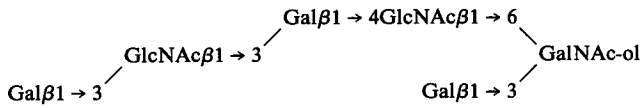

(28)

anomeric region (δ = 4.463 ppm; δ = 4.459 ppm; δ = 4.441 ppm), and two doublets in the β-GlcNAc anomeric region (δ = 4.740 ppm; δ = 4.555 ppm). The core element is indicated by the chemical shifts of GalNAc-ol H-2 at δ = 4.392 ppm and H-5 at δ = 4.277 ppm. Comparison of the Gal^3 H-1 structural-reporter group at δ = 4.463 ppm in **28** with those in **7** and **25** supports a terminal position for Gal^3. This means that a trisaccharide element is attached to GlcNAc^6. The structural reporters of the Galβ1 → 3GlcNAcβ1 → 3Galβ1 → 4 sequence are identical to those of the same element in **20** (Table 5). The H-4 signal of Gal^{4,6} at δ = 4.151 ppm indicates the additional GlcNAc^3 to be β1 → 3 linked to Gal^{4,6}. (See also Hounsell *et al.*, 1989.)

4. PERIPHERAL FUCOSE IN NEUTRAL OLIGOSACCHARIDE-ALDITOLS

4.1. Extensions of the Galβ1 → 3GalNAc-ol Core Structure

In this section, the ^{1}H-NMR data of the fucose-containing carbohydrates **29–33** will be presented, all having Galβ1 → 3GalNAc-ol as the core structure. The relevant ^{1}H-NMR parameters of **29–33** are found in Table 9. The Galβ1 → 3GalNAc-ol core type is characterized by the H-2 and H-5 signals of GalNAc-ol at δ = 4.38–4.40 and 4.14–4.20 ppm, respectively (see Section 11). The GalNAc-ol H-3 signal is detected at δ = 4.0–4.1 ppm. The NAc singlet of GalNAc-ol appears at δ = 2.045–2.049 ppm.

In Figure 28 the ^{1}H-NMR spectrum of **29** is presented (Van Halbeek *et al.*, 1982b). The occurrence of α-Fuc is evident from the following set

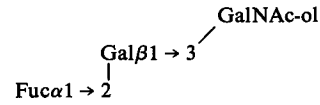

(29)

TABLE 9

^{1}H Chemical Shifts of Structural-Reporter Groups of Constituent Monosaccharides for Fucosylated Oligosaccharide-Alditols with the Galβ1 → 3GalNAc-ol Core Structure (29–33)

Residue	Reporter group	29 	30 	31 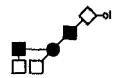	32 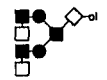	33 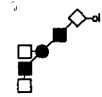
GalNAc-ol	H-2	4.399	4.397	4.396	4.386	4.400
	H-3	4.091	4.050	4.046	3.991	4.084
	H-4	3.522	3.495	3.496	3.509	n.d.
	H-5	4.163	4.183	4.177	4.142	4.179
	NAc	2.046	2.046	2.046	2.045	2.049
Gal^3	H-1	4.584	4.464	4.463	4.468	4.446
	H-4	3.926	4.127	4.111	4.104	4.142
GlcNAc^3	H-1	—	4.692	4.69	4.685	4.582
	H-6	—	3.966	3.992	n.d.[a]	n.d.
	NAc	—	2.032	2.035	2.043	2.068
GlcNAc^6	H-1	—	—	—	4.584	—
	NAc	—	—	—	2.055	—
Gal^{4,3}	H-1	—	4.461	4.510	4.550	—
	H-4	—	3.900	3.870	3.890	—
Gal^{3,3}	H-1	—	—	—	—	4.665
Gal^{4,6}	H-1	—	—	—	4.532	—
	H-4	—	—	—	3.888	—
Fuc^2	H-1	5.256	—	5.273	5.313/5.310	5.153
	H-5	4.279	—	4.248	4.221[b]	4.354
	CH_3	1.243	—	1.266	1.230[b]	1.276
Fuc^3	H-1	—	5.140	5.127	—	—
	H-5	—	4.833	4.873	—	—
	CH_3	—	1.177	1.236	—	—
Fuc^4	H-1	—	—	—	—	5.026
	H-5	—	—	—	—	4.880[c]
	CH_3	—	—	—	—	1.252

[a] n.d. means value could not be determined merely by inspection of the spectrum.
[b] Signal stemming from two Fuc residues.
[c] Spectrum recorded at 77 °C.

of structural-reporter groups: H-1, δ = 5.256 ppm ($J_{1,2}$ = 3.8 Hz); H-5, δ = 4.279 ppm; CH_3, δ = 1.243 ppm. Compared with Galβ1 → 3GalNAc-ol (**2**, Table 1), the presence of Fuc in α1 → 2 linkage to Gal^3 gives rise to downfield shifts for Gal^3 H-1 (δ = 4.584 ppm; $\Delta\delta$ = +0.106 ppm; $J_{1,2}$ = 7.8 Hz), H-2 (δ = 3.688 ppm; $\Delta\delta$ = +0.124 ppm), H-3 (δ = 3.880 ppm; $\Delta\delta$ = +0.209 ppm), and H-4 (δ = 3.926 ppm; $\Delta\delta$ = +0.025 ppm). In addition, the attachment of Fuc^2 causes shift increments for GalNAc-ol H-3 ($\Delta\delta$ = +0.026 ppm), H-4 ($\Delta\delta$ = +0.015 ppm), and H-5 ($\Delta\delta$ = −0.033 ppm). Other

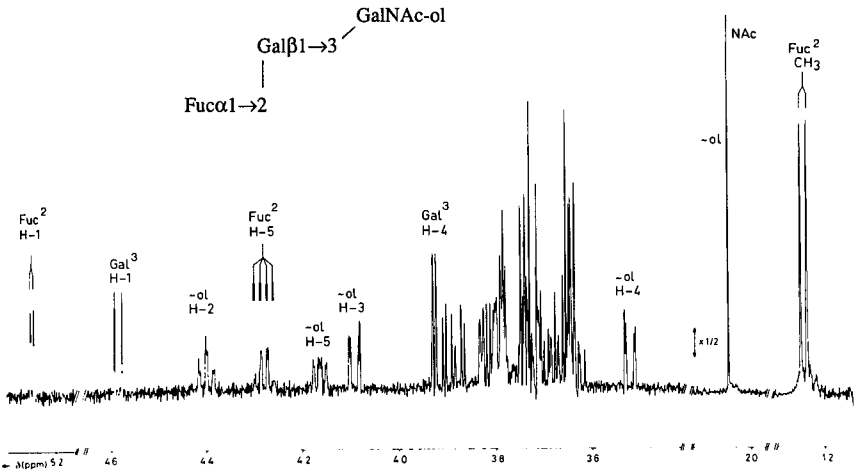

Figure 28. Resolution-enhanced ^{1}H-NMR spectrum of **29**. The relative-intensity scale of the *N*-acetyl methyl proton region of the spectrum differs from that of the other parts, as indicated.

reference data of this blood group H-containing substance can be found in Dua *et al.* (1984, 1986), Klein *et al.* (1988), Lamblin *et al.* (1984b), Rao *et al.* (1985), Van Halbeek *et al.* (1981a), and Vliegenthart *et al.* (1980). For a complete assignment of the 300-MHz ^{1}H-NMR spectrum and NOE experiments, see Rao *et al.* (1985).

The ^{1}H-NMR spectrum of **30** is depicted in Figure 29 (Klein *et al.*, 1988; Lamblin *et al.*, 1984b; Van Halbeek *et al.*, 1982b). Compound **30** is

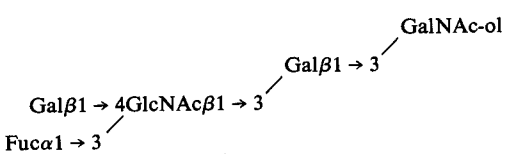

(30)

an extension of **12** (see Table 2) with Fuc in $\alpha 1 \rightarrow 3$ linkage to GlcNAc, representing the immuno group X determinant. The substitution of Gal^3 (H-1, $\delta = 4.464$ ppm) at C-3 is obvious from the chemical shift of the Gal^3 H-4 signal at $\delta = 4.127$ ppm, being characteristic for a $\rightarrow$GlcNAc$\beta 1 \rightarrow$ 3Gal$\beta 1\rightarrow$ sequence (Table 2). In comparison to **12**, the GlcNAc^3 NAc signal has undergone an upfield shift of $\Delta\delta = -0.010$ ppm. The chemical shift of GlcNAc^3 H-1 is hardly affected ($\Delta\delta = +0.004$ ppm), but the signal is relatively broad. The Gal^{4,3} H-1 resonance is shifted by $\Delta\delta = -0.019$ ppm. These effects are indicative of substitution of an *N*-acetyllactosamine unit at C-3 of the GlcNAc residue by α-Fuc (Vliegenthart *et al.*, 1983). The $\alpha 1 \rightarrow$

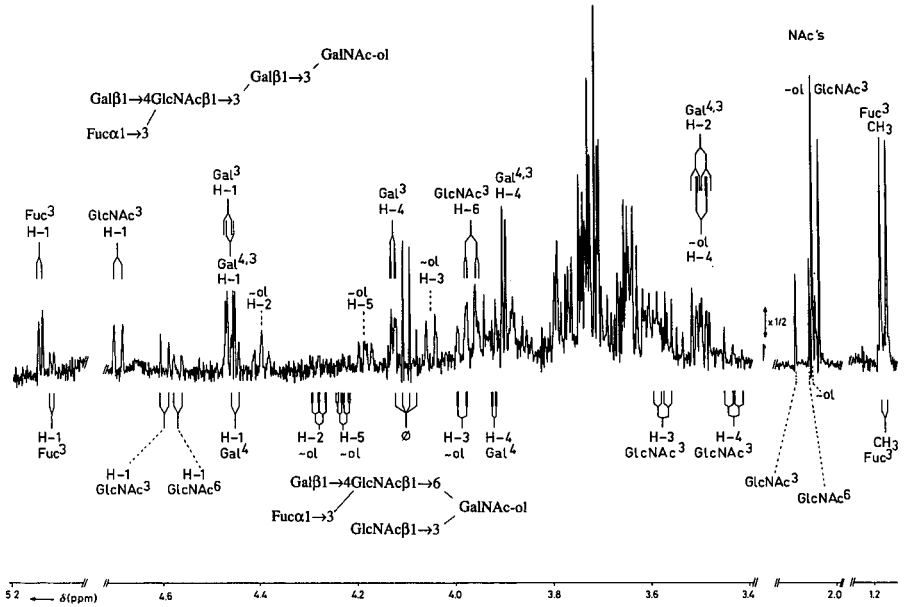

Figure 29. Resolution-enhanced ^{1}H-NMR spectrum of a mixture of **30** (upper) and **49** (lower). For comments, see Figure 28. The signal(s) marked by ϕ stem(s) from (a) frequently occurring, nonprotein noncarbohydrate contaminant(s).

3-linked Fuc residue is characterized by the following set of structural-reporter-group signals: H-1, δ = 5.140 ppm; H-5, δ = 4.833 ppm; CH_3, δ = 1.177 ppm (compare to Vliegenthart *et al.*, 1983). The chemical shift values of the Gal^{4,3} and GlcNAc^3 residues of **30** make clear that the presence of Fuc^3 at GlcNAc influences the specific structural-reporter groups reported for the discrimination between backbone type-1 and type-2 chains (see Table 3; compare to **13** and **12**).

In Figure 30 the ^{1}H-NMR spectrum of **31** is shown (Klein *et al.*, 1988). This compound is an elongation of **30**, having an additional α-Fuc residue,

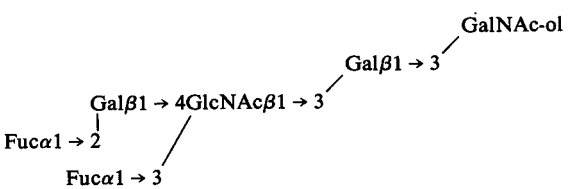

(31)

1 → 2 linked to Gal^{4,3}. The Gal^3 unit is substituted at C-3, as is evident from the chemical shift values of Gal^3 H-1 (δ = 4.463 ppm) and Gal^3 H-4 (δ = 4.111 ppm). One set of Fuc structural-reporter groups, i.e., H-1, H-5, and

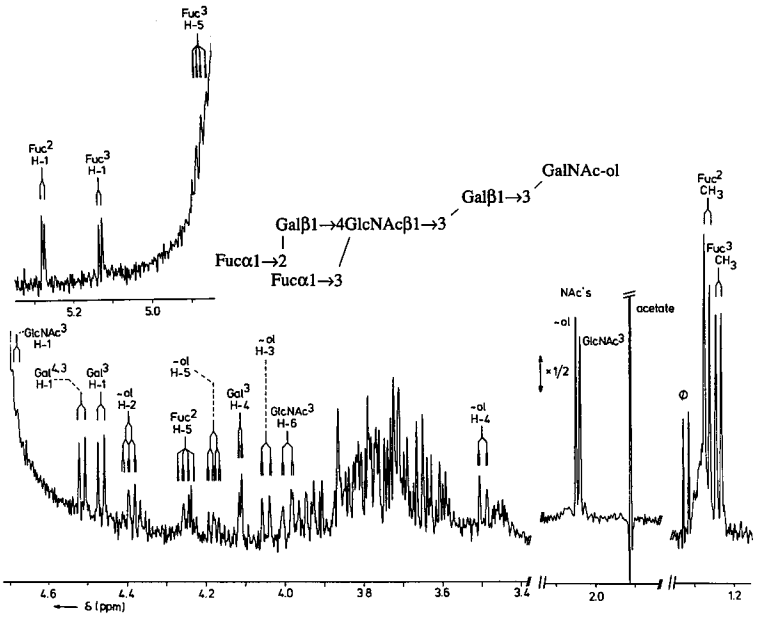

Figure 30. Resolution-enhanced ^{1}H-NMR spectrum of **31**. The relative-intensity scale of the *N*-acetyl methyl proton region of the spectrum differs from that of the other parts, as indicated. Contaminating acetate gives rise to a signal at $\delta = 1.908$ ppm. The signal(s) marked by ϕ stem(s) from (a) frequently occurring, nonprotein noncarbohydrate contaminant(s).

TABLE 10
^{1}H Chemical Shift Differences for Pertinent Reporter Groups, Comparing Blood Group H and X to the Y Determinant Sequence

Residue	Reporter group	Chemical shift differences for H → Y **34 → 36**	Chemical shift differences for X → Y **35 → 36**
Gal	H-1	−0.043	+0.050
	H-4	−0.030	−0.033
GlcNAc	H-1	+0.018	−0.016
	H-6	+0.036	+0.012
	NAc	−0.011	+0.002
Fuc^2	H-1	−0.032	—
	H-5	+0.033	—
	CH_3	+0.040	—
Fuc^3	H-1	—	−0.018
	H-5	—	+0.053
	CH_3	—	+0.061

CH_3 at $\delta = 5.273$, 4.248, and 1.266 ppm, respectively, indicates Fuc in an $\alpha 1 \rightarrow 2$ linkage to $Gal^{4,3}$. The other set, i.e., H-1, H-5, and CH_3 at $\delta = 5.127$, 4.873, and 1.236 ppm, respectively, points to Fuc in an $\alpha 1 \rightarrow 3$ type of linkage. The assignment of the CH_3 signals of Fuc^2 and Fuc^3 has been verified by irradiation of Fuc^2 H-5 at $\delta = 4.248$ ppm. The exact positions of both Fuc sets, together with the $Gal^{4,3}$ H-1 signal at $\delta = 4.510$ ppm, correspond to the data indicating the immuno group Y determinant, being the Fucα1 → 2Galβ1 → 4(Fucα1 → 3)GlcNAcβ1 → structural element (compare Hindsgaul *et al.*, 1982; Van Halbeek *et al.*, 1985a, in *N*-linked carbohydrate chains). To generalize some effects of fucosylation of the *N*-acetyllactosamine element, a survey of ^{1}H chemical shift differences for pertinent reporter groups comparing blood group H and X to the Y determinant sequence is presented in Table 10.

The ^{1}H-NMR spectrum of **32**, presented in Figure 31 (Van Halbeek *et al.*, 1982c; see also Van Kuik *et al.*, 1991), reveals the characteristics for a

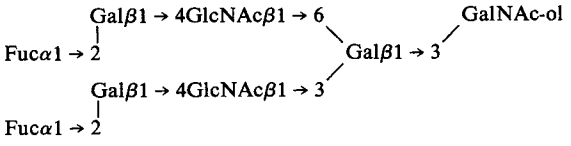

(32)

Gal^3 branching point. In this case the Gal^3 H-4 signal serves as the reporter group for the 3,6-disubstitution of Gal^3. As was shown earlier (see for

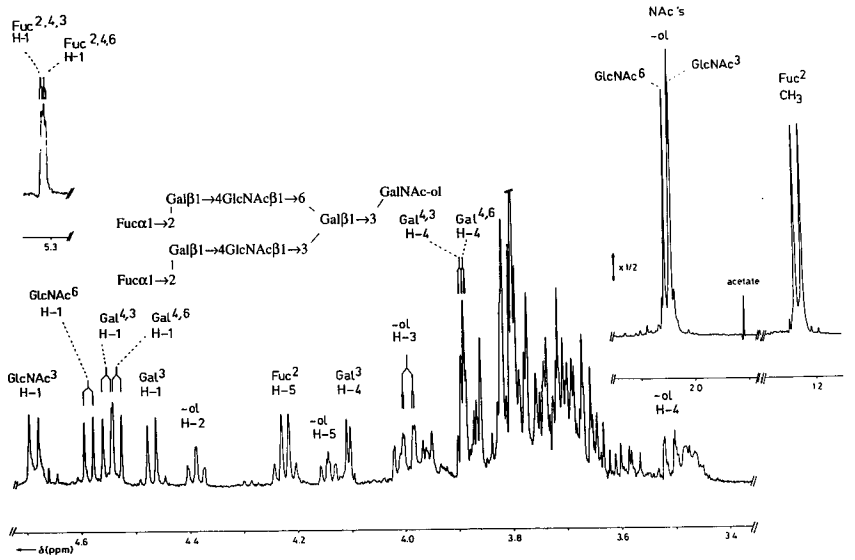

Figure 31. Resolution-enhanced ^{1}H-NMR spectrum of **32**. For comments, see Figure 30.

instance **12** and **13**, Table 2), the H-4 signal is the reporter group for $\beta 1 \rightarrow 3$ substitution of Gal by GlcNAc. Assuming independency of the influences of attachment of the $\beta 1 \rightarrow 3$- and $\beta 1 \rightarrow 6$-linked *N*-acetyllactosamine elements on the chemical shifts of the Gal[3] reporter groups, it may be concluded from a comparison of **32** with **12** that the introduction of the $\beta 1 \rightarrow 6$ branch causes an additional shift alteration for Gal[3] H-4 ($\Delta\delta = -0.022$ ppm). Moreover, the presence of the $\beta 1 \rightarrow 6$-linked *N*-acetyllactosamine unit causes considerable shift effects on some GalNAc-ol signals, e.g., on H-3 ($\Delta\delta = -0.060$ ppm) and on H-5 ($\Delta\delta = -0.042$ ppm). A similar trend of shift increments is observed going from **13** to **15** (Table 2). The GlcNAc[3] H-1 signal is observed at $\delta = 4.685$ ppm ($J_{1,2} = 8.5$ Hz; see **12**: $\delta = 4.688$ ppm), whereas that of GlcNAc[6] at $\delta = 4.584$ ppm ($J_{1,2} = 8.3$ Hz; see **15**: $\delta = 4.607$ ppm). The remaining two doublets at $\delta = 4.550$ ppm and $\delta = 4.532$ ppm ($J_{1,2} = 7.8$ Hz) in the β-anomeric region of the spectrum belong to the Gal[4] residues. The signal at $\delta = 4.550$ ppm is assigned to Gal[4,3] H-1 because of its shift increment coming from **12** ($\Delta\delta \approx +0.07$ ppm), which is typical of substitution of a Gal[4,3] by an $\alpha 1 \rightarrow 2$-linked Fuc residue. Consequently, the signal at $\delta = 4.532$ ppm is attributed to Gal[4,6]. Finally, the set of chemical shifts for the Fuc structural-reporter groups (H-1, $\delta = 5.313/5.310$ ppm; H-5, $\delta = 4.221$ ppm; CH_3, $\delta = 1.230$ ppm) is indicative of the Fuc$\alpha 1 \rightarrow$ 2Gal$\beta 1 \rightarrow$ 4GlcNAc$\beta 1 \rightarrow$ element. For ^{1}H-NMR data of the related compounds GlcNAc$\beta 1 \rightarrow$ 6(GlcNAc$\beta 1 \rightarrow$ 3)Gal, Gal$\beta 1 \rightarrow$ 4GlcNAc$\beta 1 \rightarrow$ 6(GlcNAc$\beta 1 \rightarrow$ 3)Gal, and Gal$\beta 1 \rightarrow$ 4GlcNAc$\beta 1 \rightarrow$ 6(Gal$\beta 1 \rightarrow$ 4GlcNAc$\beta 1 \rightarrow$ 3)Gal, see Van Halbeek *et al.* (1982c).

The oligosaccharide-alditol **33** gives rise to a very characteristic ^{1}H-NMR spectrum (300 MHz), as reported by Dua *et al.* (1984). Of the anomeric

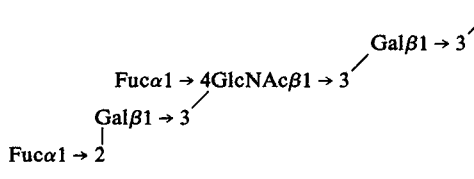

(33)

protons, the assignment of the Gal[3] H-1 signal at $\delta = 4.446$ ppm is supported by the NOE effect between Gal[3] H-1 and GalNAc-ol H-3. The signal at $\delta = 4.142$ ppm corresponds with Gal[3] H-4, indicating a 3-substituted Gal[3] residue. The two sets of Fuc structural-reporter groups have been established by comparison of these sets with those observed for the milk oligosaccharide lacto-*N*-difucohexaose I with the blood group Le[b] determinant (Breg *et al.*, 1988a; Dua and Bush, 1983). The Fuc$\alpha 1 \rightarrow$ 2Gal$\beta 1 \rightarrow$ element is reflected by the following Fuc reporters: H-1, $\delta = 5.153$ ppm; H-5, $\delta = 4.354$ ppm; CH_3, $\delta = 1.276$ ppm. For the Fuc$\alpha 1 \rightarrow$ 4GlcNAc$\beta 1 \rightarrow$ element the reporters are: H-1, $\delta = 5.026$ ppm; H-5, $\delta = 4.880$ ppm (77 °C); CH_3, $\delta = 1.252$ ppm.

It has to be noted that in view of the chemical shift values of the NAc signals of GalNAc-ol in **29–32**, the assignments of the NAc singlets of GalNAc-ol and GlcNAc[3] for **33** have been interchanged with respect to the original proposal by Dua *et al.* (1984).

4.2. Extensions of the GlcNAcβ1 → 3GalNAc-ol Core Structure

In this section, the ^{1}H-NMR data of the fucose-containing saccharides **34–37** will be presented, all having GlcNAcβ1 → 3GalNAc-ol as the core structure. The relevant ^{1}H-NMR parameters of these compounds have been summarized in Table 11. The GlcNAcβ1 → 3GalNAc-ol core type is characterized by the H-2 and H-5 signals of GalNAc-ol at δ = 4.27–4.29 and 4.11–4.14 ppm, respectively (see Section 11). The GalNAc-ol NAc signal resonates at δ = 2.030–2.037 ppm. The precise chemical shifts of these

TABLE 11

^{1}H Chemical Shifts of Structural-Reporter Groups of Constituent Monosaccharides for Fucosylated Oligosaccharide-Alditols with the GlcNAcβ1 → 3GalNAc-ol Core Structure (34–37)

Residue	Reporter group	**34** 	**35**[a] 	**36** 	**37** 
GalNAc-ol	H-2	4.282	4.272	4.266	4.267
	H-3	3.989	3.996	3.986	3.982
	H-4	3.542	3.564	n.d.[b]	3.587
	H-5	4.143	4.126	4.128	4.115
	NAc	2.037	2.031	2.030	2.036
GlcNAc[3]	H-1	4.609	4.643	4.627	4.656
	H-3	n.d.	n.d.	n.d.	4.017
	H-6	4.010	4.034	4.046	3.952
	NAc	2.086	2.073	2.075	2.113
Gal[3]	H-1	—	—	—	4.580
	H-4	—	—	—	3.891
Gal[4]	H-1	4.523	4.430	4.480	—
	H-4	3.894	3.897	3.864	—
Fuc[2]	H-1	5.310	—	5.278	5.210
	H-5	4.219	—	4.252	4.270
	CH_3	1.234	—	1.274	1.231
Fuc[3]	H-1	—	5.140	5.122	—
	H-5	—	4.813	4.866	—
	CH_3	—	1.177	1.238	—

[a] Spectrum recorded at 22 °C.
[b] n.d. means value could not be determined merely by inspection of the spectrum.

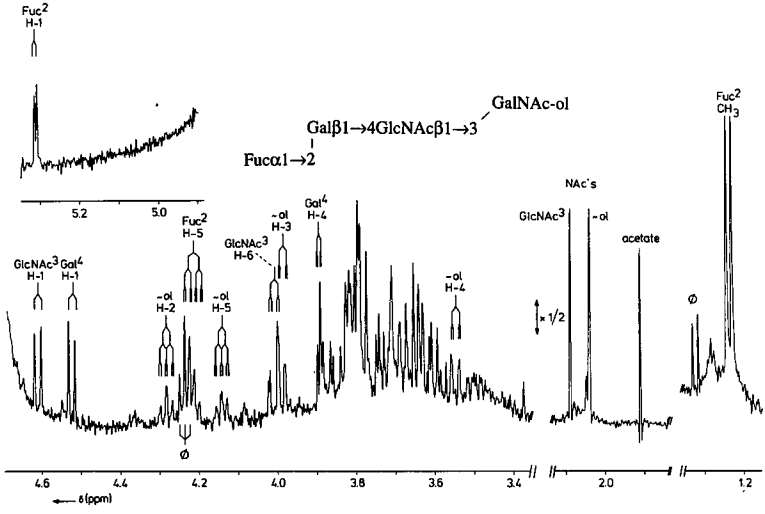

Figure 32. Resolution-enhanced ^{1}H-NMR spectrum of **34**. For comments, see Figure 30.

structural reporters as well as those of GlcNAc^3 are dependent on substitutions in GlcNAc^3.

The ^{1}H-NMR spectrum of the $\alpha 1 \rightarrow 2$ fucosylated form of **17**, namely **34**, is depicted in Figure 32 (Breg *et al.*, 1988b). The presence of

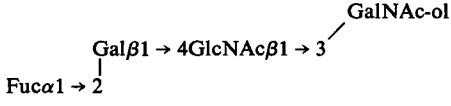

(34)

Fuc $\alpha 1 \rightarrow 2$ linked to Gal in an *N*-acetyllactosamine element is represented by the following set of Fuc structural-reporter-group signals: H-1, δ = 5.310 ppm; H-5, δ = 4.219 ppm; CH_3, δ = 1.234 ppm. The same set of Fuc reporters is observed for the blood group H structural element in **32** (Table 9). As compared to **17**, the attachment of α-Fuc to C-2 of Gal^4 leads to a number of shifts for structural-reporter groups of the Gal$\beta 1 \rightarrow$ 4GlcNAc$\beta 1 \rightarrow$ element. For the GlcNAc^3 H-1 signal an upfield shift of $\Delta\delta = -0.022$ ppm is observed. Furthermore, a downfield shift of $\Delta\delta$ = +0.068 ppm for Gal^4 H-1 and an upfield shift of $\Delta\delta = -0.032$ ppm for Gal^4 H-4 are detected.

In Figure 33 the ^{1}H-NMR spectrum of another monofucosylated form of **17**. namely, **35** (Lamblin *et al.*, 1984a), is presented. The attachment of

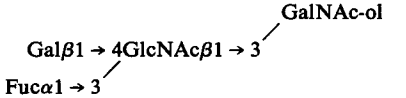

(35)

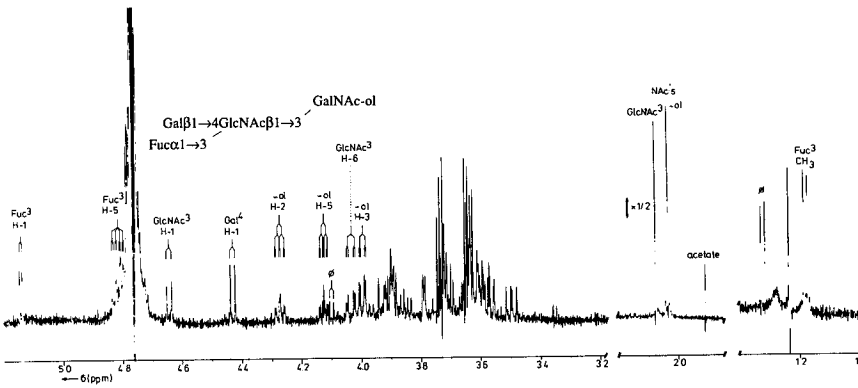

Figure 33. Resolution-enhanced ^{1}H-NMR spectrum of **35** at 22 °C. For comments, see Figure 30.

α-Fuc to GlcNAc^3 C-3 being part of an *N*-acetyllactosamine unit gives rise to the following set of Fuc structural-reporter groups: H-1, δ = 5.140 ppm; H-5, δ = 4.813 ppm; CH_3, δ = 1.177 ppm, similar to that of the immuno group X determinant as found in the spectrum of **30** (Table 9). Also the effects of introduction of the Fucα1 → 3 residue into **17**, namely, the upfield shift of Gal^4 H-1 from δ = 4.455 ppm to δ = 4.430 ppm ($\Delta\delta$ = −0.025 ppm), and in particular the upfield shift of the GlcNAc^3 NAc singlet from δ = 2.083 ppm to δ = 2.073 ppm ($\Delta\delta$ = −0.010 ppm), corroborate the α1 → 3 type of linkage of Fuc to GlcNAc that forms part of an *N*-acetyllactosamine element (Vliegenthart *et al.*, 1983; see also **30**). Finally, the attachment of Fuc^3 to the core GlcNAc^3 residue causes upfield shifts for GalNAc-ol H-2 ($\Delta\delta$ = −0.018 ppm), H-3 ($\Delta\delta$ = −0.006 ppm), H-5 ($\Delta\delta$ = −0.017 ppm), and NAc ($\Delta\delta$ = −0.007 ppm).

The ^{1}H-NMR spectrum of the difucosylated form of **17**, namely, **36**, is shown in Figure 34 (Breg *et al.*, 1988b). The total set of structural-reporter

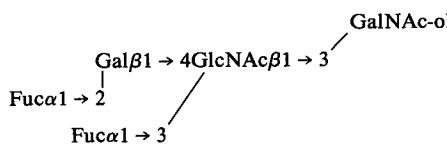

(36)

groups of the two Fuc residues, i.e., H-1, H-5, and CH_3 for each residue (Fuc^2: δ = 5.278 ppm/4.252 ppm/1.274 ppm; Fuc^3: δ = 5.122 ppm/4.866 ppm/1.238 ppm), is indicative of the presence of the immuno group Y determinant. A similar set has been discussed for **31** (Table 9). Comparison of the structural-reporter groups of **34**, **35**, and **36** demonstrates a series of typical shift increments, as summarized in Table 10.

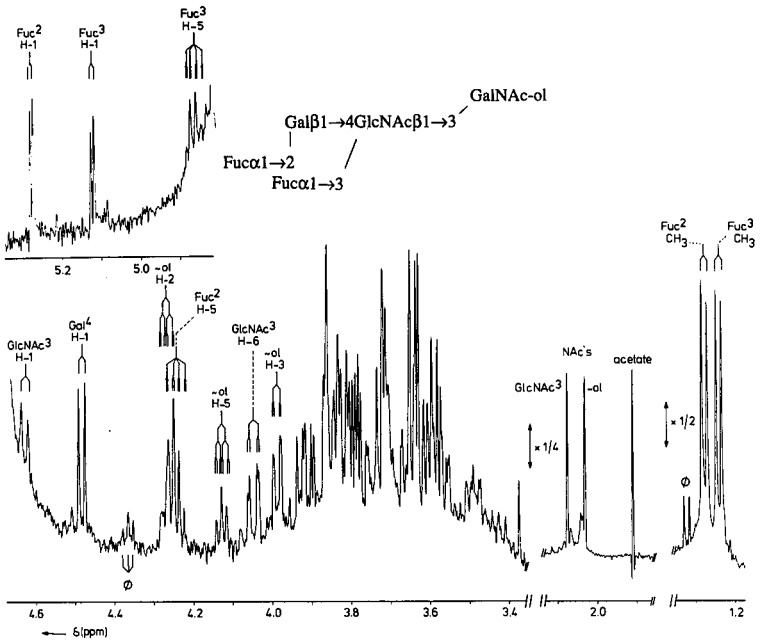

Figure 34. Resolution-enhanced ^{1}H-NMR spectrum of **36**. The relative-intensity scale of the *N*-acetyl and Fuc methyl proton regions of the spectrum differ from that of the other parts, as indicated. Contaminating acetate gives rise to a signal at $\delta = 1.908$ ppm. The signal(s) marked by ϕ stem(s) from (a) frequently occurring, nonprotein noncarbohydrate contaminant(s).

In Figure 35 the ^{1}H-NMR spectrum of **37** is depicted (Breg *et al.*, 1988b; Dua *et al.*, 1984; Lamblin *et al.*, 1984b; Rao *et al.*, 1985; Van Halbeek

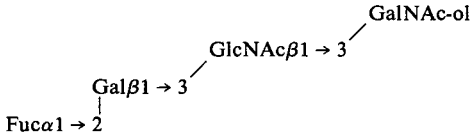

(37)

et al., 1982b). This structure is an $\alpha 1 \rightarrow 2$ fucosylated form of **18** (Table 4). The GlcNAc^3 H-3 signal at $\delta = 4.017$ ppm ($J_{2,3} = 10.4$ Hz; $J_{3,4} = 8.5$ Hz), resonating outside the bulk of skeleton protons, is indicative of β-substitution of GlcNAc^3 at C-3 (even more downfield than reported for **18**). The occurrence of the Fuc$\alpha 1 \rightarrow$ 2Gal$\beta 1 \rightarrow$ 3GlcNAc$\beta 1 \rightarrow$ element as an extension of **18**, is supported by the set of Fuc structural-reporter groups: H-1, $\delta = 5.210$ ppm, $J_{1,2} = 4.2$ Hz; H-5, $\delta = 4.270$ ppm; CH_3, $\delta = 1.231$ ppm. The shift effects of Fuc attachment upon the Gal^3 reporter

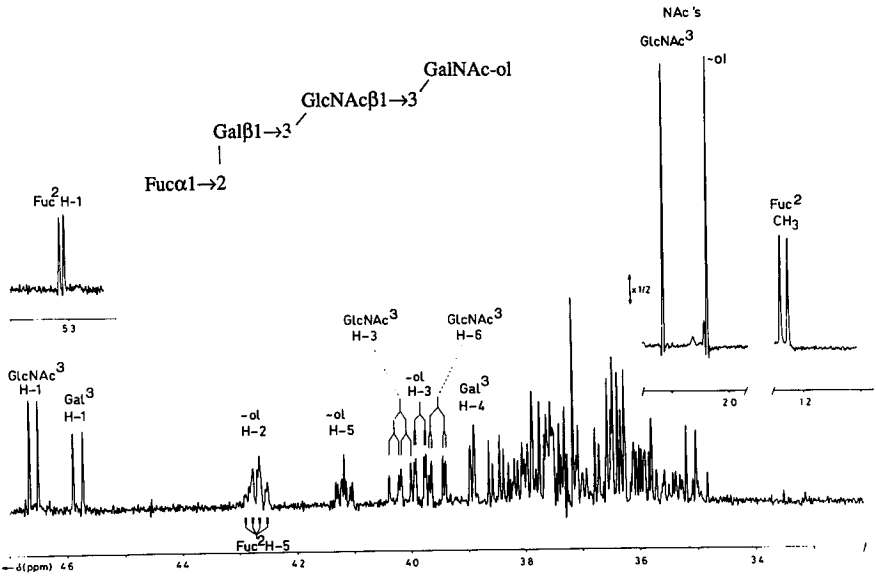

Figure 35. Resolution-enhanced ^{1}H-NMR spectrum of **37**. For comments, see Figure 30.

groups, namely, Gal^3 H-1 and H-4 ($\Delta\delta$ = +0.119 and −0.028 ppm, respectively, in comparison to **18**), corroborate the $\alpha 1 \rightarrow 2$ type of linkage. Going from **18** to **37**, also a large downfield shift for GlcNAc^3 NAc is observed ($\Delta\delta$ = +0.040 ppm). In this respect it is worthwhile to mention that $\alpha 1 \rightarrow 2$ fucosylation of Gal$\beta 1 \rightarrow$ 4GlcNAc$\beta 1 \rightarrow$ 3GalNAc-ol (step **17** to **34**) gives for GlcNAc^3 NAc only rise to a downfield shift of $\Delta\delta$ = +0.003 ppm. Complete assignment of the 300-MHz ^{1}H-NMR spectrum of **37** and NOE experiments have been reported by Rao *et al.* (1985).

4.3. Extensions of the GlcNAc$\beta 1 \rightarrow$ 6(Gal$\beta 1 \rightarrow$ 3)GalNAc-ol Core Structure

In this section the ^{1}H-NMR data are summarized of the fucose-containing saccharides **38–47**, all having GlcNAc$\beta 1 \rightarrow$ 6(Gal$\beta 1 \rightarrow$ 3)GalNAc-ol as the core structure. The relevant ^{1}H-NMR parameters of these carbohydrates are summarized in Table 12. The establishment of compounds with the GlcNAc$\beta 1 \rightarrow$ 6(Gal$\beta 1 \rightarrow$ 3)GalNAc-ol core type element is based on the H-2 signal of GalNAc-ol at δ = 4.38–4.41 ppm, together with the GalNAc-ol H-3 and H-5 signals at δ = 4.0–4.1 and 4.22–4.29 ppm, respectively (see Section 11).

The ^{1}H-NMR spectrum of the $\alpha 1 \rightarrow 2$ fucosylated form of **7**, namely, **38**, is presented in Figure 36 (Dua *et al.*, 1984; Klein *et al.*, 1988; Rao *et*

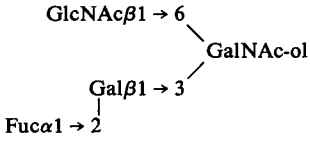

(38)

al., 1985). A comparison of the ^{1}H-NMR data of both compounds reveals that the introduction of the Fuc$\alpha 1 \rightarrow 2$ residue at Gal^3 causes a number of shift effects. Significant shifts are observed for several GalNAc-ol protons (H-3, $\Delta\delta = +0.024$ ppm; H-4, $\Delta\delta = +0.033$ ppm; H-5, $\Delta\delta = -0.045$ ppm; NAc, $\Delta\delta = -0.012$ ppm). Especially, the GalNAc-ol NAc signal at $\delta = 2.054$ ppm seems to be a specific reporter for the Fuc$\alpha 1 \rightarrow 2$Gal$\beta 1 \rightarrow 3$(GlcNAc$\beta 1 \rightarrow 6$)GalNAc-ol structure, even when it occurs as structural element in more complex carbohydrate chains (see **39** and **42–44**). The effects of the Fuc attachment on the chemical shifts of the anomeric protons of Gal^3 ($\Delta\delta = +0.104$ ppm) and GlcNAc^6($\Delta\delta = +0.013$ ppm) are analogous to the shift effects observed for the corresponding protons, when comparing **2** and **29**, **25** and **39**, and **40** and **42**, respectively. The assignment of the NAc signals has been achieved by comparison of the chemical shifts of the NAc signals of **38** and **39**: extension of the upper branch by Gal in $\beta 1 \rightarrow 4$ linkage induces a small upfield shift for GlcNAc^6 NAc (Vliegenthart *et al.*, 1983) and a minor downfield shift for the GalNAc-ol NAc signal. Finally, the $\alpha 1 \rightarrow 2$-linked Fuc to Gal^3 comes to expression in the typical set of chemical shifts of Fuc, i.e., H-1 ($\delta = 5.221$ ppm), H-5 ($\delta = 4.274$ ppm), and CH_3 ($\delta = 1.244$ ppm). For a complete interpretation of the 300-MHz ^{1}H-NMR spectrum, see Rao *et al.* (1985).

The oligosaccharide-alditols **39–44** are all fucosylated analogs of **25** (Table 7). The relevant ^{1}H-NMR data of **39** (Capon *et al.*, 1989; Dua *et al.*,

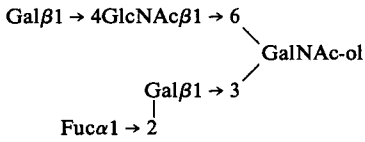

(39)

1984; Klein *et al.*, 1988; Lamblin *et al.*, 1984b; Pierce-Cretel *et al.*, 1989; Rao *et al.*, 1985) (see Figure 37), **40** (Dua *et al.*, 1984; Klein *et al.*, 1988; Korrel *et al.*, 1985; Lamblin *et al.*, 1984b; Rao *et al.*, 1985) (see Figure 38),

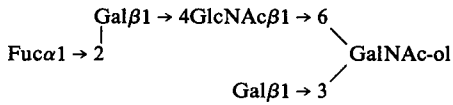

(40)

TABLE 12

^{1}H Chemical Shifts of Structural-Reporter Groups of Constituent Monosaccharides for Fucosylated Oligosaccharide-Alditols with the GlcNAcβ1 → 6(Galβ1 → 3)GalNAc-ol Core Structure (38–47)

Residue	Reporter group	38 	25 	39[a] 	40[a] 	41 	42[a] 	43 	44 	45 	46 	47 
GalNAc-ol	H-2	4.401	4.394	4.405	4.398	4.393	4.400	4.401	4.401	4.395	4.397	4.392
	H-3	4.085	4.060	4.085	4.060	4.060	4.083	4.085	4.081	n.d.	4.048	3.993
	H-4	3.501[b]	3.465	3.499	3.464	3.454	3.496	n.d.[d]	3.486	n.d.	3.452	3.472
	H-5	4.236[b]	4.282	4.256[c]	4.287	4.270	4.260	n.d.	4.249[e]	4.285	4.266	4.219
	NAc	2.054	2.067	2.055	2.066	2.067	2.053	2.055	2.054	2.066	2.066	2.046
Gal[3]	H-1	4.572	4.465	4.573	4.463	4.463	4.576	4.575	4.570	4.470	4.447	4.457
	H-4	3.924[b]	3.900	3.923	3.900	3.899	3.924	3.923	3.921	n.d.	4.126	4.103
GlcNAc[6]	H-1	4.551	4.560	4.570	4.535	4.560	4.554	4.569	4.563	4.560	4.554	4.526
	H-6	3.937[b]	3.998	3.998[c]	3.99	4.010	3.999	4.010	4.030	n.d.	3.995	3.931
	NAc	2.057	2.064	2.055	2.066	2.056	2.058	2.047	2.049	2.066	2.059	2.066
Gal[4,6]	H-1	—	4.470	4.469	4.536	4.448	4.537	4.448	4.497	4.484	4.466	4.529
	H-4	—	3.925	3.923	n.d.	3.927	3.924	3.92	n.d.	4.154	3.925	3.888
GlcNAc[3]	H-1	—	—	—	—	—	—	—	—	4.70	4.69	4.681
	H-6	—	—	—	—	—	—	—	—	n.d.	3.966	n.d.
	NAc	—	—	—	—	—	—	—	—	2.036	2.029	2.041

$Gal^{4,3}$	H-1	—	—	—	—	—	—	—	—	—	4.464	4.551
	H-4	—	—	—	—	—	—	—	—	—	3.900	3.892
$GlcNAc^{6,3}$	H-1	—	—	—	—	—	—	—	—	—	—	4.577
	NAc	—	—	—	—	—	—	—	—	—	—	2.051
$Gal^{3,3}$	H-1	—	—	—	—	—	—	—	—	4.470	—	—
$Fuc^{2,3}$	H-1	5.221	—	5.221	—	—	5.216	5.218	5.217	—	—	—
	H-5	4.274[b]	—	4.278	—	—	4.274	4.273	4.273	—	—	—
	CH_3	1.244	—	1.244	—	—	1.244	1.233	1.244	—	—	—
$Fuc^{2,4}$	H-1	—	—	—	5.309	—	5.306	—	5.279	—	—	5.311[g]
	H-5	—	—	—	4.227	—	4.226	—	4.242	—	—	4.225[g]
	CH_3	—	—	—	1.233	—	1.229	—	1.271	—	—	1.232[g]
Fuc^{3}	H-1	—	—	—	—	5.109	—	5.112	5.100	—	5.138	—
	H-5	—	—	—	—	4.835	—	n.d.	4.871	—	n.d.	—
	CH_3	—	—	—	—	1.174	—	1.175	1.235	—	1.176	—
Fuc^{4}	H-1	—	—	—	—	—	—	—	—	5.030	—	—
	H-5	—	—	—	—	—	—	—	—	4.782[f]	—	—
	CH_3	—	—	—	—	—	—	—	—	1.183	—	—

[a] Spectrum recorded at 22 °C.
[b] 300-MHz ^{1}H-NMR data at 24 °C from Dua *et al.* (1984) and Rao *et al.* (1985): GalNAc-ol H-4, $\delta = 3.482$ ppm; GalNAc-ol H-5, $\delta = 4.285/4.257$ ppm; Gal^3 H-4, $\delta = 3.915$ ppm; $GlcNAc^6$ H-6, $\delta = 3.900$ ppm; $Fuc^{2,3}$ H-5, $\delta = 4.263$ ppm.
[c] 300-MHz ^{1}H-NMR data at 24 °C from Rao *et al.* (1985): GalNAc-ol H-5, $\delta = 4.284$ ppm; $GlcNAc^6$ H-6, $\delta = 3.978$ ppm.
[d] n.d. means value could not be determined merely by inspection of the spectrum.
[e] 300-MHz ^{1}H-NMR data at 24 °C from Dua *et al.* (1984): GalNAc-ol H-5, $\delta = 4.286$ ppm.
[f] Spectrum recorded at 75 °C.
[g] Derived from two Fuc residues.

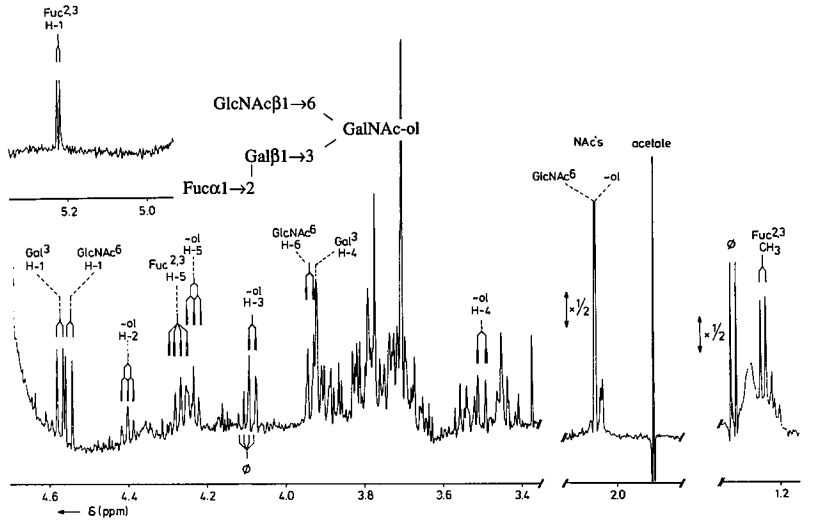

Figure 36. Resolution-enhanced ^{1}H-NMR spectrum of **38**. For comments, see Figure 34.

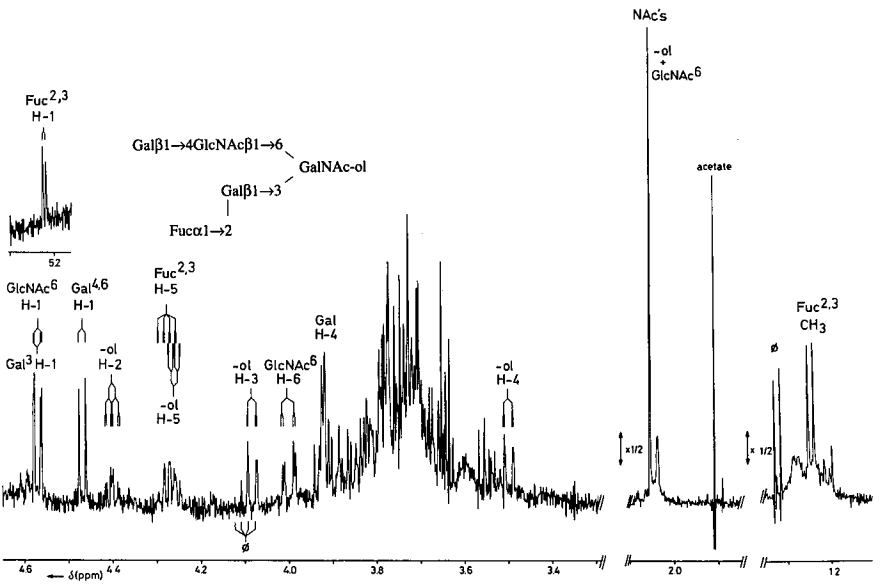

Figure 37. Resolution-enhanced ^{1}H-NMR spectrum of **39** at 22 °C. For comments, see Figure 34.

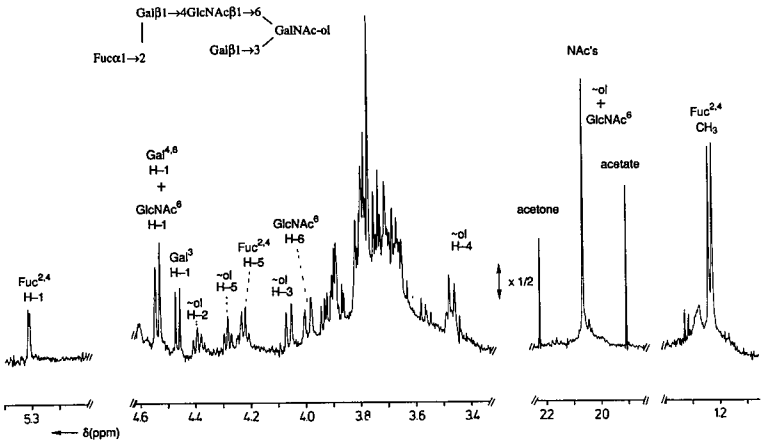

Figure 38. Resolution-enhanced ^{1}H-NMR spectrum of **40** at 22 °C. For comments, see Figure 30.

41 (Fiat *et al.*, 1988; Klein *et al.*, 1988; Lamblin *et al.*, 1984b; Van Halbeek *et al.*, 1982b) (see Figure 39), **42** (Dua *et al.*, 1984; Klein *et al.*, 1988; Lamblin *et al.*, 1984b; Rao *et al.*, 1985) (see Figure 40), **43** (Klein *et al.*, 1988), and **44** (Dua *et al.*, 1984; Klein *et al.*, 1988) (see Figure 41) are presented in Table 12. For reference purposes the structural-reporter groups of **25** have

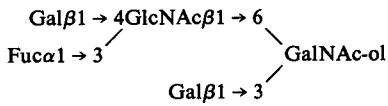

(41)

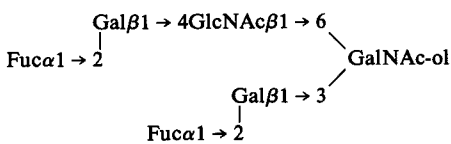

(42)

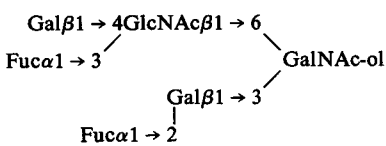

(43)

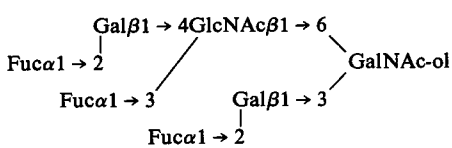

(44)

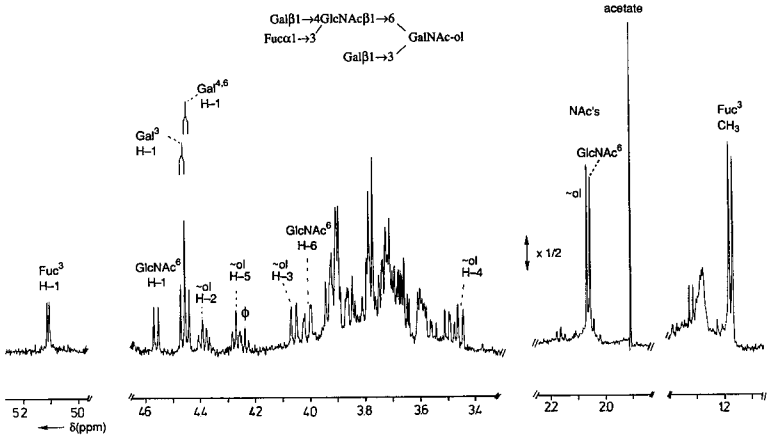

Figure 39. Resolution-enhanced ^{1}H-NMR spectrum of **41**. For comments, see Figure 30.

been included. From a comparison of the ^{1}H-NMR data of **39–44**, it is clear that each compound gives rise to a highly characteristic ^{1}H-NMR spectrum. The three positions for attachment of Fuc to **25** are correlated with the following typical sets of Fuc structural-reporter groups. For Fucα1 → 2Galβ1 → 3GalNAc-ol (Fuc^{2,3}): H-1, δ = 5.21–5.22 ppm; H-5, δ = 4.27–4.28 ppm; CH_3, δ = 1.23–1.24 ppm (see also **38**). For Fucα1 → 2Galβ1 →

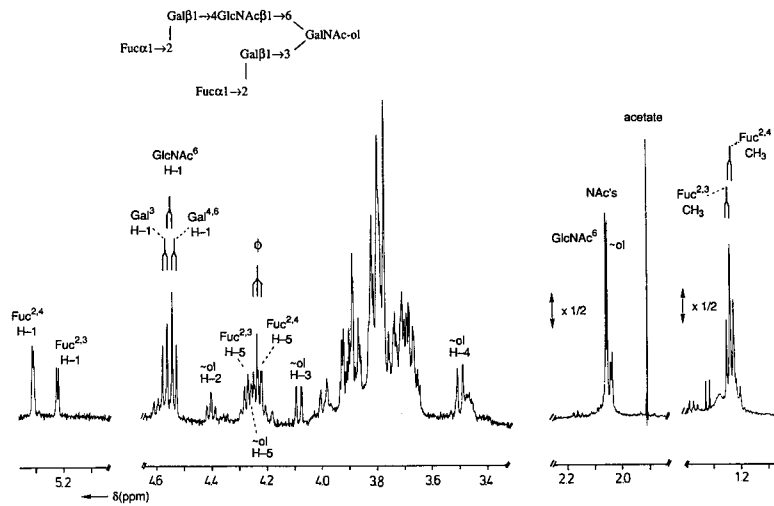

Figure 40. Resolution-enhanced ^{1}H-NMR spectrum of **42** at 22 °C. For comments, see Figure 34.

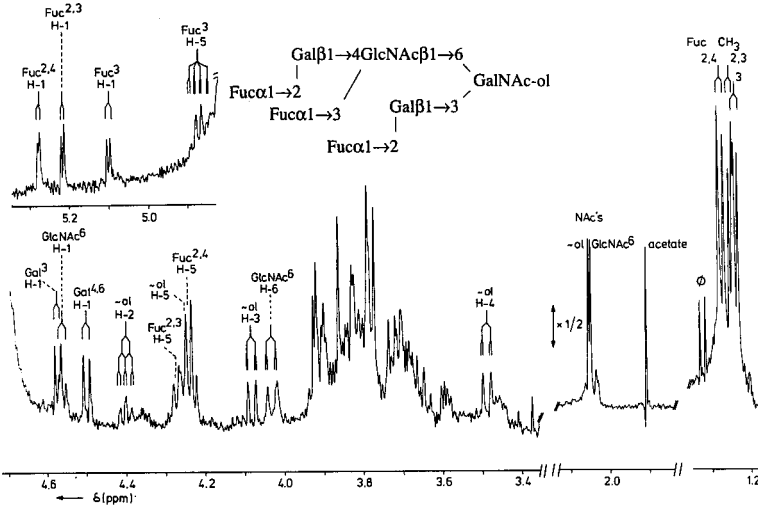

Figure 41. Resolution-enhanced ^{1}H-NMR spectrum of **44**. For comments, see Figure 30.

4GlcNAcβ1 → 6(Fuc^{2,4}): H-1, δ = 5.30–5.31 ppm; H-5, δ = 4.22–4.23 ppm; CH_3, δ = 1.23 ppm. For Galβ1 → 4(Fucα1 → 3)GlcNAcβ1 → 6: H-1, δ = 5.11 ppm; H-5, δ = 4.83 ppm; CH_3, δ = 1.17 ppm. For Fucα1 → 2Galβ1 → 4(Fucα1 → 3)GlcNAcβ1 → 6: (Fuc^{2,4}) H-1, δ = 5.28 ppm; H-5, δ = 4.24 ppm; CH_3, δ = 1.27 ppm; (Fuc^3) H-1, δ = 5.10 ppm; H-5, δ = 4.87 ppm; CH_3, δ = 1.23 ppm. They can easily be recognized when they occur alone or in combination. In the case of the presence of the Fucα1 → 2Galβ1 → 3GalNAc-ol element (**38**, **39**, and **42–44**), the GalNAc-ol H-3 signal undergoes a downfield shift from δ = 4.060 ppm (**25**, **40**, and **41**) to δ = 4.081–4.085 ppm, whereas the GalNAc-ol NAc singlet shows an upfield shift from $\delta \sim$ 2.067 ppm to $\delta \sim$ 2.054 ppm. Furthermore, the Gal^3 H-1 signal is observed at δ = 4.570–4.576 ppm (for **25**, **40**, and **41**, δ = 4.463–4.465 ppm). The Fucα1 → 2Galβ1 → 4GlcNAcβ1 → 6 element (**40** and **42**) gives rise to a specific Gal^{4,6} H-1 signal at δ = 4.536 ppm ($\Delta\delta$ = +0.066 ppm, as compared to **25**). The occurrence of the immuno group X determinant Galβ1 → 4(Fucα1 → 3)GlcNAcβ1 → 6 is reflected by an upfield shift of the Gal^{4,6} H-1 signal from δ = 4.470 ppm in **25** to δ = 4.448 ppm in **41** and **43**. Finally, in the case of the immuno group Y determinant Fucα1 → 2Galβ1 → 4(Fucα1 → 3)GlcNAcβ1 → 6 especially the position of the Gal^{4,6} H-1 signal has to be mentioned. Furthermore, the shift increment data for going from H to Y and from X to Y blood group determinants, as summarized in Table 10, hold also for the series **42–44**. It has to be noted that in the case of Fucα1 → 2Galβ1 → 3GalNAc-ol itself (**29**), the chemical shift value for Fuc H-1 deviates from those reported for **38**, **39**, and **42–44**

(δ = 5.256 ppm versus δ = 5.21–5.22 ppm). This demonstrates that the Fuc H-1 signal is extremely sensitive to structural changes in the carbohydrate chain. Concerning **40**, it should be noted that the doublets at δ = 4.535 ppm ($J_{1,2}$ = 8.6 Hz) and at δ = 4.536 ppm ($J_{1,2}$ = 7.3 Hz) have been assigned to H-1 of GlcNAc^6 and Gal^{4,6}, respectively, on the basis of the pronounced difference in coupling constant (see Section 3).

Compound **45** is the $\alpha 1 \rightarrow 4$ fucosylated analog of **28** (Dua *et al.*, 1985). The ^{1}H-NMR data of **45** have been derived from a 300-MHz ^{1}H-NMR spectrum. The observed set of Fuc structural-reporter-group signals, i.e., H-1 (δ = 5.030 ppm), H-5 (δ = 4.782 ppm at 75 °C), and CH_3 (δ = 1.183 ppm), deviates from those reported for $\alpha 1 \rightarrow 2$- and $\alpha 1 \rightarrow 3$-linked Fuc residues. For **33** (Table 9) having also an $\alpha 1 \rightarrow 4$-linked Fuc residue, the spectrum gives rise to the following set: H-1, δ = 5.026 ppm; H-5, δ = 4.880 ppm (at 77 °C); CH_3, δ = 1.252 ppm. Comparison of the ^{1}H-NMR data of **45**, containing the blood group Le^a determinant, and **28** (Table 7)

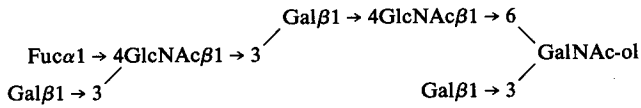

(45)

demonstrates that the $\alpha 1 \rightarrow 4$ fucosylation induces typical shifts for GlcNAc^3 H-1 ($\Delta\delta$ = −0.027 ppm) and GlcNAc^3 NAc ($\Delta\delta$ = +0.007 ppm). The same upfield shift for GlcNAc^3 H-1 is found, when the ^{1}H-NMR spectra of the milk oligosaccharides Fuc$\alpha 1 \rightarrow 4$(Gal$\beta 1 \rightarrow 3$)GlcNAc$\beta 1 \rightarrow 3$Gal$\beta 1 \rightarrow 4$Glc and Gal$\beta 1 \rightarrow 3$GlcNAc$\beta 1 \rightarrow 3$Gal$\beta 1 \rightarrow 4$Glc are compared (Dua and Bush, 1983).

The ^{1}H-NMR spectrum of the $\alpha 1 \rightarrow 3$ fucosylated form of **26**, namely, **46**, is depicted in Figure 42 (Klein *et al.*, 1988, Van Kuik *et al.*, 1991). The

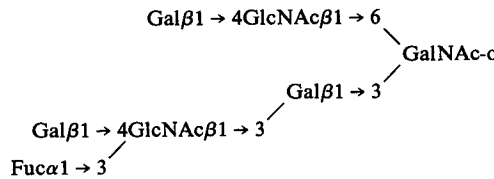

(46)

structural-reporter groups of the residues remote from the fucosylated element are similar in both cases. The structural-reporter groups of the Fuc residue, i.e., H-1 at δ = 5.138 ppm and CH_3 at δ = 1.176 ppm, are indicative of the immuno group X determinant. This element is further evidenced by the Gal^{4,3} H-1 signal at δ = 4.464 ppm ($\Delta\delta$ = −0.017 ppm, as compared to **26**). Additional effects are observed at GlcNAc^3 H-6 ($\Delta\delta$ = +0.014 ppm), GlcNAc^3 NAc ($\Delta\delta$ = −0.010 ppm), and Gal^{4,3} H-4 ($\Delta\delta$ = −0.025 ppm). The effects of the extension are similar to those observed in the spectra when

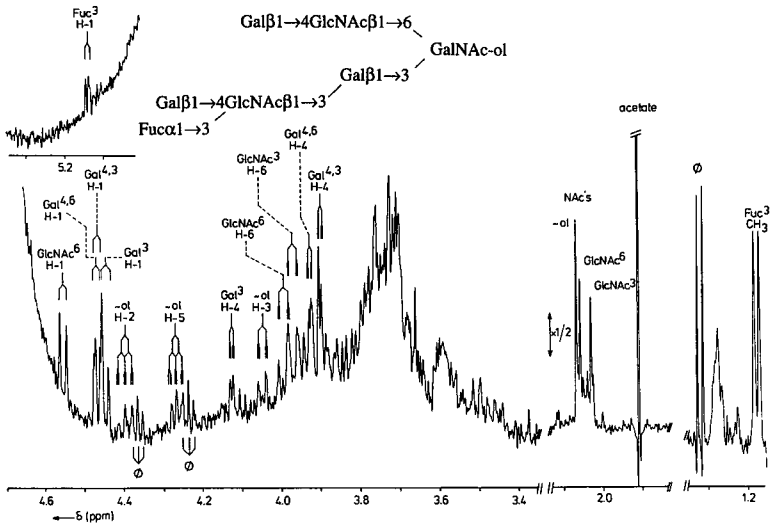

Figure 42. Resolution-enhanced ^{1}H-NMR spectrum of **46**. For comments, see Figure 30.

going from **12** to **30** (GlcNAc^3 NAc, $\Delta\delta = -0.010$ ppm; Gal^{4,3} H-1, $\Delta\delta = -0.019$ ppm) (Vliegenthart *et al.*, 1983).

Compound **47** can be conceived as an extension of **32** (Table 9) with GlcNAc in $\beta 1 \rightarrow 6$ linkage to GalNAc-ol (Van Halbeek *et al.*, 1982c). The

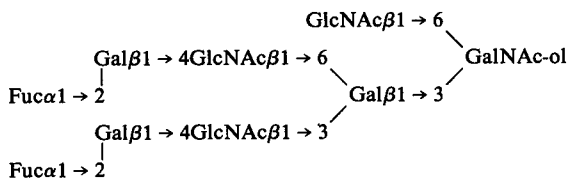

(47)

structural-reporter-group signals of the bulky, dibranched part of the structure at Gal^3 fit those presented earlier for **32**. For the core structure the chemical shift of GalNAc-ol H-5 at $\delta = 4.219$ ppm is lower than generally found (see Section 11), illustrating the influence of the bulky, dibranched part.

4.4. Extensions of the GlcNAcβ1 → 6(GlcNAcβ1 → 3)GalNAc-ol Core Structure

In this section, the ^{1}H-NMR structural-reporter-group data of a series of fucose-containing saccharides, which have the GlcNAcβ1 → 6(GlcNAcβ1 → 3)GalNAc-ol core structure in common, are reviewed. This

group of structures can be divided into three subgroups, corresponding to the three nonfucosylated analogs **21**, **22**, and **23**, respectively, described in Section 3.4.

The ^{1}H-NMR structural-reporter-group data of the first subgroup, comprising the three fucosylated analogs **48** (Breg *et al.*, 1988b; Lamblin *et al.*, 1984b), **49** (Van Halbeek *et al.*, 1982b), and **50** (Breg *et al.*, 1988b)

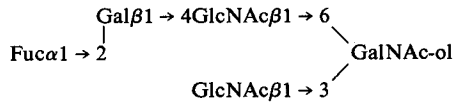

(48)

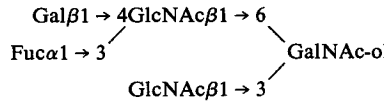

(49)

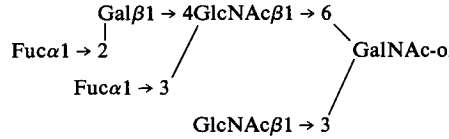

(50)

derived from Galβ1 → 4GlcNAcβ1 → 6(GlcNAcβ1 → 3)GalNAc-ol (**21**), have been summarized in Table 13. Recurrent features in the structural-reporter-group chemical shifts of this series are H-2, H-5, and NAc of GalNAc-ol at δ = 4.26–4.29, 4.20–4.24, and 2.044–2.046 ppm, respectively (see Section 11). The GlcNAc^3 H-1 and NAc signals appear at δ = 4.60 and 2.08 ppm, respectively, indicative of GlcNAc^3 in a terminal position. Comparison of the ^{1}H-NMR data of the Fuc residues in **48** (blood group H determinant), **49** (immuno X determinant) (see Figure 29), and **50** (immuno group Y determinant) (Figure 43) with those of the same determinants in **42**, **43**, and **44** (Table 12), respectively, shows a great similarity. The three sets can be defined as follows. For the Fucα1 → 2Galβ1 → 4GlcNAcβ1 → 6 element (**48**), the set is H-1, δ = 5.307 ppm; H-5, δ = 4.225 ppm; CH_3, δ = 1.233 ppm. The Galβ1 → 4(Fucα1 → 3)GlcNAcβ1 → 6 element (**49**) is represented by the set H-1, δ = 5.118 ppm; H-5, δ = 4.83 ppm; CH_3, δ = 1.177 ppm. The Fucα1 → 2Galβ1 → 4(Fucα1 → 3)GlcNAcβ1 → 6 element (**50**) gives rise to: (Fuc^2) H-1, δ = 5.275 ppm; H-5, δ = 4.259 ppm; CH_3, δ = 1.273 ppm; and (Fuc^3) H-1, δ = 5.102 ppm; H-5, δ = 4.872 ppm; CH_3, δ = 1.236 ppm. The downfield shift for Gal^4 H-1 in **48** ($\Delta\delta$ = +0.067 ppm, as compared to **21**), the upfield shift for Gal^4 H-1 in **49** ($\Delta\delta$ = −0.020 ppm), and the downfield shift of Gal^4 H-1 in **50** ($\Delta\delta$ = +0.028 ppm), are similar to those observed for the steps going from **39** to

TABLE 13
^{1}H Chemical Shifts of Structural-Reporter Groups of Constituent Monosaccharides for Fucosylated Oligosaccharide-Alditols with the Galβ1 → 4GlcNAcβ1 → 6(GlcNAcβ1 → 3)GalNAc-ol Backbone Structure in Common (48–50)

Residue	Reporter group	21 	48 	49 	50 
GalNAc-ol	H-2	4.282	4.282	4.280	4.282
	H-3	3.986	3.986	3.988	3.985
	H-4	3.515	3.517	3.5–3.6	3.503
	H-5	4.239	4.241	4.230	4.231
	NAc	2.045	2.044	2.046	2.044
GlcNAc^3	H-1	4.599	4.597	4.597	4.595
	H-6	3.951	3.949	3.966	3.947
	NAc	2.081	2.081	2.081	2.080
GlcNAc^6	H-1	4.564	4.546	4.570	4.553
	H-6	3.998	3.991	4.0[a]	4.026
	NAc	2.061	2.065	2.052	2.055
Gal^4	H-1	4.473	4.540	4.453	4.501
	H-4	3.927	3.891	3.921	n.d[b]
Fuc^2	H-1	—	5.307	—	5.275
	H-5	—	4.225	—	4.259
	CH_3	—	1.233	—	1.273
Fuc^3	H-1	—	—	5.118	5.102
	H-5	—	—	4.83	4.872
	CH_3	—	—	1.177	1.236

[a] Value could not be determined more accurately due to overlap with other carbohydrate originating signals.
[b] n.d. means value could not be determined merely by inspection of the spectrum.

42, **43**, or **44**, respectively. Moreover, the shifts for the steps going from **48** to **50** (H → Y), and from **49** to **50** (X → Y) fit those summarized in Table 10. It has to be noted that the position of the Fuc^3 H-1 signal at δ = 5.102 ppm in **50** points to GlcNAc being β1 → 6 linked to GalNAc-ol (see also **44**).

The second subgroup of fucosylated structures with the GlcNAcβ1 → 6(GlcNAcβ1 → 3)GalNAc-ol core element are the mono-, di-, and trifucosylated analogs **51–56** of Galβ1 → 4GlcNAcβ1 → 6(Galβ1 → 4GlcNAcβ1 → 3)GalNAc-ol (**22**). The ^{1}H-NMR characteristics of these substances have been summarized in Table 14. Typical ^{1}H-NMR signals for the common moieties in this subgroup, including **22**, are as follows. GalNAc-ol: H-2, H-5, and NAc at δ = 4.26–4.29, 4.20–4.24, and 2.038–2.045 ppm, respectively (see Section 11): GlcNAc^3: H-1 and NAc at δ = 4.60–4.62 and 2.070–2.083 ppm, respectively; GlcNAc^6: H-1 and NAc at δ = 4.54–4.56 and 2.056–2.070 ppm, respectively. The ^{1}H-NMR chemical shifts of the Gal^{4,3}

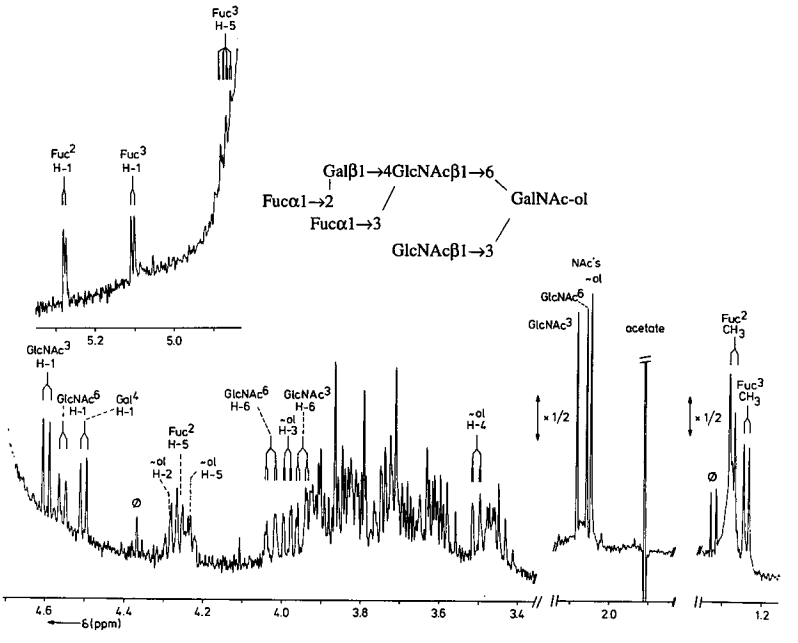

Figure 43. Resolution-enhanced ^{1}H-NMR spectrum of **50**. For comments, see Figure 34.

and Gal^{4,6} residues are largely influenced by extensions of the lower and upper branch, respectively.

Comparison of the ^{1}H-NMR data of **51** (Breg *et al.*, 1988b; Lamblin *et al.*, 1984b) with those of **22** shows that the structural-reporter groups of

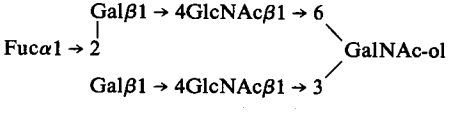

(51)

the *N*-acetyllactosamine unit attached to GalNAc-ol C-3 are essentially unaltered. The introduction of the Fucα1 → 2 residue at the *N*-acetyllactosamine unit of the upper branch gives rise to specific shifts for the GlcNAc^6 and Gal^{4,6} structural-reporter groups. The GlcNAc^6 H-1 signal shifts upfield ($\Delta\delta = -0.019$ ppm) and the GlcNAc^6 NAc singlet downfield ($\Delta\delta = +0.004$ ppm). For the Gal^{4,6} H-1 and H-4 signals, $\Delta\delta$ values of +0.066 and −0.033 ppm, respectively, are found. Similar α1 → 2 fucosylation effects have been determined for the Fucα1 → 2Galβ1 → 4GlcNAcβ1 → 6 element in **48**. The structural reporters of the Fuc residue are consistent with those found generally for such a fucosylated *N*-acetyllactosamine element, i.e., H-1, $\delta = 5.305$ ppm; H-5, $\delta = 4.227$ ppm; CH_3, $\delta = 1.235$ ppm.

TABLE 14
^{1}H Chemical Shifts of Structural-Reporter Groups of Constituent Monosaccharides for Fucosylated Oligosaccharide-Alditols with the Galβ1 → 4GlcNAcβ1 → 6(Galβ1 → 4GlcNAcβ1 → 3)GalNAc-ol Backbone Structure in Common (51–56)

Residue	Reporter group	22 	51 	52 	53 	54 	55 	56 
GalNAc-ol	H-2	4.283	4.283	4.27	4.28	4.27	4.265	4.27
	H-5	4.240	4.234	4.23	4.23	4.22	4.223	4.22
	NAc	2.045	4.044	2.043	2.043	2.045	2.038	2.044
GlcNAc^3	H-1	4.624	4.621	4.603	4.602	4.621	4.617	4.601
	NAc	2.079	2.079	2.083	2.082	2.078	2.070	2.082
Gal^{4,3}	H-1	4.456	4.454	4.523	4.525	4.456	4.481	4.526
	H-4	3.927	3.927	3.89	3.89	n.d.[a]	n.d.	n.d.
GlcNAc^6	H-1	4.565	4.546	4.560	4.541	4.55[b]	4.538	4.551
	NAc	2.062	2.066	2.062	2.066	2.057	2.070	2.056
Gal^{4,6}	H-1	4.474	4.540	4.475	4.539	4.501	4.538	4.501
	H-4	3.927	3.894	3.93	3.89	n.d.	3.89	n.d.
Fuc^{2,4,6}	H-1	—	5.305	—	5.304	5.275	5.306	5.273
	H-5	—	4.227	—	4.23	n.d.	4.23	n.d.
	CH_3	—	1.235	—	1.235	1.273	1.237	1.273
Fuc^{2,4,3}	H-1	—	—	5.305	5.311	—	5.279	5.309
	H-5	—	—	4.23	4.23	—	4.24	n.d.
	CH_3	—	—	1.229	1.235	—	1.276	1.230
Fuc^3	H-1	—	—	—	—	5.104	5.118	5.104
	H-5	—	—	—	—	n.d.	4.867	n.d.
	CH_3	—	—	—	—	1.236	1.237	1.234

[a] n.d. means value could not be determined merely by inspection of the spectrum.
[b] Value could not be determined more accurately, probably due to virtual coupling.

Compound **52** is an isomer of **51**, which has been found as a minor component in a fraction containing mainly **51** (Breg *et al.*, 1988b). Comparison of the ^{1}H-NMR data of **52** with those of **22** and **51** leads to the

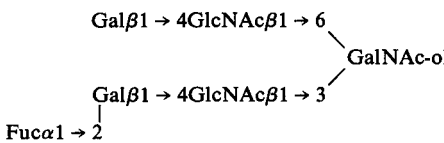

(52)

conclusion that in **52** the structural-reporter groups of the *N*-acetyllactosamine unit attached to GalNAc-ol C-6 indicate a nonfucosylated upper branch. The typical shift effects, due to the coupling of the Fucα1 → 2 residue at an *N*-acetyllactosamine unit, are now observed for the GlcNAc^3 and Gal^{4,3} structural-reporter groups. The GlcNAc^3 H-1 and NAc signals

give rise to $\Delta\delta$ values of -0.021 and $+0.004$ ppm, respectively, as compared to **22**. The $Gal^{4,3}$ H-1 and H-4 signals show $\Delta\delta$ values of $+0.067$ and -0.037 ppm, respectively. The Fuc structural reporters (H-1, H-5, CH_3) are similar to those observed for **51**.

The difucosylated oligosaccharide-alditol **53** has the fucosylated elements of both **51** and **52** (Breg *et al.*, 1988b). The structural reporters of $Fuc^{2,4,3}$ (H-1, $\delta = 5.311$ ppm; CH_3, $\delta = 1.235$ ppm) and $Fuc^{2,4,6}$ (H-1, $\delta = 5.304$ ppm; CH_3, $\delta = 1.235$ ppm) are both indicative of Fuc in $\alpha 1 \rightarrow 2$ linkage to Gal of an *N*-acetyllactosamine unit. In fact, the typical shift effects found in **51** and **52** separately, occur now jointly in **53**.

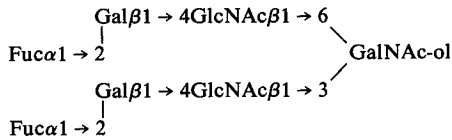

(53)

The ^{1}H-NMR spectrum of **54** (Breg *et al.*, 1988b) indicates the presence of the immuno group Y determinant (Fucα1 → 2Galβ1 → 4(Fucα1

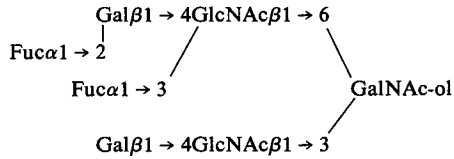

(54)

→ 3)GlcNAcβ1 →), reflected by the combined sets of structural-reporter groups of $Fuc^{2,4,6}$ (H-1, $\delta = 5.275$ ppm; CH_3, $\delta = 1.273$ ppm) and Fuc^3 (H-1, $\delta = 5.104$ ppm; CH_3, $\delta = 1.236$ ppm). The NAc signal for $GlcNAc^6$ at $\delta = 2.057$ ppm and the $Gal^{4,6}$ H-1 signal at $\delta = 4.501$ ppm also point to the presence of this element. The anomeric doublet of $GlcNAc^6$ at $\delta = 4.55$ ppm is, similar to the GlcNAc H-1 signals in the spectra of **44** and **59**, severely distorted, probably due to virtual coupling. The position of Fuc^3 H-1 ($\delta = 5.104$ ppm) indicates the GlcNAc residue in this determinant to be $\beta 1 \rightarrow 6$ linked to GalNAc-ol (see also **44** and **50**). Comparison of the ^{1}H-NMR data of **54** and **22** shows clearly that the *N*-acetyllactosamine element attached to GalNAc-ol C-3 is unsubstituted (see also **51**).

In Figure 44 the ^{1}H-NMR spectrum is depicted of **55**, a trifucosylated form of **22** (Breg *et al.*, 1988b; see also Van Kuik *et al.*, 1991). The presence

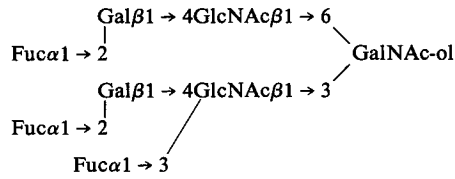

(55)

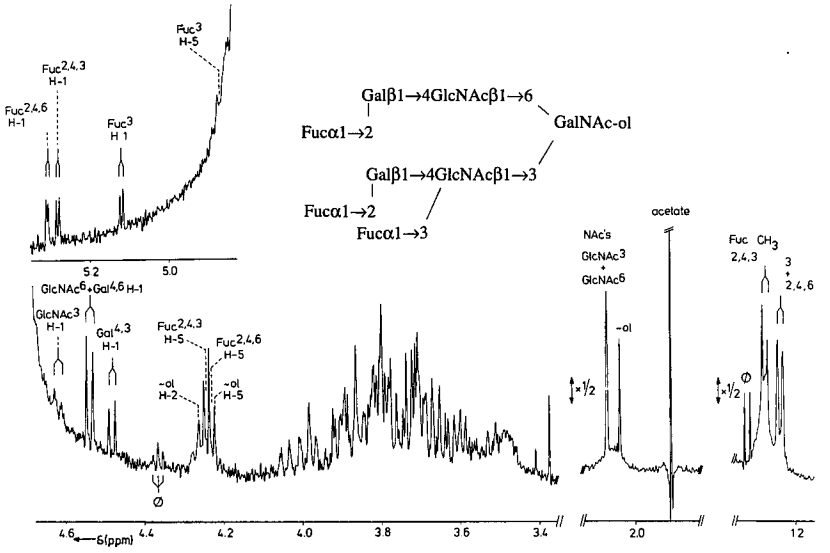

Figure 44. Resolution-enhanced ^{1}H-NMR spectrum of **55**. For comments, see Figure 34.

of the immuno group Y determinant is evidenced by the combined sets of structural-reporter groups of Fuc^{2,4,3} (H-1, δ = 5.279 ppm; CH_3, δ = 1.276 ppm) and Fuc^3 (H-1, δ = 5.118 ppm; CH_3, δ = 1.237 ppm). The Fuc^3 H-1 shift value (δ = 5.118 ppm) indicates that the immuno group Y determinant is involved in a 1 → 3 linkage to GalNAc-ol, analogous to the same element in **31** and **36**. This partial structure is supported by the GlcNAc^3 NAc signal at δ = 2.070 ppm and the Gal^{4,3} H-1 signal at δ = 4.481 ppm. The GlcNAc^3 H-1 doublet at δ = 4.617 ppm is heavily distorted, probably due to virtual coupling with its H-3. The third Fuc residue is α1 → 2 linked to Gal in an *N*-acetyllactosamine unit attached to GalNAc-ol C-6. Comparison of the ^{1}H-NMR data of this element in **55** with the same element in **51** and **53** shows similar structural-reporter-group signals. For **55** the anomeric signals of Gal^{4,6} and GlcNAc^6 coincide at δ = 4.538 ppm. It has to be noted that the GalNAc-ol H-2 and H-5 signals are partly obscured by two Fuc H-5 signals. This means that the complete structure in fact is assembled from separately recognizable peripheral structural elements (see Section 11).

The ^{1}H-NMR data of the trifucosylated compound **56** (Breg *et al.*, 1988b) can be directly related to those of **54**. The set of two Fuc reporter groups, i.e., H-1 at δ = 5.273 and 5.104 ppm, and CH_3 signals at δ = 1.273 and 1.234 ppm, are indicative of the immuno group Y determinant, i.e., Fucα1 → 2Galβ1 → 4(Fucα1 → 3)GlcNAcβ1 → . The 1 → 6 linkage of

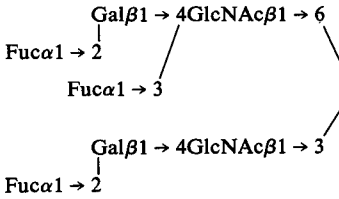

(56)

GlcNAc is indicated by the exact position of Fuc^3 H-1 at δ = 5.104 ppm, as in the identical element in **44**, **50**, and **54**. The analogy to these oligosaccharide-alditols holds also for the GlcNAc^6 H-1 and NAc signals at δ = 4.551 and 2.056 ppm, respectively, and for the Gal^{4,6} H-1 signal at δ = 4.501 ppm. The third Fuc residue, as indicated by its H-1 and CH_3 at δ = 5.309 and 1.230 ppm, respectively, is part of the Fucα1 → 2Galβ1 → 4GlcNAcβ1 → element. The various structural-reporter groups belonging to this element are similar to those observed for that in **52** and **53**.

The third subgroup of fucosylated structures with the GlcNAcβ1 → 6(GlcNAcβ1 → 3)GalNAc-ol core element are the mono-, di-, and trifucosylated analogs **57**–**59** of Galβ1 → 4GlcNAcβ1 → 6(Galβ1 → 3GlcNAcβ1 → 3)GalNAc-ol (**23**). In Table 15 the ^{1}H-NMR parameters of these compounds are presented. Characteristic GalNAc-ol signals in the various spectra, including that of **23**, are H-2, H-5, and NAc at δ = 4.26–4.29, 4.20–4.24, and 2.042 ppm, respectively (see Section 11). In each case the 1 → 3-linked branch of GalNAc-ol is elongated by Fucα1 → 2Galβ1 → 3. The GlcNAc^3 H-1 and NAc signals resonate at δ = 4.653 and 2.108 ppm, respectively, the Gal^{3,3} H-1 signal at δ = 4.56–4.57 ppm, and the Fuc^{2,3} H-1, H-5, and CH_3 signals at δ = 5.210, 4.270, and 1.232 ppm, respectively. The chemical shift of the Gal^{4,6} H-1 resonance is strongly influenced by extension of the 1 → 6-linked branch by Fuc residues.

Compound **57** (Breg *et al.*, 1988b; Lamblin *et al.*, 1984b; Hounsell *et al.*, 1989) is derived from **23** by adding one Fuc residue in α1 → 2 linkage

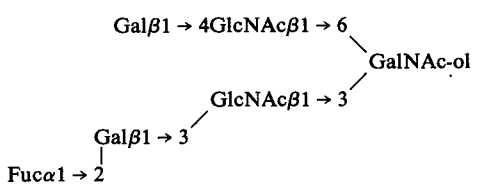

(57)

to the lower branch. The Fuc structural-reporter groups H-1 at δ = 5.210 ppm and H-5 at δ = 4.270 ppm indicate that Fuc^{2,3} is attached to Gal^{3,3} rather than to Gal^{4,6} (compare to **37**, **40**, and **42**; Tables 11 and 12). In accordance with this extension, the Gal^{3,3} H-1 signal resonates at δ = 4.569 ppm, nearly coinciding with the GlcNAc^6 H-1 signal. The location of Fuc^{2,3} at Gal^{3,3} is further evidenced by the highly typical shift of the GlcNAc^3

TABLE 15
^{1}H Chemical Shifts of Structural-Reporter Groups of Constituent Monosaccharides for Fucosylated Oligosaccharide-Alditols with the Galβ1 → 4GlcNAcβ1 → 6(Galβ1 → 3GlcNAcβ1 → 3)GalNAc-ol Backbone Structure in Common (57–59)

Residue	Reporter group	23	57	58	59
GalNAc-ol	H-2	4.287	4.264	4.26	4.290
	H-5	4.233	4.214	4.22	4.202
	NAc	2.043	2.042	2.042	2.042
GlcNAc^3	H-1	4.648	4.653	4.652	4.653
	NAc	2.069	2.108	2.108	2.106
Gal^{3,3}	H-1	4.453	4.569	4.562	4.560
	H-4	3.92	3.89	3.89	3.89
GlcNAc^6	H-1	4.559	4.564	4.551	4.56[b]
	H-6	n.d.[a]	n.d.	n.d.	4.022
	NAc	2.062	2.060	2.065	2.057
Gal^{4,6}	H-1	4.472	4.468	4.535	4.498
	H-4	3.92	3.925	3.89[c]	n.d.
Fuc^{2,3}	H-1	—	5.210	5.210	5.210
	H-5	—	4.270	4.270	4.271
	CH_3	—	1.232	1.232	1.233
Fuc^{2,4}	H-1	—	—	5.304	5.274
	H-5	—	—	4.224	4.256
	CH_3	—	—	1.232	1.271
Fuc^3	H-1	—	—	—	5.098
	H-5	—	—	—	4.874
	CH_3	—	—	—	1.233

[a] n.d. means value could not be determined merely by inspection of the spectrum.
[b] Value could not be determined more accurately, probably due to virtual coupling.
[c] Value could not be determined more accurately due to overlap with other carbohydrate originating signals.

NAc singlet (δ = 2.108 ppm; $\Delta\delta$ = +0.039 ppm, as compared to **23**). The shift effects observed for the GalNAc-ol H-2 and H-5 multiplets (H-2, $\Delta\delta$ = −0.023 ppm; H-5, $\Delta\delta$ = −0.019 ppm) are also interesting. Finally, the structural-reporter groups of the *N*-acetyllactosamine unit attached to GalNAc-ol C-6 are similar to those observed for **23**.

In the difucosylated **58** (Breg *et al.*, 1988b; see the ^{1}H-NMR spectrum in Figure 45), one Fuc residue forms part of the element Fucα1 → 2Galβ1 → 3GlcNAcβ1 → 3. This is evidenced by the set of structural reporters for Fuc^{2,3} (H-1, δ = 5.210 ppm; H-5, δ = 4.270 ppm; CH_3, δ = 1.232 ppm), the Gal^{3,3} H-1 signal at δ = 4.562 ppm, and the GlcNAc^3 H-1 and NAc signals

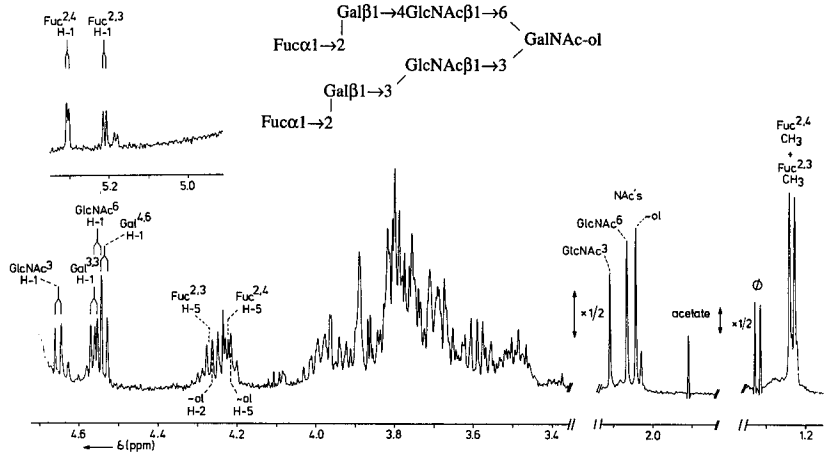

Figure 45. Resolution-enhanced ^{1}H-NMR spectrum of **58**. For comments, see Figure 34.

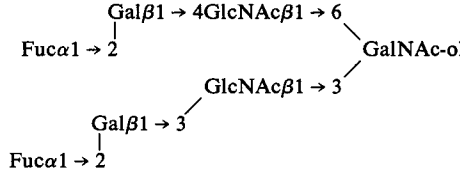

(58)

at $\delta = 4.652$ and 2.108 ppm, respectively (see **57**). The second set of Fuc resonances is characteristic of Fuc $\alpha 1 \rightarrow 2$ linked to Gal in an *N*-acetyllactosamine unit, and is comparable to that observed for the $1 \rightarrow 6$ branch in **48**, **51**, **53**, and **55** (H-1, $\delta = 5.304$ ppm; H-5, $\delta = 4.224$ ppm; CH_3, $\delta = 1.232$ ppm). It has to be noted that the exact positions of the GalNAc-ol H-2 and H-5 signals cannot be deduced directly from the spectrum because they are each obscured by Fuc H-5 signals (see Section 11).

The trifucosylated oligosaccharide-alditol **59** (Figure 46) is an extension of **58** with a $1 \rightarrow 3$-linked Fuc residue (Breg *et al.*, 1988b). A very characteristic GlcNAc^3 NAc signal at $\delta = 2.106$ ppm, together with Fuc H-1, H-5, and

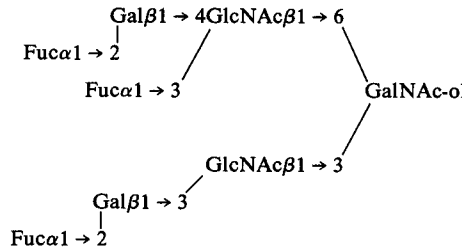

(59)

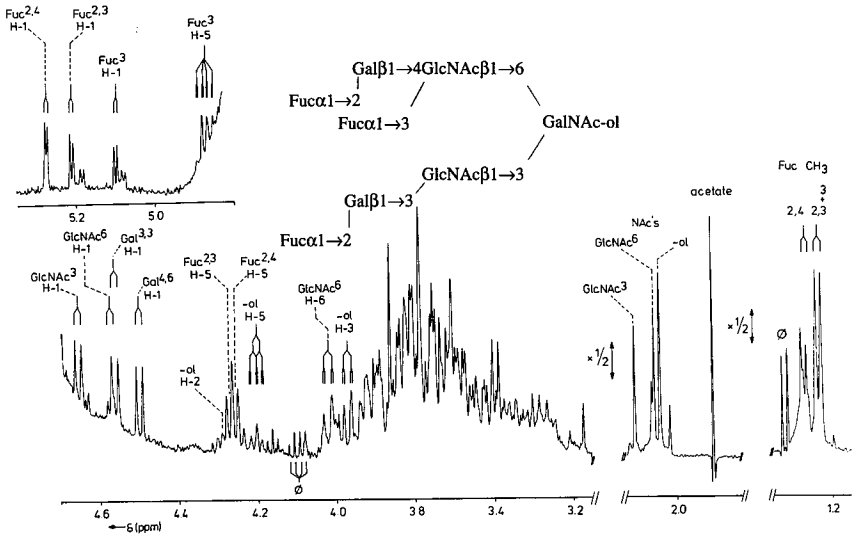

Figure 46. Resolution-enhanced ^{1}H-NMR spectrum of **59**. For comments, see Figure 34.

CH_3 signals at $\delta = 5.210$, 4.271, and 1.233 ppm, respectively, point to the element Fucα1 → 2Galβ1 → 3GlcNAcβ1 → 3 (see **57** and **58**). The occurrence of the immuno group Y determinant Fucα1 → 2Galβ1 → 4(Fucα1 → 3)-GlcNAcβ1 → is clear from the combined sets of structural reporters of Fuc^{2,4} (H-1, $\delta = 5.274$ ppm; H-5, $\delta = 4.256$ ppm; CH_3, $\delta = 1.271$ ppm) and Fuc^3 (H-1, $\delta = 5.098$ ppm; H-5, $\delta = 4.874$ ppm; CH_3, $\delta = 1.233$ ppm). The position of Fuc^3 H-1 ($\delta = 5.098$ ppm) indicates that GlcNAc is involved in a β1 → 6 linkage to GalNAc-ol, as observed for the upper branch in **50** and **44**. The disturbance in the intensity of the GlcNAc^6 H-1 doublet at $\delta =$ 4.56 ppm can be ascribed to a virtual coupling with its H-3 signal in the bulk region of the spectrum.

5. PERIPHERAL α1 → 4-LINKED *N*-ACETYLGLUCOSAMINE

The oligosaccharide-alditols **60–65** contain terminal α1 → 4-linked GlcNAc, and have a GlcNAcβ1 → 6(Galβ1 → 3)GalNAc-ol core structure in common, except the simplest one, which has only a Galβ1 → 3GalNAc-ol core. The relevant ^{1}H-NMR parameters of these compounds have been summarized in Table 16. The common presence of the Galβ1 → 3GlcNAc-ol unit is reflected by the chemical shift for GalNAc-ol H-2 at $\delta =$ 4.38–4.41 ppm, and the GalNAc-ol H-3 signal resonates at $\delta = 4.0$–4.1 ppm (see Section 11). The GlcNAcα1 → 4Galβ1 → element is characterized by

TABLE 16

^{1}H Chemical Shifts of Structural-Reporter Groups of Constituent Monosaccharides for $\alpha 1 \rightarrow$ 4-Linked GlcNAc-Containing Oligosaccharide-Alditols (60–65)

Residue	Reporter group	60 	61 	62[b] 	63 	64 	65 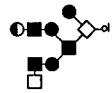
GalNAc-ol	H-2	4.404	4.405	4.405	4.406	4.392	4.392
	H-3	4.081	4.081	4.083	4.082	3.994	3.994
	H-4	3.541	3.572	3.574[b]	3.574	3.474	3.474
	H-5	4.193	4.261	4.264	4.264	4.218	4.218
	H-6	3.76	3.92	3.952	3.92	3.9	3.9
	NAc	2.058	2.054	2.054	2.055	2.047	2.047
Gal[3]	H-1	4.525	4.518	4.521	4.520	4.461	4.457
	H-4	3.971	3.976	3.980	3.985	4.108	4.115
GlcNAc[6]	H-1	—	4.546	4.579	4.548	4.526	4.526
	H-6	—	n.d.[a]	4.019	n.d.	3.932	3.932
	NAc	—	2.067	2.067	2.067	2.065	2.065
GlcNAc[3,3]	H-1	—	—	—	—	4.722	4.684
	NAc	—	—	—	—	2.042	2.039
GlcNAc[6,3]	H-1	—	—	—	—	4.578	4.604
	NAc	—	—	—	—	2.053	2.051
Gal[4,3]	H-1	—	—	—	—	4.533	4.542
	H-4	—	—	—	—	3.990	3.896
Gal[4,6]	H-1	—	—	4.526	4.535	4.549	4.529
	H-4	—	—	3.987	3.980	3.892	3.983
GlcNAc[4,(4,)3]	H-1	4.869	4.868	4.870	4.867	4.866	—
	H-4	3.542	n.d.	3.542	n.d.	3.545	—
	H-5	4.183	4.174	4.167	4.176	4.185	—
	NAc	2.089	2.103	2.104	2.102	2.069	—
GlcNAc[4,(4,)6]	H-1	—	—	4.873[b]	—	—	4.869
	H-4	—	—	3.544	—	—	3.548
	H-5	—	—	4.182[b]	—	—	4.185
	NAc	—	—	2.069	—	—	2.069
Fuc[2,4,3]	H-1	—	—	—	—	—	5.312
	H-5	—	—	—	—	—	4.226
	CH_3	—	—	—	—	—	1.233
Fuc[2,4,6]	H-1	—	—	—	5.305	5.312	—
	H-5	—	—	—	4.221	4.226	—
	CH_3	—	—	—	1.230	1.231	—

[a] n.d. means value could not be determined merely by inspection of the spectrum.

[b] Hounsell *et al.* (1989): GalNAc-ol H-4, δ = 3.517 ppm; GlcNAc[4,6] H-1, δ = 4.853 ppm (285 K); GlcNAc[4,6] H-5, δ = 4.194 ppm.

a set of α-GlcNAc structural-reporter-group signals, consisting of H-1 at $\delta = 4.86$–4.87 ppm and H-5 at $\delta = 4.17$–4.19 ppm. The definite position of the α-GlcNAc NAc signal is influenced by changes in the environment of the residue in the chain ($\delta = 2.069$–2.104 ppm).

The ^{1}H-NMR spectrum of **60** (Van Halbeek *et al.*, 1982c; Vliegenthart *et al.*, 1981) is presented in Figure 47. The terminal α-GlcNAc residue is

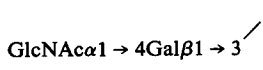

(60)

evidenced by four structural-reporter groups, namely, H-1 ($\delta = 4.869$ ppm; $J_{1,2} = 4.0$ Hz), H-4 ($\delta = 3.542$ ppm), H-5 ($\delta = 4.183$ ppm), and NAc ($\delta = 2.089$ ppm). The GlcNAc H-5 resonance is obscured, because of partial overlap of this multiplet with the GalNAc-ol H-5 signal at $\delta = 4.193$ ppm. The chemical shift of GlcNAc H-4 is practically identical with that of GalNAc-ol H-4 ($\delta = 3.541$ ppm); however, the resonance patterns of these two protons are quite distinct, owing to the significant differences in their vicinal coupling constants (α-GlcNAc, $J_{3,4} = 8.9$ Hz; $J_{4,5} = 10.3$ Hz; GalNAc-ol, $J_{3,4} = 8.8$ Hz; $J_{4,5} = 1.5$ Hz). The assignments of the α-GlcNAc skeleton proton signals were proved by double-resonance, spin-tickling experiments. The introduction of GlcNAc^{4,3} in α1 → 4 linkage to Gal causes downfield shifts of the Gal structural-reporter groups, as compared to the corresponding data of Galβ1 → 3GalNAc-ol (**2**): Gal^3 H-1, $\Delta\delta = +0.047$ ppm; Gal^3 H-4, $\Delta\delta = +0.070$ ppm.

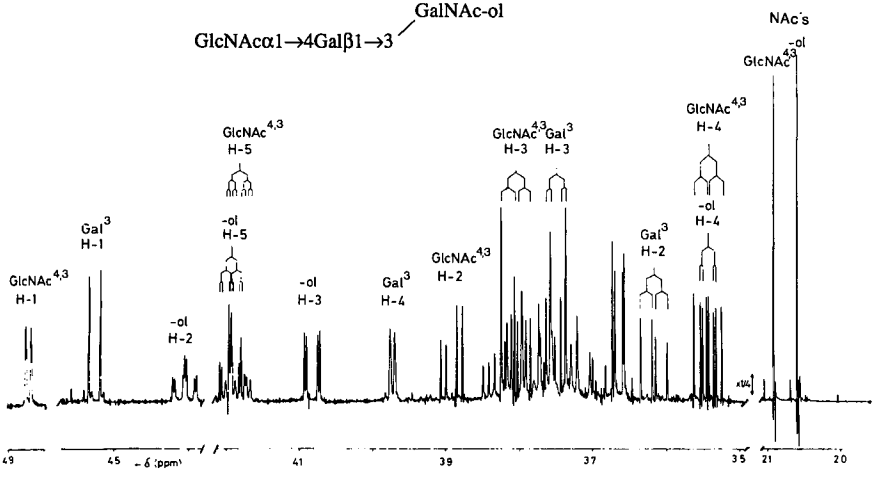

Figure 47. Resolution-enhanced ^{1}H-NMR spectrum of **60**. For comments, see Figure 30.

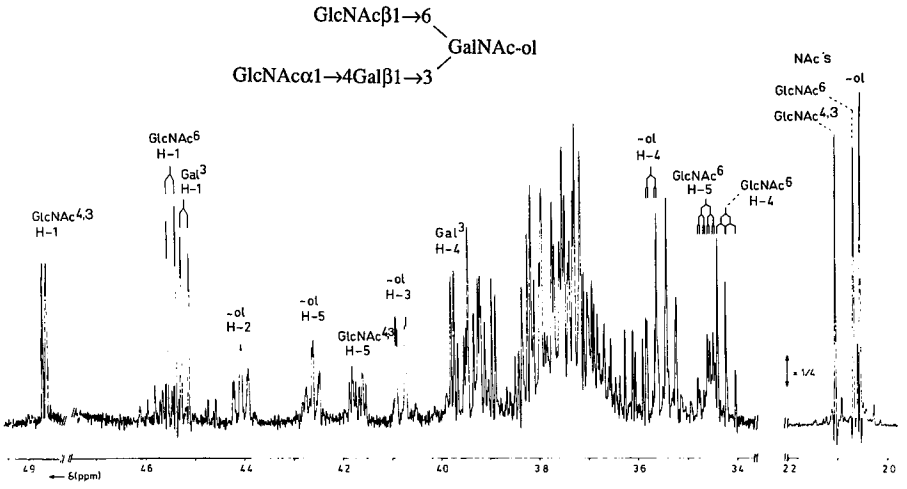

Figure 48. Resolution-enhanced ^{1}H-NMR spectrum of **61**. For comments, see Figure 30.

In Figure 48 the ^{1}H-NMR spectrum of **61** (Van Halbeek *et al.*, 1983a) is depicted. The presence of the GlcNAcβ1 → 6(Galβ1 → 3)GalNAc-ol core

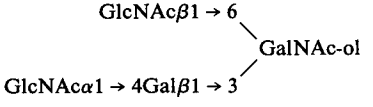

(61)

structure is evident from the GalNAc-ol H-2 (δ = 4.405 ppm), H-5 (δ = 4.261 ppm), and H-6 (δ = 3.92 ppm) structural-reporter groups. The terminal α-GlcNAc residue is demonstrated by its H-1 (δ = 4.868 ppm; $J_{1,2}$ = 3.8 Hz), H-5 (δ = 4.174 ppm), and NAc (δ = 2.103 ppm) signals. The attachment of GlcNAc^{4,3} at Gal^3 gives rise to similar effects on the Gal^3 H-1 and H-4 signals, as discussed for **60** (H-1, $\Delta\delta$ = +0.050 ppm; H-4, $\Delta\delta$ = +0.075 ppm; as compared to **7**).

Oligosaccharide-alditol **62** is an extension of **25** with two terminating α-GlcNAc residues in 1 → 4 linkage to Gal, and its ^{1}H-NMR spectrum is

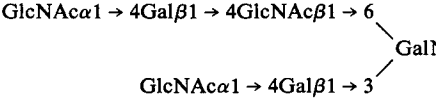

(62)

shown in Figure 49 (Capon *et al.*, 1989; Hounsell *et al.*, 1989; Van Halbeek *et al.*, 1982c). The influences of introduction of the α-GlcNAc residues upon the chemical shifts of the Gal^3 and Gal^{4,6} H-1 signals are independent of each other, illustrated by the difference in chemical shift between these

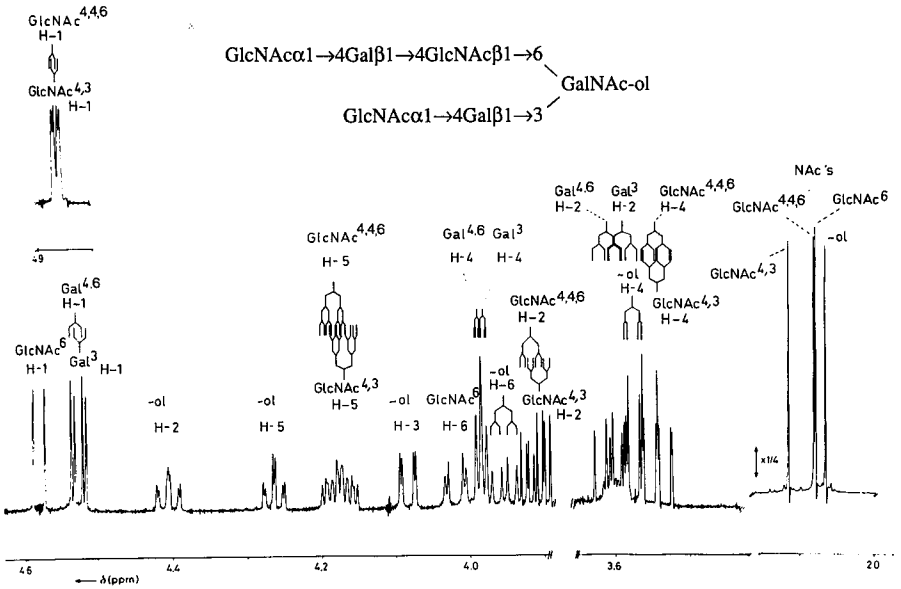

Figure 49. Resolution-enhanced ^{1}H-NMR spectrum of **62**. For comments, see Figure 30.

signals ($\Delta\delta = -0.005$ ppm) being maintained as compared to **25**. Owing to the introduction of $\alpha 1 \rightarrow 4$-linked GlcNAc into the upper branch, the GlcNAc^6 H-1 signal is shifted downfield ($\Delta\delta = +0.019$ ppm). Each of the terminal α-linked GlcNAc residues gives rise to its own set of H-1, H-4, and H-5 signals. The assignments of the signals to GlcNAc^{4,3} or GlcNAc^{4,4,6} are based upon comparison with the spectral data of **60** and **61**. The application of homonuclear *J*-resolved 2D ^{1}H-NMR spectroscopy enabled unraveling of the total spectrum, thereby confirming the aforementioned assignments. For assigning the various NAc singlets, use has been made of the ^{1}H-NMR data of **61** and **63**.

Compound **63** has been identified in a mixture of **62** and **63** (Van Halbeek *et al.*, 1983a). Besides the characteristics of **62**, a set of structural-

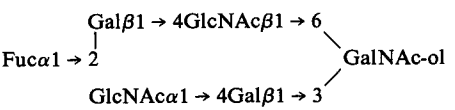

(63)

reporter-group signals for Fuc in $\alpha 1 \rightarrow 2$ linkage to Gal^{4,6}, namely, H-1, H-5, and CH_3 at $\delta = 5.305$, 4.221, and 1.230 ppm, respectively, can be observed (see **40**, **42**, and **48** with the same Fuc$\alpha 1 \rightarrow 2$Gal$\beta 1 \rightarrow 4$GlcNAc$\beta 1 \rightarrow 6$ upper branch).

The oligosaccharide-alditols **64** and **65** have only been studied as a mixture (3:4). The ^{1}H-NMR spectrum is shown in Figure 50 (Van Halbeek

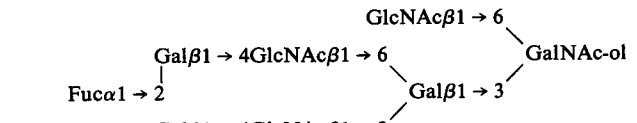

(64)

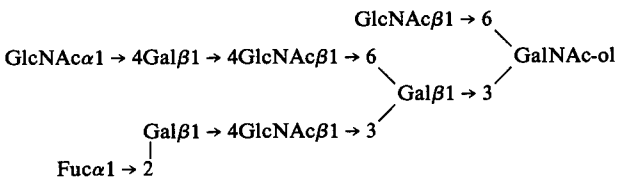

(65)

et al., 1982c). Both structures are variants of **47**, by replacing one of the Fuc residues by $\alpha 1 \rightarrow 4$-linked GlcNAc. The structural-reporter groups of GalNAc-ol and GlcNAc^6, being identical to those of the same residues in **47**, have the highest relative intensities in their spectral regions. The presence of two $\alpha 1 \rightarrow 4$-linked GlcNAc residues is indicated by H-1 signals at δ = 4.869 and 4.866 ppm (ratio 4:3), and of two $\alpha 1 \rightarrow 2$-linked Fuc residues by CH_3 signals at δ = 1.233 and 1.231 ppm (ratio 4:3). In the β-anomeric region the Gal^3 H-1 signals are observed at δ = 4.457 and 4.461 ppm (ratio 4:3). The remaining eight doublets can be divided into two groups on the basis of their relative intensity. Within such a group, they can be attributed to a Gal or a GlcNAc residue on the basis of their $J_{1,2}$ value (for Gal, $J_{1,2} < 8$ Hz; for GlcNAc, $J_{1,2} > 8$ Hz; see Section 3). Comparison with the data for the reporter groups of the fucosylated upper and lower branches in **47** makes an assignment to **64** and **65** possible. A similar procedure has been applied for the interpretation of the NAc singlets.

6. PERIPHERAL $\alpha 1 \rightarrow 3$-LINKED *N*-ACETYLGALACTOSAMINE

The oligosaccharide-alditols **66–74**, summarized in this section, contain terminal $\alpha 1 \rightarrow 3$-linked GalNAc as part of the blood group A determinant [GalNAc$\alpha 1 \rightarrow 3$(Fuc$\alpha 1 \rightarrow 2$)Gal$\beta 1 \rightarrow$]. The relevant ^{1}H-NMR parameters of **66–74**, obtained from 300-MHz ^{1}H-NMR spectra (Dua *et al.*, 1986), are presented in Table 17. The spectra have been fully assigned by spin difference decoupling spectroscopy in combination with spin simulation, whereas extensive NOE measurements have also been reported (Dua *et al.*, 1986). For urinary blood group A (and B) oligosaccharides, see Strecker *et al.* (1989c) and Wieruszeski *et al.* (1990).

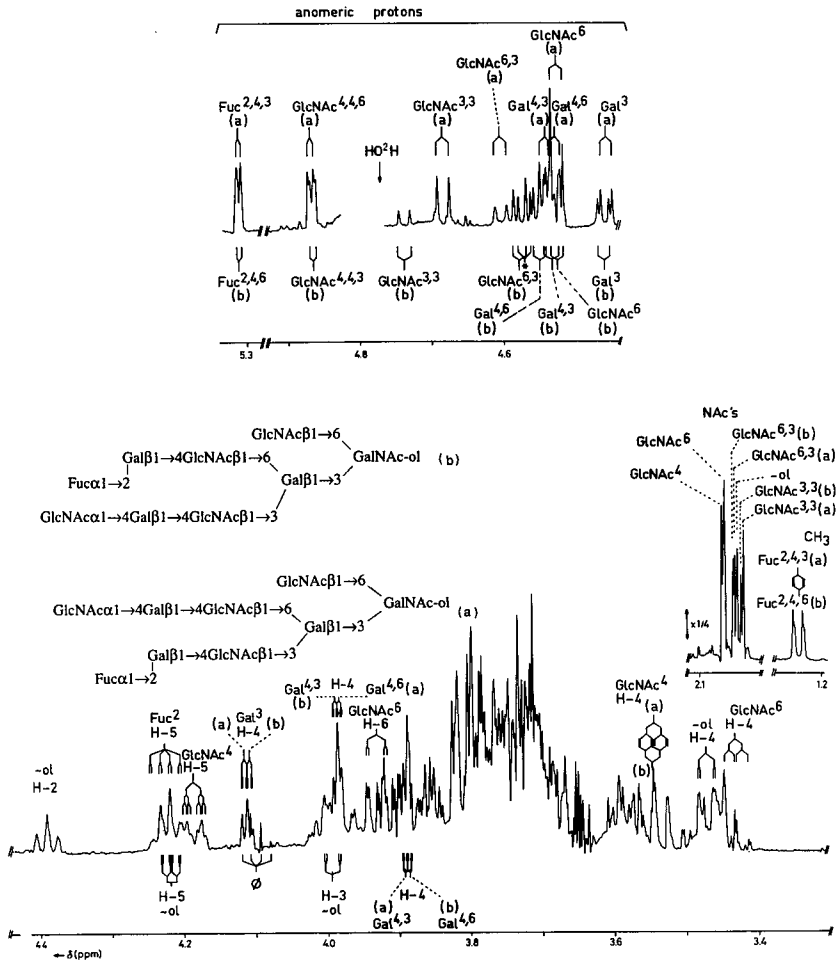

Figure 50. Resolution-enhanced ^{1}H-NMR spectrum of a mixture of **64** (b) and **65** (a). For comments, see Figure 30.

The ^{1}H-NMR spectrum of **66** (Dua *et al.*, 1986) shows three anomeric signals, namely, β-Gal^3 H-1 at $\delta = 4.710$ ppm ($J_{1,2} = 7.4$ Hz), α-GalNAc^3 H-1 at $\delta = 5.189$ ppm ($J_{1,2} = 3.8$ Hz), and α-Fuc^{2,3} H-1 at $\delta = 5.389$ ppm ($J_{1,2}$ not determined, because the line shape is distorted due to virtual

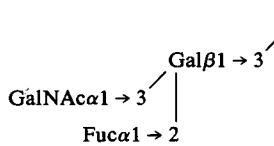

(66)

TABLE 17

^{1}H Chemical Shifts (24 °C) of Structural-Reporter Groups of Constituent Monosaccharides of Blood Group A-Containing Oligosaccharide-Alditols (66–74)

Residue	Reporter group	66 	67 	68 	69 	70 	71 	72 	73 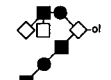	74 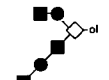
GalNAc-ol	H-2	4.304	4.309	4.302	4.392	4.402	4.270	4.280	4.402	4.400
	H-3	4.100	4.081	4.095	4.077	4.083	4.088	3.981	4.040	4.059
	H-5	4.125	4.225	4.220	4.270	4.275	4.220	4.116	4.261	4.282
	H-6	3.675	3.915	3.920	3.940	3.945	3.940	3.635	3.940	3.940
	H-6′	3.675	3.704	3.720	3.710	3.685	3.700	3.635	3.700	3.700
	NAc	2.048	2.047	2.049	2.046	2.058	2.047	2.036	2.063	2.063
Gal[3]	H-1	4.710	4.700	4.700	4.462	4.575	4.700	—	4.436	4.433
	H-3	4.019	4.011	4.025	3.667	3.847	4.010	—	3.720	3.722
	H-4	4.225	4.215	4.225	3.895	3.930	4.220	—	4.118	4.142
GlcNAc[6]	H-1	—	4.560	4.587	4.533	4.558	4.571	—	4.524	4.558
	H-6	—	3.942	4.018	4.000	4.010	4.007	—	4.005	4.005
	NAc	—	2.055	2.049	2.066	2.058	2.058	—	2.063	2.063

GlcNAc^{3}	H-1	—	—	—	—	—	—	4.581	—	—
	H-3	—	—	—	—	—	—	4.037	—	—
	NAc	—	—	—	—	—	—	2.117	—	—
Gal^{4,6}	H-1	—	—	4.472	4.594	4.598	4.597	—	4.599	4.466
	H-4	—	—	3.920	4.226	4.218	4.220	—	4.213	3.915
Gal^{3,3}	H-1	—	—	—	—	—	—	4.714	4.710	4.704
	H-4	—	—	—	—	—	—	4.225	4.213	4.223
GlcNAc^{3,3}	H-1	—	—	—	—	—	—	—	4.599	4.621
	H-3	—	—	—	—	—	—	—	4.010	4.011
	NAc	—	—	—	—	—	—	—	2.063	2.063
GalNAc^{3}	H-1	5.189	5.189	5.189	5.175	5.177	5.188[a]/5.176[b]	5.187	5.177[c]/5.177[d]	5.181
	H-2	4.247	4.247	4.249	4.230	4.237	4.247	4.222	4.219/4.237	4.233
	H-4	4.019	4.02	4.02	4.010	4.010	4.010/3.990	3.980	3.973/4.002	3.967
	H-5	4.156	4.160	4.162	4.210	4.235	4.161/4.220	4.265	4.294/4.221	4.295
	NAc	2.048	2.047	2.049	2.046	2.039	2.047	2.036	2.039	2.036
Fuc^{2,3}	H-1	5.389	5.381	5.379	—	5.217	5.372	5.264	5.252	5.251
	H-5	4.337	4.336	4.325	—	4.277	4.322	4.326	4.338	4.335
	CH_3	1.237	1.232	1.235	—	1.247	1.230	1.243	1.252	1.245
Fuc^{2,4}	H-1	—	—	—	5.348	5.349	5.348	—	5.353	—
	H-5	—	—	—	4.319	4.317	4.322	—	4.317	—
	CH_3	—	—	—	1.248	1.247	1.248	—	1.252	—

[a] GalNAc^{3,3}; [b] GalNAc^{3,4}; [c] GalNAc^{3,3}; [d] GalNAc^{3,4}.

coupling). The chemical shift value of the GalNAc-ol H-2 signal (δ = 4.304 ppm) is greatly affected by the presence of the $\alpha 1 \rightarrow 3$-linked GalNAc residue [$\Delta\delta = -0.091$ ppm, when compared to Gal$\beta 1 \rightarrow 3$GalNAc-ol (**2**); $\Delta\delta = -0.095$ ppm, when compared to Fuc$\alpha 1 \rightarrow 2$Gal$\beta 1 \rightarrow 3$GalNAc-ol (**29**)]. For this reason, the GalNAc-ol H-2 resonance at $\delta = 4.304$ ppm appears outside the general region for this structural-reporter group, being δ = 4.38–4.40 ppm (see Section 11). Also the GalNAc-ol H-5 signal undergoes an upfield shift ($\Delta\delta = -0.071$ ppm, when compared to **2**; $\Delta\delta = -0.038$ ppm, when compared to **29**). The Gal^3 H-1 signal is highly sensitive for introduction of the α-GalNAc residue. The downfield shift caused by $\alpha 1 \rightarrow 2$ fucosylation of **2** (→**29**, $\Delta\delta = +0.106$ ppm) increases upon attachment of α-GalNac (**29** → **66**, $\Delta\delta = +0.126$ ppm). The Gal^3 H-3 resonance shows a downfield shift of $\Delta\delta = +0.139$ ppm. It has to be noted that some earlier reported proton assignments made by Van Halbeek *et al.* (1981a) have been revised by Dua *et al.* (1986) on the basis of COSY experiments, 1D decoupling and simulation of all multiplet structures. The reported NOE data are interesting for the following reasons. Irradiation of the GalNAc H-1 signal gives, in addition to the effect at GalNAc H-2, a very small enhancement at the Gal H-3 resonance but a large effect at Gal H-4 adjacent to the position of the glycosidic linkage. This result contrasts with the more common observation for oligosaccharides that upon irradiation of the anomeric proton the major interresidue NOE effect is at the proton attached to the aglycone position (Bock *et al.*, 1984; Brisson and Carver, 1983; Koerner *et al.*, 1983, 1984). It is clear that the blood group A determinant adopts a conformation in which GalNAc H-1 is closer to Gal H-4 than to Gal H-3 (Lemieux *et al.*, 1980). This finding demonstrates that the application of NOE data as a proof for the determination of the position of the glycosidic linkage has to be done with great care, preferably on guidance of a 3D model. The presence of the blood group A determinant directly attached at GalNAc-ol C-3 is reflected by specific structural-reporter sets for $GalNAc^3$ (H-1, δ = 5.189 ppm; H-5, δ = 4.156 ppm) and for $Fuc^{2,3}$ (H-1, δ = 5.389 ppm; H-5, δ = 4.337 ppm; CH_3, δ = 1.237 ppm); identical sets are present in the spectra of **67**, **68**, and **71** (Table 17). For conformational energy calculations, see Bush *et al.* (1986).

Oligosaccharide-alditol **67** is an extension of **66** with β-GlcNAc at C-6 of GalNAc-ol (Dua *et al.*, 1986). The various structural-reporter-group signals specific for the occurrence of the GalNAc$\alpha 1 \rightarrow 3$(Fuc$\alpha 1$

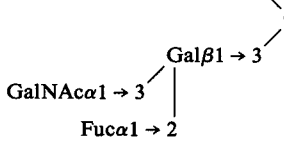

(**67**)

→ 2)Galβ1 → element at GalNAc-ol C-3 are identical to those found in **66**. The GlcNAc^6 residue shows signals for H-1 at $\delta = 4.560$ ppm, H-6 at $\delta = 3.942$ ppm, and NAc at $\delta = 2.055$ ppm, being comparable to those observed for Fucα1 → 2Galβ1 → 3(GlcNAcβ1 → 6)GalNAc-ol **38** (Table 12). The GalNAc-ol H-2 chemical shift region usually found for the GlcNAcβ1 → 6(Galβ1 → 3)GalNAc-ol core structure (H-2, δ = 4.38–4.41 ppm) (see Section 11) does not hold for **67** (GalNAc-ol H-2, $\delta = 4.309$ ppm), demonstrating the large effect of α1 → 3-linked GalNAc at Gal^3.

Compound **68** is an extension of **67** with an additional β-Gal residue at C-4 of GlcNAc^6 (Dua *et al.*, 1986). The blood group A determinant at

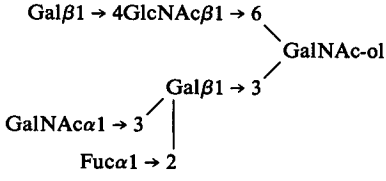

(68)

C-3 of GalNAc-ol can be deduced from the ^{1}H-NMR spectrum in a similar way as reported for **66** and **67**. The structural-reporter groups for the Galβ1 → 4GlcNAcβ1 → 6 element are in agreement with those already discussed (see, e.g., **39**, Table 12).

The oligosaccharide-alditol **69** is an isomer of **68** (Dua *et al.*, 1986). Because of the absence of GalNAcα1 → 3, directly linked to Gal^3, the

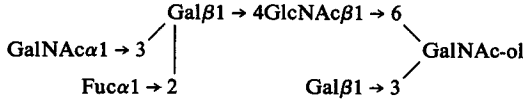

(69)

establishment of the GlcNAcβ1 → 6(Galβ1 → 3)GalNAc-ol core type structure can directly be based on the usual GalNAc-ol H-2 and H-5 signals at $\delta = 4.392$ and 4.270 ppm, respectively (see Section 11). The terminal position of the Gal^3 residue is evident from the H-1 signal at $\delta = 4.462$ ppm ($J_{1,2}$ = 8.1 Hz) and its H-4 signal at $\delta = 3.895$ ppm, being similar to those observed for **25** (Table 7) and **40** (Table 12). Based on coupling constants (see Section 3), the other two β-anomeric signals at $\delta = 4.533$ ppm ($J_{1,2} = 8.0$ Hz) and $\delta = 4.594$ ppm ($J_{1,2} = 7.3$ Hz) have been assigned to GlcNAc^6 H-1 and Gal^{4,6} H-1, respectively. It should be noted that in this case a Gal H-1 signal resonates at a more downfield position than a GlcNAc H-1 doublet (see Section 3). The attachment of the α-Fuc and α-GalNAc residues at the Gal^{4,6} residue of the *N*-acetyllactosamine element has been shown by NOE experiments. The GlcNAc^6 H-1, H-6, and NAc structural reporters at $\delta = 4.533$, 4.000, and 2.066 ppm are identical to those established for

GlcNAc^6 in Fucα1 → 2Galβ1 → 4GlcNAcβ1 → 6(Galβ1 → 3)GalNAc-ol (**40**). As compared to **40**, the additional α1 → 3-linked GalNAc residue causes downfield shifts for the Gal^{4,6} H-1 ($\Delta\delta$ = +0.058 ppm) and H-4 signals. The presence of a blood group A determinant in a backbone type-2 chain [GalNAcα1 → 3(Fucα1 → 2)Galβ1 → 4GlcNAcβ1 →] shows structural-reporter sets for GalNAc^3 and Fuc^{2,4}, that are different from those discussed for **66–68**. The GalNAc^3 set consists of H-1 at δ = 5.175 ppm and H-5 at δ = 4.210 ppm, whereas the Fuc^{2,4} set has H-1 at δ = 5.348 ppm, H-5 at δ = 4.319 ppm, and CH_3 at δ = 1.248 ppm.

Compound **70** is an α1 → 2 fucosylated form of **69** (Dua *et al.*, 1986).

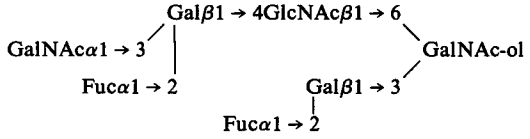

(70)

The GlcNAcβ1 → 6(Galβ1 → 3)GalNAc-ol core type is evidenced by the GalNAc-ol structural reporters H-2 at δ = 4.402 ppm and H-5 at δ = 4.275 ppm. As has been discussed for **38** and **39** (Table 12), the occurrence of a Fucα1 → 2Galβ1 → 3GalNAc-ol element comes to expression in the Fuc^{2,3} H-1, H-5, and CH_3 signals at δ = 5.217, 4.277, and 1.247 ppm, respectively, and in the Gal^3 H-1 and H-4 signals at δ = 4.575 and 3.930 ppm, respectively. The blood group A/backbone type-2 chain upper branch is reflected by a similar series of structural-reporter groups for the constituting monosaccharides as presented for **69**. The observed shift effects for GlcNAc^6 H-1 and NAc, when going from **25** to **39** (α1 → 2 fucosylation; Table 12) are also evident from the step **69** → **70**. The fucosylation at Gal^3 leads to small shift effects in the upper branch, especially at the GalNAc^3 NAc and H-5 signals (Table 17).

For the interpretation of the ^{1}H-NMR data of **71** (Dua *et al.*, 1986), use can be made of the spectra of **68** and **69**. The chemical shifts of the

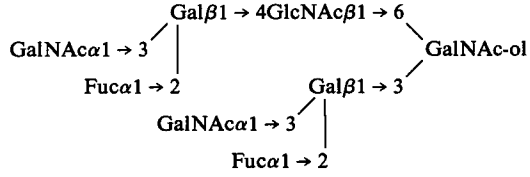

(71)

GalNAc-ol H-2 (δ = 4.270 ppm) and H-5 (δ = 4.220 ppm) signals imply substitution at C-3 by a blood group A determinant and at C-6 by GlcNAc^6. The various ^{1}H-NMR parameters of the A determinant attached at C-3 of GalNAc-ol match those reported for that element in **68**. The structural-

reporter groups of the blood group A determinant present in the upper branch fit those parameters discussed for **69**. The difference between the chemical shift values of the GlcNAc^6 H-1 (δ = 4.571 ppm) and NAc (δ = 2.058 ppm) signals, when comparing **69** and **71**, is due to the presence of the blood group A structure in the lower branch (compare with **67** and **68**).

Compound **72** is an oligosaccharide-alditol having a blood group A/backbone type-1 chain portion (Dua *et al.*, 1986). The ^{1}H-NMR spectrum of **72** shows two β-anomeric signals, namely, GlcNAc^3 H-1 at δ = 4.581 ppm

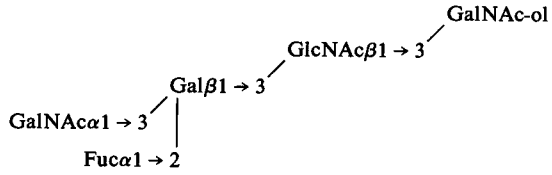

(72)

($J_{1,2}$ = 8.0 Hz) and Gal^{3,3} H-1 at δ = 4.714 ppm ($J_{1,2}$ = 7.3 Hz). This furnishes a further example wherein the Gal H-1 signal is at a more downfield position than the GlcNAc H-1 signal (see Section 3), as a result of the presence of the blood group A determinant. The finding of GalNAc-ol H-2 and H-5 signals at δ = 4.280 and 4.116 ppm, respectively, is in accordance with the general regions given for the GlcNAcβ1 → 3GalNAc-ol core structure (H-2, δ = 4.27–4.29 ppm; H-5, δ = 4.11–4.14 ppm) (see Section 11). Also the GalNAc-ol NAc singlet at δ = 2.036 ppm resonates in the defined region of δ = 2.034–2.038 ppm. The GlcNAc^3 H-3 signal at δ = 4.037 ppm, resonating outside the bulk of skeleton protons, is indicative of β-substitution of GlcNAc^3 at C-3. The Galβ1 → 3GlcNAcβ1 → element (backbone type-1 chain) has been confirmed by the observation of a NOE effect at GlcNAc^3 H-3 on irradiation of Gal^{3,3} H-1. The GlcNAc^3 H-3 position is even more downfield than observed for Galβ1 → 3GlcNAcβ1 → 3GalNAc-ol (**18**) (δ = 3.911 ppm) and for Fucα1 → 2Galβ1 → 3GlcNAcβ1 → 3GalNAc-ol (**37**) (δ = 4.017 ppm). Additional NOE effects have been observed at Gal^{3,3} H-2 on irradiation of Fuc^{2,3} H-1 and at Gal^{3,3} H-4 on irradiation of GalNAc^3 H-1. The presence of the blood group A constituents GalNAc and Fuc in another molecular environment leads to a third combination of structural-reporter sets for these residues. In this case GalNAc^3 is reflected by the H-1 and H-5 signals at δ = 5.187 and 4.265 ppm, respectively, and Fuc^{2,3} by the H-1, H-5, and CH_3 signals at δ = 5.264, 4.326, and 1.243 ppm, respectively.

Compound **73** is an oligosaccharide-alditol having blood group A determinants involved in both backbone type-1 and type-2 chains (Dua *et al.*, 1986). The occurrence of the GlcNAcβ1 → 6(Galβ1 → 3)GalNAc-ol core structure is evident from the GalNAc-ol H-2 and H-5 signals at δ = 4.402 and 4.261 ppm, respectively. The backbone type-2 chain linked

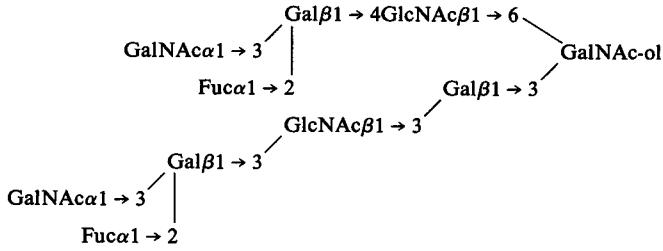

(73)

to GalNAc-ol C-6 is concluded from a comparison of the structural-reporter groups of $Fuc^{2,4}$, $GalNAc^{3,4}$, $Gal^{4,6}$, and $GlcNAc^{6}$ with those in **69–71**. They are further supported by NOE experiments. The Galβ1 → 3GalNAc-ol linkage is supported by a NOE effect at GalNAc-ol H-3 on irradiation of Gal^{3} H-1. The chemical shift of Gal^{3} H-4 at $\delta = 4.118$ ppm implies that this residue is substituted at C-3 by $GlcNAc^{3,3}$ (see **26**, **27** in Table 7 and **12/13** in Table 2). The structural reporters of the $Fuc^{2,3}$, $GalNAc^{3,3}$, and $Gal^{3,3}$ residues in the backbone type-1 chain in the lower branch are comparable to those of the analogous chain in **72**. They differ from those of the backbone type-2 chain in the upper branch, and from those of the A determinant directly connected to Gal^{3} (see **66–68**). The β1 → 3 linkage of $Gal^{3,3}$ to $GlcNAc^{3,3}$ (backbone type-1 chain) has been demonstrated by the observation of a NOE effect at the $GlcNAc^{3,3}$ H-3 resonance on irradiation of $Gal^{3,3}$ H-1.

Compound **74** (Dua *et al.*, 1986) is missing the blood group A determinant in the upper branch, when compared with **73**. The occurrence

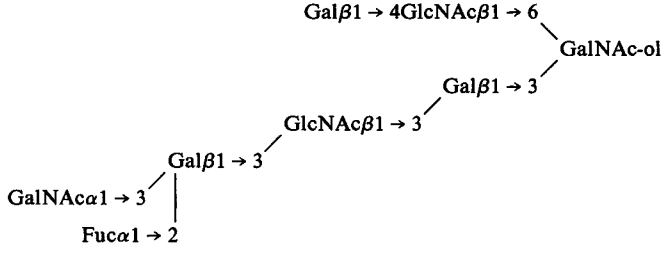

(74)

of the GlcNAcβ1 → 6(Galβ1 → 3)GalNAc-ol core structure is clear from the GalNAc-ol H-2 and H-5 signals at $\delta = 4.400$ and 4.282 ppm, respectively. The structural-reporter groups of the Galβ1 → 4GlcNAcβ1 → 6(→3Galβ1 → 3)GalNAc-ol part have been identified by comparison with those reported for **27** (Table 7). The structural-reporter-group signals of the lower branch have been identified on guidance of those of the lower branch in **73**. The structural assignments have been confirmed by various NOE experiments.

7. NEUTRAL *N*-ACETYL-β-D-GALACTOSAMINE-CONTAINING OLIGOSACCHARIDE-ALDITOLS

Three neutral oligosaccharide-alditols **75**–**77** containing β-GalNAc residues have been reported [**75**, Shimamura *et al.*, 1983, 1984; **76**, Kitajima *et al.*, 1984; **77** (after sialidase treatment), Iwasaki *et al.*, 1987a]. The available 270-MHz ^{1}H-NMR data are given in Table 18. In each case the Galβ1 → GalNAc-ol

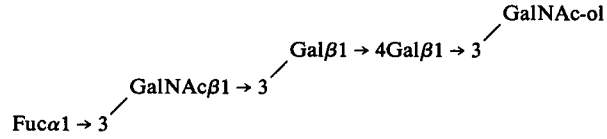

(75)

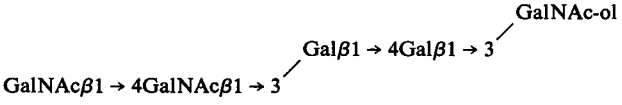

(76)

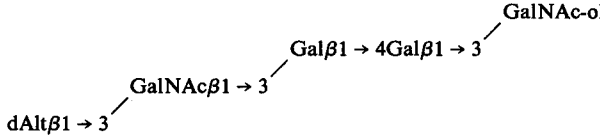

(77)

TABLE 18

^{1}H Chemical Shifts of Structural-Reporter Groups of Constituent Monosaccharides for Three Neutral β-GalNAc-Containing Oligosaccharide-Alditols Having the Galβ1 → 3GalNAc-ol Core Structure in Common (75–77)

Residue	Reporter group	**2** 	**75**[a] 	**76**[a] 	**77** 
GalNAc-ol	H-2	4.395	4.391	4.392	4.39
	NAc	2.050	2.032	2.062	2.05
Gal[3]	H-1	4.478	4.504 (7.9)[b]	4.501 (7.7)	4.50
Gal[4]	H-1	—	4.604 (7.1)	4.593 (7.7)	4.60
GalNAc[3]	H-1	—	4.718 (8.8)	4.652 (8.1)	4.71
	NAc	—	2.048	2.033	2.05
Fuc	H-1	—	4.998 (4.4)	—	—
	CH_3	—	1.204	—	—
GalNAc[4]	H-1	—	—	4.652 (8.1)	—
	NAc	—	—	2.049	—
dAlt	H-1	—	—	—	4.95
	CH_3	—	—	—	1.27
	H-5	—	—	—	3.79

[a] Spectrum recorded at 23 °C.
[b] Coupling constants are shown in parentheses.

3GalNAc-ol core element is supported by the presence of the GalNAc-ol H-2 signal at $\delta = 4.39$ ppm (see Section 11).

8. SIALYLATED OLIGOSACCHARIDE-ALDITOLS

8.1. Extensions of the Galβ1 → 3GalNAc-ol Core Structure

In this section, the relevant ^{1}H-NMR data of the sialylated saccharides **78–82** are summarized, all having Galβ1 → 3GalNAc-ol as the core structure (Table 19). The Galβ1 → 3GalNAc-ol core type is characterized by the H-2 and H-5 signals of GalNAc-ol at $\delta = 4.38$–4.40 and 4.14–4.20 ppm, respectively (see Section 11). The NAc singlet of GalNAc-ol is observed at $\delta = 2.045$–2.049 ppm.

The ^{1}H-NMR spectrum of **78** (Akiyama *et al.*, 1987; Damm *et al.*, 1987; Fiat *et al.*, 1988; Herkt *et al.*, 1985; Korrel *et al.*, 1984; Marti *et al.*, 1988;

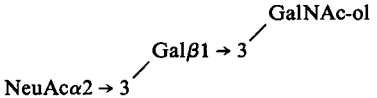

(78)

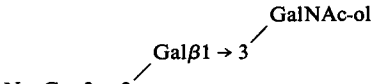

(78A)

Nato *et al.*, 1986; Savage *et al.*, 1986; Strecker *et al.*, 1985; Van Halbeek *et al.*, 1980, 1981b, 1988; Van Pelt *et al.*, 1988; Vliegenthart *et al.*, 1980, 1982) is depicted in Figure 51. The substitution at C-3 of GalNAc-ol is reflected by the GalNAc-ol H-2 and H-5 signals at $\delta = 4.390$ and 4.187 ppm, respectively. The structural-reporter groups of NeuAc, namely, H-3a at $\delta =$ 1.800 ppm and H-3e at $\delta = 2.774$ ppm, are indicative of α-NeuAc linked to C-3 of a Gal residue (Vliegenthart *et al.*, 1983). The downfield shifts of the Gal^3 H-1 and H-3 resonances ($\Delta\delta = +0.069$ and $+0.451$ ppm, respectively), as compared to Galβ1 → 3GalNAc-ol (**2**), are characteristic for the NeuAcα2 → 3Galβ1 → sequence (Vliegenthart *et al.*, 1983). For ^{1}H-NMR data of corresponding glycopeptides, see Berman (1987), Gejyo *et al.* (1983), Hirabayashi *et al.* (1990), and Weisshaar *et al.* (1987). In Figure 52 the ^{1}H-NMR spectrum of the NeuGc analog of **78**, namely, **78A**, is presented (Savage *et al.*, 1986). The structural reporters of **78A** are almost identical to those of **78**. The set of chemical shifts for NeuGc comprises H-3a at $\delta = 1.817$ ppm, H-3e at $\delta = 2.787$ ppm, and NGc at $\delta = 4.122$ ppm. It has to be noted that the NeuGc H-3 signals appear at slightly more downfield positions than those of NeuAc H-3 in **78**. This is a general feature; see also **6**/**6A** and **9**/**9A**, Table 1.

Compound **79** is an extension of **78**, with a β-GalNAc residue at C-4 of Gal[3] (Herkt *et al.*, 1985). The ^{1}H-NMR data support the monosubstitution

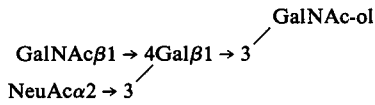

(79)

at C-3 of GalNAc-ol by Gal[3] (GalNAc-ol H-2, $\delta = 4.380$ ppm; GalNAc-ol H-5, $\delta = 4.157$ ppm). The β-GalNAc[4] residue is reflected by its H-1 and NAc reporters at $\delta = 4.725$ ppm ($J_{1,2} = 8.1$ Hz) and $\delta = 2.028$ ppm, respectively. The combination of the chemical shift values for the GalNAc[4], Gal[3], and NeuAc[3] reporter groups is specific for the blood group Cad determinant, being the GalNAcβ1 → 4(NeuAcα2 → 3)Galβ1 → structural element. In particular, the relatively downfield position of NeuAc H-3a ($\delta = 1.935$ ppm) together with the upfield position of NeuAc H-3e ($\delta = 2.682$ ppm), as compared to NeuAc in **78**, and the upfield shift of H-5 of GalNAc-ol ($\Delta\delta = -0.030$ ppm), are of interest. For ^{1}H-NMR data of the ganglioside-derived oligosaccharide GalNAcβ1 → 4(NeuAcα2 → 3)Galβ1 → 4Glc, see Dorland *et al.* (1986).

Compound **80** is an extension of **12** with a NeuAcα2 → 6 linked to Gal[4]. It has only been investigated in mixtures, namely, together with **92**

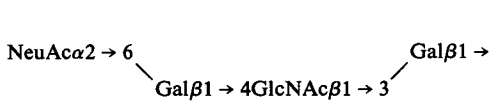

(80)

(Breg *et al.*, 1987) (Figure 53) and together with **82** (Van Halbeek *et al.*, 1988) (Figure 54). The core structure of **80** is evident from the GalNAc-ol H-2 and H-5 chemical shift values at $\delta = 4.398$ and 4.191 ppm, respectively. The Gal[3] residue bears at C-3 a β-GlcNAc residue, as can be derived from the chemical shift of the Gal[3] H-4 signal at $\delta = 4.130$ ppm, being characteristic for the →GlcNAcβ1 → 3Galβ1 → sequence (see Section 3.1). The chemical shift values of NeuAc H-3a at $\delta = 1.723$ ppm and H-3e at $\delta = 2.671$ ppm are indicative of the presence of NeuAc in α2 → 6 linkage to an *N*-acetyllactosamine unit (Vliegenthart *et al.*, 1983). As compared to **12**, the Gal[4] H-1 signal is shifted upfield ($\Delta\delta = -0.022$ ppm), whereas the GlcNAc[3] H-1 and NAc signals are shifted downfield ($\Delta\delta = +0.021$ and +0.019 ppm) (see Table 2).

Compound **81**, which is the α2 → 3 sialylated isomer of **80**, has been identified in a complex mixture of oligosaccharide-alditols (Van Halbeek

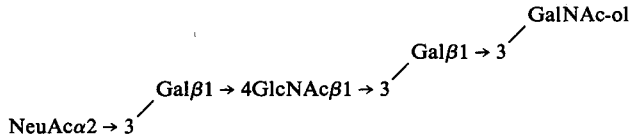

(81)

TABLE 19

^{1}H Chemical Shifts of Structural-Reporter Groups of Constituent Monosaccharides for Sialylated Oligosaccharide-Alditols with the Galβ1 → 3GalNAc-ol Core Structure in Common (78–82)

Residue	Reporter group	2 	78 	78A 	79[a] 	12 	80 	81 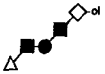	82[a] 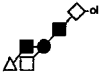
GalNAc-ol	H-2	4.395	4.390	4.389	4.380	4.396	4.398	4.394	4.395
	H-3	4.065	4.074	4.073	4.062	4.051	4.049	4.052	4.047
	H-4	3.507	3.498	3.495	3.510	3.497	3.494	3.491	3.492
	H-5	4.196	4.187	4.188	4.157	4.184	4.191	4.185	4.184
	NAc	2.050	2.046	2.045	2.048	2.048	2.049	2.047	2.046
Gal[3]	H-1	4.478	4.547	4.547	4.565	4.463	4.464[c]	4.464	4.459
	H-3	3.671	4.122	4.132	4.162	n.d.	n.d.	n.d.	n.d.
	H-4	3.901	3.931	n.d.[b]	4.095	4.126	4.130	4.126	4.129
NeuAc[3]	H-3a	—	1.800	—	1.935	—	—	1.797	1.793
	H-3e	—	2.774	—	2.682	—	—	2.759	2.765
	NAc	—	2.034	—	2.034	—	—	2.031	2.031

NeuGc[3]	H-3a	—	—	1.817	—	—	—	—	—
	H-3e	—	—	2.787	—	—	—	—	—
	NGc	—	—	4.122	—	—	—	—	—
GalNAc[4]	H-1	—	—	—	4.725	—	—	—	—
	H-4	—	—	—	3.925	—	—	—	—
	NAc	—	—	—	2.028	—	—	—	—
GlcNAc[3]	H-1	—	—	—	—	4.688	4.709	4.698	4.684
	H-6	—	—	—	—	3.953	n.d.	n.d.	3.96
	NAc	—	—	—	—	2.042	2.061	2.039	2.029
Gal[4]	H-1	—	—	—	—	4.480	4.458[c]	4.557	4.528
	H-3	—	—	—	—	n.d.	n.d.	4.114	4.084
	H-4	—	—	—	—	3.928	n.d.	n.d.	3.932
Fuc[3]	H-1	—	—	—	—	—	—	—	5.130
	H-5	—	—	—	—	—	—	—	4.821
	CH_3	—	—	—	—	—	—	—	1.170
NeuAc[6]	H-3a	—	—	—	—	—	1.723	—	—
	H-3e	—	—	—	—	—	2.671	—	—
	NAc	—	—	—	—	—	2.029	—	—

[a] Spectrum recorded at 22 °C.
[b] n.d. means value could not be determined merely by inspection of the spectrum.
[c] Assignments may have to be interchanged.

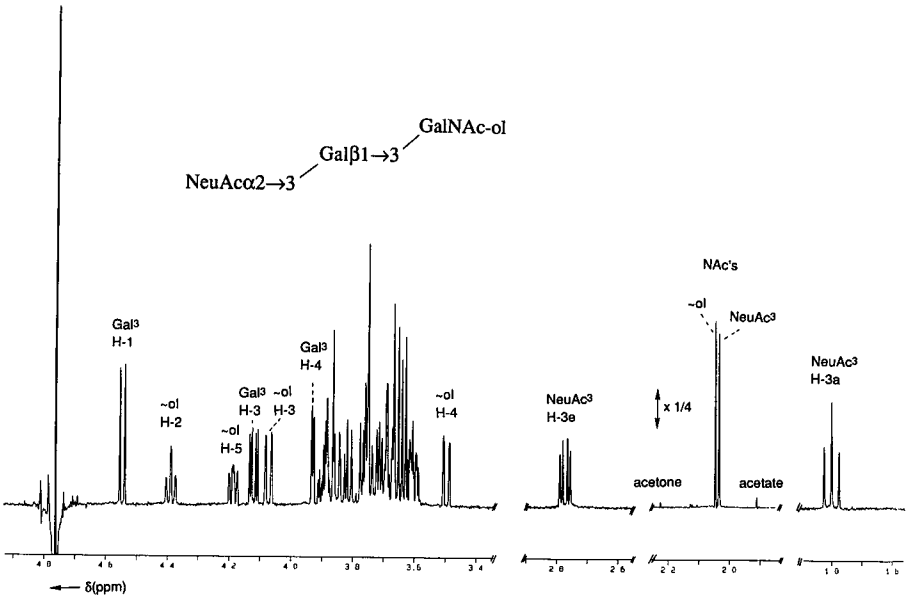

Figure 51. Resolution-enhanced ^{1}H-NMR spectrum of **78**. The relative-intensity scale of the *N*-acetyl methyl proton region of the spectrum differs from that of the other parts, as indicated.

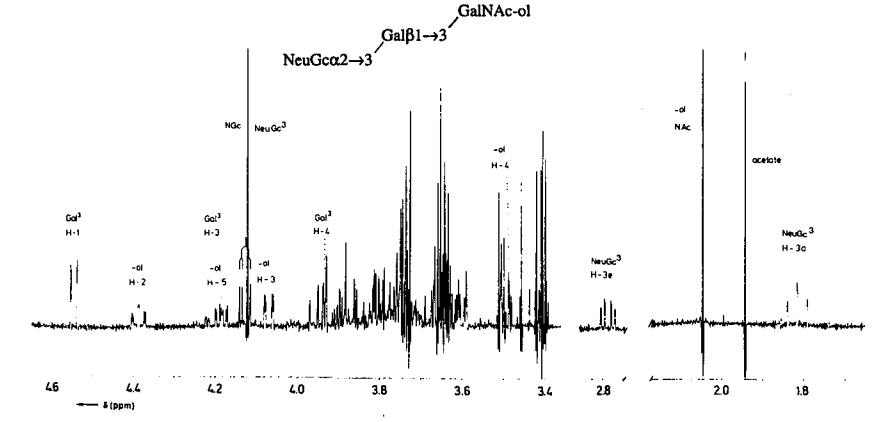

Figure 52. Resolution-enhanced ^{1}H-NMR spectrum of **78A**.

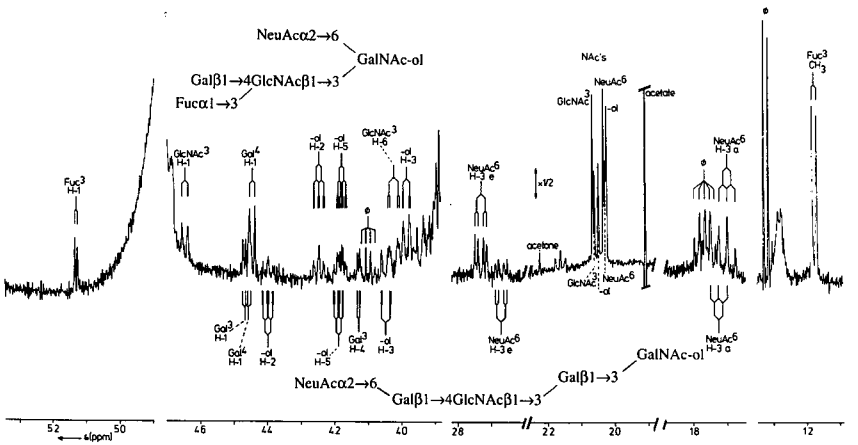

Figure 53. Resolution-enhanced ^{1}H-NMR spectrum of a mixture of **80** (lower) and **92** (upper). The relative-intensity scale of the *N*-acetyl methyl proton region of the spectrum differs from that of the other parts, as indicated. Contaminating acetate gives rise to a signal at δ = 1.908 ppm. The signal(s) marked by ϕ stem(s) from (a) frequently occurring, nonprotein noncarbohydrate contaminant(s).

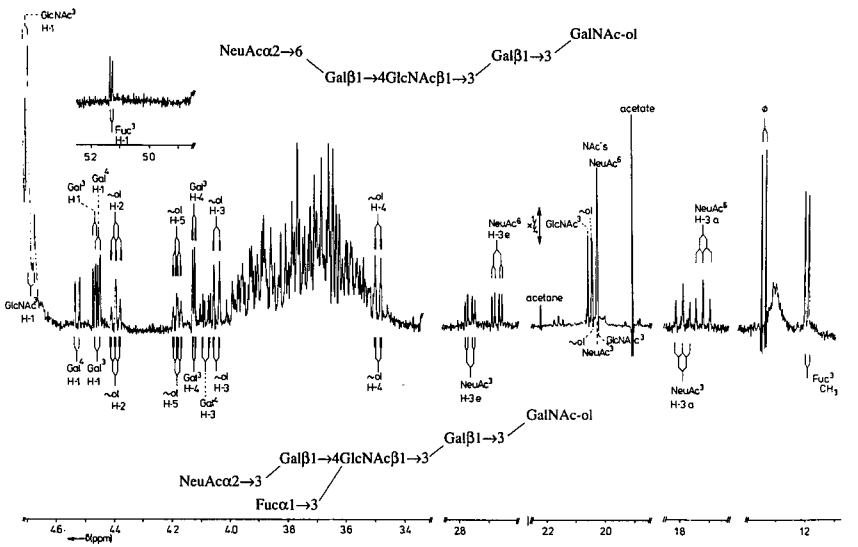

Figure 54. Resolution-enhanced ^{1}H-NMR spectrum of a mixture of **80** (upper) and **82** (lower). For comments, see Figure 53.

et al., 1988). The structural-reporter-group signals of GalNAc-ol H-2 (δ = 4.394 ppm), GalNAc-ol H-5 (δ = 4.185 ppm), and Gal^3 H-4 (δ = 4.126 ppm) demonstrate the basic structure to be identical to **12**. The presence of the NeuAcα2 → 3Galβ1 → 4GlcNAcβ1 → sequence is supported by the NeuAc H-3a and H-3e signals at δ = 1.797 and 2.759 ppm, respectively. Furthermore, the Gal^4 H-1 resonance is observed at δ = 4.557 ppm ($\Delta\delta$ = +0.077 ppm, as compared to **12**), the Gal^4 H-3 signal at the relatively downfield position of δ = 4.114 ppm, and the GlcNAc^3 NAc singlet at δ = 2.039 ppm ($\Delta\delta$ = −0.003 ppm) (see Vliegenthart *et al.*, 1983).

The ^{1}H-NMR spectrum of **82** (Lamblin *et al.*, 1984a; Van Halbeek *et al.*, 1988) is depicted in Figure 55. The occurrence of the Galβ1 →

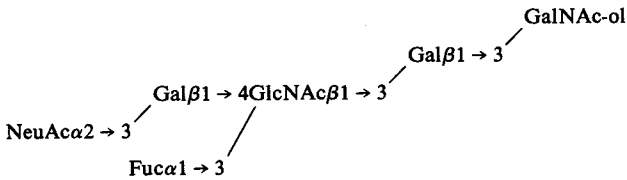

(82)

3GalNAc-ol core structure is established by the GalNAc-ol H-2 signal at δ = 4.395 ppm and the H-5 signal at δ = 4.184 ppm, whereas the extension by an *N*-acetyllactosamine unit attached in β1 → 3 linkage to the Gal^3 residue is evidenced by the Gal^3 H-4 signal at δ = 4.129 ppm. In a similar way as discussed for **81**, the α2 → 3-linked NeuAc at Gal^4 gives rise to the specific set of NeuAc^3 H-3a and H-3e structural reporters at δ = 1.793 and 2.765 ppm, respectively. Furthermore, the Gal^4 H-3 signal is found at δ = 4.084 ppm. In accordance with the nonsialylated analog **30** (Table 9), the Fuc residue in α1 → 3 linkage to GlcNAc^3 of the *N*-acetyllactosamine moiety has a typical set of Fuc structural-reporter-group signals, namely, H-1 (δ = 5.130 ppm), H-5 (δ = 4.821 ppm), and CH_3 (δ = 1.170 ppm). The simultaneous substitution of the *N*-acetyllactosamine unit by NeuAc^3 and Fuc^3 gives rise to the immuno group sialyl-X determinant in **82**. The effects of fucosylation (**12** → **30**) and sialylation (**30** → **82**) on the chemical shifts of the Gal^4 H-1 and GlcNAc^3 NAc signals are additive. The Gal^4 H-1 signal goes from δ = 4.480 ppm to δ = 4.461 ppm due to fucosylation of GlcNAc^3 (**81** → **82**, $\Delta\delta$ = −0.029 ppm), and then to δ = 4.528 ppm due to α2 → 3 sialylation of Gal^4 (**12** → **81**, $\Delta\delta$ = +0.077 ppm). The GlcNAc^3 NAc signal moves from δ = 2.042 ppm to δ = 2.032 ppm upon fucosylation (**81** → **82**, $\Delta\delta$ = −0.010 ppm), and then to δ = 2.029 ppm upon sialylation (**12** → **81**, $\Delta\delta$ = −0.003 ppm).

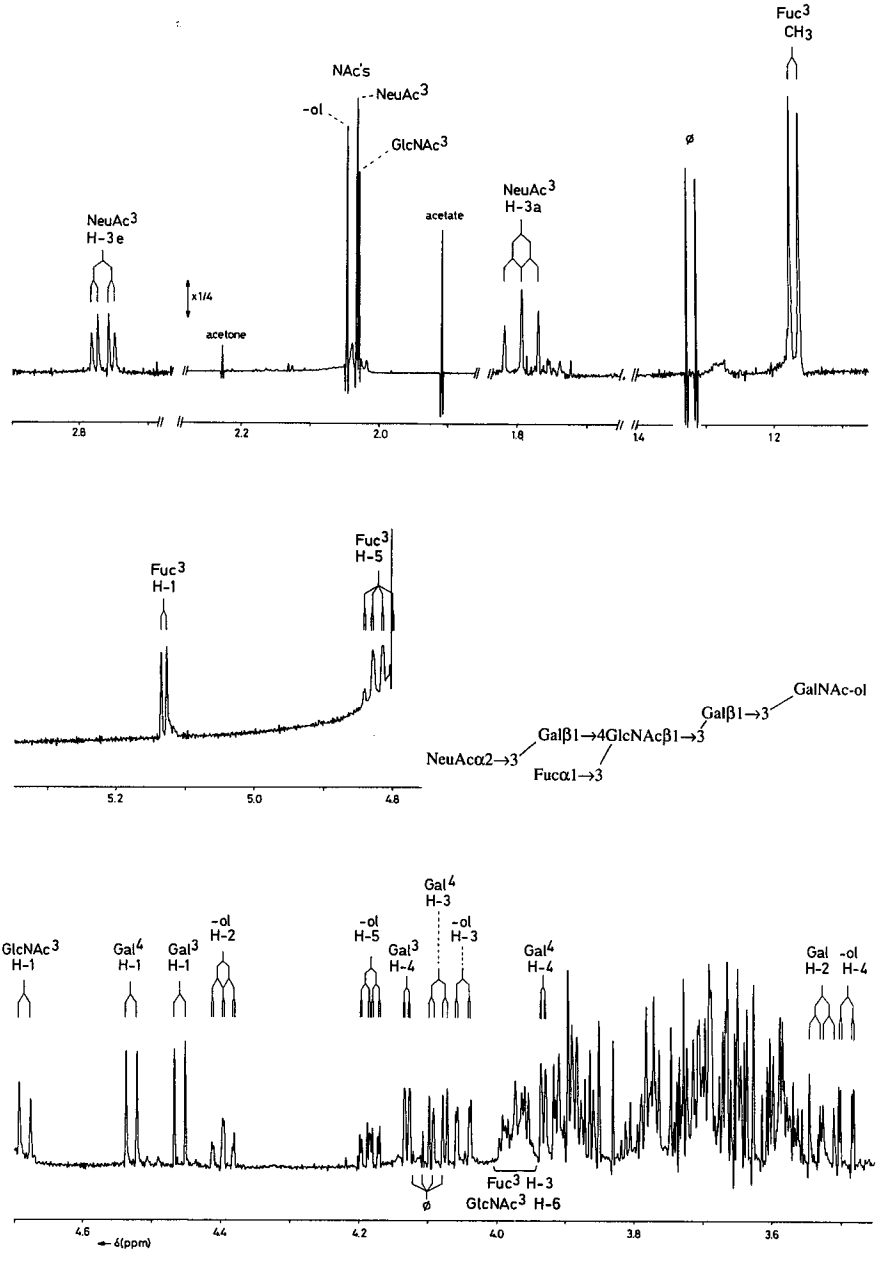

Figure 55. Resolution-enhanced ^{1}H-NMR spectrum of **82** at 22 °C. For comments, see Figure 53.

8.2. Extensions of the NeuAc/NeuGcα2 → 6(Galβ1 → 3)GalNAc-ol Core Structure

In this section, the ^{1}H-NMR spectra of the sialylated carbohydrates **83–88**, having the NeuAcα2 → 6(Galβ1 → 3)GalNAc-ol or the NeuGcα2 → 6(Galβ1 → 3)GalNAc-ol core structure, will be discussed (Table 20). In general, the GalNAc-ol H-2 signals are found in the region δ = 4.36–4.39 ppm, but exceptions occur (see **84**). The GalNAc-ol H-5 signals resonate in the region δ = 4.18–4.25 ppm (see Section 11). Concomitantly, GalNAc-ol H-6′ gives rise to a doublet of doublets at δ = 3.44–3.49 ppm, clearly upfield from the bulk of skeleton proton signals. The set of chemical shifts of NeuAc H-3a at δ = 1.69–1.71 ppm and H-3e at δ = 2.72–2.73 ppm is typical for the α2 → 6 linkage to GalNAc-ol. NeuGc H-3 signals resonate more downfield than NeuAc H-3 signals.

The ^{1}H-NMR spectrum of **83** (Nasir-Ud-Din *et al.*, 1986; Van Halbeek *et al.*, 1988), an α1 → 2 fucosylated extension of **9** (Table 1), is shown in

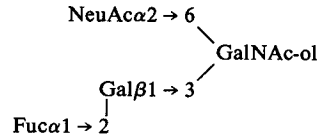

(83)

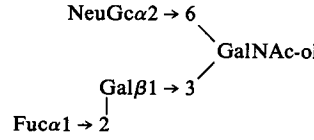

(83A)

Figure 56. The substitution pattern of the GalNAc-ol residue follows from the GalNAc-ol H-2 and H-5 signals at δ = 4.381 and 4.221 ppm, respectively, together with the GalNAc-ol H-6′ resonance at δ = 3.482 ppm. The set of structural-reporter-group signals for Fuc in α1 → 2 linkage to Gal^3, i.e., H-1 at δ = 5.268 ppm, H-5 at δ = 4.269 ppm, and CH_3 at δ = 1.235 ppm, deviates slightly from that reported for **29** (Table 9), being the asialo analog of **83**. The position of the Gal^3 H-1 doublet is similar to that observed in the spectrum of **29**. The presence of the α2 → 6-linked NeuAc residue is reflected by the H-3a and H-3e signals at δ = 1.700 and 2.730 ppm, respectively. As compared to **9**, the introduction of Fuc has an effect on the exact positions of the GalNAc-ol H-3, H-5, and NAc resonances. Compound **83A** (Van Halbeek *et al.*, 1981a) is the NeuGc analog of **83**. The structural reporters established for **83A** are almost identical to those of **83**. The specific set of chemical shifts for NeuGc comprises H-3a at δ = 1.714 ppm, H-3e at δ = 2.747 ppm, and NGc at δ = 4.122 ppm (compare with **9A**). The NeuGc H-3

multiplets resonate at more downfield positions, as compared with the NeuAc H-3 signals in **83**.

Compound **84** is an extension of **83A** with a GalNAc residue in $\alpha 1 \rightarrow 3$ linkage to Gal^3. Its ^{1}H-NMR spectrum (Nasir-Ud-Din *et al.*, 1986; Van

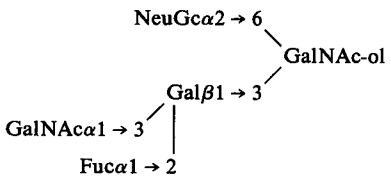

(84)

Halbeek *et al.*, 1981a) is depicted in Figure 57. In accordance with the substitution pattern of GalNAc-ol, the GalNAc-ol H-2 and H-5 signals resonate at $\delta = 4.291$ and 4.185 ppm, respectively. It has to be noted that the introduction of the GalNAc residue has a strong influence on the latter chemical shift values (compare with **83A**) (see Section 11). The presence of the blood group A determinant is reflected by the Fuc^2 H-1, H-5, and CH_3 signals at $\delta = 5.395$, 4.335, and 1.242 ppm, respectively, and the $GalNAc^3$ H-1, H-2, H-4, and H-5 signals at $\delta = 5.184$, 4.250, 4.023, and 4.166 ppm, respectively. Similar sets have been found for **66–68** (see also Gal^3 H-1, $\delta = 4.719$ ppm; Gal^3 H-3, $\delta = 4.014$ ppm; Gal^3 H-4, $\delta = 4.212$ ppm) (Table 17). The structural reporters for the NeuGc residue are identical to those found in **83A**.

In Figure 58 the ^{1}H-NMR spectrum of **85** is shown (Vliegenthart *et al.*, 1981). For additional references, see Akiyama *et al.* (1984, 1987), Capon

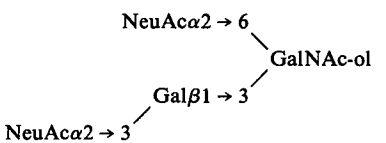

(85)

et al. (1989), Damm *et al.* (1987), Herkt *et al.* (1985), Korrel *et al.* (1984), Marti *et al.* (1988), Van Halbeek *et al.* (1980, 1981b), and Van Pelt *et al.* (1988). The substitution pattern of GalNAc-ol is clear from the GalNAc-ol H-2 and H-5 resonances at $\delta = 4.378$ and 4.240 ppm, and the GalNAc-ol H-6′ signal at $\delta = 3.475$ ppm. As compared to **9** (Table 1), substitution of Gal^3 affects the following NMR parameters of Gal^3: H-1, $\delta = 4.541$ ppm, $\Delta\delta = +0.067$ ppm; H-3, $\delta = 4.117$ ppm, $\Delta\delta = +0.45$ ppm; and H-4, $\delta = 3.927$ ppm, $\Delta\delta = +0.033$ ppm. Similar downfield shifts have been obtained from NMR spectra of carbohydrate chains containing NeuAcα2 → 3Galβ1 → units derived from *N*-glycoproteins (Vliegenthart *et al.*, 1983). In contrast to the situation of a $\beta 1 \rightarrow 3$ substitution at Gal^3 (see, e.g., **12–16**, Table 2), the resonance position of the Gal^3 H-4 signal is only slightly

TABLE 20

^{1}H Chemical Shifts of Structural-Reporter Groups of Constituent Monosaccharides for Sialylated Oligosaccharide-Alditols with the NeuAc/Gcα2 → 6(Galβ1 → 3)GalNAc-ol Core Structure in Common (83–88)

Residue	Reporter group	9 	83 	83A 	84 	85 	86 	87 	88 
GalNAc-ol	H-2	4.378	4.381	4.386	4.291	4.378	4.360	4.380	4.379
	H-3	4.055	4.083	4.087	4.089	4.067	4.047	4.041	4.041
	H-4	3.534	3.540	3.545	3.624	3.524	3.500	n.d.[c]	n.d.
	H-5	4.244	4.221	4.226	4.185	4.240	4.181	4.231	4.225
	H-6′	3.486	3.482	3.484	3.493	3.475	3.445	3.479	3.47
	NAc	2.047	2.038	2.043	2.044[a]	2.042	2.039	2.045	2.045
Gal[3]	H-1	4.474	4.583	4.586	4.719	4.541	4.561	4.461	4.464
	H-4	3.894	3.916	3.915	4.212	3.927	4.091	4.119	4.119
NeuAc[6]	H-3a	1.692	1.700	—	—	1.692	1.707	1.689	1.688
	H-3e	2.726	2.730	—	—	2.723	2.733	2.725	2.724
	NAc	2.033	2.034	—	—	2.032	2.032	2.033	2.032
NeuGc[6]	H-3a	—	—	1.714	1.711	—	—	—	—
	H-3e	—	—	2.747	2.750	—	—	—	—
	NGc	—	—	4.122	4.123	—	—	—	—

Fuc^2	H-1	—	5.268	5.271	5.395	—	—	—	—
	H-5	—	4.269	4.271	4.335	—	—	—	—
	CH_3	—	1.235	1.239	1.242	—	—	—	—
$GalNAc^3$	H-1	—	—	—	5.184	—	—	—	—
	NAc	—	—	—	2.046[a]	—	—	—	—
$NeuAc^3$	H-3a	—	—	—	—	1.800	1.933	—	—
	H-3e	—	—	—	—	2.774	2.681	—	—
	NAc	—	—	—	—	2.032	2.032	—	—
$GalNAc^4$	H-1	—	—	—	—	—	4.714[b]	—	—
	H-4	—	—	—	—	—	3.913	—	—
	NAc	—	—	—	—	—	2.025	—	—
$GlcNAc^3$	H-1	—	—	—	—	—	—	4.69	4.69
	NAc	—	—	—	—	—	—	2.042	2.032
Gal^4	H-1	—	—	—	—	—	—	4.480	4.458
	H-4	—	—	—	—	—	—	n.d.	n.d.
Fuc^3	H-1	—	—	—	—	—	—	—	5.136
	H-5	—	—	—	—	—	—	—	4.833
	CH_3	—	—	—	—	—	—	—	1.176

[a] Assignments may have to be interchanged.
[b] Measured at 12 °C (signal is hidden under HO^2H line at 27 °C).
[c] n.d. means values could not be determined merely by inspection of the spectrum.

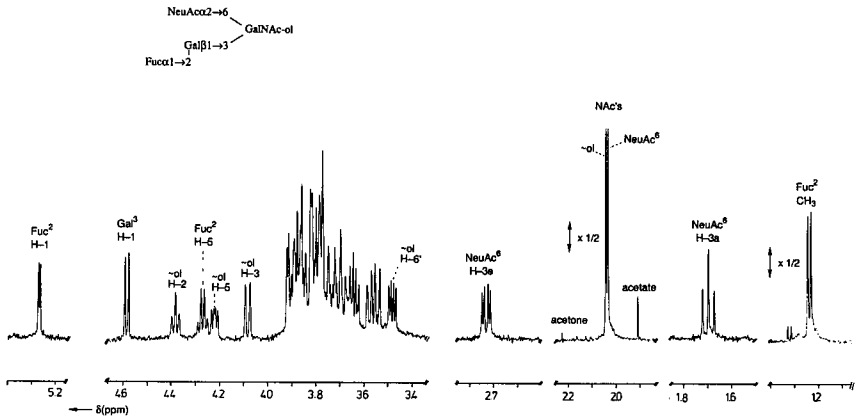

Figure 56. Resolution-enhanced ^{1}H-NMR spectrum of **83**. The relative-intensity scale of the *N*-acetyl and Fuc methyl proton regions of the spectrum differ from that of the other parts, as indicated. Contaminating acetate gives rise to a signal at $\delta = 1.908$ ppm.

altered in the step **9** → **85**. The structural-reporter-group signals for the NeuAc^6 residue are H-3a at $\delta = 1.692$ ppm and H-3e at $\delta = 2.723$ ppm, whereas the NeuAc^3 residue is characterized by H-3a and H-3e signals at $\delta = 1.800$ and 2.774 ppm, respectively. The latter set is similar to that reported for NeuAcα2 → 3Galβ1 → sequences in *N*-linked carbohydrate chains (Vliegenthart *et al.*, 1983). For ^{1}H-NMR data of corresponding glycopeptides, see Lecat *et al.* (1984), Hirabayashi *et al.* (1990), Linden *et al.* (1989), and Weisshaar *et al.* (1987).

The ^{1}H-NMR spectrum of the blood group Cad determinant-containing **86** is presented in Figure 59 (Blanchard *et al.*, 1983; Herkt *et al.*, 1985). The

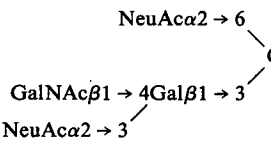

(86)

chemical shifts of the GalNAc-ol H-2, H-5, and H-6′ signals at $\delta = 4.360$, 4.181, and 3.445 ppm, respectively, point to the presence of a Gal residue in β1 → 3 linkage and a sialic acid residue in α2 → 6 linkage to GalNAc-ol. This NeuAc^6 residue is further characterized by its set of H-3 chemical shifts (H-3a, $\delta = 1.707$ ppm; H-3e, $\delta = 2.733$ ppm). The H-3 signals of NeuAc^3 occur at $\delta = 1.933$ ppm (H-3a) and $\delta = 2.681$ ppm (H-3e), whereas the GalNAc^4 residue gives rise to signals for H-1 at $\delta = 4.714$ ppm ($J_{1,2} = 7.6$ Hz) and NAc at $\delta = 2.025$ ppm. As has already been shown for the monosialo form **79** missing NeuAc^6 (Table 19), the combination of the

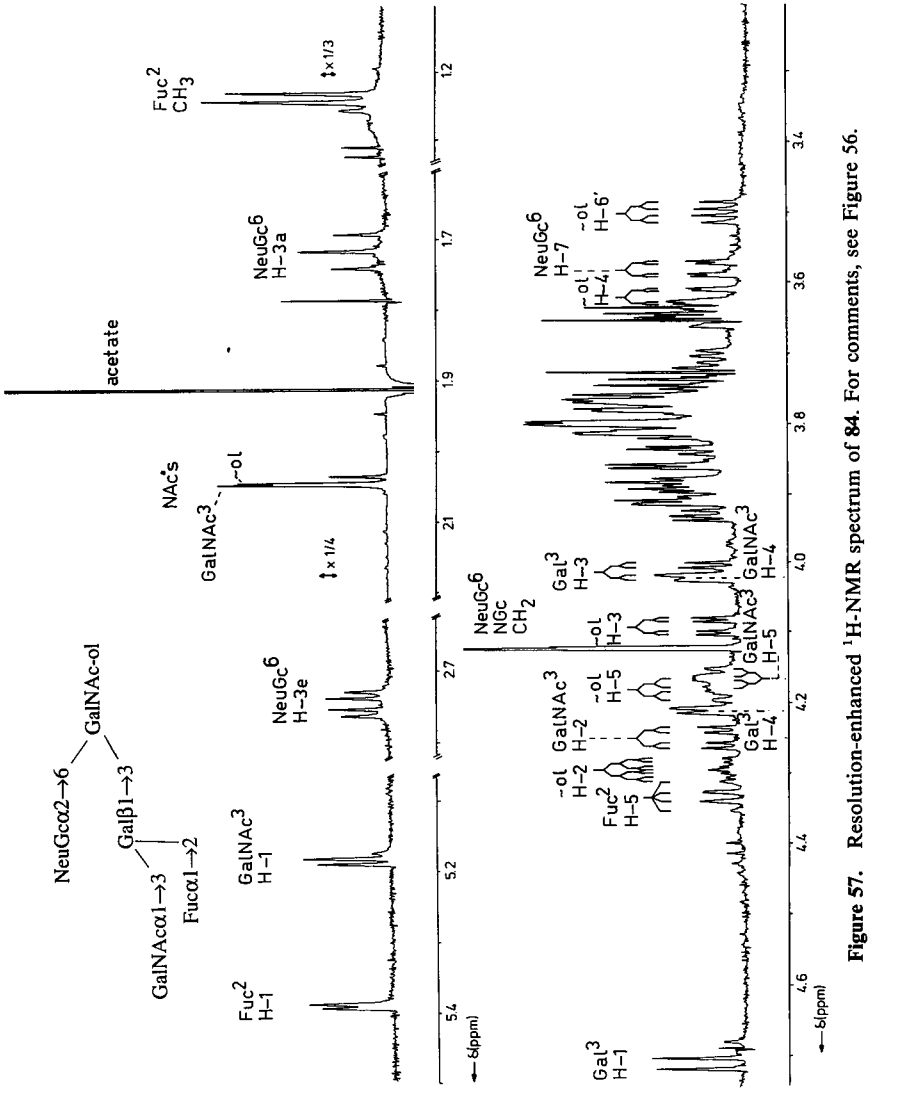

Figure 57. Resolution-enhanced ^{1}H-NMR spectrum of **84**. For comments, see Figure 56.

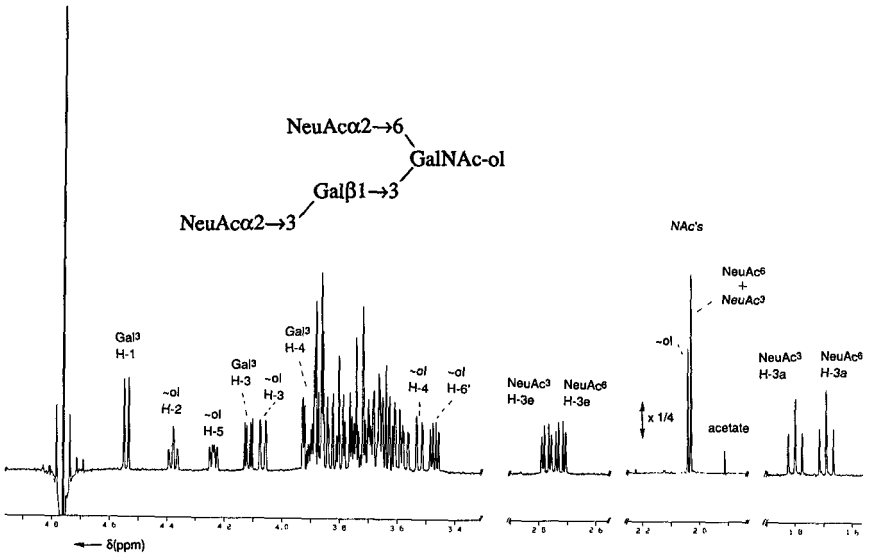

Figure 58. Resolution-enhanced ^{1}H-NMR spectrum of **85**. For comments, see Figure 53.

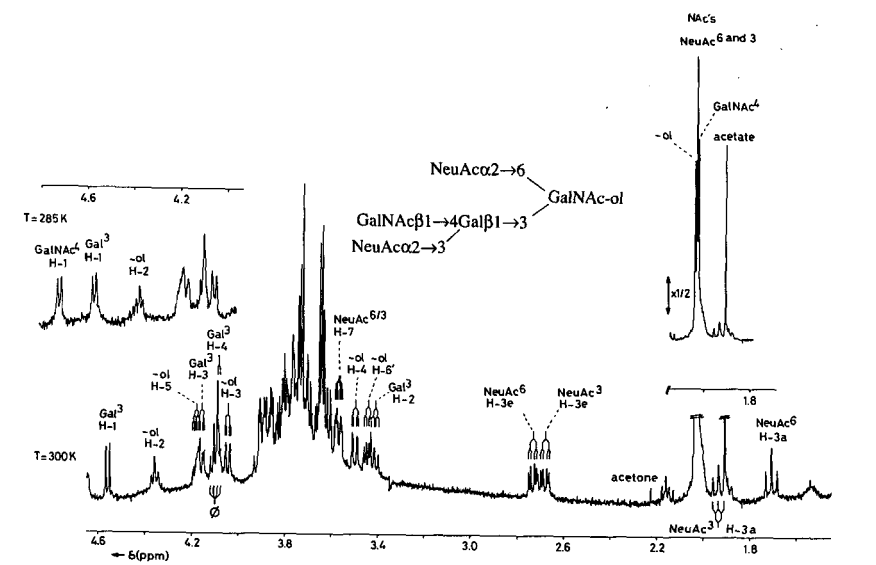

Figure 59. Resolution-enhanced ^{1}H-NMR spectrum of **86**. For comments, see Figure 53. The inset shows the $4.0 < \delta < 4.8$ ppm spectral region at 12 °C.

chemical shifts for the GalNAc[4], Gal[3], and NeuAc[3] reporters is highly diagnostic for the occurrence of the blood group Cad determinant. See also Dorland *et al.* (1986) for the ganglioside-derived oligosaccharides GalNAcβ1 → 4Galβ1 → 4Glc and GalNAcβ1 → 4(NeuAcα2 → 3)Galβ1 → 4Glc.

Compound **87** is an α2 → 6 sialylated extension of **12**. So far, it has not been obtained in a pure state (Van Halbeek *et al.*, 1988) (Figure 59a).

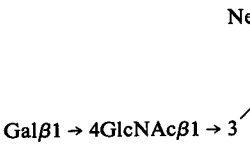

(87)

The core structure NeuAcα2 → 6(Galβ1 → 3)GalNAc-ol of **87** is established by NeuAc H-3a and H-3e signals at δ = 1.689 and 2.725 ppm, respectively, in conjunction with GalNAc-ol H-2 and H-5 signals at δ = 4.380 and 4.231 ppm, respectively. For a discussion of the data of the lower branch, see **12** (Table 2).

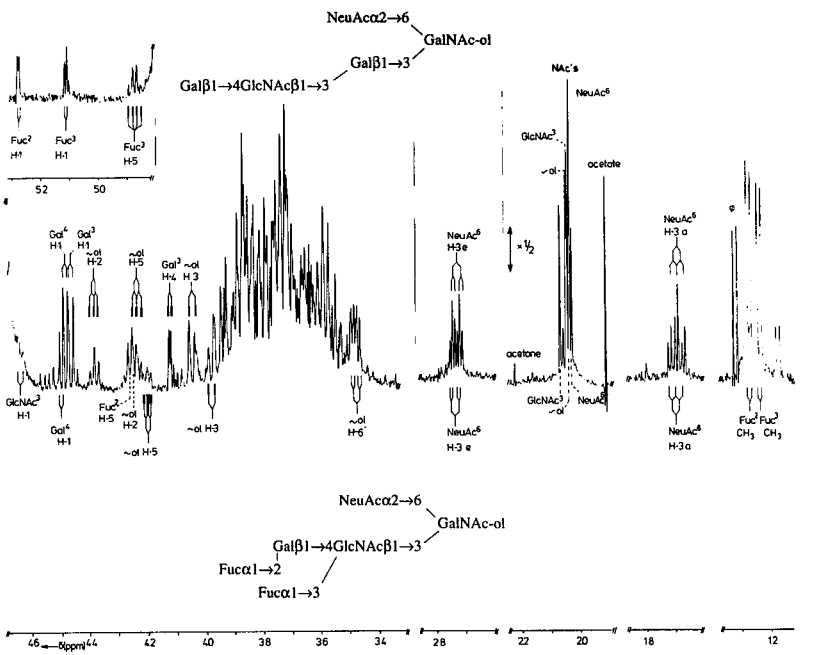

Figure 59a. Resolution-enhanced ^{1}H-NMR spectrum of a mixture of **87** (upper) and **93** (lower). For comments, see Figure 53.

Compound **88** is the sialylated form of **30** (Van Halbeek *et al.*, 1988). The substitution pattern of GalNAc-ol is reflected by GalNAc-ol H-2, H-5,

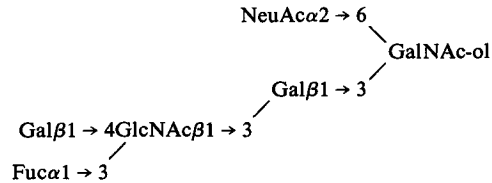

(88)

and H-6′ signals at $\delta = 4.379$, 4.225, and 3.47 ppm, respectively. The H-3 signals for NeuAc in $\alpha 2 \rightarrow 6$ linkage occur at $\delta = 1.688$ ppm (H-3a) and $\delta = 2.724$ ppm (H-3e). The ^{1}H-NMR parameters of the carbohydrate chain forming the lower branch at GalNAc-ol fit those discussed for **30** (Table 9). The immuno group X determinant is reflected by the characteristic set of the Fuc structural-reporter-group signals H-1 ($\delta = 5.136$ ppm), H-5 ($\delta =$ 4.833 ppm), and CH_3 ($\delta = 1.176$ ppm) for Fuc in $\alpha 1 \rightarrow 3$ linkage to GlcNAc of *N*-acetyllactosamine, in conjunction with the chemical shift value of the GlcNAc[3] NAc singlet at $\delta = 2.032$ ppm. It should be emphasized that the chemical shift of Fuc H-1 indicates not only the occurrence of the immuno group X determinant, but, in addition, that the GlcNAc residue forming part of the X determinant is involved in a $\beta 1 \rightarrow 3$ linkage to another residue, instead of in a $\beta 1 \rightarrow 6$ linkage.

8.3. Extension of the GlcNAcβ1 → 3GalNAc-ol Core Structure

Up to now, **89** is the only sialylated representative of the GlcNAc$\beta 1 \rightarrow$ 3GalNAc-ol core type, including an immuno group sialyl-X determinant (Lamblin *et al.*, 1984a; Van Halbeek *et al.*, 1988; Capon *et al.*, 1989). The

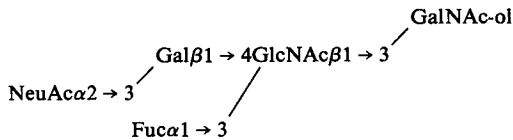

(89)

^{1}H-NMR data of **89** (Figure 60), together with those of the nonsialylated form **35**, are presented in Table 21. The substitution of GalNAc-ol at C-3 by GlcNAc is evident from the GalNAc-ol H-2 and H-5 signals at $\delta = 4.275$ and 4.129 ppm, respectively (see **35** and Section 11. The set of structural-reporter-group signals for NeuAc (H-3a, $\delta = 1.792$ ppm; H-3e, $\delta =$ 2.763 ppm) reflects that the NeuAc residue is $\alpha 2 \rightarrow 3$ linked to Gal of a Gal$\beta 1 \rightarrow$ 4GlcNAc$\beta 1 \rightarrow$ sequence (Vliegenthart *et al.*, 1983). Comparison of the ^{1}H-NMR data of **35** and **89** shows downfield shifts for Gal[4] H-1 ($\Delta\delta = +0.066$ ppm), H-3, and H-4 ($\Delta\delta = +0.032$ ppm). These shifts are in

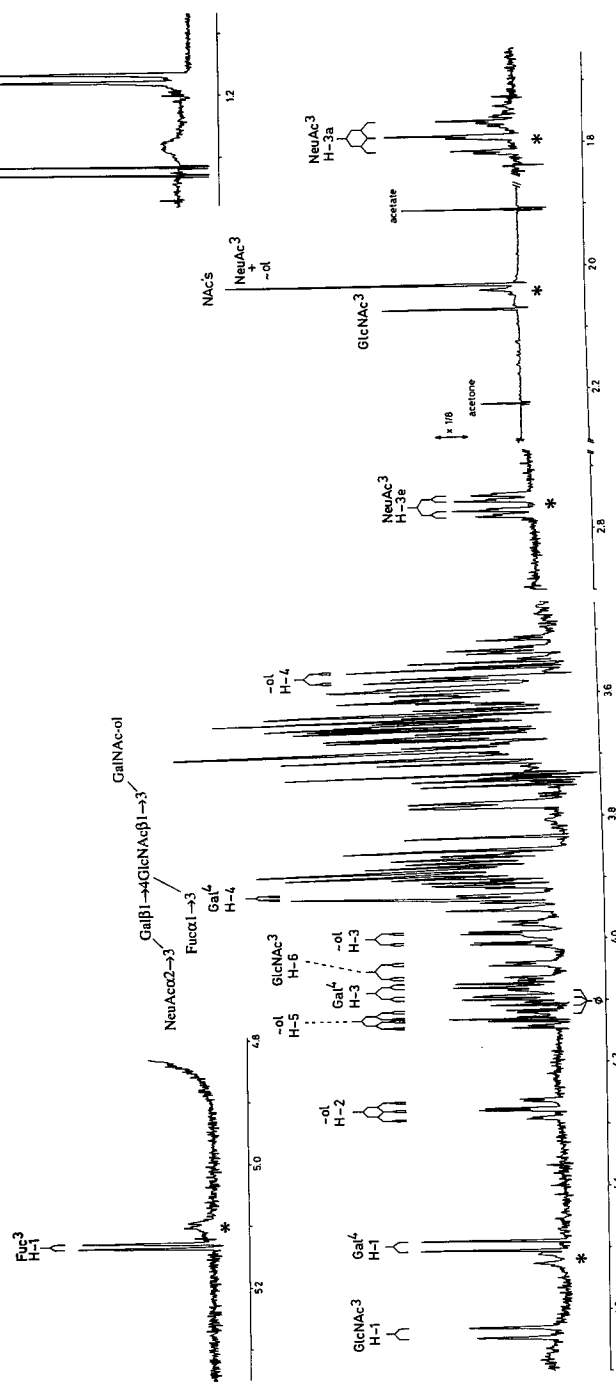

Figure 60. Resolution-enhanced ^{1}H-NMR spectrum of **89**. For comments, see Figure 56. The signal(s) marked by ϕ stem(s) from (a) frequently occurring, nonprotein noncarbohydrate contaminant(s).

TABLE 21
^{1}H Chemical Shifts of Structural-Reporter Groups of Constituent Monosaccharides for a Sialylated Oligosaccharide-Alditol with the GlcNAcβ1 → 3GalNAc-ol Core Structure (89)

Residue	Reporter group	35 	89[a] 
GalNAc-ol	H-2	4.272	4.275
	H-3	3.996	3.997
	H-4	3.564	3.563
	H-5	4.126	4.129
	NAc	2.031	2.030
GlcNAc[3]	H-1	4.643	4.638
	H-6	4.034	4.052
	NAc	2.073	2.070
Gal[4]	H-1	4.430	4.496
	H-3	n.d.[b]	4.084
	H-4	3.897	3.929
Fuc[3]	H-1	5.140	5.131
	H-5	4.813	4.83[c]
	CH_3	1.177	1.169
NeuAc[3]	H-3a	—	1.792
	H-3e	—	2.763
	NAc	—	2.030

[a] Spectrum recorded at 22 °C.
[b] n.d. means value could not be determined merely by inspection of the spectrum.
[c] Capon *et al.* (1989): δ = 4.801 ppm (27 °C).

the same order of magnitude as those observed for the step going from **9** to **85** (see also Vliegenthart *et al.*, 1983, for *N*-linked carbohydrate chains). The structural-reporter-group resonances for Fuc, i.e., H-1 (δ = 5.131 ppm), H-5 (δ = 4.83 ppm), and CH_3 (δ = 1.169 ppm), are found at positions that confirm the Galβ1 → 4(Fucα1 → 3)GlcNAcβ1 → 3 structural element (see **35**).

8.4. Extensions of the NeuAcα2 → 6(GlcNAcβ1 → 3)GalNAc-ol Core Structure

In this section, the ^{1}H-NMR data of the sialylated carbohydrates **90–97** will be discussed. The relevant ^{1}H-NMR parameters of these compounds, and of the core structure **10**, are summarized in Table 22. The GalNAc-ol H-2 and H-5 signals in the various spectra are found at δ = 4.24–4.27 and

4.15–4.21 ppm, respectively, whereas GalNAc-ol H-6′ resonates at δ = 3.47–3.49 ppm, upfield from the bulk of skeleton proton signals. The chemical shifts of NeuAc[6] H-3a at δ = 1.69–1.70 ppm and H-3e at δ = 2.73–2.74 ppm indicate an $\alpha 2 \rightarrow 6$ linkage to GalNAc-ol.

The ^{1}H-NMR spectrum of **90** is depicted in Figure 61 (Breg *et al.*, 1987; Capon *et al.*, 1989; Savage *et al.*, 1987; Van Halbeek *et al.*, 1988).

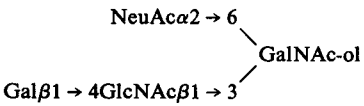

(90)

The shift values of H-3a (δ = 1.697 ppm) and H-3e (δ = 2.733 ppm) of NeuAc, together with the chemical shift values of GalNAc-ol H-2 (δ = 4.260 ppm) and H-5 (δ = 4.185 ppm) are indicative of the NeuAc$\alpha 2 \rightarrow$ 6(GlcNAc$\beta 1 \rightarrow$ 3)GalNAc-ol core element. The extension of GlcNAc[3] with a terminal Gal residue is evident from the Gal[4] H-1 and H-4 signals at δ = 4.464 ppm ($J_{1,2}$ = 7.8 Hz) and δ = 3.927 ppm, respectively. The Gal$\beta 1 \rightarrow$ 4GlcNAc sequence (backbone type-2 chain) is reflected by the position of the GlcNAc[3] H-1 signal at δ = 4.635 ppm ($\Delta\delta$ = +0.027 ppm, as compared to **10**; step **3** → **17**, $\Delta\delta$ = +0.027 ppm) in combination with the GlcNAc[3] H-6 signal at δ = 4.009 ppm ($\Delta\delta$ = +0.070 ppm; step **3** → **17**, $\Delta\delta$ = +0.071 ppm) and the GlcNAc[3] NAc singlet at δ = 2.076 ppm ($\Delta\delta$ = −0.003 ppm; step **3** → **17**, $\Delta\delta$ = −0.002 ppm). The absence of a doublet of doublets for GlcNAc[3] H-3 at $\delta \approx$ 3.91 ppm excludes the possibility of a $\beta 1 \rightarrow 3$ linkage (see **18**, Table 4). For NeuGc analog **90A**, see Addendum.

Compound **91** can be conceived as an extension of **90** with an $\alpha 1 \rightarrow$ 2-linked Fuc residue attached at Gal[4]. The ^{1}H-NMR data of **91** have been

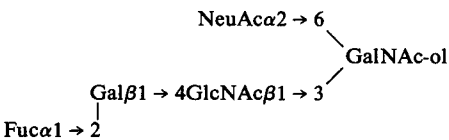

(91)

reported by Savage *et al.* (1987) and D'Arcy *et al.* (1989). The substitution pattern of GalNAc-ol is reflected by the GalNAc-ol H-2, H-5, and H-6′ signals at δ = 4.263, 4.210, and 3.490 ppm, respectively. The typical NeuAc H-3a and H-3e signals occur at δ = 1.699 and 2.734 ppm, respectively. Comparison of the ^{1}H-NMR data of the lower branches in **34** (asialo form, Table 11) and **91** demonstrates that most of the structural-reporter-group signals resonate at nearly the same positions. The Fuc set (H-1, δ = 5.313 ppm; H-5, δ = 4.223 ppm; CH_3, δ = 1.233 ppm) points to the occurrence of the blood group H/backbone type-2 structural element (compare with **95**). For NeuGc analog **91A**, see Addendum.

TABLE 22

^{1}H Chemical Shifts of Structural-Reporter Groups of Constituent Monosaccharides for Sialylated Oligosaccharide-Alditols with the NeuAcα2 → 6(GlcNAcβ1 → 3)GalNAc-ol Core Structure in Common (90–97)

Residue	Reporter group	10 	90 	91 	92 	93 	94 	95 	96 	97 
GalNAc-ol	H-2	4.260	4.260	4.263	4.247	4.250	4.261	4.237	4.262	4.249
	H-3	3.985	3.990	3.984	3.984	3.976	4.011	3.974	3.991	3.983
	H-4	n.d.[a]	n.d.	n.d.	n.d.	n.d.	n.d.	n.d.	3.597	n.d.
	H-5	4.185	4.185	4.210	4.179	4.198	4.171	4.153	4.186	4.176
	H-6′	3.487	3.491	3.490	3.489	3.48	n.d.	3.468	3.487	3.485
	NAc	2.035	2.035	2.034	2.034[b]	2.033[c]	2.036[d]	2.034[e]	2.035	2.024
GlcNAc^3	H-1	4.608	4.635	4.613	4.645	4.635[f]	4.660	4.653	4.626	4.641
	H-3	n.d.	n.d.	n.d.	n.d.	n.d.	n.d.	4.018	n.d.	n.d.
	H-6	3.939	4.009	4.010	4.021	n.d.	3.970	3.944	4.020	4.015
	NAc	2.079	2.076	2.080	2.066	2.069	2.067	2.107	2.073	2.063
NeuAc^6	H-3a	1.697	1.697	1.699	1.698	1.699	1.697	1.696	1.698	1.697
	H-3e	2.733	2.733	2.734	2.732	2.735	2.735	2.730	2.729	2.730
	NAc	2.031	2.031	2.034	2.025[b]	2.026[c]	2.032[d]	2.030[e]	2.031	2.031

Gal^4	H-1	—	4.464	4.534	4.444	4.493	—	—	4.540	4.509
	H-4	—	3.927	n.d.	n.d.	n.d.	—	—	3.962	n.d.
Fuc^2	H-1	—	—	5.313	—	5.276	—	5.206	—	—
	H-5	—	—	4.223	—	4.258	—	4.273	—	—
	CH_3	—	—	1.233	—	1.274	—	1.235	—	—
Fuc^3	H-1	—	—	—	5.132	5.113	—	—	—	5.122
	H-5	—	—	—	4.819	4.874	—	—	—	4.804
	CH_3	—	—	—	1.177	1.238	—	—	—	1.169
Gal^3	H-1	—	—	—	—	—	4.455	4.574	—	—
	H-4	—	—	—	—	—	3.918	3.885	—	—
$NeuAc^3$	H-3a	—	—	—	—	—	—	—	1.802	1.797
	H-3e	—	—	—	—	—	—	—	2.768	2.760
	NAc	—	—	—	—	—	—	—	2.031	2.031

[a] n.d. means value could not be determined merely by inspection of the spectrum.
[b] Assignments may have to be interchanged.
[c] Assignments may have to be interchanged.
[d] Assignments may have to be interchanged.
[e] Assignments may have to be interchanged.
[f] The shape of this GlcNAc. H-1 doublet is distorted due to virtual coupling (δ H-2 $\approx$ δ H-3).

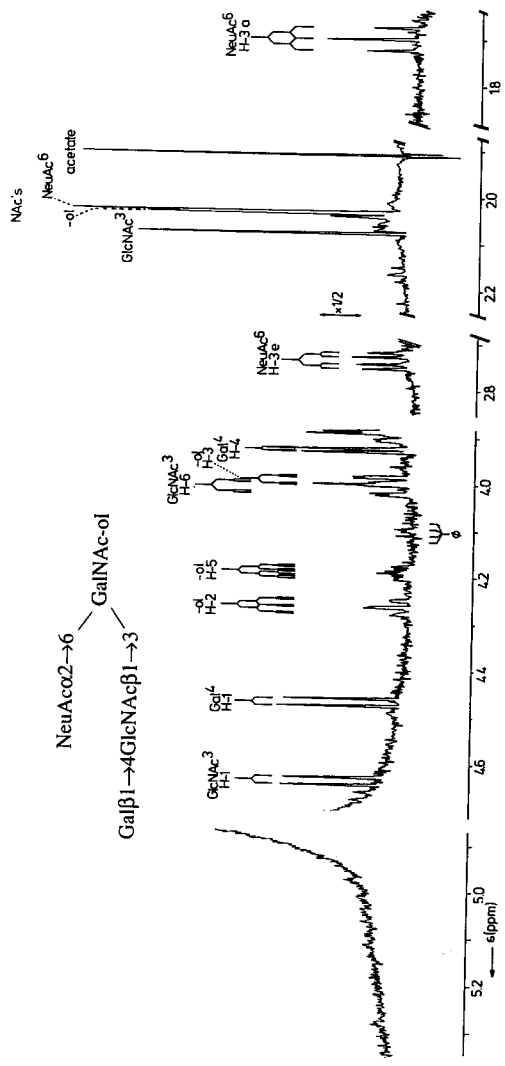

Figure 61. Resolution-enhanced ^{1}H-NMR spectrum of **90**. For comments, see Figure 53.

Compound **92** has been demonstrated to occur as a major component in a mixture together with **80** (Breg *et al.*, 1987; see also Capon *et al.*, 1989;

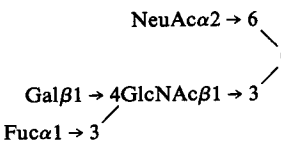

(92)

Van Halbeek *et al.*, 1988; Savage *et al.*, 1990b) (Figure 53). The chemical shift values for NeuAc H-3a at $\delta = 1.698$ ppm and H-3e at $\delta = 2.732$ ppm, in combination with those for GalNAc-ol H-2 at $\delta = 4.247$ ppm and H-5 at $\delta = 4.179$ ppm, are indicative of the NeuAcα2 → 6(GlcNAcβ1 → 3)GalNAc-ol core. The structural-reporter-group resonances of Fuc, namely, H-1 at $\delta = 5.132$ ppm, H-5 at $\delta = 4.819$ ppm, and CH_3 at $\delta = 1.177$ ppm, are found at positions characteristic of the immuno group X determinant Galβ1 → 4(Fucα1 → 3)GlcNAcβ1 → 3. The terminal position of Gal^4 is reflected by its anomeric doublet at $\delta = 4.444$ ppm.

Compound **93** can be considered as a fucosylated extension of **91** or **92**, and has been shown in a mixture together with **87** (Van Halbeek

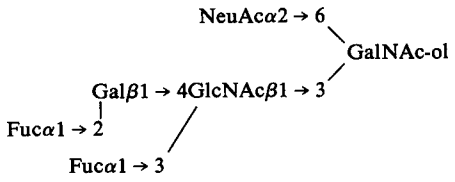

(93)

et al., 1988) (Figure 59a). It belongs to the NeuAcα2 → 6(GlcNAcβ1 → 3)GalNAc-ol core type, on the basis of the chemical shifts of the NeuAc H-3a and H-3e signals at $\delta = 1.699$ and 2.735 ppm, respectively, and the GalNAc-ol H-2 and H-5 signals at $\delta = 4.250$ and 4.198 ppm, respectively. Two Fuc H-1 signals are observed at $\delta = 5.276$ and 5.113 ppm, respectively. These doublets, in conjunction with the H-5 signals at $\delta = 4.258$ and 4.874 ppm, respectively, and the CH_3 doublets at $\delta = 1.274$ and 1.238 ppm, respectively, show the occurrence of two Fuc residues, one α1 → 2 linked to Gal^4 and the other α1 → 3 linked to $GlcNAc^3$ of the same *N*-acetyllactosamine unit. The combined sets of Fuc structural-reporter-group signals are diagnostic for the immuno group Y determinant sequence (see also nonsialylated **36**, Table 11).

The 400-MHz ^{1}H-NMR data of the structural isomer of **90**, namely **94**, have been reported by Capon *et al.* (1989). The occurrence of the NeuAcα2 → 6(GlcNAcβ1 → 3)GalNAc-ol core structure is reflected by the typical NeuAc H-3 and GalNAc-ol H-2 and H-5 structural-reporter-group signals. The Galβ1 → 3GlcNAc sequence is indicated by $GlcNAc^3$ H-1 at

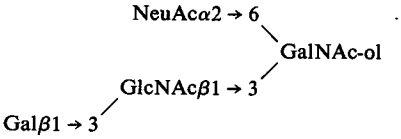

(94)

δ = 4.660 ppm ($\Delta\delta$ = +0.052 ppm, as compared to **10**; step **3** → **18**, $\Delta\delta$ = +0.050 ppm), H-6 at δ = 3.970 ppm ($\Delta\delta$ = +0.031 ppm; step **3** → **18**, $\Delta\delta$ = +0.004 ppm), and NAc at δ = 2.067 ppm ($\Delta\delta$ = −0.012 ppm; step **3** → **18**, $\Delta\delta$ = −0.012 ppm). See also the comparison of the asialo forms **17** and **18** (Table 4).

Compound **95** is an $\alpha 1 \rightarrow 2$ fucosylated form of **94** (Breg *et al.*, 1987; Capon *et al.*, 1989; Van Halbeek *et al.*, 1988) (Figure 62). The substitution

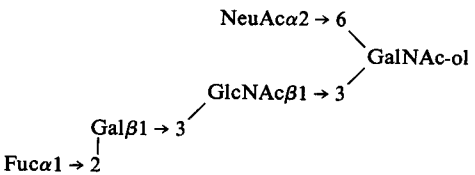

(95)

pattern of GalNAc-ol is evident from the GalNAc-ol H-2 (δ = 4.237 ppm), H-5 (δ = 4.153 ppm), and H-6′ (δ = 3.468 ppm) signals, together with the NeuAc H-3a (δ = 1.696 ppm) and H-3e (δ = 2.730 ppm) resonances. The set of Fuc structural-reporter-group signals H-1 at δ = 5.206 ppm, H-5 at

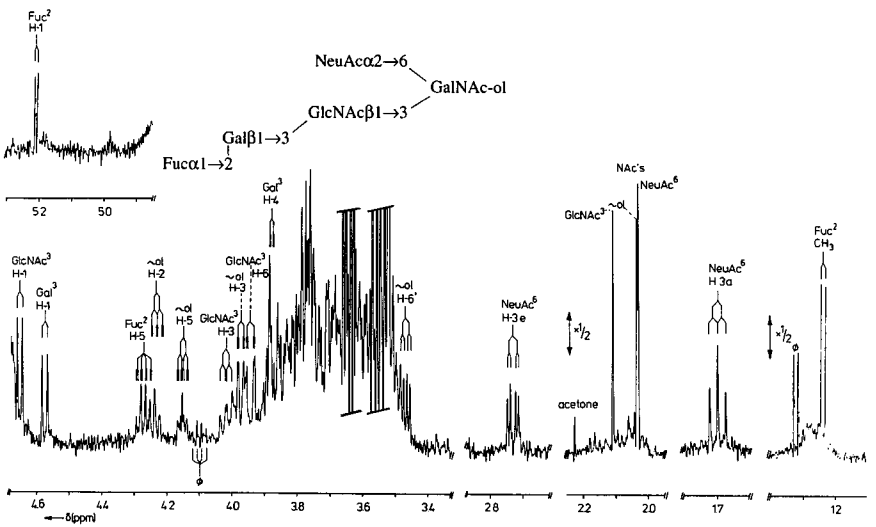

Figure 62. Resolution-enhanced ^{1}H-NMR spectrum of **95**. For comments, see Figures 56 and 60.

$\delta = 4.273$ ppm, and CH_3 at $\delta = 1.235$ ppm confirms the presence of the blood group H/backbone type-1 structural element Fucα1 → 2Galβ1 → 3GlcNAcβ1 → (see also nonsialylated **37**, Table 11). The lower branches in **37** and **95** have the same sets of structural reporters.

Compound **96** is an α2 → 3 sialylated form of **90** (Capon *et al.*, 1989). The presence of the NeuAcα2 → 3Galβ1 → 4GlcNAcβ1 → sequence follows from the NeuAc H-3a and H-3e signals at $\delta = 1.802$ and 2.768 ppm,

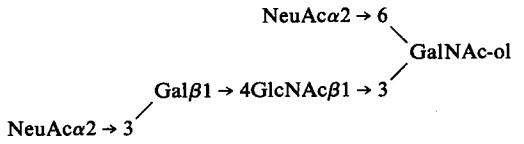

(96)

respectively. The Gal[4] H-1 doublet is observed at $\delta = 4.540$ ppm ($\Delta\delta$ = +0.076 ppm, as compared to **90**), the Gal[4] H-3 signal at the downfield position of $\delta = 4.118$ ppm, the GlcNAc[3] H-1 doublet at $\delta = 4.626$ ppm ($\Delta\delta = -0.009$ ppm), and the GlcNAc[3] NAc singlet at $\delta = 2.073$ ppm ($\Delta\delta$ = −0.003 ppm) (see Vliegenthart *et al.*, 1983; and compare with the step **22** → **116**). As discussed for **90**–**95**, the NeuAc residue α2 → 6 linked to GalNAc-ol is reflected by another set of structural-reporter groups, namely, H-3a at $\delta = 1.698$ ppm and H-3e at $\delta = 2.729$ ppm (400-MHz ^{1}H-NMR data).

Compound **97** is a further extension of **90** (Capon *et al.*, 1989), leading to the presence of an immuno group sialyl-X determinant. The structural-

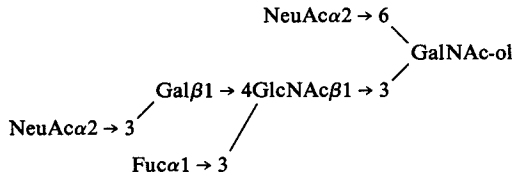

(97)

reporter-group resonances for Fuc, i.e., H-1 ($\delta = 5.122$ ppm), H-5 (δ = 4.804 ppm), and CH_3 ($\delta = 1.169$ ppm), are in agreement with the occurrence of the blood group element linked at GlcNAc[3]. This compound can also be conceived as the asialo (upper branch) form of **89**. Comparison of both lower branch sets shows small variations in the chemical shift data of the constituting monosaccharide residues, reflecting the influence of the sialylation at C-6 of GalNAc-ol (400-MHz ^{1}H-NMR data).

8.5. Extensions of the Galβ1 → 4GlcNAcβ1 → 6(Galβ1 → 3)GalNAc-ol Backbone Structure

In this section, the ^{1}H-NMR data of the sialylated saccharides **98**–**104**, having the Galβ1 → 4GlcNAcβ1 → 6(Galβ1 → 3)GalNAc-ol backbone

TABLE 23

^{1}H Chemical Shifts of Structural-Reporter Groups of Constituent Monosaccharides for Sialylated Oligosaccharide-Alditols with the Galβ1 → 4GlcNAcβ1 → 6(Galβ1 → 3)GalNAc-ol Backbone Structure in Common (98–104)

Residue	Reporter group	25 	98 	99 	100 	101 	102 	103 	104 
GalNAc-ol	H-2	4.394	4.392	4.400	4.399	4.392	4.399	4.294	4.324
	H-3	4.060	4.059	4.082	4.083	4.058	4.085	4.076	4.085
	H-4	3.465	3.463	3.49	n.d.[a]	3.485	3.482	3.482	3.482
	H-5	4.282	4.282	4.253	4.249	4.280	4.254	4.210	4.219
	NAc	2.067	2.065	2.054	2.055[b]	2.067	2.053	2.049[c]	2.050
Gal[3]	H-1	4.465	4.461	4.572	4.568	4.462	4.571	4.676	4.697
	H-3	n.d.	n.d.	n.d.	n.d.	n.d.	n.d.	4.012	4.026
	H-4	3.900	3.899	3.922	n.d.	3.907[d]	3.923	4.214	4.278
GlcNAc[6]	H-1	4.560	4.551	4.567	4.570	4.550	4.560	4.576	4.576
	H-6	3.998	4.008	4.018	4.023	4.000	4.003	4.010	4.002
	NAc	2.064	2.061	2.054	2.044[b]	2.062	2.053	2.049[c]	2.050
Gal[4]	H-1	4.470	4.548	4.550	4.515	4.546	4.544	4.547	4.547
	H-2	n.d.	n.d.	n.d.	n.d.	3.352	3.354	3.354	3.355
	H-3	n.d.	4.115	4.114	4.083	4.150	4.152	4.152	4.152
	H-4	3.925	n.d.	3.957	n.d.	4.112	4.112	4.113	4.113

$NeuAc^3$	H-3a	—	1.799	1.798	1.795	1.925	1.927	1.925	1.925
	H-3e	—	2.755	2.756	2.763	2.659	2.660	2.659	2.660
	NAc	—	2.030	2.031	2.032	2.032	2.031	2.032	2.031
Fuc^2	H-1	—	—	5.224	5.222	—	5.226	5.378	5.349
	H-5	—	—	4.273	4.274	—	4.272	4.322	4.317
	CH_3	—	—	1.245	1.244	—	1.244	1.232	1.227
Fuc^3	H-1	—	—	—	5.105	—	—	—	—
	H-5	—	—	—	4.82	—	—	—	—
	CH_3	—	—	—	1.168	—	—	—	—
$GalNAc^4$	H-1	—	—	—	—	4.711[e]	4.722[f]	4.713[e]	4.738 (4.714)[e]
	H-4	—	—	—	—	3.917[d]	3.914	3.916	3.916
	NAc	—	—	—	—	2.014	2.014	2.015	2.014
$GalNAc^3$	H-1	—	—	—	—	—	—	5.185	—
	H-2	—	—	—	—	—	—	4.251	—
	H-4	—	—	—	—	—	—	4.020	—
	H-5	—	—	—	—	—	—	4.160	—
	NAc	—	—	—	—	—	—	2.052[c]	—
$Gal^{3,3}$	H-1	—	—	—	—	—	—	—	5.259
	H-2	—	—	—	—	—	—	—	3.872
	H-4	—	—	—	—	—	—	—	4.015
	H-5	—	—	—	—	—	—	—	4.119

[a] n.d. means value could not be determined merely by inspection of the spectrum.
[b] Assignments may have to be interchanged.
[c] Assignments may have to be interchanged.
[d] Assignments may have to be interchanged.
[e] Measured at 5 °C.
[f] Measured at 10 °C.

structure, are presented (see Table 23). For comparison, the data of the nonsialylated backbone structure **25** are also considered. For **98–102**, the core structures are recognized from their ^{1}H-NMR spectra by the generally found chemical shift values of GalNAc-ol H-2 and H-5 at $\delta = 4.38$–4.41 and 4.22–4.29 ppm, respectively (see Section 11). A further characteristic of the common element is the GlcNAc^6 H-1 signal at $\delta = 4.55$–4.58 ppm.

The ^{1}H-NMR spectrum of **98** is depicted in Figure 63 (Breg *et al.*, 1987; Nato *et al.*, 1986). From the chemical shift values of GalNAc-ol H-2

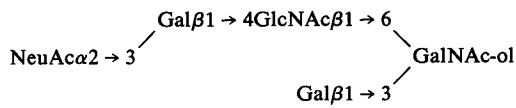

(98)

($\delta = 4.392$ ppm) and H-5 ($\delta = 4.282$ ppm), the core structure is established to be GlcNAcβ1 → 6(Galβ1 → 3)GalNAc-ol. NeuAc is α2 → 3 linked to Gal of an *N*-acetyllactosamine unit, as is evident from the NeuAc H-3a and H-3e signals at $\delta = 1.799$ and 2.755 ppm, respectively (Vliegenthart *et al.*, 1983). The effects of the NeuAc attachment to *N*-acetyllactosamine follow from a comparison with the data of **25**, showing upfield shifts for GlcNAc^6 H-1 ($\Delta\delta = -0.009$ ppm) and NAc ($\Delta\delta = -0.003$ ppm), and downfield shifts for GlcNAc^6 H-6 ($\Delta\delta = +0.010$ ppm) and Gal^4 H-1 ($\Delta\delta = +0.078$ ppm). The Gal^4 H-3 signal is observed outside the bulk of skeleton protons at $\delta = 4.115$ ppm.

Compound **99** is an α1 → 2 fucosylated form of **98** (Van Halbeek *et al.*, 1988) (Figure 63a). The GlcNAcβ1 → 6(Galβ1 → 3)GalNAc-ol core

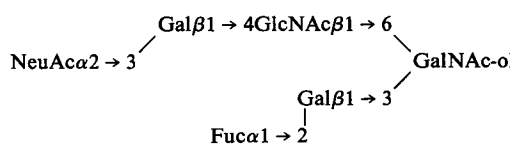

(99)

type is demonstrated by the GalNAc-ol H-2 and H-5 signals at $\delta = 4.400$ and 4.253 ppm, respectively. The structural-reporter-group signals of NeuAc (H-3a, $\delta = 1.798$ ppm; H-3e, $\delta = 2.756$ ppm) and Gal^4 (H-1, $\delta = 4.550$ ppm; H-3, $\delta = 4.114$ ppm) are identical to those of the corresponding residues in **98**. The structural reporters of the Fucα1 → 2Galβ1 → 3GalNAc-ol element, i.e., Fuc H-1 ($\delta = 5.224$ ppm), H-5 ($\delta = 4.273$ ppm), and CH_3 ($\delta = 1.245$ ppm), and Gal^3 H-1 ($\delta = 4.572$ ppm) and H-4 ($\delta = 3.922$ ppm), are identical to those observed for nonsialylated **39** (Table 12). The fucosylation shift effects on the various GalNAc-ol and GlcNAc^6 structural-reporter-group signals going from **98** to **99** are similar to those observed going from **25** to **39**.

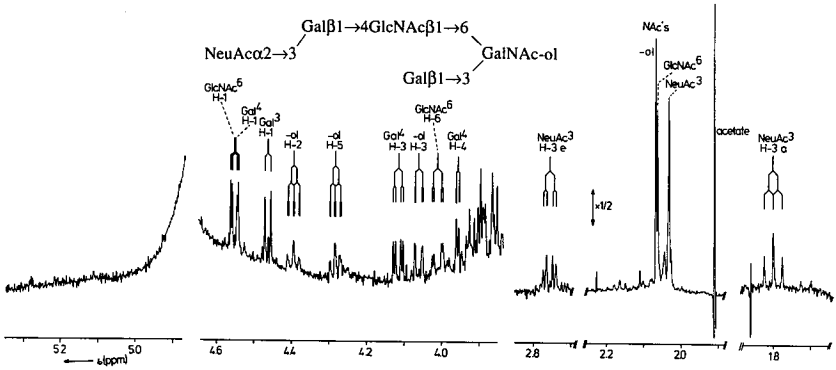

Figure 63. Resolution-enhanced ^{1}H-NMR spectrum of **98**. The relative-intensity scale of the *N*-acetyl methyl proton region of the spectrum differs from that of the other parts, as indicated. Contaminating acetate gives rise to a signal at $\delta = 1.908$ ppm.

Compound **100** is an $\alpha 1 \rightarrow 3$ fucosylated form of **99** (Van Halbeek *et al.*, 1988). The chemical shifts of GalNAc-ol H-2 and H-5 at $\delta = 4.399$ and 4.249 ppm, respectively, classify **100** as having a GlcNAc$\beta 1 \rightarrow$

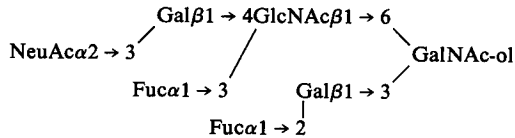

(100)

6(Gal$\beta 1 \rightarrow 3$)GalNAc-ol core element. The blood group H determinant Fuc$\alpha 1 \rightarrow 2$Gal$\beta 1 \rightarrow 3$ in the lower branch gives rise to structural-reporter-group signals for Fuc^2 (H-1, $\delta = 5.222$ ppm; H-5, $\delta = 4.274$ ppm; CH_3, $\delta = 1.244$ ppm) and Gal^3 (H-1, $\delta = 4.568$ ppm), as observed for such a branch in **99**. As compared to **99**, the attachment of a Fuc residue (H-1, $\delta = 5.105$ ppm; CH_3, $\delta = 1.168$ ppm) at C-3 of GlcNAc^6 of the *N*-acetyllactosamine unit induces upfield shifts for GlcNAc^6 NAc ($\Delta\delta = -0.010$ ppm) and Gal^4 H-1 ($\Delta\delta = -0.035$ ppm). Similar shift trends for these two reporters have been observed in the step from **39** to **43** (nonsialylated **100**; Table 12). Finally, the NeuAc^3 residue of the immuno group sialyl-X determinant is evident from its H-3a and H-3e signals at $\delta = 1.795$ and 2.763 ppm, respectively.

In the ^{1}H-NMR spectrum of **101** (Nasir-Ud-Din *et al.*, 1986) the positions of the GalNAc-ol H-2 ($\delta = 4.392$ ppm) and H-5 ($\delta = 4.280$ ppm) signals point to the presence of the GlcNAc$\beta 1 \rightarrow$ 6(Gal$\beta 1 \rightarrow 3$)GalNAc-ol

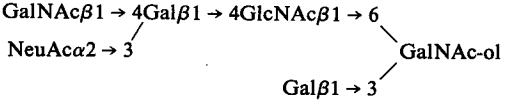

(101)

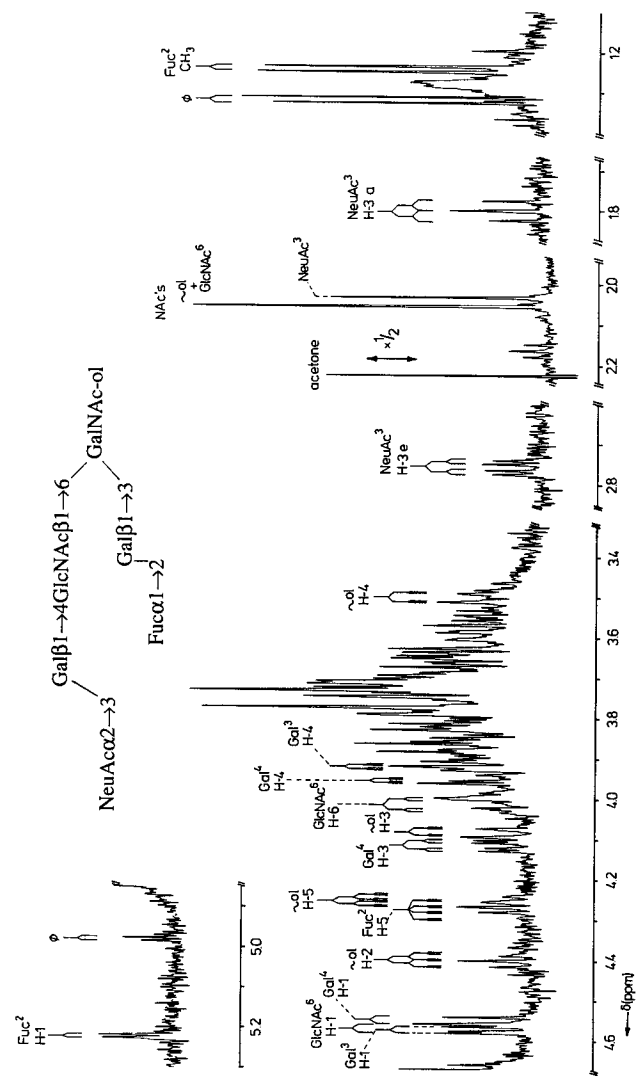

Figure 63a. Resolution-enhanced ^{1}H-NMR spectrum of **99**. For comments, see Figure 63. The signal(s) marked by ϕ stem(s) from (a) frequently occurring, nonprotein noncarbohydrate contaminant(s).

core. The Gal^3 H-1 doublet at $\delta = 4.462$ ppm ($J_{1,2} = 7.8$ Hz), together with the Gal^3 H-4 signal at $\delta = 3.907$ ppm, demonstrate a terminal position for the Gal^3 residue. The upper branch at GalNAc-ol contains the blood group Cad determinant (see also **79** and **86**). The set of chemical shifts observed for NeuAc H-3a and H-3e ($\delta = 1.925$ and 2.659 ppm, respectively) is typical for the presence (Blanchard *et al.*, 1983) of NeuAcα2 → 3 linked to a Gal residue which also bears a monosaccharide at C-4. Here, the Gal^4 H-3 signal is observed at $\delta = 4.150$ ppm. The β-linked GalNAc residue at C-4 of Gal^4 exhibits its H-1 signal at $\delta = 4.711$ ppm ($J_{1,2} = 8.1$ Hz) (see **79** and **86**) and its NAc singlet at $\delta = 2.014$ ppm. The former signal is partly hidden under the HO^2H line when recording the NMR spectrum at room temperature, but can be visualized at 5–10 °C. The disubstituted Gal residue is in turn β1 → 4 linked to $GlcNAc^6$, as follows from the chemical shifts of $GlcNAc^6$ H-1, H-6, and NAc at $\delta = 4.550$, 4.000, and 2.062 ppm, respectively (compare **98**).

Compound **102** is an α1 → 2 fucosylated form of **101**, leading to an additional blood group H determinant (Nasir-Ud-Din *et al.*, 1986) (Figure

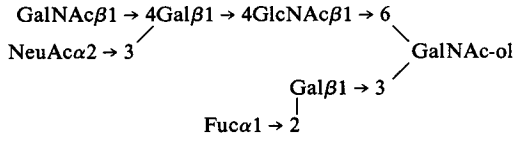

(102)

64). The substitution pattern of GalNAc-ol is evident from the GalNAc-ol H-2 and H-5 signals at $\delta = 4.399$ and 4.254 ppm, respectively. The blood group Cad determinant GalNAcβ1 → 4(NeuAcα2 → 3)Galβ1 → shows similar reporter sets for the individual monosaccharides, as discussed for **101**. The structural-reporter-group signals of Fuc α1 → 2 linked to Gal^3 are H-1 at $\delta = 5.226$ ppm, H-5 at $\delta = 4.272$ ppm, and CH_3 at $\delta = 1.244$ ppm (compare with **99**). The Gal^3 H-1 doublet is observed at $\delta = 4.571$ ppm, identical to that found in **99**.

The ^{1}H-NMR spectrum of **103** (Nasir-Ud-Din *et al.*, 1986) is depicted in Figure 65. The occurrence of the GlcNAcβ1 → 6(Galβ1 → 3)GalNAc-ol

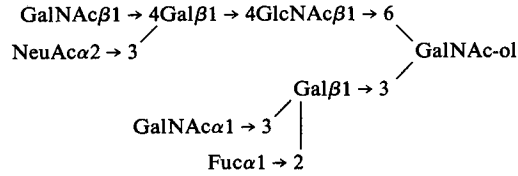

(103)

core structure is indicated by the GalNAc-ol H-2 and H-5 signals at $\delta = 4.294$ and 4.210 ppm, respectively. These values differ considerably from those usually found for this type of core structure (see Section 11). However,

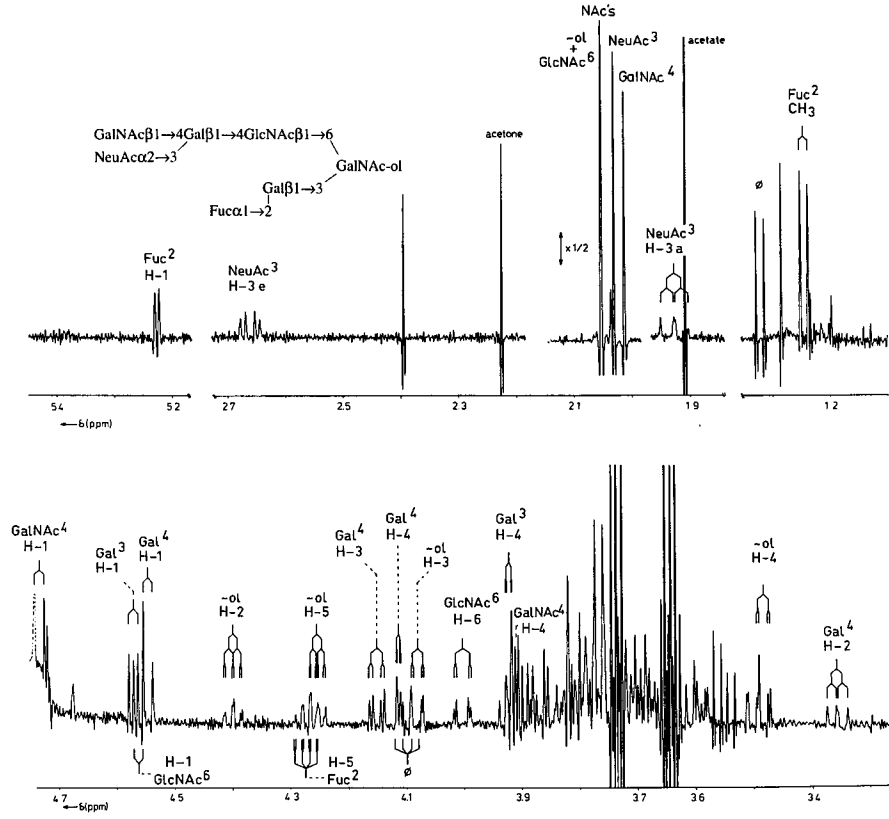

Figure 64. Resolution-enhanced ^{1}H-NMR spectrum of **102**. The relative-intensity scale of the *N*-acetyl methyl proton region of the spectrum differs from that of the other parts, as indicated. Contaminating acetate gives rise to a signal at $\delta = 1.908$ ppm. The signal(s) marked by ϕ stem(s) from (a) frequently occurring, nonprotein noncarbohydrate contaminant(s).

similar values have been observed for **68**, also containing a blood group A determinant (Table 17). The occurrence of the blood group Cad determinant GalNAcβ1 → 4(NeuAcα2 → 3)Galβ1 → is demonstrated by the set of structural-reporter-group signals, as discussed for **101**. The blood group A determinant GalNAcα1 → 3(Fucα1 → 2)Galβ1 → is reflected by the structural-reporter groups of GalNAc^3 (H-1, $\delta = 5.185$ ppm; H-2, $\delta = 4.251$ ppm; H-4, $\delta = 4.020$ ppm; H-5, $\delta = 4.160$ ppm; NAc, $\delta = 2.052$ ppm) and Fuc^2 (H-1, $\delta = 5.378$ ppm; H-5, $\delta = 4.322$ ppm; CH_3, $\delta = 1.232$ ppm). As compared to **102**, the attachment of GalNAc^3 to Gal^3 causes downfield shifts for Gal^3 H-1 ($\Delta\delta = +0.105$ ppm), Gal^3 H-3, and Gal^3 H-4 ($\Delta\delta = +0.291$ ppm) (see also **66–68**).

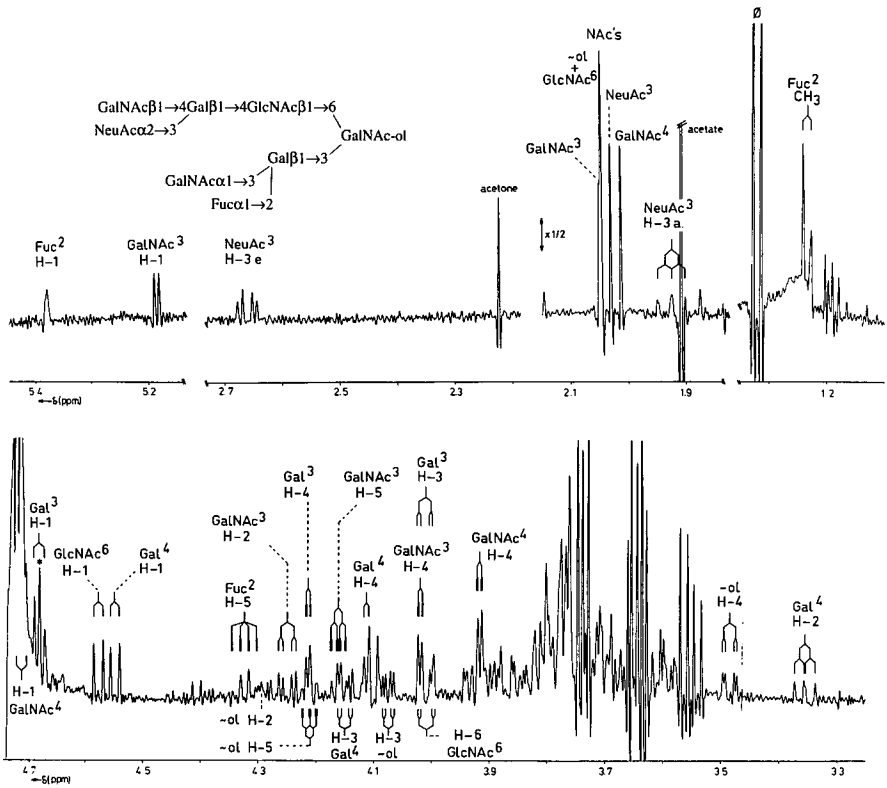

Figure 65. Resolution-enhanced ^{1}H-NMR spectrum of **103**. For comments, see Figure 64. Asterisk indicates spinning side band.

Compound **104** differs from **103** by the replacement of the blood group A structural element by a B determinant. Its ^{1}H-NMR spectrum is shown

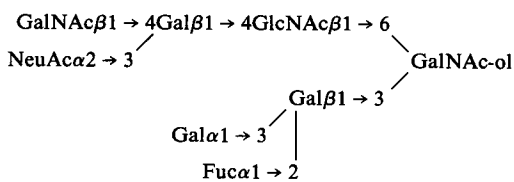

(104)

in Figure 66 (Nasir-Ud-Din *et al.*, 1986). The blood group B determinant is demonstrated by the set of structural-reporter-group signals for Gal^{3,3} (H-1, δ = 5.259 ppm; H-2, δ = 3.872 ppm; H-4, δ = 4.015 ppm; H-5, δ = 4.119 ppm) and Fuc^2 (H-2, δ = 5.349 ppm; H-5, δ = 4.317 ppm; CH_3, δ = 1.227 ppm). The extension of **102** with an $\alpha 1 \rightarrow 3$-linked Gal residue, yielding

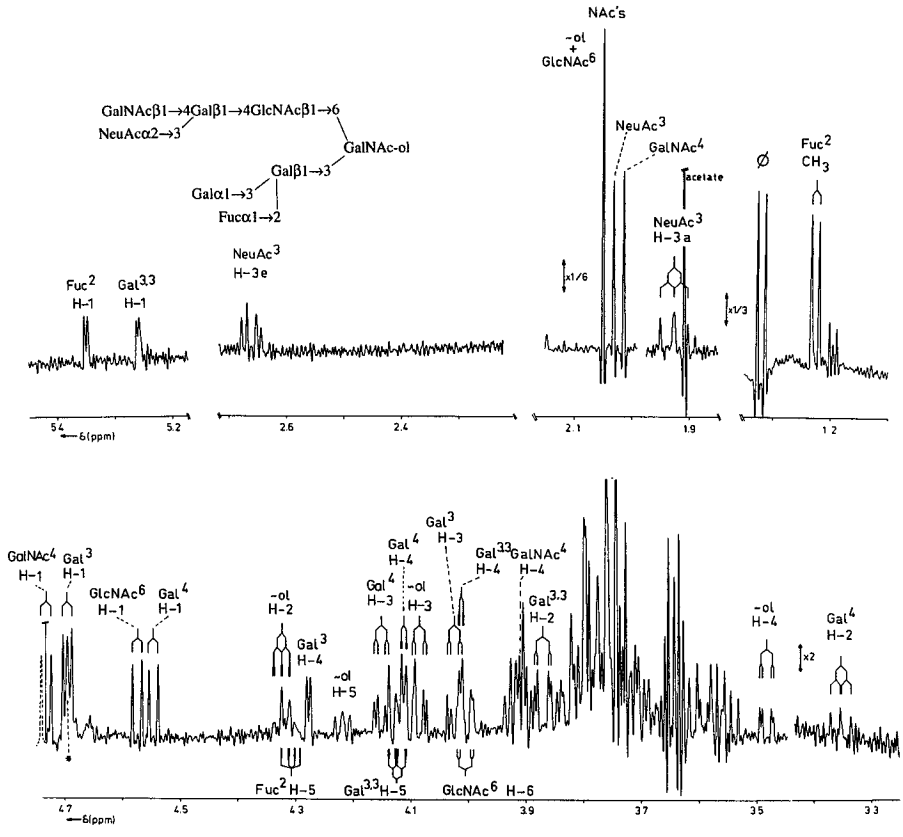

Figure 66. Resolution-enhanced ^{1}H-NMR spectrum of **104**. For comments, see Figure 64. Asterisk indicates spinning side band.

104, causes profound shift effects on GalNAc-ol H-2 ($\Delta\delta = -0.075$ ppm), GalNAc-ol H-5 ($\Delta\delta = -0.035$ ppm), Gal^3 H-1 ($\Delta\delta = +0.126$ ppm), Gal^3 H-3, and Gal^3 H-4 ($\Delta\delta = +0.355$ ppm) (see also Section 11). Comparison of the ^{1}H-NMR data of **79** and **86** with those of **101–104** demonstrates that discrimination is possible between GalNAcβ1 → 4(NeuAcα2 → 3)Galβ1 → 3GalNAc-ol and GalNAcβ1 → 4(NeuAcα2 → 3)Galβ1 → 4GlcNAcβ1 → structural elements.

8.6. Extensions of the Galβ1 → 4GlcNAcβ1 → 6(NeuAcα2 → 3Galβ1 → 3)GalNAc-ol Structure

In this section, the ^{1}H-NMR data of a series of oligosaccharide-alditols, having the Galβ1 → 4GlcNAcβ1 → 6(NeuAcα2 → 3Galβ1 → 3)GalNAc-ol

structure, namely, **105–111**, are discussed. The relevant ^{1}H-NMR parameters of these compounds are presented in Table 24. For general features, see Section 8.5.

Compound **105** (Breg *et al.*, 1987; Capon *et al.*, 1989; Hanisch *et al.*, 1990; Nato *et al.*, 1986; Pierce-Cretel *et al.*, 1989; Van Halbeek *et al.*, 1981b,

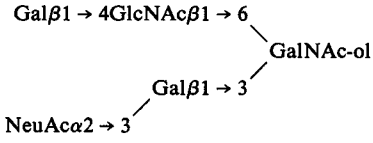

(105)

1988) is an extension of **25** with $\alpha 2 \rightarrow 3$-linked sialic acid at Gal^3. The GlcNAc$\beta 1 \rightarrow 6$(Gal$\beta 1 \rightarrow 3$)GalNAc-ol core is evident from the GalNAc-ol H-2 and H-5 signals at $\delta = 4.390$ and 4.272 ppm, respectively. The GalNAc-ol H-6 signal resonates at $\delta = 3.927$ ppm. Comparison of the ^{1}H-NMR data of **25** and **105** demonstrates that the chemical shift values of the structural reporters of the GlcNAc^6 and Gal^{4,6} residues match completely. The attachment of NeuAc at C-3 of the Gal^3 core residue gives rise to downfield shifts for Gal^3 H-1 ($\Delta\delta = +0.069$ ppm), H-4 ($\Delta\delta = +0.031$ ppm), and H-3. The occurrence of the NeuAc$\alpha 2 \rightarrow 3$Gal$\beta 1 \rightarrow 3$ element is reflected by the NeuAc H-3a and H-3e signals at $\delta = 1.801$ and 2.774 ppm, respectively. It has to be noted that in the case of the NeuAc$\alpha 2 \rightarrow 3$Gal$\beta 1 \rightarrow 4$GlcNAc$\beta 1 \rightarrow$ sequence, the NeuAc H-3e signal appears at $\delta = 2.76$ ppm (**98**, Table 23). It will be shown for **106–111** that the structural-reporter-group signals of the lower branch are hardly influenced by extensions in the upper branch.

The oligosaccharide-alditols **106** (Breg *et al.*, 1987; Van Halbeek *et al.*, 1988), **107** (Breg *et al.*, 1987; Pierce-Cretel *et al.*, 1989; Van Halbeek *et al.*, 1988), and **108** (Van Halbeek *et al.*, 1988) are fucosylated forms of **105**. The presence of the blood group H/backbone type-2 determinant in **106**

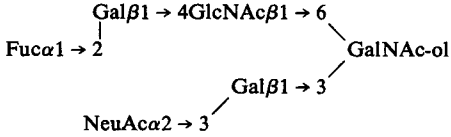

(106)

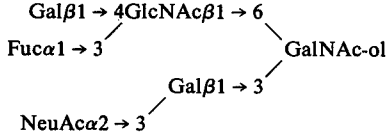

(107)

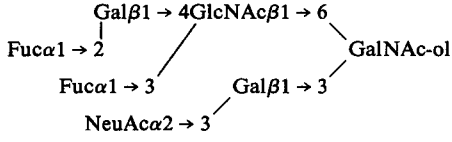

(108)

TABLE 24

[1]H Chemical Shifts of Structural-Reporter Groups of Constituent Monosaccharides for Sialylated Oligosaccharide-Alditols with the Galβ1 → 4GlcNAcβ1 → 6(NeuAcα2 → 3Galβ1 → 3)GalNAc-ol Structure in Common (105–111)

Residue	Reporter group	25 	105 	106 	107 	108 	109 	110 	111 
GalNAc-ol	H-2	4.394	4.390	4.388	4.387	4.387	4.387	4.385	4.387
	H-3	4.060	4.072	4.067	4.067	4.067	4.066	4.065	4.067
	H-4	3.465	3.435	3.442	3.426	n.d.	3.441	3.435	3.435
	H-5	4.282	4.272	4.271	4.258	4.260	4.265	4.267	4.268
	NAc	2.067	2.066	2.067[b]	2.066	2.064	2.065	2.064	2.066
Gal[3]	H-1	4.465	4.534	4.533	4.530	4.529	4.529	4.530	4.530
	H-3	n.d.[a]	4.116	4.115	4.114	4.112	4.113	4.113	4.113
	H-4	3.900	3.930	3.928	3.933	3.929	3.928	3.928	3.930
NeuAc[3,3]	H-3a	—	1.801	1.800	1.800	1.800	1.800	1.799	1.800
	H-3e	—	2.774	2.774	2.774	2.773	2.775	2.770	2.773
	NAc	—	2.033	2.034	2.033	2.033	2.033	2.033	2.033
GlcNAc[6]	H-1	4.560	4.559	4.537	4.559	4.544	4.550	4.555	4.558
	H-6	3.998	3.993	3.988	4.006	4.025	4.004	3.996	3.997
	NAc	2.064	2.066	2.064[b]	2.056	2.056	2.062	2.064	2.066

$Gal^{4,6}$	H-1	4.470	4.470	4.537	4.447	4.498	4.545	4.498	4.503
	H-3	n.d.	n.d.	n.d.	n.d.	n.d.	4.113	n.d.	n.d.
	H-4	3.925	3.922	3.891	3.895	n.d.	3.956	4.188	4.204
Fuc^2	H-1	—	—	5.307	—	5.280	—	—	—
	H-5	—	—	4.230	—	4.251	—	—	—
	CH_3	—	—	1.231	—	1.271	—	—	—
Fuc^3	H-1	—	—	—	5.107	5.094	—	—	—
	H-5	—	—	—	4.829	4.870	—	—	—
	CH_3	—	—	—	1.174	1.235	—	—	—
$NeuAc^{3,4}$	H-3a	—	—	—	—	—	1.800	—	—
	H-3e	—	—	—	—	—	2.755	—	—
	NAc	—	—	—	—	—	2.031	—	—
$Gal^{4,4,6}$	H-1	—	—	—	—	—	—	4.595	4.709
	H-4	—	—	—	—	—	—	3.903	4.028
$Gal^{4,4,4,6}$	H-1	—	—	—	—	—	—	—	4.953
	H-4	—	—	—	—	—	—	—	4.035
	H-5	—	—	—	—	—	—	—	4.366

[a] n.d. means value could not be determined merely by inspection of the spectrum.
[b] Assignments may have to be interchanged.

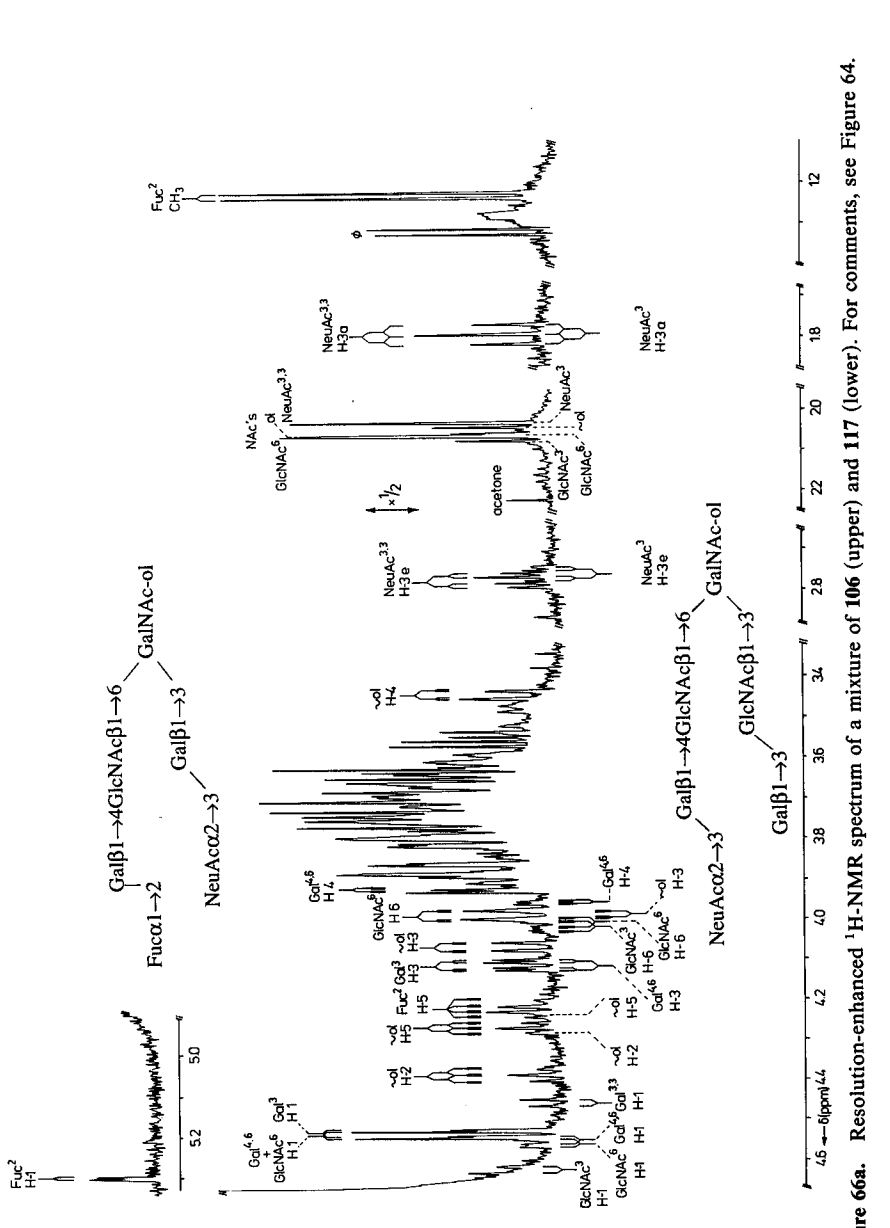

Figure 66a. Resolution-enhanced ^{1}H-NMR spectrum of a mixture of **106** (upper) and **117** (lower). For comments, see Figure 64.

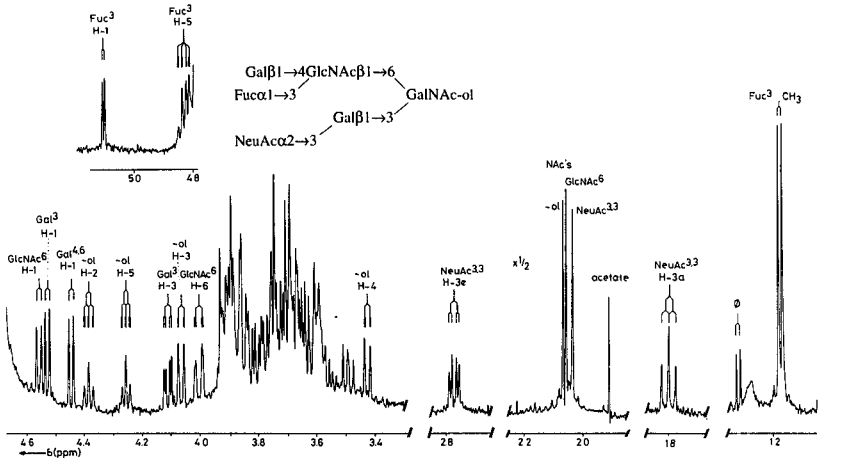

Figure 67. Resolution-enhanced ^{1}H-NMR spectrum of **107**. For comments, see Figure 64.

(Figure 66a) is clear from the set of Fuc structural-reporter groups, i.e., H-1 at $\delta = 5.307$ ppm, H-5 at $\delta = 4.230$ ppm, and CH_3 at $\delta = 1.231$ ppm. The values for the H-1 signals of Gal^{4,6} ($\delta = 4.537$ ppm; $\Delta\delta = +0.067$ ppm as compared to **105**) and GlcNAc^6 ($\delta = 4.537$ ppm; $\Delta\delta = -0.022$ ppm) are in accordance with this structural element (see also the nonsialylated form **40**, Table 12). In **107** the set of Fuc structural-reporter groups (H-1, $\delta =$ 5.107 ppm; H-5, $\delta = 4.829$ ppm; CH_3, $\delta = 1.174$ ppm) points to the immuno group X determinant (Figure 67). The position of Fuc^3 H-1 ($\delta = 5.107$ ppm) proves the GlcNAc residue in this determinant to be $\beta 1 \rightarrow 6$-linked (upper branch). As compared to **105**, upfield shifts are observed for Gal^{4,6} H-1 ($\Delta\delta = -0.023$ ppm) and for GlcNAc^6 NAc ($\Delta\delta = -0.010$ ppm), and a downfield shift for the GlcNAc^6 H-6 signal ($\Delta\delta = +0.013$ ppm) (see also the nonsialylated form **41**, Table 12). The ^{1}H-NMR spectrum of **108** (Figure 67a) indicates the occurrence of the immuno group Y determinant in the upper branch. The two specific sets for $\alpha 1 \rightarrow$ 2-linked Fuc and $\alpha 1 \rightarrow$ 3-linked Fuc are observed at $\delta = 5.280$ ppm (H-1)/$\delta = 4.251$ ppm (H-5)/$\delta =$ 1.271 ppm (CH_3) and $\delta = 5.094$ ppm (H-1)/$\delta = 4.870$ ppm (H-5)/$\delta =$ 1.235 ppm (CH_3), respectively (compare to **44**, Table 12).

The ^{1}H-NMR spectrum of **109** is depicted in Figure 68 (Akiyama *et al.*, 1984, 1987; Damm *et al.*, 1987; Korrel *et al.*, 1984; Nato *et al.*, 1986;

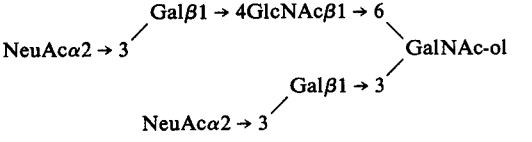

(109)

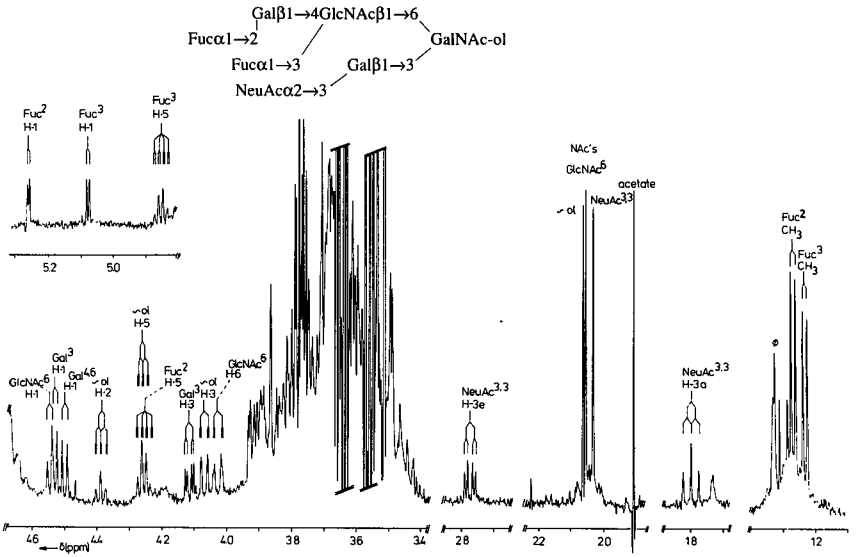

Figure 67a. Resolution-enhanced ^{1}H-NMR spectrum of **108**. For comments, see Figure 64.

Van Pelt *et al.*, 1988). The two NeuAc residues in $\alpha 2 \rightarrow 3$ linkage each have a typical set of H-3 signals, namely, NeuAc^{3,3} H-3a at $\delta = 1.800$ ppm/H-3e at $\delta = 2.775$ ppm, and NeuAc^{3,4} H-3a at $\delta = 1.800$ ppm/H-3e at $\delta = 2.755$ ppm. The latter set matches the NeuAc$\alpha 2 \rightarrow 3$Gal$\beta 1 \rightarrow 4$GlcNAc$\beta 1 \rightarrow$ sequence (Vliegenthart *et al.*, 1983). The sialylation of the *N*-acetyllactosamine unit gives rise to downfield shifts for Gal^{4,6} H-1 ($\Delta\delta = +0.075$ ppm), H-4 ($\Delta\delta = +0.034$ ppm), and H-3. It is interesting that the two NeuAc residues which are both $\alpha 2 \rightarrow 3$ linked to a β-Gal residue can be distinguished from each other on the basis of the chemical shift value for H-3e. For ^{1}H-NMR data of corresponding glycopeptides, see Hirabayashi *et al.* (1990) and Linden *et al.* (1989).

Compound **110** is an extension of **105** with a β-Gal residue attached at C-4 of Gal^{4,6}. Its ^{1}H-NMR spectrum is presented in Figure 69 (Wieruszeski *et al.*, 1987). The Gal^{4,4,6} residue has an H-1 signal at $\delta = 4.595$ ppm ($J_{1,2} = 7.8$ Hz). In a NOE experiment, presaturation of H-1 at $\delta = 4.595$ ppm leads to a clearly observable interglycosidic NOE effect on Gal^{4,6} H-4 at $\delta = 4.188$ ppm. Attachment of Gal^{4,4,6} to Gal^{4,6} affords considerable

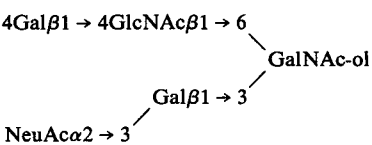

(110)

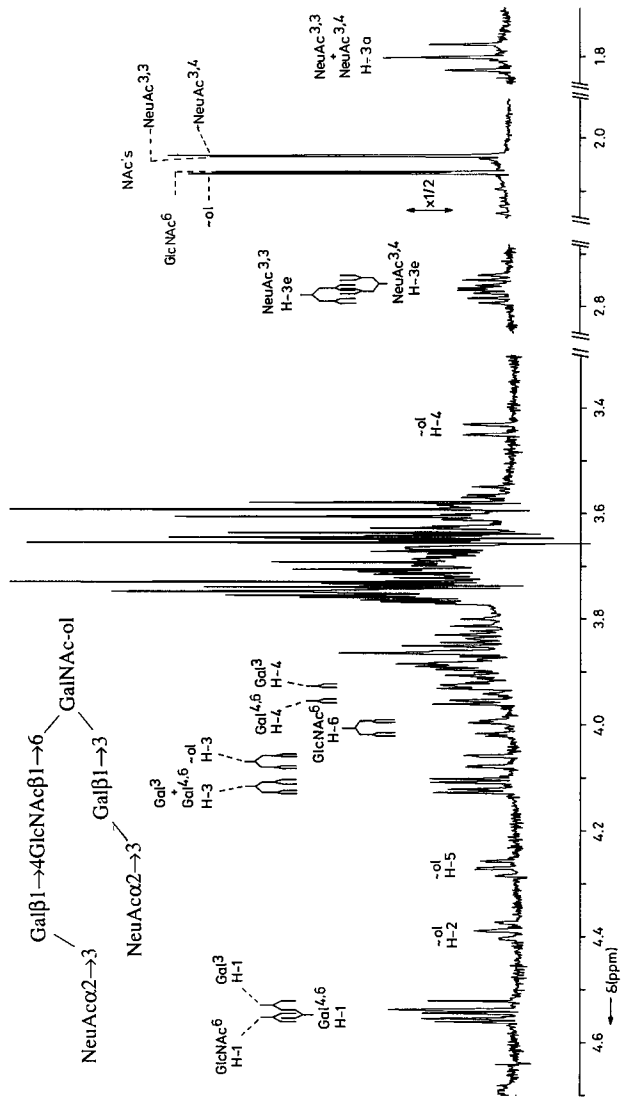

Figure 68. Resolution-enhanced ^{1}H-NMR spectrum of **109**. For comments, see Figure 64.

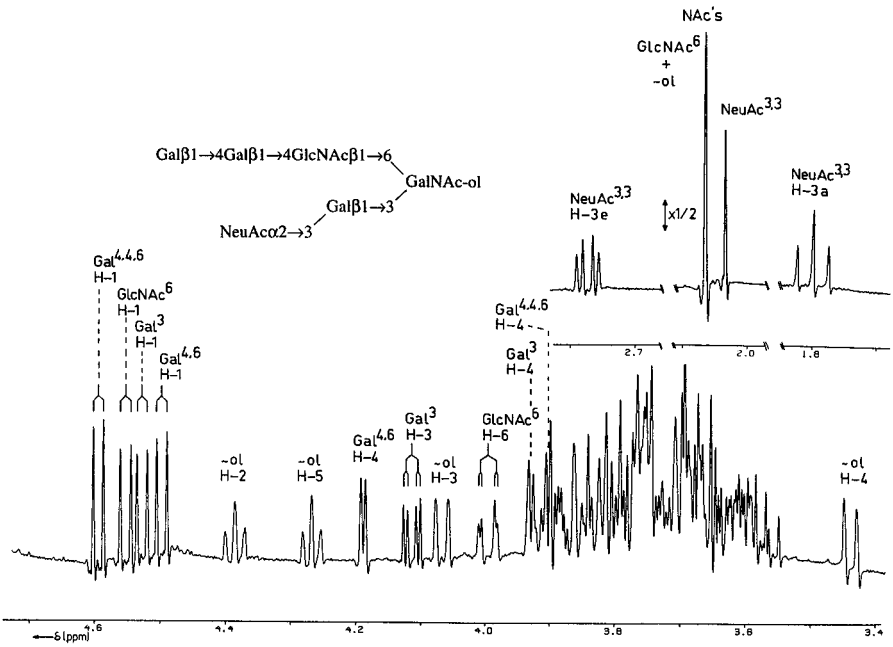

Figure 69. Resolution-enhanced ^{1}H-NMR spectrum of **110**. For comments, see Figure 64.

downfield shift effects for Gal^{4,6} H-1 ($\Delta\delta$ = +0.028 ppm) and H-4 ($\Delta\delta$ = +0.266 ppm). These reporter-group signals have chemical shifts different from the Galβ1 → 3Galβ1 → 4 element (Van Halbeek *et al.*, 1982a).

Compound **111** is an extension of **110** with an α1 → 4-linked Gal residue at Gal^{4,4,6}. The ^{1}H-NMR spectrum is shown in Figure 70 (Wieruszeski *et*

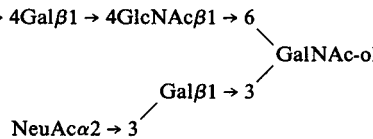

(111)

al., 1987). The Galα1 → 4Galβ1 → 4 sequence is reflected by the Gal^{4,4,4,6} H-5 signal at δ = 4.366 ppm and the Gal^{4,4,4,6} H-1 signal at δ = 4.953 ppm ($J_{1,2}$ = 4.1 Hz). The extension of **110** with α1 → 4-linked Gal leads to considerably large downfield shift effects for Gal^{4,4,6} H-1 ($\Delta\delta$ = +0.114 ppm) and H-4 ($\Delta\delta$ = +0.125 ppm). The parameters typical of the Galα1 → 4Galβ1 → sequence differ significantly from those of the Galα1 → 3Galβ1 → sequence (Dorland *et al.*, 1984; Van Halbeek *et al.*, 1983b). The

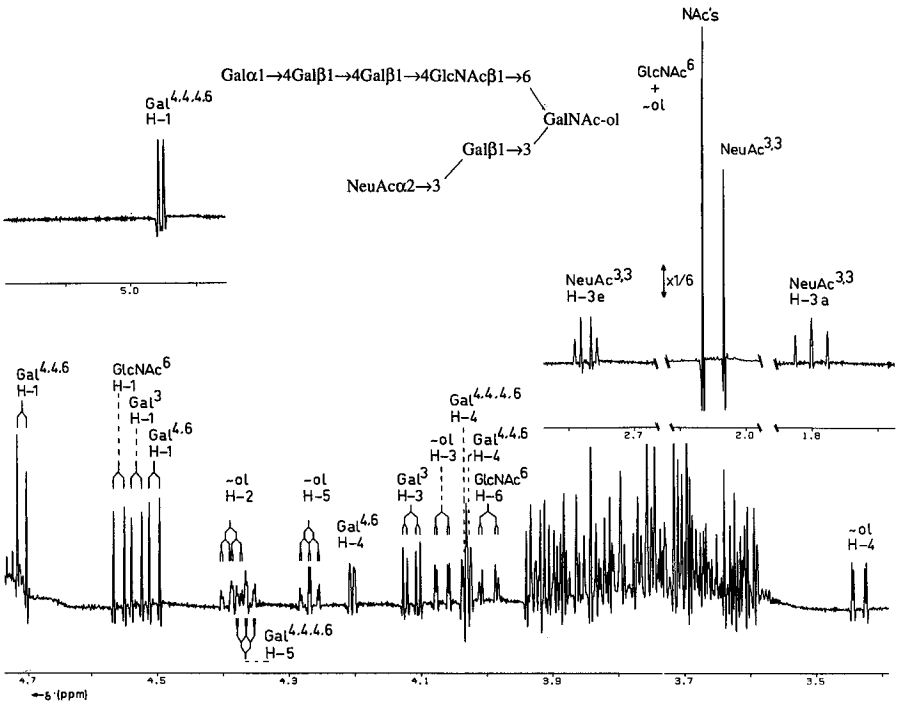

Figure 70. Resolution-enhanced ^{1}H-NMR spectrum of **111**. For comments, see Figure 64.

terminal Galα1 → 4Galβ1 → 4 element is known to occur in the blood group P_1 determinant.

8.7. Extensions of the Galβ1 → 4GlcNAcβ1 → 6(GlcNAcβ1 → 3)GalNAc-ol Backbone Structure

In this section, the ^{1}H-NMR data are presented for the sialylated oligosaccharide-alditols **112–118** containing the Galβ1 → 4GlcNAcβ1 → 6(GlcNAcβ1 → 3)GalNAc-ol backbone structure. The relevant ^{1}H-NMR parameters of these compounds are presented in Table 25. The GlcNAcβ1 → 6(GlcNAcβ1 → 3)GalNAc-ol core type is represented by the set of GalNAc-ol H-2 and H-5 chemical shifts at δ = 4.26–4.29 and 4.20–4.24 ppm, respectively (see Section 11). Other interesting features in the ^{1}H-NMR spectra are the GalNAc-ol NAc singlet at δ = 2.041–2.046 ppm, the GlcNAc^6 H-1 doublet at δ = 4.55–4.57 ppm, and the GlcNAc^6 NAc signal at δ = 2.049–2.066 ppm.

TABLE 25

[1]H Chemical Shifts of Structural-Reporter Groups of Constituent Monosaccharides for Sialylated Oligosaccharide-Alditols with the Galβ1 → 4GlcNAcβ1 → 6(GlcNAcβ1 → 3)GalNAc-ol Backbone Structure in Common (112–118)

Residue	Reporter group	21 	112[a] 	113[a] 	114 	115[a] 	116 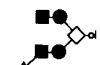	117 	118 
GalNAc-ol	H-2	4.282	4.279	4.278	4.293	4.281	4.286	4.278	4.256
	H-3	3.986	3.984	3.982	n.d.	n.d.	n.d.	n.d.	3.983
	H-4	3.515	3.519	3.509	n.d.	n.d.	n.d.	n.d.	n.d.
	H-5	4.239	4.235	4.227	4.235	4.230	4.238	4.238	4.205
	NAc	2.045	2.044	2.044	2.044	2.044	2.046	2.042	2.041
GlcNAc[3]	H-1	4.599	4.597	4.595	4.622	4.621	4.615	4.648	4.651
	H-6	3.951	3.947	3.947	4.021	4.019	n.d.	n.d.	3.948
	NAc	2.081	2.080	2.080	2.078	2.078	2.076	2.068	2.108
GlcNAc[6]	H-1	4.564	4.556	4.561	4.551	4.560	4.568	4.552	4.564
	H-6	3.998	4.008	4.019	4.009	4.019	n.d.	n.d.	4.003
	NAc	2.061	2.058	2.049	2.059	2.052	2.066	2.058	2.057

$Gal^{4,6}$	H-1	4.473	4.550	4.519	4.551	4.523	4.475	4.554	4.546
	H-3	n.d.[b]	4.115	4.085	4.113	4.088	n.d.	4.114	4.114
	H-4	3.927	3.957	3.932	3.960	3.932	n.d.	n.d.	n.d.
$NeuAc^3$	H-3a	—	1.800	1.795	1.800	1.798	1.798	1.799	1.800
	H-3e	—	2.760	2.764	2.757	2.764	2.757	2.760	2.760
	NAc	—	2.031	2.031	2.033	2.031	2.032	2.032	2.030
Fuc^3	H-1	—	—	5.108	—	5.110	—	—	—
	H-5	—	—	4.820	—	4.83	—	—	—
	CH_3	—	—	1.169	—	1.168	—	—	—
$Gal^{4,3}$	H-1	—	—	—	4.457	4.457	4.533	—	—
	H-3	—	—	—	n.d.	3.67	4.112	—	—
	H-4	—	—	—	n.d.	3.925	n.d.	—	—
$Gal^{3,3}$	H-1	—	—	—	—	—	—	4.451	4.564
	H-4	—	—	—	—	—	—	n.d.	3.961
Fuc^2	H-1	—	—	—	—	—	—	—	5.209
	H-5	—	—	—	—	—	—	—	4.272
	CH_3	—	—	—	—	—	—	—	1.230

[a] Spectrum recorded at 22 °C.
[b] n.d. means value could not be determined merely by inspection of the spectrum.

The ^{1}H-NMR spectrum of **112** is shown in Figure 71 (Breg *et al.*, 1987; Lamblin *et al.*, 1984a; Van Halbeek *et al.*, 1988). The set of chemical shifts of GalNAc-ol H-2 (δ = 4.279 ppm) and H-5 (δ = 4.235 ppm) indicates that **112** possesses GalNAc-ol, disubstituted by GlcNAc residues in β1 → 3 and

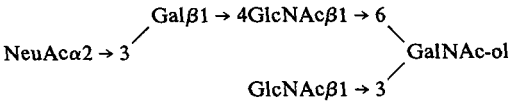

(112)

β1 → 6 linkage, respectively. The position of GlcNAc^3 H-1 (δ = 4.597 ppm; $J_{1,2}$ = 8.3 Hz), together with the H-4 and H-5 signals upfield from the bulk resonance, point to the nonreducing terminal position of this residue (compare with **21**, Table 6). In contrast, GlcNAc^6 bears a β1 → 4-linked Gal

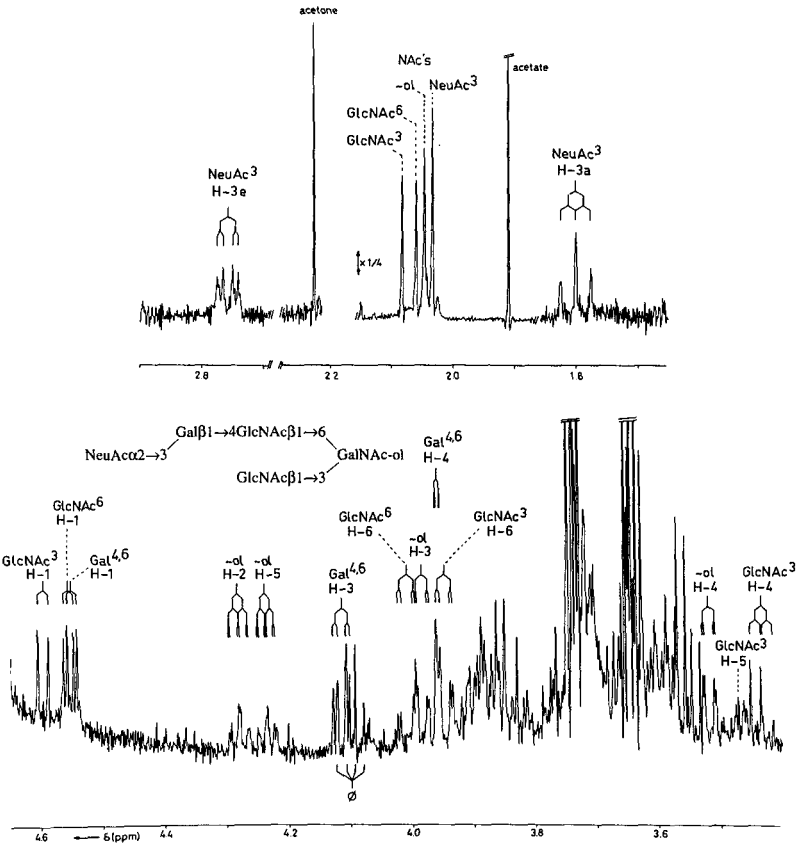

Figure 71. Resolution-enhanced ^{1}H-NMR spectrum of **112** at 22 °C. For comments, see Figure 64.

residue as substituent, as demonstrated by the GlcNAc^6 H-1 chemical shift ($\delta = 4.556$ ppm; $J_{1,2} = 8.1$ Hz). In agreement with the NeuAcα2 → 3Galβ1 → 4GlcNAcβ1 → sequence, the signals of NeuAc H-3a and H-3e resonate at $\delta = 1.800$ and 2.760 ppm, respectively (Vliegenthart *et al.*, 1983). As compared to **21**, the attachment of NeuAc gives rise to downfield shifts for Gal^{4,6} H-1 ($\Delta\delta = +0.077$ ppm), H-4 ($\Delta\delta = +0.030$ ppm), and H-3.

Compound **113** is an α1 → 3 fucosylated extension of **112**, containing the immuno group sialyl-X determinant. In Figure 72 the ^{1}H-NMR spectrum of **113** is depicted (Lamblin *et al.*, 1984a). The chemical shifts of GalNAc-ol

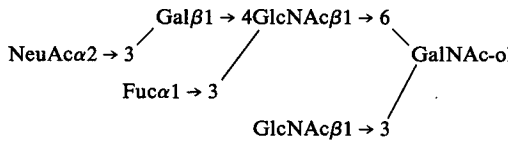

(113)

H-2 and H-5 at $\delta = 4.278$ and 4.227 ppm, respectively, classify **113** as belonging to the GlcNAcβ1 → 6(GlcNAcβ1 → 3)GalNAc-ol core type. The attachment of the α-Fuc residue via a 1 → 3 linkage to GlcNAc^6 is established from the chemical shifts of Fuc^3 H-1 at $\delta = 5.108$ ppm, H-5 at $\delta = 4.820$ ppm, and CH_3 at $\delta = 1.169$ ppm. As compared to **112**, upfield shifts for GlcNAc^6 NAc ($\Delta\delta = -0.009$ ppm) and Gal^{4,6} H-1 ($\Delta\delta = -0.031$ ppm) were observed [compare the shifts going from **39** to **43** (Table 12), and from **99** to **100** (Table 23)]. It should be mentioned that the H-1 value of Fuc^3, α1 → 3 linked to GlcNAc^6 in **113**, differs significantly from that of Fuc^3, α1 → 3 linked to GlcNAc^3 in **89** (Table 21) and **82** (Table 19).

Up to now, **114** has only been detected in a mixture with other oligosaccharide-alditols (Breg *et al.*, 1987; Van Halbeek *et al.*, 1988). The core

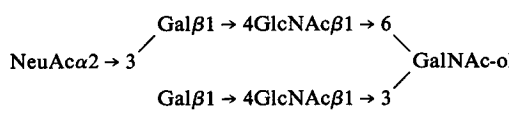

(114)

structure GlcNAcβ1 → 6(GlcNAcβ1 → 3)GalNAc-ol is confirmed by the chemical shift values of GalNAc-ol H-2 ($\delta = 4.293$ ppm) and H-5 ($\delta = 4.235$ ppm). The resonances of NeuAc H-3e ($\delta = 2.757$ ppm) and H-3a ($\delta = 1.800$ ppm) point to a NeuAcα2 → 3Galβ1 → 4GlcNAcβ1 → sequence. In the anomeric region, two Gal H-1 signals are observed, one specific for a terminal Galβ1 → 4 residue ($\delta = 4.457$ ppm), the other demonstrating a Gal residue substituted with NeuAc in α2 → 3 linkage ($\delta = 4.551$ ppm) (Vliegenthart *et al.*, 1983). To distinguish which Gal residue bears NeuAc, the chemical shift values of both Gal H-1 signals have been compared to those in the nonsialylated form **22** (Table 6); for a terminal Gal^{4,3} residue $\delta = 4.456$ ppm is characteristic, and for a terminal Gal^{4,6} residue $\delta = 4.474$ ppm. In accordance with a nonsialylated lower branch,

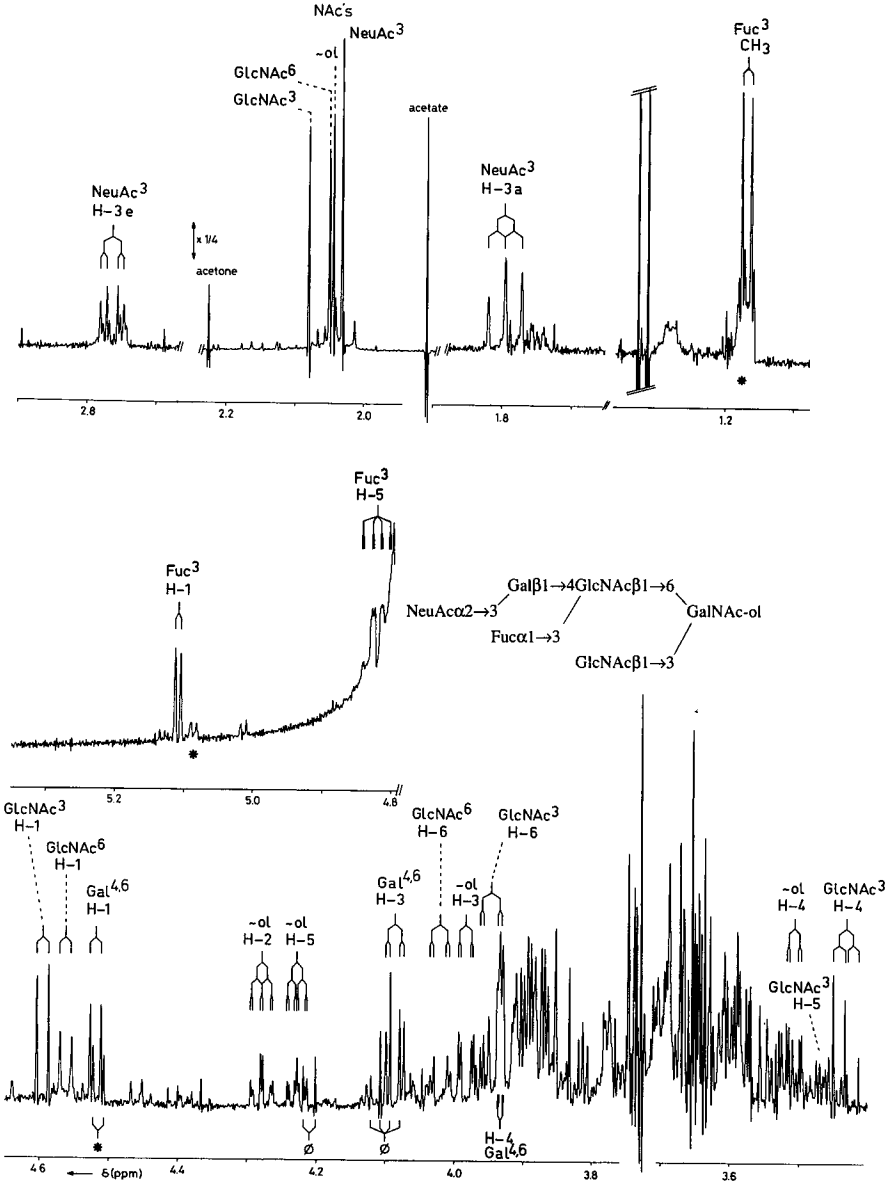

Figure 72. Resolution-enhanced ^{1}H-NMR spectrum of **113**. For comments, see Figure 64.

a downfield shift for the $Gal^{4,6}$ H-1 signal ($\Delta\delta = +0.077$ ppm) and an upfield shift for the $GlcNAc^{6}$ NAc signal ($\Delta\delta = -0.003$ ppm) evidenced the NeuAcα2 → 3 attachment to $Gal^{4,6}$ in the upper branch (compare with **112**).

Compound **115** has been found in a mixture with other oligosaccharide-alditols (Lamblin *et al.*, 1984a) and can be conceived as an extension of

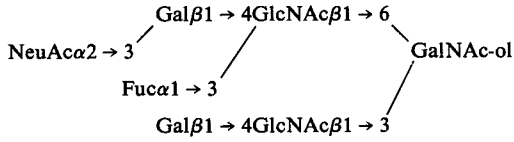

(115)

114 with $\alpha 1 \rightarrow 3$-linked Fuc. The structural-reporter-group signals of the constituting residues of the lower branch at GalNAc-ol match completely those of the same branch in **114**. For the upper branch containing the immuno group sialyl-X determinant, the structural-reporter-group signals are identical to those in the upper branch of **113**. It has to be noted that the chemical shift of Fuc H-1 found for **115** is indicative of the location of the residue at $GlcNAc^{6}$ rather than at $GlcNAc^{3}$ (see remarks at **113**).

Compound **116** is an isomer of **114** (Breg *et al.*, 1987). The GalNAc-ol residue is substituted by GlcNAc residues in $\beta 1 \rightarrow 3$ and $\beta 1 \rightarrow 6$ linkage,

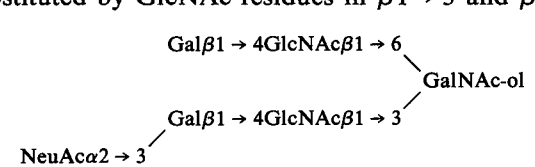

(116)

as follows from the values of GalNAc-ol H-2 ($\delta = 4.286$ ppm) and H-5 ($\delta = 4.238$ ppm). The values of NeuAc H-3a ($\delta = 1.798$ ppm) and H-3e ($\delta = 2.757$ ppm) are typical for NeuAcα2 → 3Galβ1 → 4GlcNAcβ1→. Similar to **114**, in the ^{1}H-NMR spectrum of **116** two Gal H-1 signals are observed, one pointing to a terminal Galβ1 → 4 residue ($\delta = 4.475$ ppm), the other to Gal extended with NeuAc in $\alpha 2 \rightarrow 3$ linkage ($\delta = 4.533$ ppm). Comparing **116** to **22** (Table 6), the presence of the nonsialylated upper branch in **116** is indicated by the $Gal^{4,6}$ H-1 signal at $\delta = 4.475$ ppm, the $GlcNAc^{6}$ H-1 signal at $\delta = 4.568$ ppm, and the $GlcNAc^{6}$ NAc singlet at $\delta = 2.066$ ppm. Owing to the attachment of NeuAc in $\alpha 2 \rightarrow 3$ linkage, the H-1 signals of $Gal^{4,3}$ and $GlcNAc^{3}$ give rise to shifts of $\Delta\delta = +0.077$ and -0.009 ppm, respectively, and the NAc singlet of $GlcNAc^{3}$ to an upfield shift of $\Delta\delta = -0.003$ ppm.

Compound **117** has been observed in a mixture with other oligosaccharide-alditols (Breg *et al.*, 1987) (Figure 66a). The core structure of **117** is GlcNAcβ1 → 6(GlcNAcβ1 → 3)GalNAc-ol, as is clear from the chemical shift values of GalNAc-ol H-2 at $\delta = 4.278$ ppm and H-5 at $\delta = 4.238$ ppm. The attachment of β-Gal in $1 \rightarrow 3$ linkage to $GlcNAc^{3}$ is reflected by the

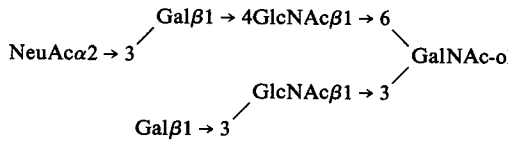

(117)

H-1 and NAc signals of GlcNAc^3 at $\delta = 4.648$ and 2.068 ppm, respectively (compare **23**; Table 6). The latter Gal residue is in terminal position as can be inferred from its H-1 signal at $\delta = 4.451$ ppm. The structural-reporter-group signals of the upper branch match completely those of the upper branch in **114**.

Figure 73 shows the ^{1}H-NMR spectrum of **118** (Breg *et al.*, 1987; Van Halbeek *et al.*, 1988). The GlcNAcβ1 → 6(GlcNAcβ1 → 3)GalNAc-ol core

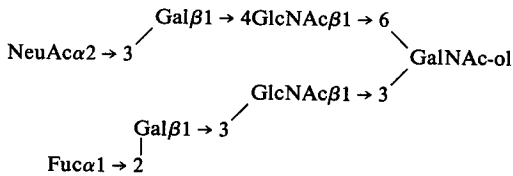

(118)

structure is confirmed by the GalNAc-ol H-2 and H-5 signals at $\delta = 4.256$ and 4.205 ppm, respectively. The GlcNAc^3 NAc singlet at $\delta = 2.108$ ppm is characteristic for the Fucα1 → 2Galβ1 → 3GlcNAcβ1 → 3GalNAc-ol (blood group H/backbone type-1) element, where in GalNAc-ol bears a substituent at C-6 (see **57** and **95**). The occurrence of this element is supported by the positions of Fuc^2 H-1 at $\delta = 5.209$ ppm and CH_3 at $\delta = 1.230$ ppm. The NeuAc residue in α2 → 3 linkage to *N*-acetyllac-

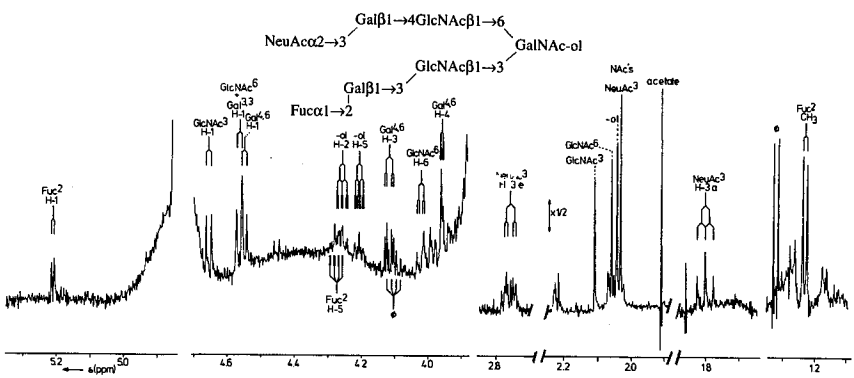

Figure 73. Resolution-enhanced ^{1}H-NMR spectrum of **118**. The relative-intensity scale of the *N*-acetyl methyl proton region of the spectrum differs from that of the other parts, as indicated. Contaminating acetate gives rise to a signal at $\delta = 1.908$ ppm. The signal(s) marked by ϕ stem(s) from (a) frequently occurring, nonprotein noncarbohydrate contaminant(s).

tosamine is demonstrated by its H-3a and H-3e signals at $\delta = 1.800$ and 2.760 ppm, respectively, and by the H-1 doublet of $Gal^{4,6}$ at $\delta = 4.546$ ppm. This compound is the sialylated form of **57** (Table 15), and the concomitant shift effects are observed: a downfield shift for $Gal^{4,6}$ H-1 ($\Delta\delta = +0.078$ ppm) and an upfield shift for $GlcNAc^{6}$ NAc ($\Delta\delta = -0.003$ ppm).

8.8. Extensions of the GalNAcα1 → 3GalNAc-ol Core Structure

In this section, the ^{1}H-NMR data of the sialylated carbohydrates **119–121**, having the GalNAcα1 → 3GalNAc-ol core structure, will be summarized. Table 26 presents the relevant ^{1}H-NMR parameters of these

TABLE 26

^{1}H Chemical Shifts of Structural-Reporter Groups of Constituent Monosaccharides for Sialylated Oligosaccharide-Alditols with the GalNAcα1 → 3GalNAc-ol Core Structure in Common (119–121)

Residue	Reporter group	**4** 	**119** 	**120** 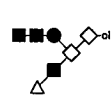	**121** 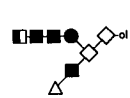	**105** 
GalNAc-ol	H-2	4.395	4.380	4.376	4.377	4.390
	H-3	3.888	3.886	3.886	3.887	4.072
	NAc	2.049	2.043	2.043	2.045	2.066
$GalNAc^{3}$	H-1	5.103	5.109	5.110	5.111	—
	H-2	4.235	4.396	4.395	4.396	—
	H-3	3.921	4.043	4.039	4.041	—
	H-4	4.043	4.262	4.262	4.262	—
	H-5	4.073	4.155	4.153	4.153	—
	H-6	3.791	4.081	4.082	4.082	—
	NAc	2.060	2.075	2.075	2.076	—
Gal^{3}	H-1	—	4.540	4.538	4.539	4.534
	H-3	—	4.074	4.074	4.070	4.116
	H-4	—	3.931	3.931	3.931	3.930
$GlcNAc^{6}$	H-1	—	4.607	4.605	4.607	4.559
	H-6	—	3.998	3.997	4.003	3.993
	NAc	—	2.037	2.037	2.038	2.066
$Gal^{4,6}$	H-1	—	4.467	4.499	4.503	4.470
	H-4	—	3.923	4.189	4.204	3.922
$Gal^{4,4,6}$	H-1	—	—	4.597	4.710	—
	H-4	—	—	3.902	4.027	—
$Gal^{4,4,4,6}$	H-1	—	—	—	4.953	—
	H-4	—	—	—	4.034	—
	H-5	—	—	—	4.365	—
$NeuAc^{3}$	H-3a	—	1.783	1.783	1.784	1.801
	H-3e	—	2.760	2.759	2.759	2.774
	NAc	—	2.028	2.028	2.029	2.033

compounds, together with those of **4** and **105** as reference substances. For general features, see Section 11.

The ^{1}H-NMR spectrum of **119** is depicted in Figure 74 (Wieruszeski *et al.*, 1987). Typical indications for the GalNAcα1 → 3GalNAc-ol core

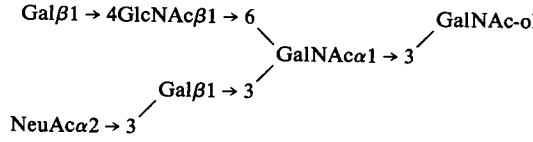

(119)

structure form the combination of the GalNAc-ol H-2 and H-3 signals at $\delta = 4.380$ and 3.886 ppm, respectively (see also **4** and Section 11). The α-GalNAc^3 H-1 signal is found at $\delta = 5.109$ ppm ($J_{1,2} = 4.1$ Hz). Other GalNAc signals are H-2 at $\delta = 4.396$ ppm, H-3 at $\delta = 4.043$ ppm, H-4 at $\delta = 4.262$ ppm, H-5 at $\delta = 4.155$ ppm, and H-6 at $\delta = 4.081$ ppm. The $\alpha 2 \rightarrow$ 3-linked NeuAc residue is reflected by the set of structural-reporter groups H-3a at $\delta = 1.783$ ppm, H-3e at $\delta = 2.760$ ppm, and NAc at $\delta = 2.028$ ppm, slightly differing from the set for the NeuAcα2 → 3Galβ1 → 3GalNAc-ol

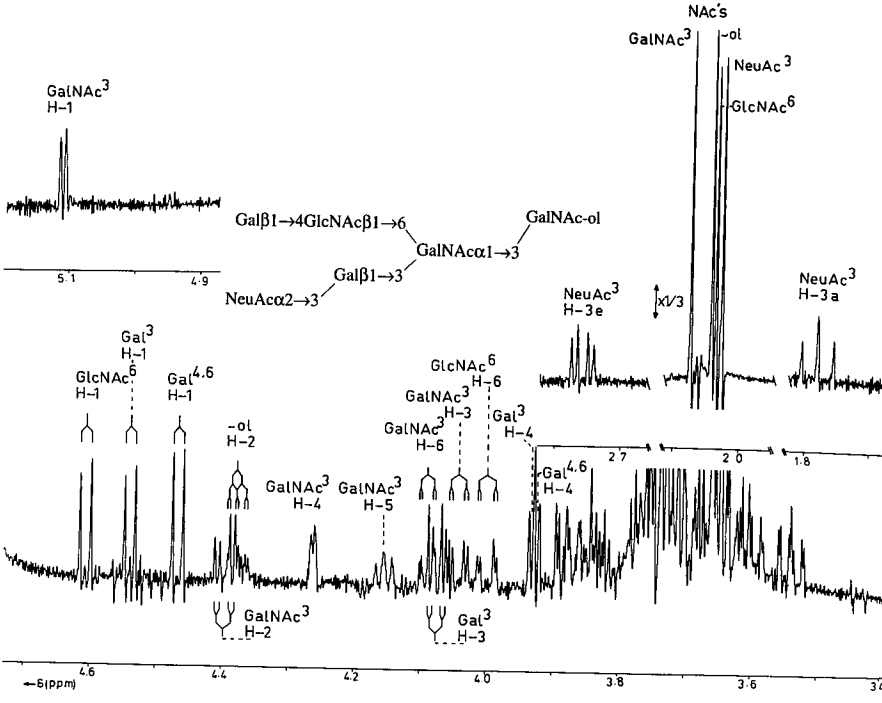

Figure 74. Resolution-enhanced ^{1}H-NMR spectrum of **119**. For comments, see Figure 73.

sequence in **105**. The positions of the Gal^3 H-1 and H-3 signals at $\delta = 4.540$ and 4.074 ppm, respectively, are in agreement with substitution at C-3 of Gal^3 but also here deviations are observed with respect to **105**. The chemical shift value of the $Gal^{4,6}$ H-1 signal at $\delta = 4.467$ ppm illustrates the terminal position of the $Gal^{4,6}$ residue (compare to **105**).

Compound **120** is an extension of **119** with β-Gal 1 → 4 linked to $Gal^{4,6}$. Its ^{1}H-NMR spectrum is presented in Figure 75 (Wieruszeski *et al.*, 1987).

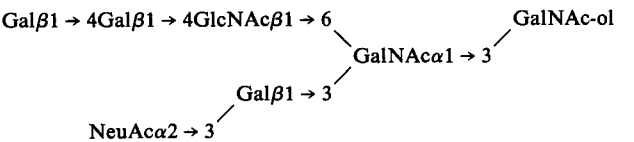

(120)

The structural-reporter groups of GalNAc-ol, $GalNAc^3$, Gal^3, $NeuAc^3$, and $GlcNAc^6$ in **120** match completely those of **119**. The assignments for the various α-GalNAc protons have been obtained by consecutive double-resonance (spin decoupling and NOE) experiments starting from GalNAc H-1 ($\delta = 5.110$ ppm; $J_{1,2} = 4.1$ Hz). The core GalNAc serves as a C-3,C-6

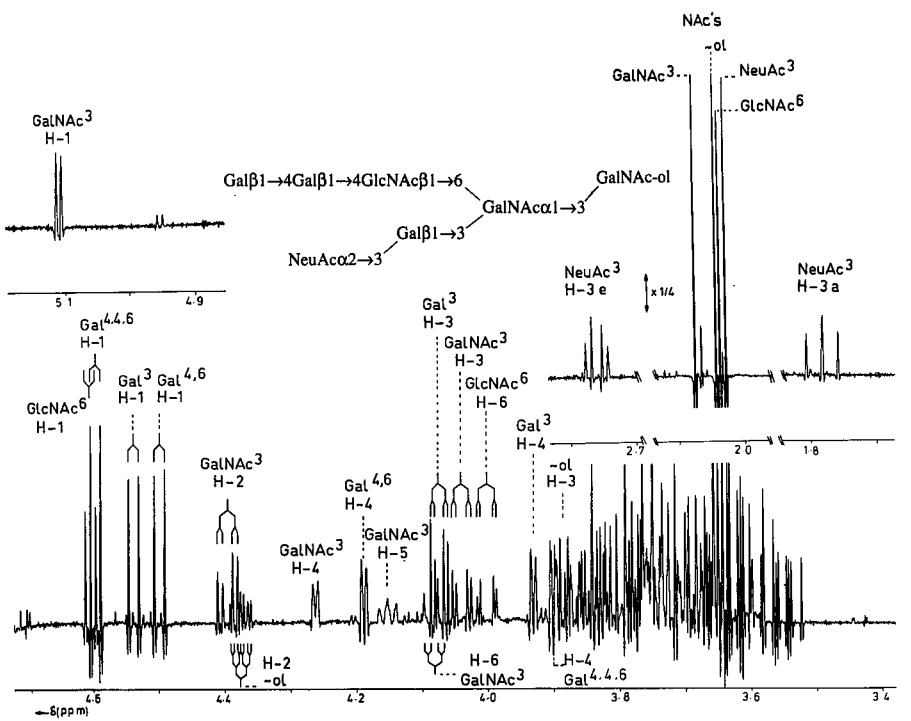

Figure 75. Resolution-enhanced ^{1}H-NMR spectrum of **120**. For comments, see Figure 73.

branching point, wherein the NeuAcα2 → 3Galβ1 → element is attached to C-3, and the Galβ1 → 4Galβ1 → 4GlcNAcβ1 → element to C-6. The sites of substitution have been established by the observation of interresidue NOE effects between Gal^3 H-1 and GalNAc^3 H-3 on the one hand, and between GlcNAc^6 H-1 and GalNAc^3 H-6 on the other. In addition, a NOE effect on the H-3 signal of GalNAc-ol at $\delta = 3.886$ ppm can be detected due to presaturation of GalNAc H-1, and vice versa. The common presence of the Galβ1 → 4Galβ1 → 4GlcNAcβ1 → sequence in **110** (Table 24) and **120** is evident from the same structural-reporter-group signals for Gal^{4,6} (H-1, $\delta = 4.499$ ppm; H-4, $\delta = 4.189$ ppm) as well as for Gal^{4,4,6} (H-1, $\delta = 4.597$ ppm; H-4, $\delta = 3.902$ ppm).

Compound **121** is an extension of **120** with α-Gal 1 → 4 linked to Gal^{4,4,6}. The ^{1}H-NMR spectrum of **121** is shown in Figure 76 (Wieruszeski

Galα1 → 4Galβ1 → 4Galβ1 → 4GlcNAcβ1 → 6 GalNAc-ol **(121)**

GalNAcα1 → 3

Galβ1 → 3

NeuAcα2 → 3

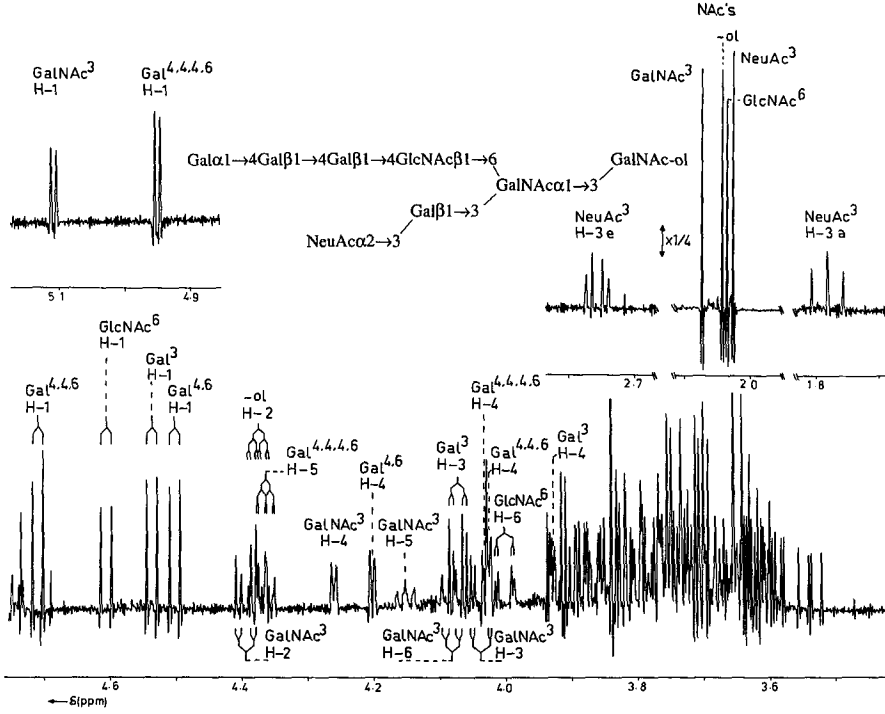

Figure 76. Resolution-enhanced ^{1}H-NMR spectrum of **121**. For comments, see Figure 73.

et al., 1987). The structural-reporter-group signals of the GalNAc-ol, GalNAc^3, Gal^3, NeuAc^3, and GlcNAc^6 match those of the corresponding residues in **119** and **120**. The common presence of the Galα1 → 4Galβ1 → 4Galβ1 → 4GlcNAcβ1 → sequence in **111** (Table 24) and **121** is reflected by the structural-reporter groups for Gal^{4,4,4,6} (H-1, δ = 4.953 ppm; H-4, δ = 4.034 ppm; H-5, δ = 4.365 ppm), Gal^{4,4,6} (H-1, δ = 4.710 ppm; H-4, δ = 4.027 ppm), and Gal^{4,6} (H-1, δ = 4.503 ppm; H-4, δ = 4.204 ppm). The terminal Galα1 → 4Galβ1 → 4 sequence is known to occur in the blood group P_1 determinant.

8.9. Additional Sialylated Oligosaccharide-Alditols

The ^{1}H-NMR data acquired at 270 MHz of the sialylated oligosaccharide-alditols **122–127** and **128–131** have been compiled in Tables 27 and 28, respectively. Compounds **122–127** are extensions of **75**, and compounds **128–131** are extensions of **76** (Table 18).

The ^{1}H-NMR parameters of **122–127** (Table 27) have been described by Shimamura *et al.* (1984) (see also Iwasaki *et al.*, 1984). The GalNAc-ol H-2 signal is found at δ = 4.37–4.39 ppm in accordance with the corresponding signal in **9A** (δ = 4.380 ppm) (see also Section 11). Making use of complex-formation with borate, the Fuc H-1, GalNAc H-1, Gal^4 H-1, and

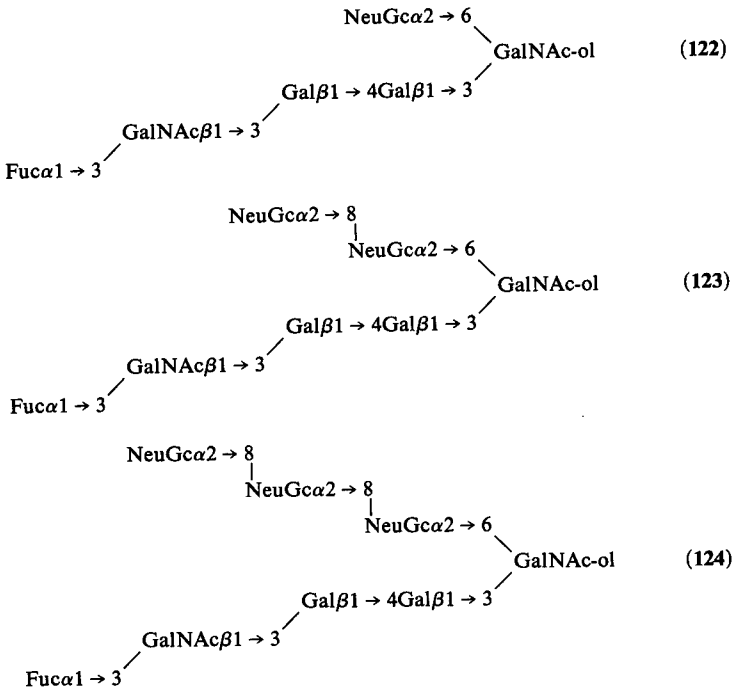

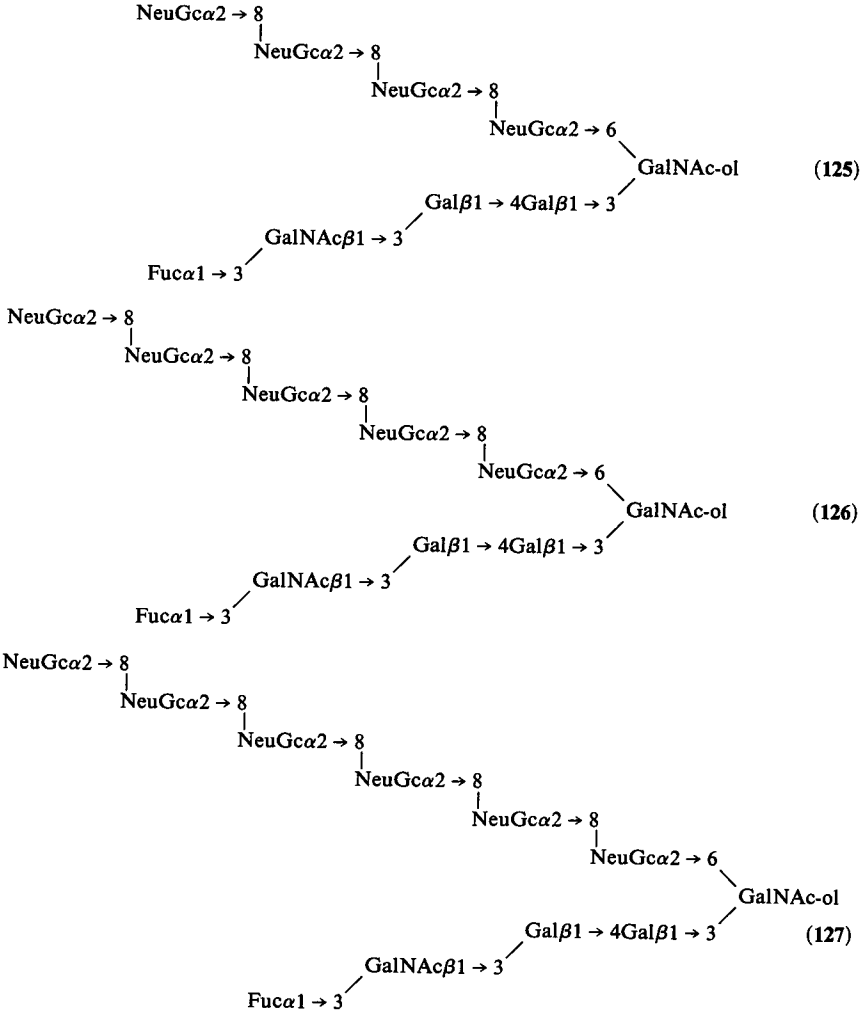

Gal[3] H-1 signals have been found at $\delta = 4.995$–4.997 ppm, $\delta = 4.779$–4.800 ppm (60 °C), $\delta = 4.608$–4.609 ppm, and $\delta = 4.500$–4.507 ppm, respectively (for comparison, see **75**; Table 18). The Fuc residue shows a CH_3 signal at $\delta = 1.204$–1.205 ppm. Comparison of the structural-reporter-group signals of the core NeuGc residue in **9A** and **122** shows identical chemical shift values for H-3a ($\delta = 1.714$ ppm) as well as for H-3e ($\delta = 2.744$ ppm). The presence of $\alpha 2 \rightarrow 8$-linked NeuGc oligomers leads to the following observations in the ^{1}H-NMR spectra of **123**–**127**: The $NeuGc_{proximal}$ residue is reflected by signals of H-3a at $\delta = 1.661$–1.667 ppm and H-3e at $\delta = 2.653$–2.660 ppm, the $NeuGc_{distal}$ residue by signals of H-3a

TABLE 27

^{1}H Chemical Shifts (23 °C) of Structural-Reporter Groups of Constituent Monosaccharides for Sialylated β-GalNAc-Containing Oligosaccharide-Alditols (122–127)

Residue	Reporter group	122 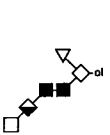	123 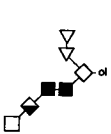	124 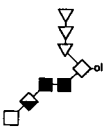	125 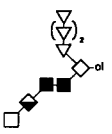	126 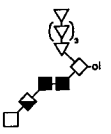	127 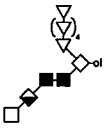
Fuc	H-1	4.997	4.995	4.996	4.996	4.995	4.997
GalNAc	H-1[a]	4.779	4.792	4.800	4.800	4.797	4.789
Gal[4]	H-1	4.608	4.608	4.608	4.609	4.608	4.609
Gal[3]	H-1	4.500	4.504	4.504	4.507	4.505	4.505
$NeuGc_p$[b]	H-3a	—	1.661	1.665	1.666	1.667	1.666
$NeuGc_i$	H-3a	—	—	1.698	1.711	1.712	1.714
$NeuGc_d$	H-3a	1.714	1.743	1.750	1.758	1.758	1.758
$NeuGc_p$	H-3e	—	2.657	2.654	2.660	2.653	2.660
$NeuGc_i$	H-3e	—	—	2.706	2.707	2.707	2.709
$NeuGc_d$	H-3e	2.744	2.780	2.778	2.779	2.779	2.780
Fuc	CH_3	1.204	1.204	1.204	1.205	1.205	1.205
GalNAc	NAc	2.042	2.042	2.040	2.042	2.041	2.043
GalNAc-ol	NAc	2.042	2.042	2.040	2.042	2.041	2.043
GalNAc-ol	H-2	4.376	4.384	4.384	4.384	4.383	4.389

[a] Measured at 60 °C.
[b] p = proximal; i = internal; d = distal.

at $\delta = 1.743$–1.758 ppm and H-3e at $\delta = 2.778$–2.780 ppm, and the $NeuGc_{internal}$ residues by signals of H-3a at $\delta = 1.698$–1.714 ppm and H-3e at $\delta = 2.706$–2.709 ppm. For some ^{1}H-NMR data of Galβ1 → 3([NeuGcα2 → 8]$_{1-2}$NeuGcα2 → 6)GalNAc-ol, see Nomoto *et al.* (1982). For additional ^{1}H-NMR data of $(NeuGc)_{2-4}$ with α2 → 8 linkages, see Kitajima *et al.* (1984); for ^{1}H-NMR data of $(NeuAc)_{2-3}$ with α2 → 8 linkages, see Nomoto *et al.* (1982). See also disialyllactose (Dorland *et al.*, 1986).

The ^{1}H-NMR parameters of **128–131** (Table 28) have been reported by Kitajima *et al.* (1984). In each case the lower branch gives rise to Gal^3 H-1 signals at $\delta = 4.50$–4.51 ppm and Gal^4 H-1 signals at $\delta = 4.59$–4.60 ppm. Similar values have been found for nonsialylated **76** (Table 18). As compared to **76**, the introduction of α2 → 3-linked NeuGc at C-3 of GalNAc^3 in **128** causes downfield shifts for both GalNAc^3 H-1 ($\Delta\delta = +0.118$ ppm) and GalNAc^4 H-1 ($\Delta\delta = +0.138$ ppm). This NeuGc^3 residue is reflected by a characteristic set of H-3a and H-3e signals at $\delta = 1.85$–186 ppm and 2.56 ppm, respectively. Compounds **129–131** are higher sialylated forms of

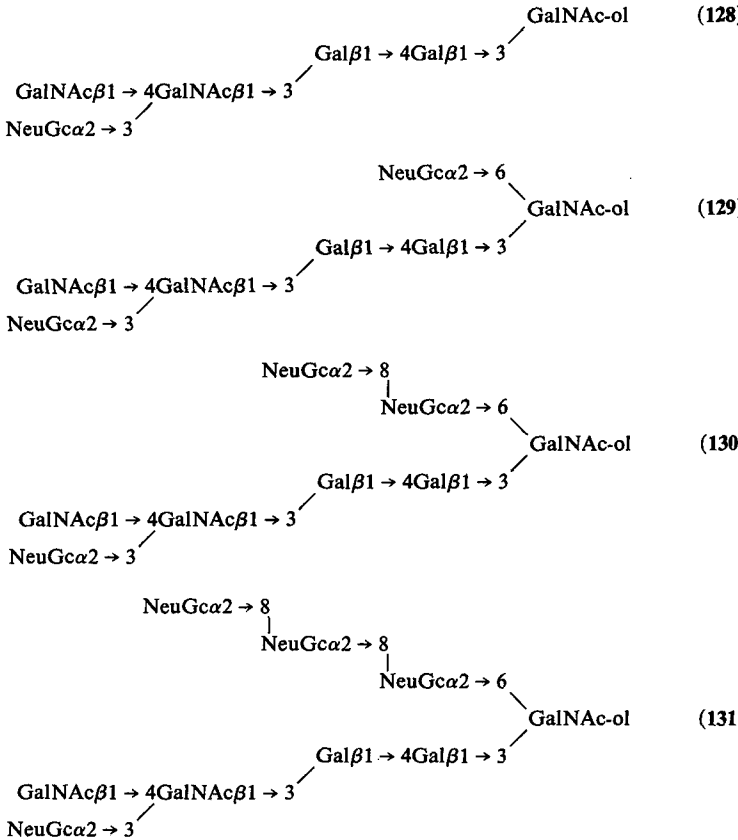

TABLE 28

^{1}H Chemical Shifts (23 °C) of Structural-Reporter Groups of Constituent Monosaccharides for (Deaminated) Sialylated β-GalNAc-Containing Oligosaccharide-Alditols (128–132)

Residue	Reporter group	128 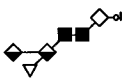	129 	130 	131 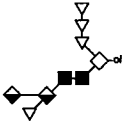	132 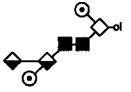
Gal[3]	H-1	4.497	4.501	4.504	4.508	4.49
Gal[4]	H-1	4.594	4.598	4.598	4.597	4.59
GalNAc[3]	H-1	4.770[a,b]	n.d.[d]	n.d.	n.d.	4.80[a]
GalNAc[4]	H-1	4.790[a,b]	n.d.	n.d.	n.d.	4.80[a]
NeuGc[3]	H-3a	1.860	1.853	1.859	1.855	1.79[c]
NeuGc[6]	H-3a	—	1.714	1.666	1.666	1.66[c]
NeuGc[8,6]	H-3a	—	—	1.741	1.696	—
NeuGc[8,8,6]	H-3a	—	—	—	1.753	—
NeuGc[3]	H-3e	2.558	2.556	2.562	2.559	2.48[c]
NeuGc[6]	H-3e	—	2.745	2.659	2.659	2.66[c]
NeuGc[8,6]	H-3e	—	—	2.779	2.708	—
NeuGc[8,8,6]	H-3e	—	—	—	2.778	—
GalNAc-ol	NAc	2.061	2.075	2.073	2.074	2.06
GalNAc[3]	NAc	2.012	2.009	2.008	2.009	2.00
GalNAc[4]	NAc	2.048	2.048	2.038	2.042	2.04

[a] Measured at 60 °C.
[b] Assignments may have to be interchanged.
[c] Kdn instead of NeuGc.
[d] n.d. means value could not be determined merely by inspection of the spectrum.

128 with NeuGc-oligomer extensions at GalNAc-ol C-6. The set of H-3 signals of the core NeuGc[6] in **129** fits the ^{1}H-NMR data known for this structural element (H-3a, δ = 1.714 ppm; H-3e, δ = 2.745 ppm, see **9A** and **122**). In a similar way the H-3 structural-reporter groups of the $NeuGc_{proximal}$, $NeuGc_{distal}$, and $NeuGc_{internal}$ residues in **130** and **131** correspond with the values observed for **123–127** (Table 27).

9. PERIPHERAL DEAMINATED SIALIC ACID

The 400-MHz ^{1}H-NMR data of a deaminated sialic acid-containing oligosaccharide-alditol (**132**), being an analog of **129**, have been described

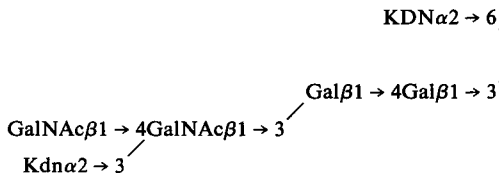

(132)

by Iwasaki *et al.* (1987b), and are included in Table 28 (see, for KDN, Nadano *et al.*, 1986).

10. SULFATED OLIGOSACCHARIDE-ALDITOLS

The ^{1}H-NMR data of only three sulfated oligosaccharide-alditols have been reported so far, namely, **133** (Strecker *et al.*, 1987, 1989a), **134** (Strecker *et al.*, 1987, 1989a), and **135** (Capon *et al.*, 1989). The structural-reporter-group data are presented in Table 29, together with reference compounds **25**, **105**, and **92**. For general features of the core structures, see also Section 11.

The 400-MHz ^{1}H-NMR spectrum of **133** (Strecker *et al.*, 1987) is depicted in Figure 77. As compared to **25**, typical downfield shifts are observed for the GlcNAc[6] H-6 ($\Delta\delta$ = +0.421 ppm) and H-6′ ($\Delta\delta$ = +0.521 ppm) resonances, in accordance with the presence of a sulfate group at C-6 of GlcNAc[6]. Additional significant alterations are found for GlcNAc[6]

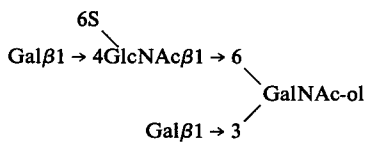

(133)

TABLE 29

^{1}H Chemical Shifts of Structural-Reporter Groups of Constituent Monosaccharides for Sulfated Oligosaccharide-Alditols (133–135)

Residue	Reporter group	25 	133 	105 	134 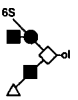	92 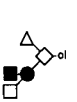	135 
GalNAc-ol	H-2	4.394	4.385	4.390	4.384	4.247	4.250
	H-3	4.060	4.058	4.072	4.066	3.984	4.005
	H-4	3.465	3.471	3.435	3.437	n.d.	3.577
	H-5	4.282	4.271	4.272	4.252	4.179	4.179
	H-6	3.931	3.943	3.927	3.937	n.d.	n.d.
	H-6′	n.d.[a]	n.d.	n.d.	n.d.	3.489	3.490
	NAc	2.067	2.065	2.066	2.066	2.034[b]	2.035[c]
Gal^3	H-1	4.465	4.462	4.534	4.527	—	—
	H-2	3.560	3.571	n.d.	3.609	—	—
	H-3	3.674	3.667	4.116	4.111	—	—
	H-4	3.900	3.898	3.930	3.925	—	—
GlcNAc^6	H-1	4.560	4.583	4.559	4.581	—	—
	H-6	3.998	4.419	3.993	4.412	—	—
	H-6′	3.828	4.349	n.d.	4.328	—	—
	NAc	2.064	2.065	2.066	2.064	—	—
GlcNAc^3	H-1	—	—	—	—	4.645	4.648
	H-6	—	—	—	—	4.021	4.029
	NAc	—	—	—	—	2.066	2.068
Gal^4	H-1	4.470	4.538	4.470	4.537	4.444	4.560
	H-2	3.538	3.555	n.d.	3.528	n.d.	n.d.
	H-3	3.669	3.677	n.d.	3.675	n.d.	4.332
	H-4	3.925	3.927	3.922	3.925	n.d.	4.272
NeuAc^{3,3}	H-3a	—	—	1.801	1.801	—	—
	H-3e	—	—	2.774	2.774	—	—
	NAc	—	—	2.033	2.032	—	—
NeuAc^6	H-3a	—	—	—	—	1.698	1.700
	H-3e	—	—	—	—	2.732	2.736
	NAc	—	—	—	—	2.025[b]	2.027[c]
Fuc^3	H-1	—	—	—	—	5.132	5.135
	H-5	—	—	—	—	4.819	4.802
	CH_3	—	—	—	—	1.177	1.180

[a] n.d. means value could not be determined merely by inspection of the spectrum.
[b] Assignments may have to be interchanged.
[c] Assignments may have to be interchanged.

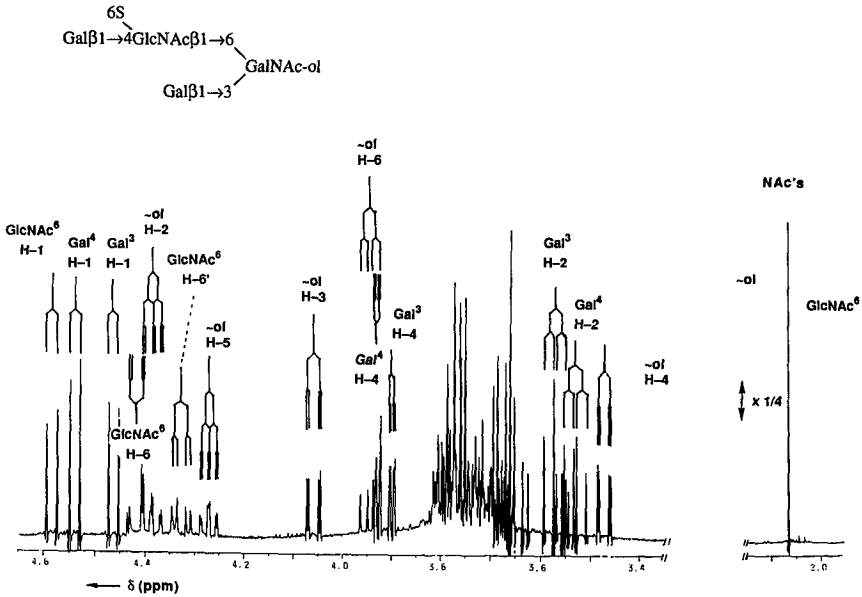

Figure 77. Resolution-enhanced 400-MHz ^{1}H-NMR spectrum of **133**. The relative-intensity scale of the *N*-acetyl methyl proton region of the spectrum differs from that of the other parts, as indicated.

H-1 ($\Delta\delta$ = +0.023 ppm), Gal^{4,6} H-1 ($\Delta\delta$ = +0.068 ppm), and Gal^{4,6} H-2 ($\Delta\delta$ = +0.017 ppm). The other structural-reporter-group signals are not influenced significantly ($\Delta\delta < 0.01$ ppm).

Compound **134** (Strecker *et al.*, 1987) is a sulfated extension of **105** (Figure 78). As compared to **105**, the GlcNAc^6 H-6 and H-6′ atoms resonate

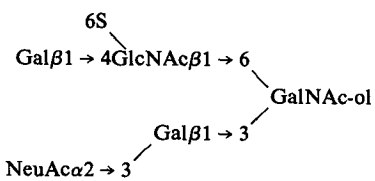

(134)

clearly outside the bulk of skeleton protons at more downfield positions (H-6, $\Delta\delta$ = +0.419 ppm). The various structural-reporter groups of the upper branch are similar to those of the same branch in **133**, whereas the structural reporters of the lower branch resemble those of the same branch in **105**. It has to be noted that the chemical shift values for GlcNAc^6 H-6 and H-6′, as published by Strecker *et al.* (1987), have been modified in this review (personal communication, G. Strecker).

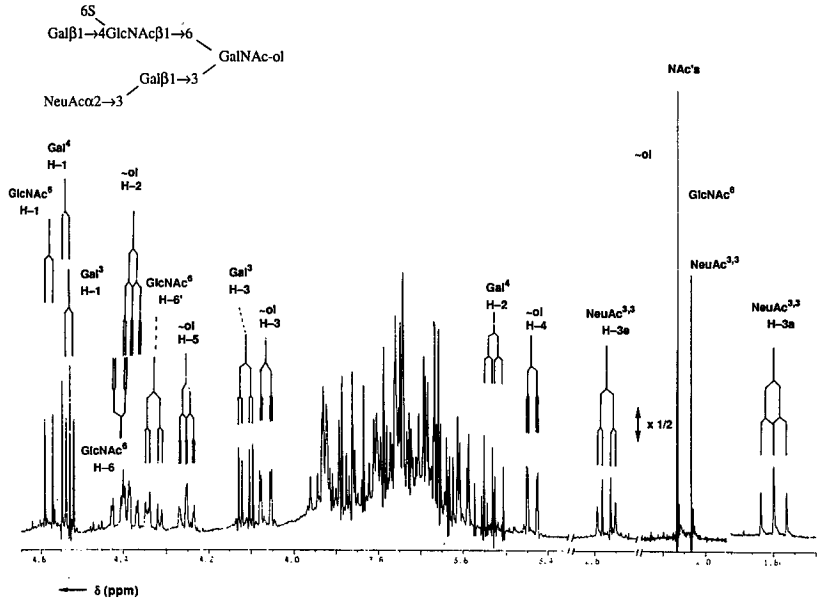

Figure 78. Resolution-enhanced 400-MHz ^{1}H-NMR spectrum of **134**. For comments, see Figure 77.

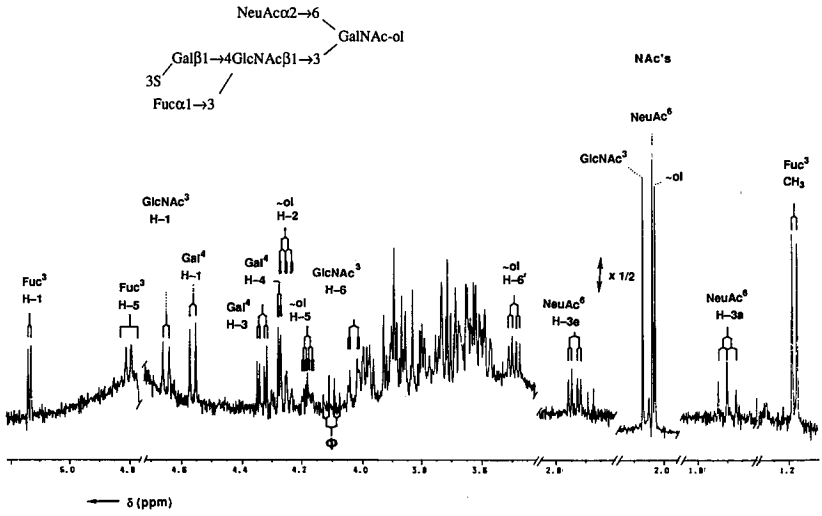

Figure 79. Resolution-enhanced 400-MHz ^{1}H-NMR spectrum of **135**. For comments, see Figure 77. The signal marked by ϕ stems from a frequently occurring, nonprotein noncarbohydrate contaminant.

The 400-MHz ^{1}H-NMR spectrum of **135** (Capon *et al.*, 1989) is presented in Figure 79. As compared to **92**, significant downfield shifts to positions

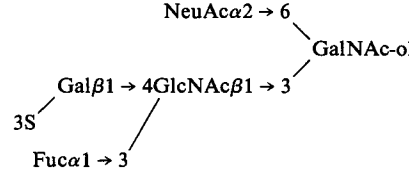

(135)

outside the bulk of skeleton protons are observed for Gal^4 H-3 (δ = 4.332 ppm) and Gal^4 H-4 (δ = 4.272 ppm). Moreover, Gal^4 H-1 undergoes a downfield shift of $\Delta\delta = +0.116$ ppm, whereas Fuc^3 H-5 shifts upfield ($\Delta\delta = -0.017$ ppm). The other structural-reporter-group signals are not influenced significantly ($\delta < 0.01$ ppm).

11. SUMMARY OF GENERAL FEATURES

For smaller oligosaccharide-alditols, the core structure, i.e., the substitution pattern of GalNAc-ol, is usually inferred from the resonance positions of GalNAc-ol H-2 and H-5, whereas in specific cases H-3 also has to be taken into account. Starting from these parameters, the total structure is then deduced from the additional structural-reporter-group signals. When analyzing larger structures, the H-2 and H-5 resonances of GalNAc-ol may be obscured by other carbohydrate signals. The complete structure is then in fact assembled from separately recognizable peripheral structural elements. The combination of shift effects arising from partial structures should account for the observed spectrum of the compound. If the amount of material is not the limiting factor, the different 2D NMR techniques available nowadays are highly valuable to reach conclusive evidence for complicated structures. Obviously, the total structure must be in accordance with restrictions imposed by other analytical methods. For the ^{1}H-NMR approach, monosaccharide analysis of unknown structures is compulsory. Moreover, knowledge of the charge and the apparent size of carbohydrate chains, as determined from their chromatographic behavior (GPC, FPLC, HPLC) during fractionation, is very helpful. In the case of compounds with high complexity in primary structure, information from glycosidase studies, methylation analysis, and different modes of mass spectrometry, especially fast atom bombardment mass spectrometry, can provide valuable information.

In this section, a survey will be presented of empirical rules deduced from the ^{1}H-NMR data of the large series of oligosaccharide-alditols

included in this chapter, divided into core structures, backbone structures, and peripheral elements.

11.1. Core Structures

Scheme 5 gives information about the structural-reporter-group data of GalNAc-ol when substituted at C-3 by β-Gal, β-GlcNAc, or α-GalNAc, and/or at C-6 by β-GlcNAc or α-NeuAc/NeuGc.

Structural element	H-2	H-5
GalNAc-ol	4.25	3.93
→Galβ1 → 3GalNAc-ol	4.38–4.40	4.13–4.20
GalNAcα1 → 3(→)Galβ1 → 3GalNAc-ol	4.30	4.13
→Galβ1 → 3(→GlcNAcβ1 → 6)GalNAc-ol	4.38–4.41	4.22–4.29
GalNAcα1 → 3(→)Galβ1 →3(→GlcNAcβ1 → 6)GalNAc-ol	4.27–4.31	4.21–4.23
Galα1 → 3(→)Galβ1 → 3(→GlcNAcβ1 → 6)GalNAc-ol	4.32	4.22
→Galβ1 → 3(→NeuAc/Gcα2 → 6)GalNAc-ol	4.36–4.39	4.18–4.25
GalNAcα1 → 3(→)Galβ1 →3(NeuAc/Gcα2 → 6)GalNAc-ol	4.29	4.19
→GlcNAcβ1 → 3GalNAc-ol	4.27–4.29	4.11–4.14
→GlcNAcβ1 → 3(→GlcNAcβ1 → 6)GalNAc-ol	4.26–4.30	4.20–4.24
→GlcNAcβ1 → 3(NeuAcα2 → 6)GalNAc-ol	4.24–4.27	4.15–4.21
→GalNAcα1 → 3GalNAc-ol	4.37–4.40	3.75
→GalNAcα1 → 3(NeuAc/Gcα2 → 6)GalNAc-ol	4.39–4.40	n.d.
→GlcNAcβ1 → 6GalNAc-ol	4.24–4.25	4.02–4.03
NeuAc/Gcα2 → 6GalNAc-ol	4.24–4.25	4.02–4.03

Scheme 5. Structural-reporter-group data of GalNAc-ol, specific for the type of core structures.

Compounds with Gal in β1 → 3 linkage at GalNAc-ol, nonsubstituted or substituted with β-GlcNAc or α-NeuAc/NeuGc at C-6, give rise to a GalNAc-ol H-2 signal in the region $\delta = 4.36$–4.41 ppm, except when blood group A or B structural elements occur, wherein this Gal residue is involved. The presence of blood group A or B determinants directly attached to GalNAc-ol (backbone type-3 in the native carbohydrate chains) strongly influences the position of the GalNAc-ol H-2 signal ($\delta = 4.27$–4.32 ppm). For compounds with GlcNAc in β1 → 3 linkage at GalNAc-ol, nonsubstituted or substituted with β-GlcNAc or α-NeuAc/NeuGc at C-6, this range is $\delta = 4.24$–4.30 ppm. It can be concluded that in each case the chemical shift values are hardly affected by elongation of the chain, neither

at Gal/GlcNAc nor at C-6 of GalNAc-ol. The occurrence of GalNAc in $\alpha 1 \rightarrow 3$ linkage at GalNAc-ol, with or without α-NeuAc/NeuGc attached to C-6, leads to the same chemical shift region for GalNAc-ol H-2 as mentioned above for $\beta 1 \rightarrow 3$-linked Gal ($\delta = 4.37$–4.40 ppm), but in this case the GalNAc-ol H-3 signal is observed at $\delta = 3.9$ ppm instead of at $\delta = 4.0$–4.1 ppm. The absence of a substituent at GalNAc-ol C-3 shows the GalNAc-ol H-2 signal to be present at $\delta = 4.24$–4.25 ppm.

For the chemical shift of the GalNAc-ol H-5 signal, the following observations have been made. In the case when GalNAc-ol is only substituted at C-6 by GlcNAc in $\beta 1 \rightarrow 6$ linkage or by NeuAc/NeuGc in $\alpha 2 \rightarrow 6$ linkage, the GalNAc-ol H-5 resonance is detected in the region $\delta = 4.02$–4.03 ppm. Additional substitution at C-3 by β-Gal or β-GlcNAc leads to broad regions of $\delta = 4.18$–4.29 or 4.15–4.24 ppm, respectively, but within subgroups the ranges are more restricted (see Scheme 5). In the case of an α-GalNAc substitution at C-3, the GalNAc-ol H-5 signal is found at $\delta = 3.75$ ppm.

Finally, substitution of GalNAc-ol by GlcNAc in $\beta 1 \rightarrow 6$ linkage causes a downfield shift for GalNAc-ol H-6 from the bulk region to $\delta \approx 3.90$–3.95 ppm, and by NeuAc/NeuGc in $\alpha 2 \rightarrow 6$ linkage an upfield shift for GalNAc-ol H-6′ from the bulk region to $\delta \approx 3.44$–3.49 ppm.

11.2. Backbone Structures

A general discussion on relatively simple oligosaccharide-alditols with backbone structures constituted of alternating β-linked Gal and β-linked GlcNAc residues has been presented in Section 3, whereby Table 3 includes chemical shift values for pertinent structural-reporter groups of Gal$\beta 1 \rightarrow$ 4GlcNAc$\beta 1\rightarrow$ (backbone type-2 chain) and Gal$\beta 1 \rightarrow$ 3GlcNAc$\beta 1\rightarrow$ (backbone type-1 chain) elements. As has been reported in Section 3, for a given oligosaccharide-alditol both sequences can be distinguished on the basis of the positions of the GlcNAc H-1, H-3, H-6, and NAc signals. The $\beta 1 \rightarrow 3$ linkage is especially indicated by the relatively downfield position of GlcNAc H-3 ($\delta = 3.91$ versus $\delta \approx 3.7$ ppm). In contrast, the $\beta 1 \rightarrow 4$ linkage is evidenced by the relatively downfield position of GlcNAc H-6 ($\delta = 4.02$ ppm versus $\delta = 3.95$ ppm). The analysis of compounds with a higher complexity in primary structure than discussed in Section 3 is often facilitated by NOE measurements. On the other hand, Fuc and/or NeuAc residues attached at backbone type-1 and type-2 chains give rise to specific sets of structural-reporter groups that are useful for discrimination purposes, as will be discussed below (Schemes 6 and 8).

A number of examples have been presented in which $\rightarrow$Gal$\beta 1 \rightarrow$ 3/4GlcNAc$\beta 1\rightarrow$ elements are connected by $\beta 1 \rightarrow 3$ linkages, yielding $\rightarrow$GlcNAc$\beta 1 \rightarrow$ 3Gal$\beta 1\rightarrow$ segments, that can be recognized from the charac-

Structural element	H-1	H-5	CH_3
*Fucα1 → 2*Galβ1 → 3GalNAc-ol	5.26	4.28	1.24
*Fucα1 → 2*Galβ1 → 3(→GlcNAcβ1 → 6)GalNAc-ol	5.21–5.23	4.27–4.28	1.23–1.25
*Fucα1 → 2*Galβ1 → 3(NeuAcα2 → 6)GalNAc-ol	5.27	4.27	1.24
Fucα1 → 2(GalNAcα1 → 3)Galβ1 → 3GalNAc-ol	5.37–5.39	4.32–4.34	1.23–1.24
Fucα1 → 2(Galα1 → 3)Galβ1 → 3GalNAc-ol	5.35	4.32	1.23
*Fucα1 → 2*Galβ1 → 4GlcNAcβ1 → 3/6	5.30–5.31	4.22–4.23	1.23–1.24
Fucα1 → 2(GalNAcα1 → 3)Galβ1 → 4GlcNAcβ1 → 3/6	5.35	4.32	1.25
*Fucα1 → 2*Galβ1 → 3GlcNAcβ1 → 3/6	5.19–5.21	4.27–4.29	1.23–1.24
Fucα1 → 2(GalNAcα1 → 3)Galβ1 → 3GlcNAcβ1 → 3/6	5.25–5.26	4.32–4.34	1.24–1.25
*Fucα1 → 2*Galβ1 → 3(Fucα1 → 4)GlcNAcβ1 → 3	5.15–5.16	4.30–4.36	1.27–1.28
Fucα1 → 2Galβ1 → 3(*Fucα1 → 4*)GlcNAcβ1 → 3	5.02–5.04	4.86–4.88	1.25–1.26
Galβ1 → 4(*Fucα1 → 3*)GlcNAcβ1 → 3	5.13–5.14	4.81–4.85	1.17–1.18
GlcNAcβ1 → 3Galβ1 → 4(*Fucα1 → 3*)GlcNAcβ1 → 3	5.13	4.87	1.15
NeuAcα2 → 3Galβ1 → 4(*Fucα1 → 3*)GlcNAcβ1 → 3	5.12–5.13	4.80–4.83	1.17
Fucα1 → 2Galβ1 → 4(*Fucα1 → 3*)GlcNAcβ1 → 3	5.11–5.13	4.86–4.88	1.23–1.24
*Fucα1 → 2*Galβ1 → 4(Fucα1 → 3)GlcNAcβ1 → 3	5.27–5.28	4.24–4.26	1.26–1.28
Galβ1 → 4(*Fucα1 → 3*)GlcNAcβ1 → 6	5.09–5.12	4.81–4.84	1.15–1.18
NeuAcα2 → 3Galβ1 → 4(*Fucα1 → 3*)GlcNAcβ1 → 6	5.10–5.11	4.82–4.83	1.17
Fucα1 → 2Galβ1 → 4(*Fucα1 → 3*)GlcNAcβ1 → 6	5.09–5.11	4.87–4.88	1.23–1.24
*Fucα1 → 2*Galβ1 → 4(Fucα1 → 3)GlcNAcβ1 → 6	5.27–5.28	4.24–4.26	1.27–1.28
Galβ1 → 3(*Fucα1 → 4*)GlcNAcβ1 → 3	5.02–5.03	4.86–4.88	1.18
*Fucα1 → 3*GalNAcβ1 → 3Galβ1→	4.99–5.00	n.d.	1.20–1.21
→Galβ1 → 3(Fucα1 → 4)GlcNAcβ1→ 3(*Fucα1 → 2*)Galβ1 → 4	4.99	4.27	1.23
→Galβ1 → 4(Fucα1 → 3)GlcNAcβ1→ 3(*Fucα1 → 2*)Galβ1 → 4	5.07–5.08	4.26	1.22
→Galβ1 → 3GlcNAcβ1 → 3(*Fucα1 → 2*)Galβ1 → 3	5.08	4.27	1.19

Scheme 6. Structural-reporter-group data of Fuc for Fuc-containing structural elements in mucin-type *O*-linked carbohydrate chains.

teristic Gal H-4 signal at $\delta = 4.11$–4.15 ppm, outside the bulk of skeleton protons. When the Gal residue serves as a branching point bearing →Galβ1 → 3/4GlcNAcβ1→ units at both C-3 and C-6, in general the Gal H-4 signal is shifted upfield ($\delta = 4.10$–4.11 ppm).

11.3. Peripheral Elements

Typical examples of Fuc-containing peripheral elements of mucin-type oligosaccharide-alditols are Fucα1 → 2Galβ1→, Fucα1 → 3GlcNAcβ1→, Fucα1 → 4GlcNAcβ1→, and Fucα1 → 3GalNAcβ1→. The terminal α-Fuc

at different positions gives rise to specific sets of structural-reporter groups, comprising the H-1, H-5, and CH_3 resonances. As can be concluded from the ^{1}H-NMR data in Scheme 6, the combination of the positions of these resonances is highly modulated by the molecular environment of Fuc. For comparison, the ^{1}H-NMR data of Fuc structural reporters known for *N*-glycoprotein-derived Fuc-containing carbohydrate chains are presented in Scheme 7 (Damm *et al.*, 1987; Paz-Parente *et al.*, 1983; Santer *et al.*, 1983; Takahashi *et al.*, 1986; Van Halbeek *et al.*, 1985a; Van Kuik *et al.*, 1986;

Structural element	H-1	H-5	CH_3
→GlcNAcβ1 → 4(*Fucα1 → 6*)GlcNAcβ1 →N(Asn)	4.87–4.88	4.12–4.13	1.20–1.21
→GlcNAcβ1 → 4(*Fucα1 → 6*)GlcNAc	4.89–4.91	4.08–4.13	1.21–1.22
→GlcNAcβ1 → 4(*Fucα1 → 6*)GlcNAc-ol	4.89–4.90	4.07–4.08	1.22–1.23
→GlcNAcβ1 → 4(*Fucα1 → 3*)GlcNAcβ1 →N(Asn)	5.13–5.14	4.71–4.72	1.27–1.29
→GlcNAcβ1 → 4(*Fucα1 → 3*)GlcNAc	5.08	4.72	1.27
→GlcNAcβ1 → 4(*Fucα1 → 3*)GlcNAc-ol	5.01–5.02	4.23	1.20
Galβ1 → 4(*Fucα1 → 3*)GlcNAcβ1 →2Manα1 → 3/6	5.12–5.13	4.83–4.84	1.17–1.18
Galβ1 → 4(*Fucα1 → 3*)GlcNAcβ1 →4/6Manα1 → 3/6	5.11–5.12	4.83–4.84	1.17–1.18
*Fucα1 → 2*Galβ1 → 4GlcNAcβ1 → 2Manα1→	5.31	4.22–4.23	1.23–1.24
Fucα1 → 2Galβ1 → 4(*Fucα1 → 3*)GlcNAcβ1 →Manα1 → 3/6	5.11	n.d.	1.23
*Fucα1 → 2*Galβ1 → 4(Fucα1 → 3)GlcNAcβ1 →Manα1 → 3/6	5.27	n.d.	1.27
Galβ1 → 4(*Fucα1 → 6*)GlcNAcβ1 → 2Manα1 → → 3/6	5.00	n.d.	1.17

Scheme 7. Structural-reporter-group data of Fuc for Fuc-containing structural elements in *N*-linked carbohydrate chains.

Vliegenthart *et al.*, 1983). Evaluation of the data from Schemes 6 and 7 leads to several generalizations. Some typical examples are: (1) The Fucα1 → 2Galβ1→ element in blood group A, B [not in combination with the Le^a determinant (see Scheme 11)], and H determinants is indicated by the Fuc CH_3 signal at δ = 1.23–1.25 ppm. The Fuc CH_3 region moves downfield when going to immuno group Y and Le^b determinants (δ = 1.26–1.28 ppm). In the case of an internal blood group H determinant the δ range is 1.19–1.23 ppm. (2) For the Fucα1 → 3GlcNAcβ1→ element, the Fuc H-1 signal resonates in the region δ = 5.09–5.14 ppm. It is of interest to note

the influence of the type of glycosidic linkage by which GlcNAc is attached to the next residue. (3) The presence of an $\alpha 1 \rightarrow 6$-linked Fuc unit at the proximal GlcNAc residue in *N*-linked carbohydrate chains is reflected by a Fuc H-1 signal at $\delta = 4.87$–4.91 ppm.

In Scheme 8 the chemical shift values of the NeuAc/NeuGc H-3a and H-3e signals for different NeuAc/NeuGc-containing structural elements have been summarized. For comparison, the data from *N*-linked oligosaccharides (Bernard *et al.*, 1984; Green *et al.*, 1988; Marti *et al.*, 1988;

Structural element	H-3a	H-3e
NeuAcα2 → 6(→3)GalNAc-ol	1.69–1.71	2.72–2.74
*NeuAcα2 → 6*Galβ1 → 4GlcNAcβ1 → 3/6	1.72	2.67
*NeuAcα2 → 3*Galβ1 → 3(→6)GalNAc-ol	1.80	2.77–2.78
*NeuAcα2 → 3*Galβ1 → 4GlcNAcβ1 → 3/6	1.80	2.75–2.77
*NeuAcα2 → 3*Galβ1 → 4(Fucα1 → 3)GlcNAcβ1 → 3/6	1.79–1.80	2.76–2.77
NeuAcα2 → 3(GalNAcβ1 → 4)Galβ1 → 3	1.93–1.94	2.68
NeuAcα2 → 3(GalNAcβ1 → 4)Galβ1 → 4	1.92–1.93	2.66
*NeuAcα2 → 3*Galβ1 → 3GalNAcβ1→	1.78	2.76
NeuGcα2 → 6(→3)GalNAc-ol	1.71–1.72	2.74–2.75
NeuGcα2 → 3(GalNAcβ1 → 4)GalNAcβ1 → 3	1.85–1.86	2.55–2.56
NeuGcα2 → 8(NeuGcα2 → 8)$_{0-4}$*NeuGcα2* →*6*(→3)GalNAc-ol	1.66–1.67	2.65–2.66
NeuGcα2 → 8(NeuGcα2 → 8)$_{0-4}$NeuGcα2 →6(→3)GalNAc-ol	1.74–1.76	2.78
NeuGcα2 → 8(*NeuGcα2 → 8*)$_{0-4}$NeuGcα2 →6(→3)GalNAc-ol	1.70–1.71	2.70–2.71

Scheme 8. Structural-reporter-group data of NeuAc/NeuGc for NeuAc/NeuGc-containing structural elements in mucin-type *O*-linked carbohydrate chains.

Vliegenthart *et al.*, 1983) and sialyl-oligosaccharides with lactose as the reducing structural element (Dorland *et al.*, 1986; Strecker *et al.*, 1989b) are presented in Schemes 9 and 10, respectively. The NAc signal of NeuAc is generally present at $\delta \approx 2.03$ ppm, slightly modulated by the molecular environment in which the sialic acid residue occurs. The combined set of H-3 structural-reporter groups of α-NeuAc gives direct information about the type of glycosidic linkage ($\alpha 2 \rightarrow 6$, $\alpha 2 \rightarrow 3$, $\alpha 2 \rightarrow 8$), and the molecular environment in which the NeuAc residue occurs. The presence of NeuGc instead of NeuAc is reflected by the NGc signal at $\delta \approx 4.12$ ppm, whereas the H-3a and H-3e multiplets show downfield shifts of $\Delta\delta \approx +0.02$ ppm, as compared to the NeuAc analogs.

Structural element	H-3a	H-3e
*NeuAcα2 → 6*Galβ1 → 4GlcNAcβ1 → 2Manα1 → 3/6	1.71–1.72	2.67
*NeuAcα2 → 6*Galβ1 → 4GlcNAcβ1 → 4Manα1 → 3	1.70–1.71	2.67
Galβ1 → 3(*NeuAcα2 → 6)*GlcNAcβ1 → 4Manα1 → 3	1.76–1.77	2.73
*NeuAcα2 → 3*Galβ1 → 4GlcNAcβ1 → 2/4/6Manα1 → 3/6	1.80	2.75–2.76
*NeuAcα2 → 3*Galβ1 → 3GlcNAcβ1 → 4Manα1 → 3	1.79	2.76
*NeuAcα2 → 3*Galβ1 → 3(NeuAcα2 → 6)GlcNAcβ1 → 2Manα1 → 3/6	1.78–1.79	2.76
NeuAcα2 → 3Galβ1 → 3(*NeuAcα2 → 6*)GlcNAcβ1 → 2Manα1 → 3/6	1.71–1.72	2.73–2.74
*NeuAcα2 → 3*Galβ1 → 3(NeuAcα2 → 6)GlcNAcβ1 → 4Manα1 → 3	1.78–1.79	2.76
NeuAcα2 → 3Galβ1 → 3(*NeuAcα2 → 6*)GlcNAcβ1 → 4Manα1 → 3	1.76–1.77	2.72–2.73
*NeuGcα2 → 6*Galβ1 → 4GlcNAcβ1 → 2Manα1 → 3/6	1.73–1.74	2.69–2.70

Scheme 9. Structural-reporter-group data of NeuAc/NeuGc for NeuAc/NeuGc-containing structural elements in *N*-linked carbohydrate chains.

Oligosaccharide	H-3a	H-3e
*NeuAcα2 → 3*Galβ1 → 4Glc	1.799	2.757
*NeuGcα2 → 3*Galβ1 → 4Glc	1.816	2.777
*NeuAcα2 → 6*Galβ1 → 4Glc	1.739	2.715
*NeuAcα2 → 8*NeuAcα2 → 3Galβ1 → 4Glc	1.741	2.779
NeuAcα2 → 8*NeuAcα2 → 3*Galβ1 → 4Glc	1.739	2.682/79
NeuAcα2 → 3(GalNAcβ1 → 4)Galβ1 → 4Glc	1.923	2.666/64
Galβ1 → 3GalNAcβ1 → 4(*NeuAcα2 → 3*)Galβ1 → 4Glc	1.929	2.664/62
*NeuAcα2 → 3*Galβ1 → 3GalNAcβ1 → 4(NeuAcα2 → 3)Galβ1 → 4Glc	1.798	2.750
NeuAcα2 → 3Galβ1 → 3GalNAcβ1 → 4(*NeuAcα2 → 3*)Galβ1 → 4Glc	1.913	2.683/81
*NeuAcα2 → 3*Galβ1 → 3GlcNAcβ1 → 3Galβ1 → 4Glc	1.783	2.760
Galβ1 → 3(*NeuAcα2 → 6*)GlcNAcβ1 → 3Galβ1 → 4Glc	1.685	2.741
*NeuAcα2 → 3*Galβ1 → 3(NeuAcα2 → 6)GlcNAcβ1 → 3Galβ1 → 4Glc	1.779	2.754
NeuAcα2 → 3Galβ1 → 3(*NeuAcα2 → 6*)GlcNAcβ1 → 3Galβ1 → 4Glc	1.685	2.736
*NeuAcα2 → 3*Galβ1 → 3(Fucα1 → 4)GlcNAcβ1 → 3Galβ1 → 4Glc	1.768	2.768
Fucα1 → 2Galβ1 → 3(*NeuAcα2 → 6*)GlcNAcβ1 → 3Galβ1 → 4Glc	1.658	2.742
*NeuAcα2 → 6*Galβ1 → 4GlcNAcβ1 → 3Galβ1 → 4Glc	1.713	2.668

Scheme 10. Structural-reporter-group data of NeuAc/NeuGc for NeuAc/NeuGc-containing oligosaccharides with lactose at reducing end.

In Schemes 11–14 the relevant structural-reporter groups for the blood group determinants A (including data from Strecker *et al.*, 1989c), B (including data from Finne *et al.*, 1989), X, Y, sialyl-X, Cad, Le^a, Le^b, pseudo B, and P_1 are presented. The reporters for blood group H can be directly

Blood group A determinant			
Backbone type 1			
Fucα1 → 2(GalNAcα1 → 3)Galβ1 → 3GlcNAcβ1	α-Fuc	H-1	5.25–5.26
→ 3/6		H-5	4.32–4.34
		CH_3	1.24–1.25
	α-GalNAc	H-1	5.18–5.19
		H-5	4.26–4.30
Backbone type 1 with internal Le^a determinant			
Fucα1 → 2(GalNAcα1 → 3)Galβ1	α-Fuc^2	H-1	5.21
→ 3(Fucα1 → 4)GlcNAcβ1 → 3		H-5	4.39–4.40
		CH_3	1.29
	α-GalNAc	H-1	5.22
		H-5	4.31
	α-Fuc^4	H-1	5.03–5.04
		H-5	4.85
		CH_3	1.29
Backbone type 2			
Fucα1 → 2(GalNAcα1 → 3)Galβ1 → 4GlcNAcβ1	α-Fuc	H-1	5.35
→ 3/6		H-5	4.32
		CH_3	1.25
	α-GalNAc	H-1	5.17–5.18
		H-5	4.21–4.24
Backbone type 3			
Fucα1 → 2(GalNAcα1 → 3)Galβ1 → 3GalNAc-ol	α-Fuc	H-1	5.37–5.39
		H-5	4.32–4.34
		CH_3	1.23–1.24
	α-GalNAc	H-1	5.18–5.19
		H-5	4.16
Blood group B determinant			
Backbone type 1 with internal Le^a determinant			
Fucα1 → 2(Galα1 → 3)Galβ1	α-Fuc^2	H-1	5.23
→ 3(Fucα1 → 4)GlcNAcβ1 → 3		H-5	4.39
		CH_3	1.27
	α-Gal	H-1	5.17
		H-5	4.26
	α-Fuc^4	H-1	5.04
		H-5	4.83
		CH_3	1.29
Backbone type 3			
Fucα1 → 2(Galα1 → 3)Galβ1 → 3GalNAc-ol	α-Fuc	H-1	5.35
		H-5	4.32
		CH_3	1.23
	α-Gal	H-1	5.26
		H-5	4.12

Scheme 11. Structural-reporter-group data for blood group A and B determinants.

deduced from Schemes 6 and 7. The data from these schemes indicate the great advantages of ^{1}H-NMR spectroscopy for the direct recognition of blood group determinants in carbohydrate structures. Finally, the structural reporters of the terminating sequences GlcNAcα1 → 4Galβ1 → 3/4, GalNAcβ1 → 4GalNAcβ1 → 3, Galβ1 → 4Galβ1 → 4, and Galβ1 → 3Galβ1 → 4 are summarized in Scheme 15.

Scheme 12. Structural-reporter-group data for immuno group X and Y determinants.

Immuno group X (SSEA-1) determinant			
Galβ1 → 4(Fucα1 → 3)GlcNAcβ1 → 3	α-Fuc	H-1	5.13–5.14
		H-5	4.81–4.85
		CH_3	1.17–1.18
→GlcNAcβ1 → 3Galβ1 → 4(Fucα1 → 3)GlcNAcβ1 → 3 (internal)	α-Fuc	H-1	5.13
		H-5	4.87
		CH_3	1.15
Galβ1 → 4(Fucα1 → 3)GlcNAcβ1 → 3(Fucα1 → 2)Galβ1 → 4 (with internal H determinant)	α-Fuc^3	H-1	5.14
		H-5	4.83
		CH_3	1.17
	α-Fuc^2	H-1	5.07
		H-5	4.26
		CH_3	1.22
Galβ1 → 4(Fucα1 → 3)GlcNAcβ1 → 6	α-Fuc	H-1	5.09–5.12
		H-5	4.81–4.84
		CH_3	1.15–1.18
Galβ1 → 4(Fucα1 → 3)GlcNAcβ1 → 2/4/6Manα1 → 3/6	α-Fuc	H-1	5.11–5.13
		H-5	4.83–4.84
		CH_3	1.17–1.18
Immuno group Y determinant			
Fucα1 → 2Galβ1 → 4(Fucα1 → 3)GlcNAcβ1 → 3	α-Fuc^2	H-1	5.27–5.28
		H-5	4.24–4.26
		CH_3	1.26–1.28
	α-Fuc^3	H-1	5.11–5.13
		H-5	4.86–4.88
		CH_3	1.23–1.24
	β-Gal	H-1	4.48–4.51
Fucα1 → 2Galβ1 → 4(Fucα1 → 3)GlcNAcβ1 → 3(Fucα1 → 2)Galβ1 → 4 (with internal H determinant)	α-Fuc^3	H-1	5.12
		H-5	4.88
		CH_3	1.23
	α-Fuc^{2,4,3}	H-1	5.27
		H-5	4.25
		CH_3	1.26
	α-Fuc^2	H-1	5.08
		H-5	4.26
		CH_3	1.22

continued.

Fucα1 → 2Galβ1 → 4(Fucα1 → 3)GlcNAcβ1 → 6	α-Fuc[2]	H-1	5.27–5.28
		H-5	4.24–4.26
		CH_3	1.27–1.28
	α-Fuc[3]	H-1	5.09–5.11
		H-5	4.87–4.88
		CH_3	1.23–1.24
	β-Gal	H-1	4.50
Fucα1 → 2Galβ1 → 4(Fucα1 → 3)GlcNAcβ1 → Manα1 → 3/6	α-Fuc[2]	H-1	5.27
		CH_3	1.27
	α-Fuc[3]	H-1	5.11
		CH_3	1.23
	β-Gal	H-1	4.50

Scheme 12. Structural-reporter-group data for immuno group X and Y determinants.

Immuno group sialyl-X determinant			
NeuAcα2 → 3Galβ1 → 4(Fucα1 → 3)GlcNAcβ1 → 3	α-Fuc	H-1	5.12–5.13
		H-5	4.80–4.83
		CH_3	1.17
	α-NeuAc	H-3a	1.79–1.80
		H-3e	2.76–2.77
		NAc	2.03
NeuAcα2 → 3Galβ1 → 4(Fucα1 → 3)GlcNAcβ1 → 6	α-Fuc	H-1	5.10–5.11
		H-5	4.82–4.83
		CH_3	1.17
	α-NeuAc	H-3a	1.79–1.80
		H-3e	2.76–2.77
		NAc	2.03
Blood group Cad (Sd^a) determinant			
NeuAcα2 → 3(GalNAcβ1 → 4)Galβ1 → 3	α-NeuAc	H-3a	1.93–1.94
		H-3e	2.68
		NAc	2.03
	β-GalNAc	H-1	4.71–4.73
		H-4	3.91–3.93
		NAc	2.02–2.03
NeuAcα2 → 3(GalNAcβ1 → 4)Galβ1 → 4	α-NeuAc	H-3a	1.92–1.93
		H-3e	2.66
		NAc	2.03
	β-GalNAc	H-1	4.71–4.76
		H-4	3.91–3.92
		NAc	2.01–2.02

Scheme 13. Structural-reporter-group data for sialyl-X and Cad determinants.

Blood group Le^a determinant			
Galβ1 → 3(Fucα1 → 4)GlcNAcβ1 → 3	Fuc^4	H-1	5.02–5.03
		H-5	4.86–4.88
		CH_3	1.18
Blood group Le^b determinant			
Fucα1 → 2Galβ1 → 3(Fucα1 → 4)GlcNAcβ1 → 3	Fuc^4	H-1	5.02–5.04
		H-5	4.86–4.88
		CH_3	1.25–1.26
	Fuc^2	H-1	5.15–5.16
		H-5	4.30–4.36
		CH_3	1.27–1.28
Fucα1 → 2Galβ1 → 3(Fucα1 → 4)GlcNAcβ1	Fuc^4	H-1	5.04
→ 3(Fucα1 → 2)Galβ1 → 4		H-5	4.86
(with internal H determinant)		CH_3	1.26
	$Fuc^{2,3}$	H-1	5.16
		H-5	4.30
		CH_3	1.27
	$Fuc^{2,4}$	H-1	4.99
		H-5	4.27
		CH_3	1.23
Blood group pseudo B determinant			
Galα1 → 3Galβ1 → 4GlcNAcβ1→	Gal^4	H-1	4.54
		H-4	4.18
	Gal^3	H-1	5.15
		H-5	4.20
Blood group P_1 determinant			
Galα1 → 4Galβ1 → 4	$Gal^4(\beta)$	H-1	4.71
		H-4	4.03
	$Gal^4(\alpha)$	H-1	4.95
		H-4	4.03
		H-5	4.37

Scheme 14. Structural-reporter-group data for blood group Le^a, Le^b, pseudo B, and P_1 determinants.

The various examples presented in this chapter make clear that, in addition to the earlier developed empirical rules for *N*-linked oligosaccharide chains (Vliegenthart *et al.*, 1983), it has also been possible to extend the NMR concept of structural-reporter groups to the mucin-type *O*-linked carbohydrate chains in a widely applicable way. Taking into account the various rules, the next step is to computerize spectrum interpretations. First approaches in this field have been reported by Hounsell and Wright (1990), Hounsell *et al.* (1984), Anderson and Grimes (1985), and Bot *et al.* (1988).

Structural element			
GlcNAcα1 → 4Galβ1 → 3/4	GlcNAc	H-1	4.86–4.87
		H-4	3.54–3.55
		H-5	4.17–4.19
GalNAcβ1 → 4GalNAcβ1 → 3	$GalNAc^4$	H-1	4.65
	$GalNAc^3$	H-1	4.65
Galβ1 → 4Galβ1 → 4GlcNAcβ1 → 6	$Gal^{4,6}$	H-1	4.50
		H-4	4.19
	$Gal^{4,4,6}$	H-1	4.59–4.60
		H-4	3.90
Galβ1 → 3Galβ1 → 4Xylose	Gal^4	H-1	4.62
		H-4	4.20
	Gal^3	H-1	4.62
		H-4	3.93

Scheme 15. Structural-reporter-group data for terminating sequences not classified as human blood group determinants.

12. ADDENDUM

In this section, the ^{1}H-NMR data of a series of mucin-type oligosaccharide-alditols, which became available after finishing Sections 2–10, are presented. Tables 30 and 31 include 400-MHz ^{1}H-NMR structural-reporter-group resonances of the oligosaccharide-alditols **136–140** and **142–145**, respectively, having the GlcNAcβ1 → 6(Galβ1 → 3)GalNAc-ol core structure in common (Pierce-Cretel *et al.*, 1989). For **141**, having the same core structure, 500-MHz ^{1}H-NMR data are given (Hounsell *et al.*, 1988); the NMR spectrum of this compound has been completely assigned by ^{1}H–^{1}H COSY experiments. For **138** and **140**, see also Hanisch *et al.* (1990); for **142**, see also Van Kuik *et al.* (1991). ^{1}H-NMR spectra of **136–145** are given in the respective references.

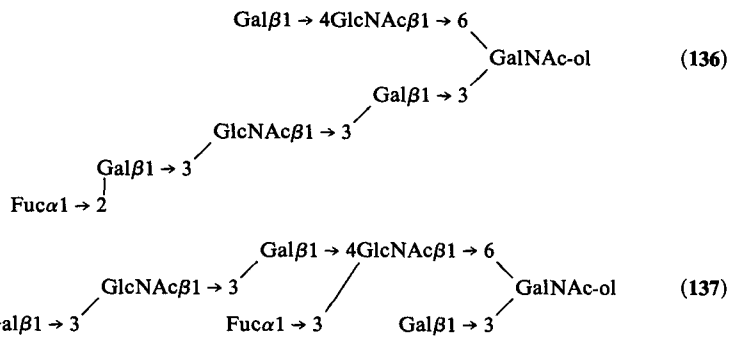

(136)

(137)

TABLE 30

^{1}H Chemical Shifts of Structural-Reporter Groups of Constituent Monosaccharides for Oligosaccharide-Alditols with the GlcNAcβ1 → 6(Galβ1 → 3)GalNAc-ol Core Structure in Common (136–140)

Residue	Reporter group	136 	137 	138 	139 	140 
GalNAc-ol	H-2	4.399	4.388	4.385	4.384	4.386
	H-3	4.044	4.056	4.067	4.066	4.067
	H-4	3.448	3.451	3.438	3.437	3.438
	H-5	4.274	4.264	4.269	4.268	4.268
	NAc	2.067	2.066	2.065	2.064	2.065
Gal^3	H-1	4.436	4.461	4.530	4.530	4.530
	H-3	n.d.[a]	n.d.	4.114	4.114	4.114
	H-4	4.116	n.d.	3.901[b]	3.929	3.927
GlcNAc^6	H-1	4.554	4.559	4.556	4.555	4.556
	H-6	3.99	4.000	3.992	3.980	3.992
	NAc	2.058	2.052	2.061	2.061	2.061
Gal^{4,6}	H-1	4.469	4.432	4.459[c]	4.439	4.459
	H-4	n.d.	4.095	4.149	4.134	4.149
GlcNAc^3	H-1	4.652	4.703	4.731	4.644	4.707
	H-6	3.96	n.d.	n.d.	n.d.	n.d.
	NAc	2.060	2.022	2.029	2.056	2.036
Gal^{3,3}	H-1	4.599	4.445	4.441[c]	4.622	—
	H-4	n.d.	n.d.	3.914	3.891	—
Gal^{4,3}	H-1	—	—	—	—	4.478
Fuc^2	H-1	5.193	—	—	5.187	—
	H-5	4.284	—	—	4.291	—
	CH_3	1.239	—	—	1.233	—
Fuc^3	H-1	—	5.094	—	—	—
	H-5	—	4.806	—	—	—
	CH_3	—	1.149	—	—	—
NeuAc^3	H-3a	—	—	1.800	1.798	1.800
	H-3e	—	—	2.774	2.774	2.774
	NAc	—	—	2.034	2.033	2.034

[a] n.d. means value could not be determined merely by inspection of the spectrum.
[b] Hanisch *et al.* (1990): δ = 3.931 ppm.
[c] Interchange according to Hanisch *et al.* (1990).

TABLE 31

^{1}H Chemical Shifts of Structural-Reporter Groups of Constituent Monosaccharides for Oligosaccharide-Alditols with the GlcNAcβ1 → 6(Galβ1 → 3)GalNAc-ol Core Structure in Common (141–145)

Residue	Reporter group	141 	142 	143 	144 	145 
GalNAc-ol	H-2	4.389	4.387	4.387	4.389	4.388
	H-3	4.013	4.002	4.01	4.002	4.070
	H-4	3.476	3.469	3.469	3.464	3.436
	H-5	4.235	4.219	4.219	4.219	4.273
	H-6	3.946	n.d.[c]	n.d.	n.d.	n.d.
	NAc	2.046[a]	2.046	2.045	2.044	2.067
Gal^3	H-1	4.470	4.458	4.459	4.445	4.531
	H-3	3.672	n.d.	n.d.	n.d.	4.116
	H-4	3.882	4.114	4.113	4.102	n.d.
GlcNAc^6	H-1	4.556	4.556	4.556	4.556	4.560
	H-6	3.998[b]	n.d.	n.d.	n.d.	n.d.
	NAc	2.066[a]	2.066	2.066	2.067	2.060
Gal^{4,6}	H-1	4.470	4.469	4.467	4.467	4.454
	H-4	3.922	n.d.	n.d.	n.d.	n.d.
Gal^{4,3}	H-1	—	4.482	—	—	—
Gal^{4,6,3}	H-1	4.470	4.469	4.467	4.469	—
	H-4	3.922	n.d.	n.d.	n.d.	n.d.
Gal^{3,3}	H-1	—	—	4.448	4.650[d]	4.440
Gal^{4,6,4}	H-1	—	—	—	—	4.463
GlcNAc^{3,3}	H-1	—	4.684	4.706	4.592[d]	—
	NAc	—	2.037	2.029	2.057	—
GlcNAc^{6,3}	H-1	4.599	4.594	4.594	4.598	—
	H-6	4.002[b]	n.d.	n.d.	n.d.	—
	NAc	2.055[a]	2.051	2.049	2.051	—
GlcNAc^{3,4}	H-1	—	—	—	—	4.728
	NAc	—	—	—	—	2.027
GlcNAc^{6,4}	H-1	—	—	—	—	4.618
	NAc	—	—	—	—	2.070
Fuc^2	H-1	—	—	—	5.191	—
	H-5	—	—	—	4.294	—
	CH_3	—	—	—	1.238	—
NeuAc^3	H-3a	—	—	—	—	1.800
	H-3e	—	—	—	—	2.774
	NAc	—	—	—	—	2.034

[a] Assignments have been made according to Van Halbeek *et al.* (1982c).
[b] Assignments may have to be interchanged.
[c] n.d. means value could not be determined merely by inspection of the spectrum.
[d] Values have been interchanged (see Van Kuik *et al.*, 1991).

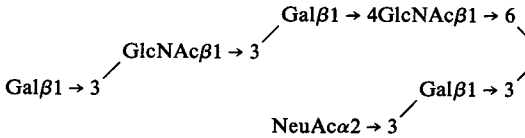

(138)

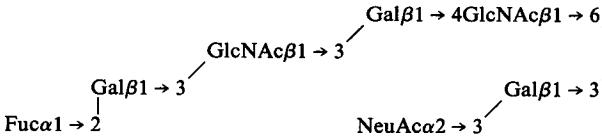

(139)

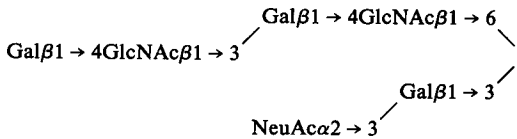

(140)

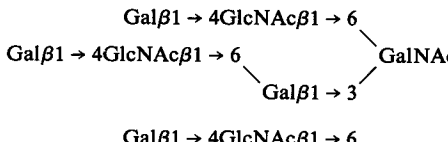

(141)

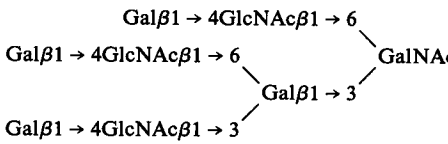

(142)

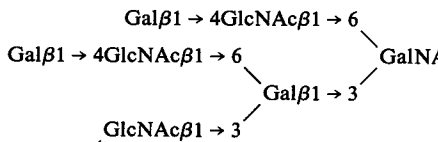

(143)

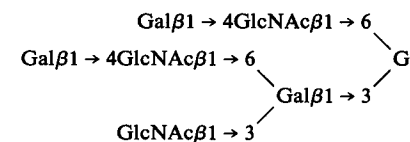

(144)

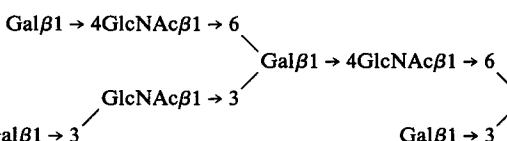

(145)

Recently, ^{1}H-NMR data became available for the NeuGc analogs of the oligosaccharide-alditols **10**, **90**, and **91**. The structural reporters established for **10A** (Savage *et al.*, 1990a) are similar to those discussed for **10**, except that the NeuAc[6] set has been replaced by the typical NeuGc[6] set (H-3a, δ = 1.716 ppm; H-3e, δ = 2.749 ppm; NGc, δ = 4.123 ppm) (270-MHz ^{1}H-NMR data). The same findings hold for the comparison of the ^{1}H-NMR data of **90** and **90A** (Savage *et al.*, 1990b) (H-3a, δ = 1.719 ppm; H-3e, δ = 2.753 ppm; NGc, δ = 4.123 ppm), and of **91** and **91A** (Savage *et al.*, 1990b) (H-3a, δ = 1.718 ppm; H-3e, δ = 2.752 ppm; NGc, δ = 4.124 ppm). For the ^{1}H-NMR spectrum of **91A**, see Savage *et al.* (1990b).

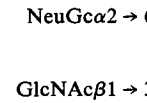

(10A)

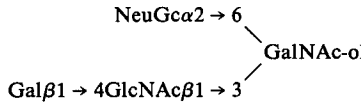

(90A)

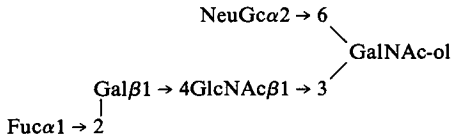

(91A)

An additional series of fucosylated oligosaccharide-alditols have been reported and the ^{1}H-NMR data are presented in Tables 32–35. Compounds **146–150** (Figures 80–84) (Table 32; Klein *et al.*, 1991) have the common element Galβ1 → 3GlcNAcβ1 → 3Galβ1 → 4GlcNAcβ1 → 6GalNAc-ol,

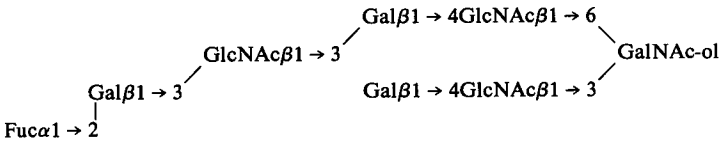

(146)

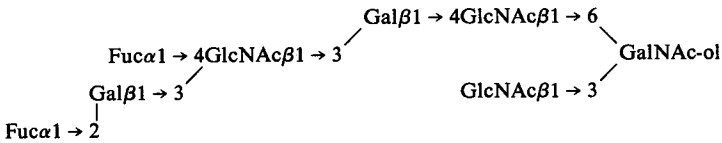

(147)

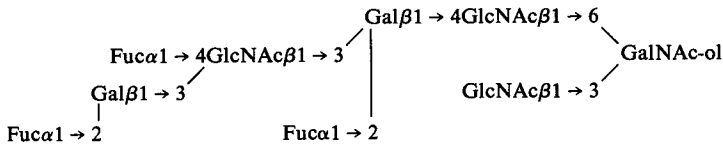

(148)

TABLE 32

^{1}H Chemical Shifts of Structural-Reporter Groups of Constituent Monosaccharides for Oligosaccharide-Alditols with the Common Element Galβ1 → 3GlcNAcβ1 → 3Galβ1 → 4GlcNAcβ1 → 6GalNAc-ol (146–150)

Residue	Reporter group	146 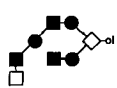	147 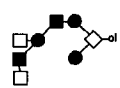	148 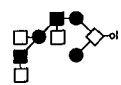	149 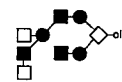	150 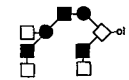
GalNAc-ol	H-2	4.284	4.282	4.296	4.282	4.401
	H-3	n.d.	3.986	n.d.	n.d.	4.083
	H-4	3.518	3.515	3.511	3.522	3.496
	H-5	4.236	4.237	4.245	4.237	4.243
	NAc	2.045	2.045	2.044	2.044	2.054
GlcNAc^6	H-1	4.561	4.561	4.535	4.562	4.570
	H-6	n.d.	4.000	n.d.	n.d.	n.d.
	NAc	2.060	2.062[a]	2.063	2.061	2.054
Gal^{4,6}	H-1	4.444	4.440	4.545	4.441	4.438
	H-4	4.139	4.138	4.158	4.137	4.136
GlcNAc^{3,4}	H-1	4.623	4.600[b]	4.722	4.605	4.602
	H-3	n.d.	4.134	4.171	4.134	4.133
	NAc	2.058	2.058[a]	2.124	2.061	2.062
Gal^{3,3}	H-1	4.646	4.659	4.678	4.659	4.658

GlcNAc^{3}	H-1	4.623	4.598[b]	4.596	4.623	—
	H-6	4.019	3.948	n.d.	4.018	—
	NAc	2.079	2.081	2.081	2.079	—
Gal^{4,3}	H-1	4.455	—	—	4.455	—
Gal^{3}	H-1	—	—	—	—	4.570
Fuc^{2,4}	H-1	—	—	4.993	—	—
	H-5	—	—	4.27[c]	—	—
	CH_3	—	—	1.226	—	—
Fuc^{2,3,3}	H-1	5.189	5.152	5.161	5.152	5.151
	H-5	4.291	4.344	4.30[c]	4.343	4.343
	CH_3	1.233	1.273	1.269	1.272	1.272
Fuc^{2,3}	H-1	—	—	—	—	5.221
	H-5	—	—	—	—	4.275
	CH_3	—	—	—	—	1.244
Fuc^{4}	H-1	—	5.025	5.035	5.025	5.025
	H-5	—	4.866	4.855	4.866	4.865
	CH_3	—	1.258	1.259	1.258	1.258

[a] Assignments may have to be interchanged.
[b] Assignments may have to be interchanged.
[c] From HOHAHA experiment, recorded at 10 °C at 600 MHz.

TABLE 33

^{1}H Chemical Shifts of Structural-Reporter Groups of Constituent Monosaccharides for Oligosaccharide-Alditols with the Common Element Galβ1 → 4GlcNAcβ1 → 3Galβ1 → 4GlcNAcβ1 → 6GalNAc-ol (151–156)

Residue	Reporter group	151 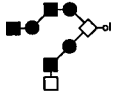	152 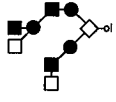	153 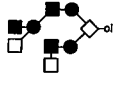	154 	155 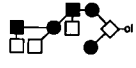	156 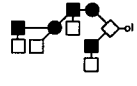
GalNAc-ol	H-2	4.259	4.259	4.279	4.279	4.279	4.402
	H-3	n.d.	n.d.	n.d.	n.d.	n.d.	4.082
	H-4	n.d.	n.d.	n.d.	n.d.	n.d.	3.494
	H-5	4.213	4.2	4.23	4.235	4.236	4.26
	NAc	2.042	2.042	2.043	2.043	2.043	2.054
GlcNAc^6	H-1	4.566	4.565	4.556	4.535	4.534	4.541
	NAc	2.058	2.057	2.060	2.062	2.062	2.054
Gal^{4,6}	H-1	4.457	4.453	4.461	4.552	4.559	4.557
	H-4	4.148	4.151	4.157	4.202	4.206	4.206
GlcNAc^{3,4}	H-1	4.695[a]	4.699[a]	4.696[a]	4.802[b]	4.788[a]	4.787[a]
	NAc	2.037	2.025	2.026	2.073	2.074	2.074
Gal^{4,3,4}	H-1	4.479	4.462	4.461	4.468	4.519	4.520
	H-4	n.d.	n.d.	n.d.	3.89[c]	n.d.	n.d.

$GlcNAc^3$	H-1	4.654	4.654	4.603	4.595	4.595	—
	NAc	2.108	2.108	2.083	2.080	2.080	—
Gal^3	H-1	4.566	4.565	—	—	—	4.571
Gal^4	H-1	—	—	4.526	—	—	—
$Fuc^{2,4,6}$	H-1	—	—	—	5.071	5.077	5.079
	H-5	—	—	—	4.257	4.26	4.26
	CH_3	—	—	—	1.224	1.222	1.221
$Fuc^{2,4,3}$	H-1	—	—	5.312	—	5.268	5.268
	H-5	—	—	4.23	—	4.25	4.25
	CH_3	—	—	1.234	—	1.261	1.261
$Fuc^{2,3}$	H-1	5.212	5.212	—	—	—	5.219
	H-5	4.269	4.269	—	—	—	4.27
	CH_3	1.231	1.231	—	—	—	1.243[d]
Fuc^3	H-1	—	5.128	5.128	5.135	5.123	5.124
	H-5	—	4.834	4.835[a]	4.831	4.880	4.880
	CH_3	—	1.175	1.175	1.173	1.234	1.231[d]

[a] Spectrum recorded at 15 °C.
[b] Spectrum recorded at 12 °C.
[c] From HOHAHA experiment.
[d] Assignments may have to be interchanged.

TABLE 34

^{1}H Chemical Shifts of Structural-Reporter Groups of Constituent Monosaccharides for Oligosaccharide-Alditols with the Common Element GlcNAcβ1 → 3(Galβ1 → 4GlcNAcβ1 → 6)Galβ1 → 3GalNAc-ol (157–160)

Residue	Reporter group	157 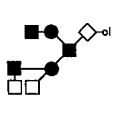	158 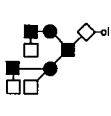	159 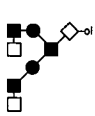	160 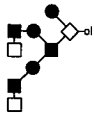
GalNAc-ol	H-2	4.384	4.399	4.387	4.395
	H-3	n.d.	4.046	4.003	4.00
	H-4	3.505	3.508	3.504	3.468
	H-5	4.134	4.139	4.143	4.23
	NAc	2.044	2.044	2.046	2.046
Gal^3	H-1	4.469	4.466	4.452	4.442
	H-4	4.102	4.100	4.104	4.102
GlcNAc^{6,3}	H-1	4.608	4.584	4.582	4.576
	NAc	2.052	2.055	2.055	2.051
Gal^{4,6}	H-1	4.469	4.531	4.530	4.534
	H-4	3.92[a]	n.d.	n.d.	n.d.
GlcNAc^{3,3}	H-1	4.684[b]	4.697	4.599	4.592
	NAc	2.031	2.032	2.060	2.057
Gal^{4,3}	H-1	4.515	4.514	—	—
Gal^{3,3}	H-1	—	—	4.650	4.651
	H-4	—	—	3.89[c]	n.d.
GlcNAc^6	H-1	—	—	—	4.534
	NAc	—	—	—	2.067
Fuc^{2,4,6}	H-1	—	5.315	5.313	5.312
	H-5	—	4.223	4.221	4.225
	CH_3	—	1.231	1.229	1.232
Fuc^{2,4,3}	H-1	5.278	5.276	—	—
	H-5	4.253	4.251	—	—
	CH_3	1.268	1.266	—	—
Fuc^{2,3}	H-1	—	—	5.192	5.199
	H-5	—	—	4.291	4.293
	CH_3	—	—	1.235	1.237
Fuc^3	H-1	5.125	5.126	—	—
	H-5	4.874	4.874	—	—
	CH_3	1.237	1.236	—	—

[a] From HOHAHA experiment.
[b] Spectrum recorded at 10 °C.
[c] From HOHAHA experiment recorded at 600 MHz.

TABLE 35
^{1}H Chemical Shifts of Structural-Reporter Groups of Constituent Monosaccharides for the Oligosaccharide-Alditols 161–164

Residue	Reporter group	161 	162 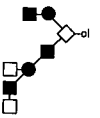	163 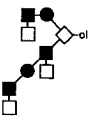	164 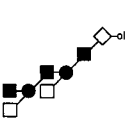
GalNAc-ol	H-2	4.27	4.393	4.401	4.396
	H-3	n.d.	4.059	n.d.	4.049
	H-4	3.505	3.463	3.539	n.d.
	H-5	4.22	4.279	n.d.	4.178
	NAc	2.037	2.066[a]	2.044	2.045
GlcNAc^6	H-1	4.546	4.556	4.586	—
	H-6	n.d.	3.987	n.d.	—
	NAc	2.059	2.061	2.056	—
Gal^{4,6}	H-1	4.501	4.464	4.543	—
Gal^3	H-1	—	4.435	4.685	4.445
	H-4	—	4.136	4.159	4.124
GlcNAc^3	H-1	4.616	4.601	4.77[b]	4.673[c,d]
	H-3	n.d.	4.132	4.03[b]	n.d.
	NAc	2.070	2.061[a]	2.124	2.029[e]
Gal^{4,3}	H-1	4.484	—	—	4.459[f]
	H-4	n.d.	—	—	4.099
Gal^{3,3}	H-1	—	4.653	4.668	—
	H-4	—	n.d.	3.88[b]	—
GlcNAc^{3,4,3}	H-1	—	—	—	4.661[c,d]
	NAc	—	—	—	2.017[e]
Gal^{4,3,4,3}	H-1	—	—	—	4.464[f]
Fuc^{2,3}	H-1	—	—	5.081	—
	H-5	—	—	4.274	—
	CH_3	—	—	1.190	—
Fuc^{2,3,3}	H-1	—	5.151	5.198	—
	H-5	—	4.344	4.274	—
	CH_3	—	1.272	1.231	—
Fuc^{2,4,3}	H-1	5.27	—	—	—
	H-5	4.258	—	—	—
	CH_3	1.275	—	—	—
Fuc^{2,4,6}	H-1	5.27	—	5.311	—
	H-5	4.258	—	4.224	—
	CH_3	1.275	—	1.231	—
Fuc^{3,3}	H-1	5.117[g]	—	—	5.125
	H-5	4.873	—	—	4.865[c,h]
	CH_3	1.238	—	—	1.150
Fuc^{3,3,4}	H-1	—	—	—	5.133
	H-5	—	—	—	4.851[c,h]
	CH_3	—	—	—	1.174
Fuc^{3,6}	H-1	5.108[g]	—	—	—
	H-5	4.873	—	—	—
	CH_3	1.238	—	—	—

continued.

TABLE 35—*continued.*

Residue	Reporter group	161 	162 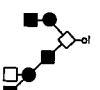	163 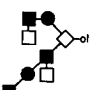	164 
Fuc[4]	H-1	—	5.024	—	—
	H-5	—	4.865	—	—
	CH_3	—	1.257	—	—

[a] Assignments may have to be interchanged.
[b] From HOHAHA experiment recorded at 15 °C at 600 MHz.
[c] Spectrum recorded at 7 °C.
[d-h] Assignments may have to be interchanged.

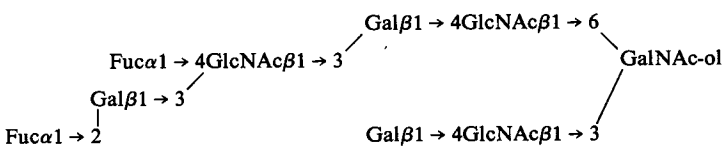

(149)

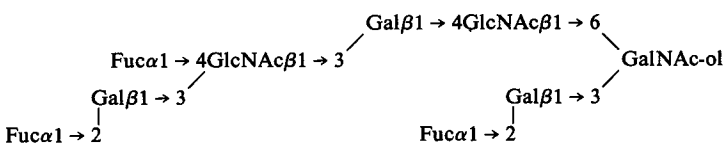

(150)

compounds **151-156** (Figures 85-90) (Table 33; Klein *et al.*, 1991) the common element Galβ1 → 4GlcNAcβ1 → 3Galβ1 → 4GlcNAcβ1 → 6GalNAc-ol, compounds **157-160** (Figures 91-94) (Table 34; Van Kuik *et al.*, 1991) the common element GlcNAcβ1 → 3(Galβ1 → 4GlcNAcβ1 → 6)Galβ1 →

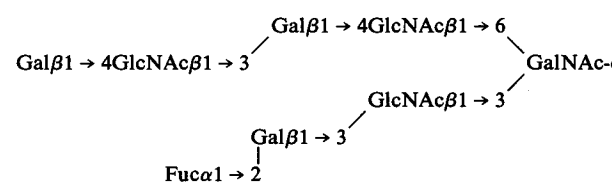

(151)

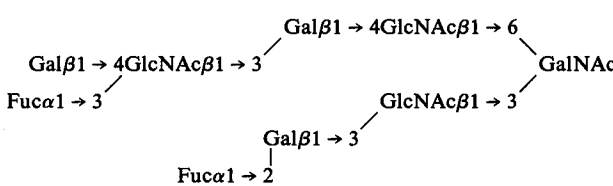

(152)

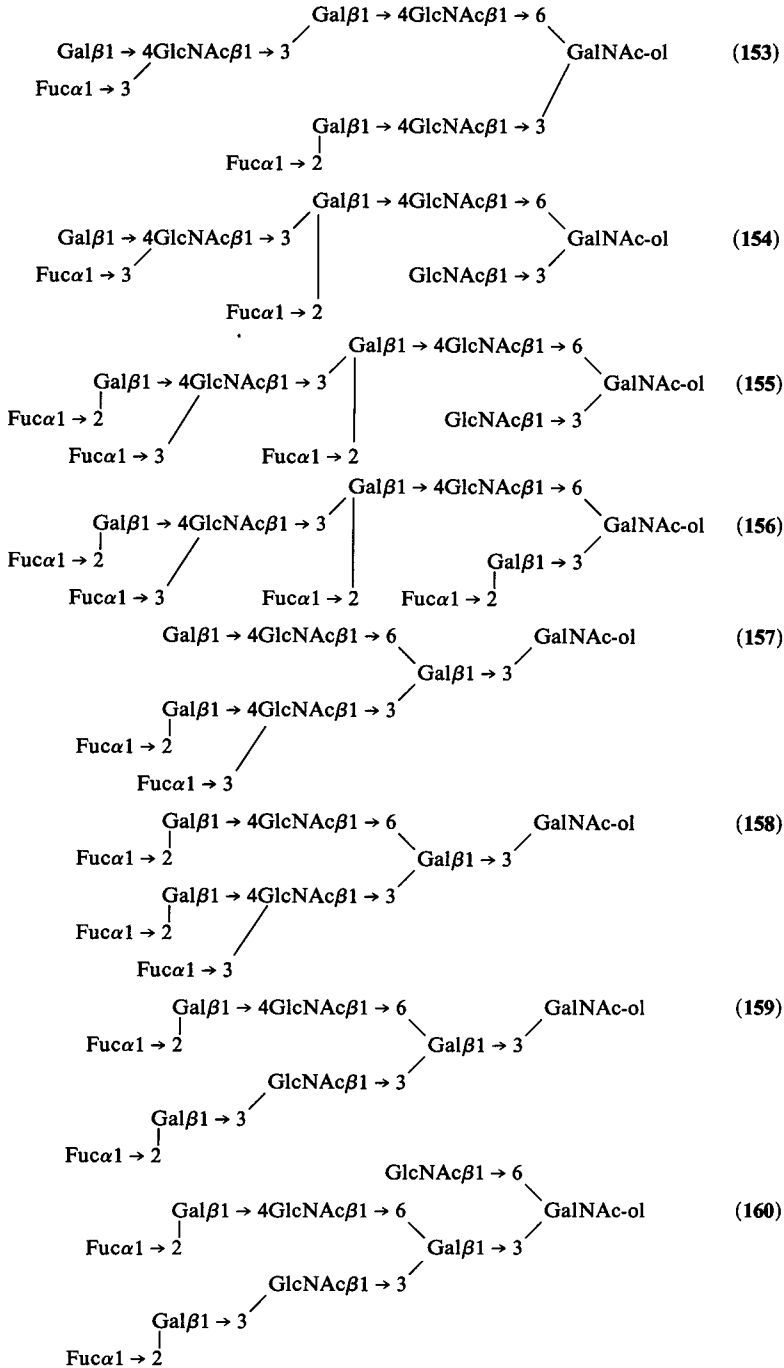
Galβ1 → 4GlcNAcβ1 → 6
Galβ1 → 4GlcNAcβ1 → 3
GalNAc-ol
Fucα1 → 3
Galβ1 → 4GlcNAcβ1 → 3
Fucα1 → 2
(153)
Galβ1 → 4GlcNAcβ1 → 6
Galβ1 → 4GlcNAcβ1 → 3
GalNAc-ol
Fucα1 → 3
GlcNAcβ1 → 3
Fucα1 → 2
(154)
Galβ1 → 4GlcNAcβ1 → 6
Galβ1 → 4GlcNAcβ1 → 3
GalNAc-ol
Fucα1 → 2
GlcNAcβ1 → 3
Fucα1 → 3
Fucα1 → 2
(155)
Galβ1 → 4GlcNAcβ1 → 6
Galβ1 → 4GlcNAcβ1 → 3
GalNAc-ol
Fucα1 → 2
Galβ1 → 3
Fucα1 → 3
Fucα1 → 2
Fucα1 → 2
(156)
Galβ1 → 4GlcNAcβ1 → 6
GalNAc-ol
Galβ1 → 3
Galβ1 → 4GlcNAcβ1 → 3
Fucα1 → 2
Fucα1 → 3
(157)
Galβ1 → 4GlcNAcβ1 → 6
GalNAc-ol
Galβ1 → 3
Galβ1 → 4GlcNAcβ1 → 3
Fucα1 → 2
Fucα1 → 3
(158)
Galβ1 → 4GlcNAcβ1 → 6
GalNAc-ol
Fucα1 → 2
Galβ1 → 3
Galβ1 → 4GlcNAcβ1 → 3
Fucα1 → 2
Fucα1 → 3
(159)
Galβ1 → 4GlcNAcβ1 → 6
GalNAc-ol
Fucα1 → 2
Galβ1 → 3
GlcNAcβ1 → 3
Galβ1 → 3
Fucα1 → 2
GlcNAcβ1 → 6
(160)
Galβ1 → 4GlcNAcβ1 → 6
GalNAc-ol
Fucα1 → 2
Galβ1 → 3
GlcNAcβ1 → 3
Galβ1 → 3
Fucα1 → 2

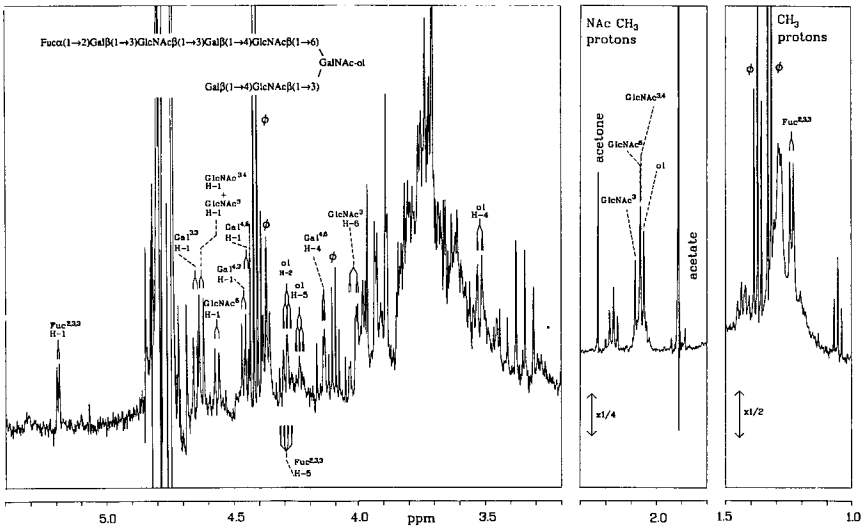

Figure 80. Resolution-enhanced 500-MHz ^{1}H-NMR spectrum of **146**. The relative-intensity scale of the *N*-acetyl methyl and Fuc methyl proton regions of the spectrum differ from that of the other parts, as indicated. The signals marked by ϕ stem from frequently occurring, nonprotein noncarbohydrate contaminants.

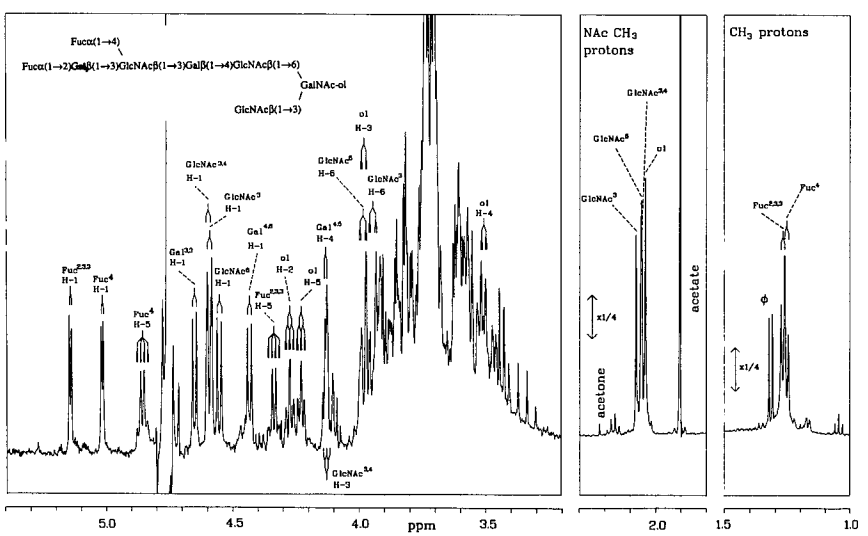

Figure 81. Resolution-enhanced 500-MHz ^{1}H-NMR spectrum of **147**. For comments, see Figure 80.

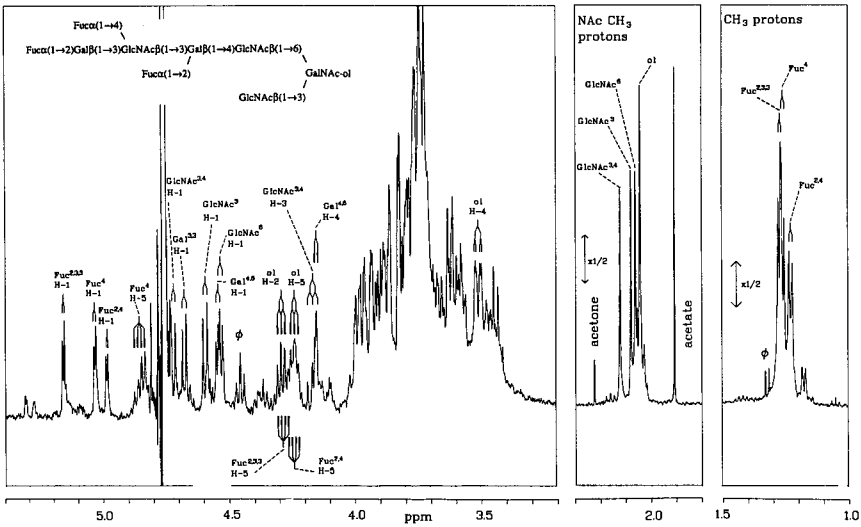

Figure 82. Resolution-enhanced 500-MHz ^{1}H-NMR spectrum of **148**. For comments, see Figure 80.

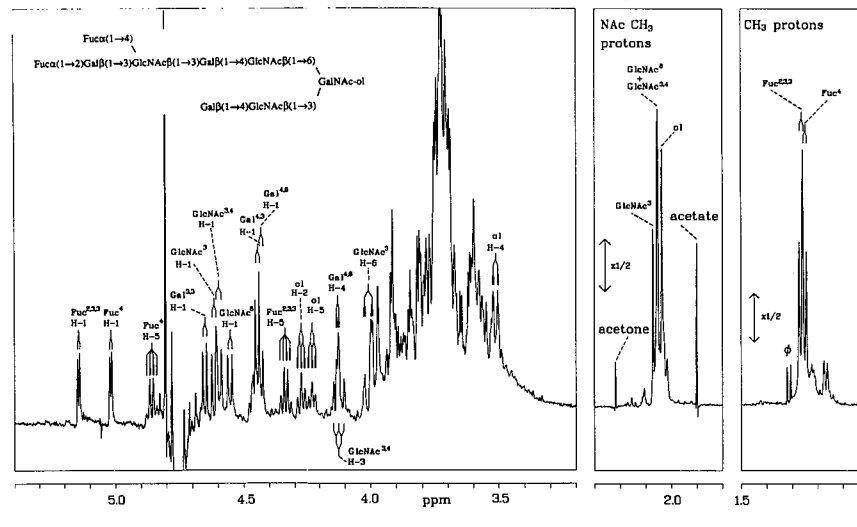

Figure 83. Resolution-enhanced 500-MHz ^{1}H-NMR spectrum of **149**. For comments, see Figure 80.

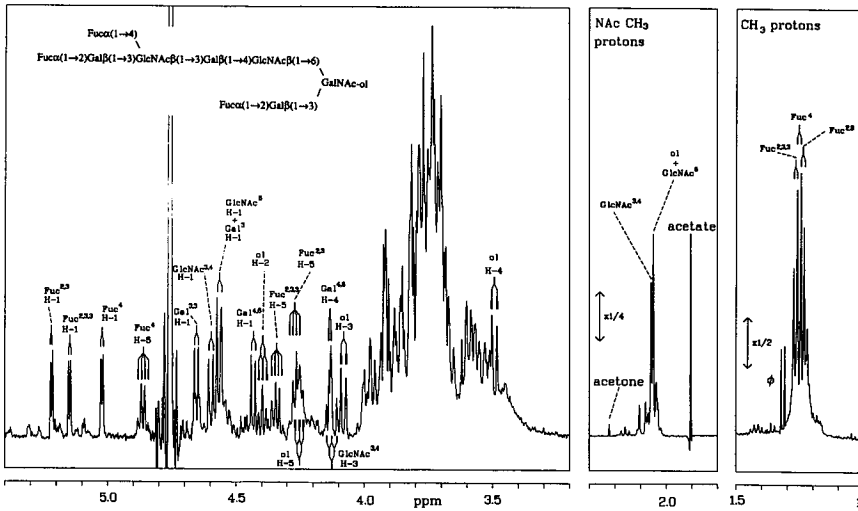

Figure 84. Resolution-enhanced 500-MHz ^{1}H-NMR spectrum of **150**. For comments, see Figure 80.

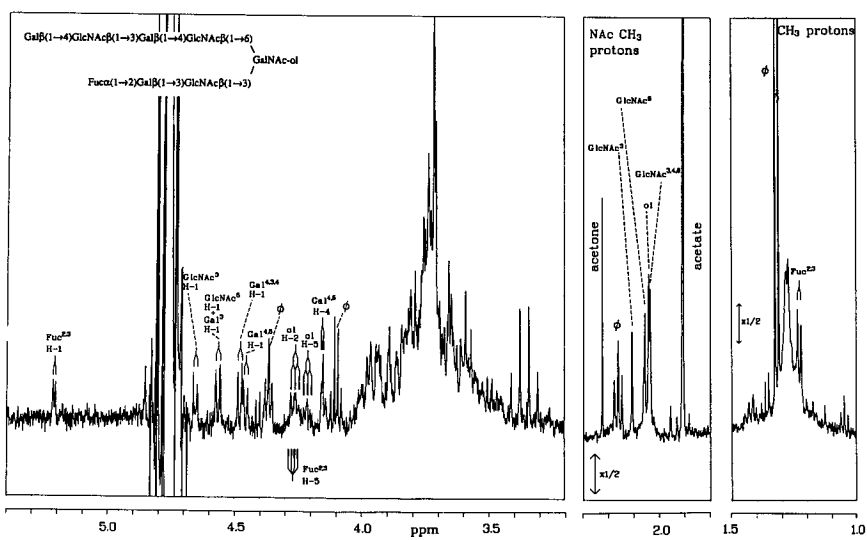

Figure 85. Resolution-enhanced 500-MHz ^{1}H-NMR spectrum of **151**. For comments, see Figure 80.

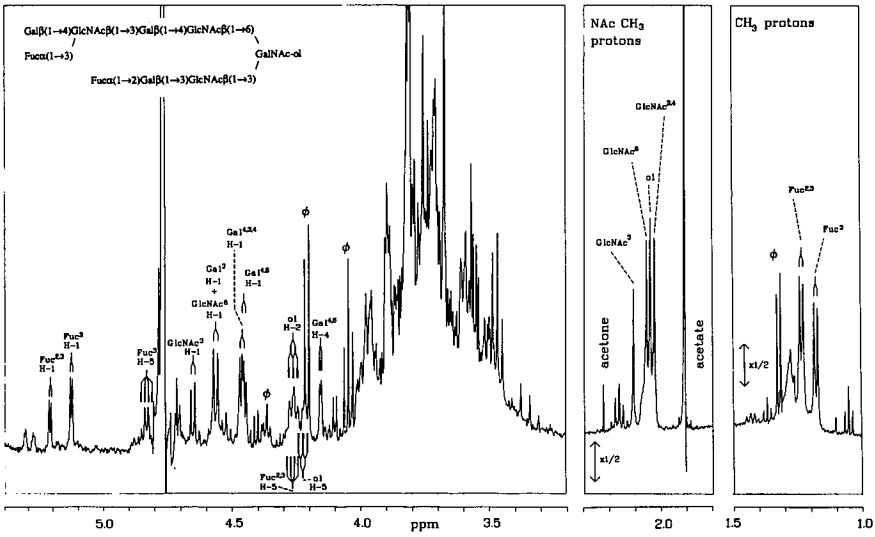

Figure 86. Resolution-enhanced 500-MHz ^{1}H-NMR spectrum of **152**. For comments, see Figure 80.

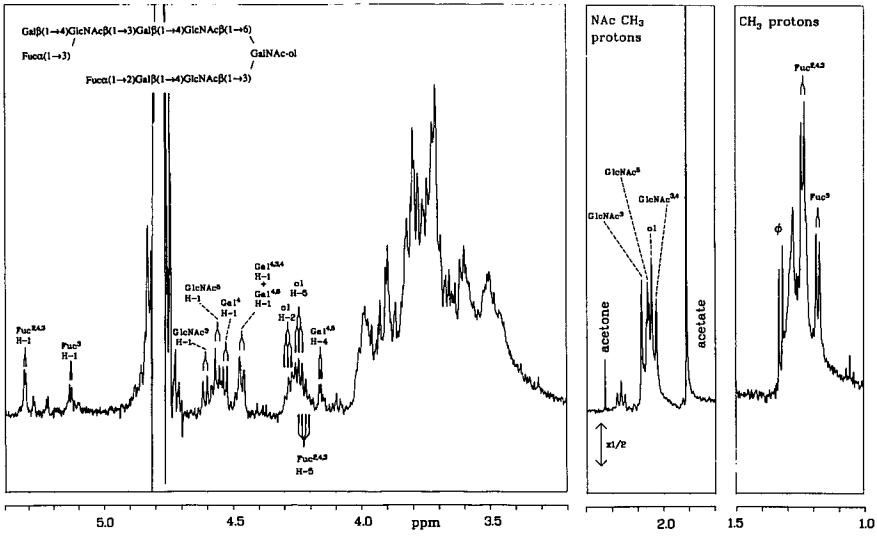

Figure 87. Resolution-enhanced 500-MHz ^{1}H-NMR spectrum of **153**. The relative-intensity scale of the *N*-acetyl methyl proton region of the spectrum differs from that of the other parts, as indicated.

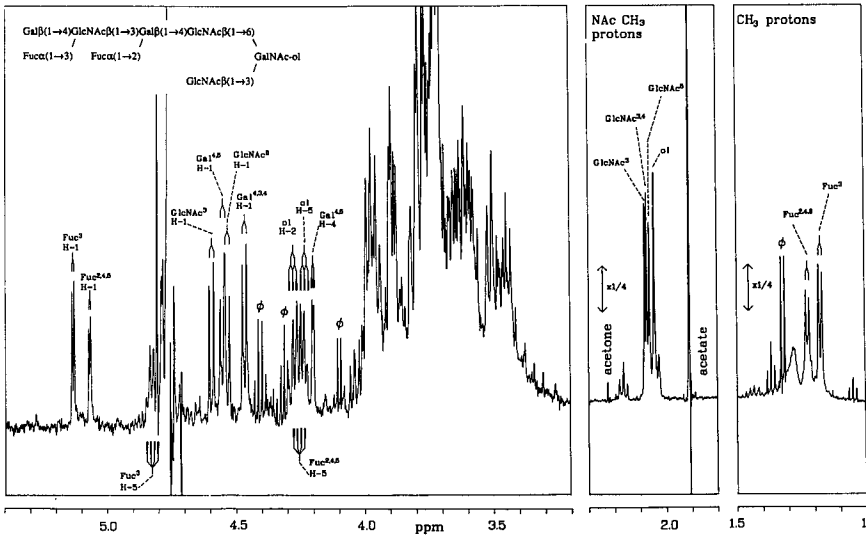

Figure 88. Resolution-enhanced 500-MHz ^{1}H-NMR spectrum of **154**. For comments, see Figure 80.

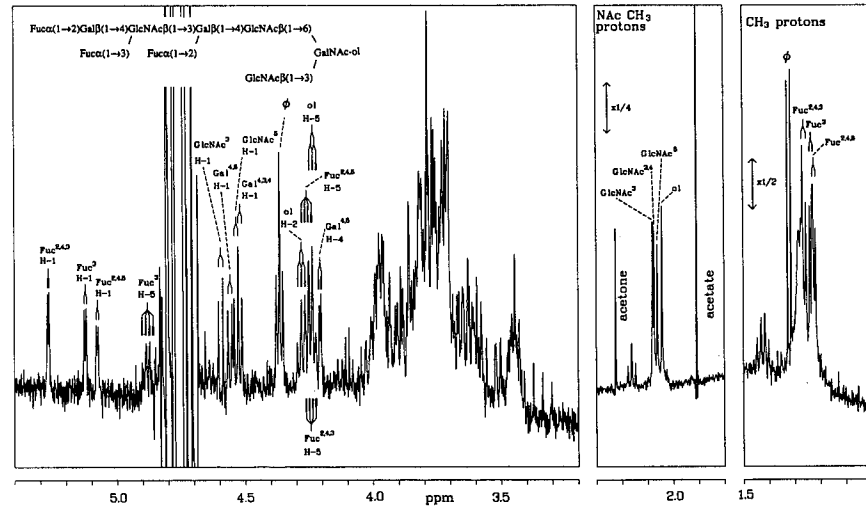

Figure 89. Resolution-enhanced 500-MHz ^{1}H-NMR spectrum of **155**. For comments, see Figure 80.

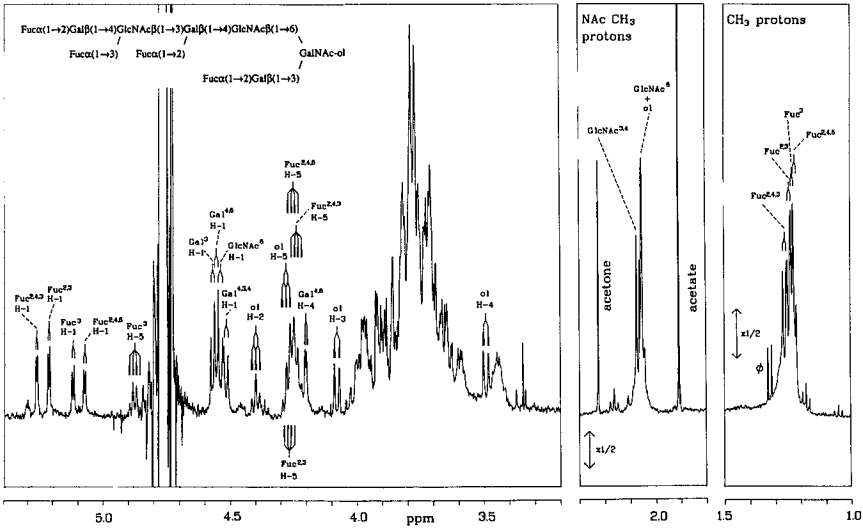

Figure 90. Resolution-enhanced 500-MHz ^{1}H-NMR spectrum of **156**. For comments, see Figure 80.

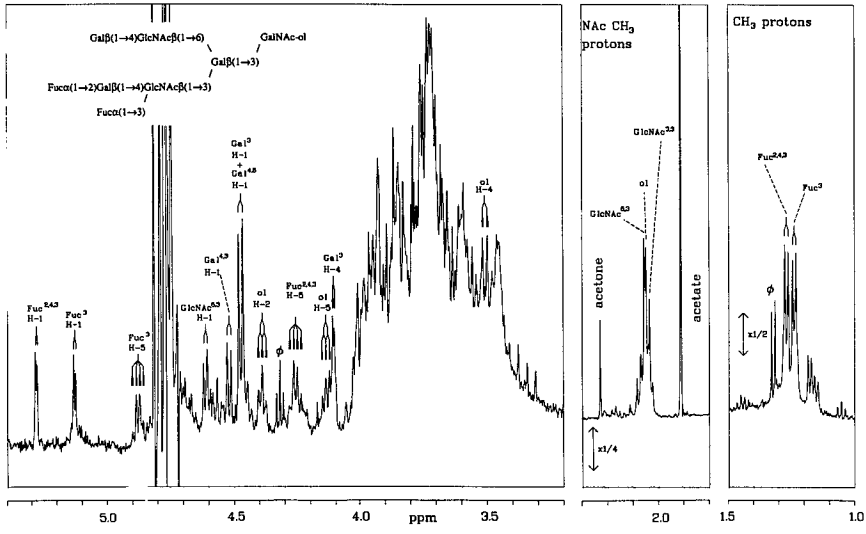

Figure 91. Resolution-enhanced 500-MHz ^{1}H-NMR spectrum of **157**. For comments, see Figure 80.

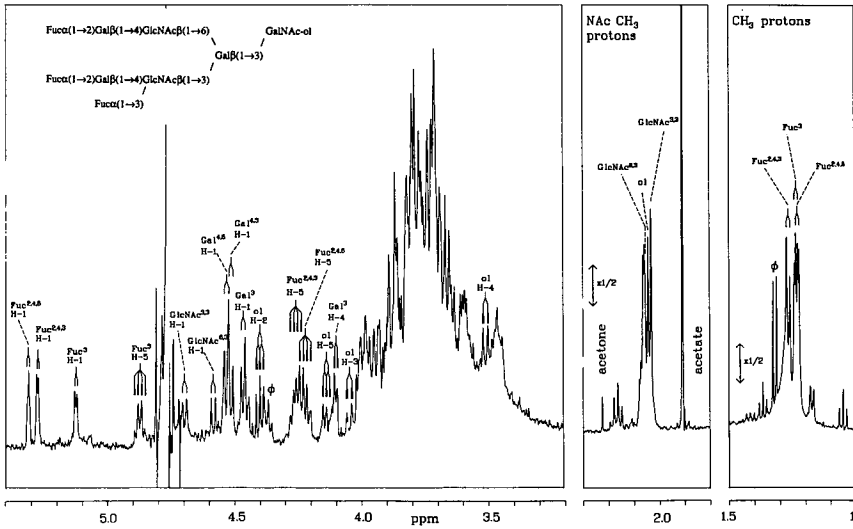

Figure 92. Resolution-enhanced 500-MHz ^{1}H-NMR spectrum of **158**. For comments, see Figure 80.

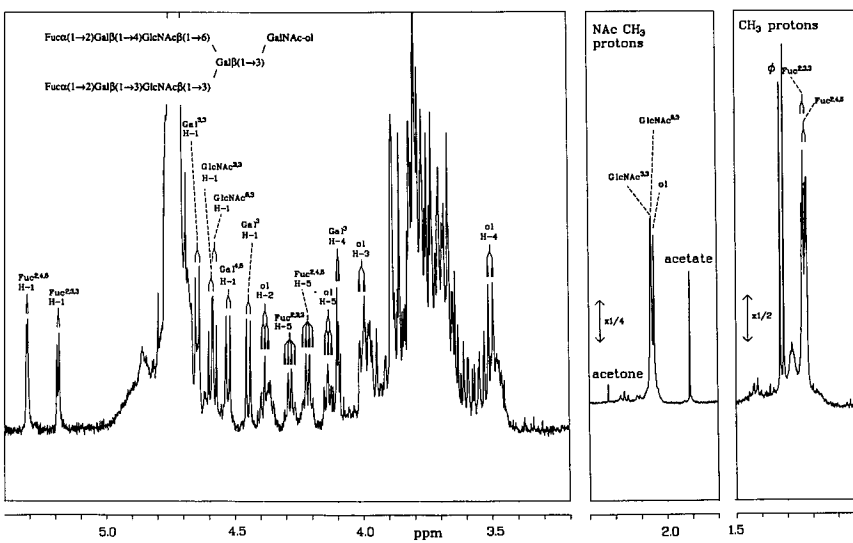

Figure 93. Resolution-enhanced 500-MHz ^{1}H-NMR spectrum of **159**. For comments, see Figure 80.

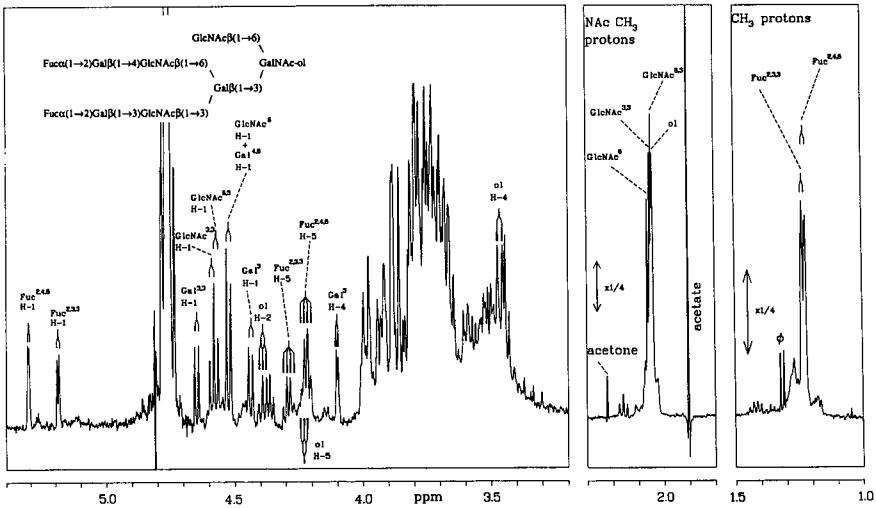

Figure 94. Resolution-enhanced 500-MHz ^{1}H-NMR spectrum of **160**. For comments, see Figure 80.

3GalNAc-ol, whereas compounds **161–164** (Figures 95–98) (Table 35; Van Kuik *et al.*, 1991) form a heterogeneous series.

The ^{1}H-NMR data of two additional sulfated oligosaccharide-alditols (**165, 166**) and of two additional oligosaccharide-alditols with terminal $\alpha 1 \rightarrow 4$-linked GlcNAc (**167, 168**) have been reported by Dickenson *et al.* (1990) and Hounsell *et al.* (1989), respectively, and are presented in

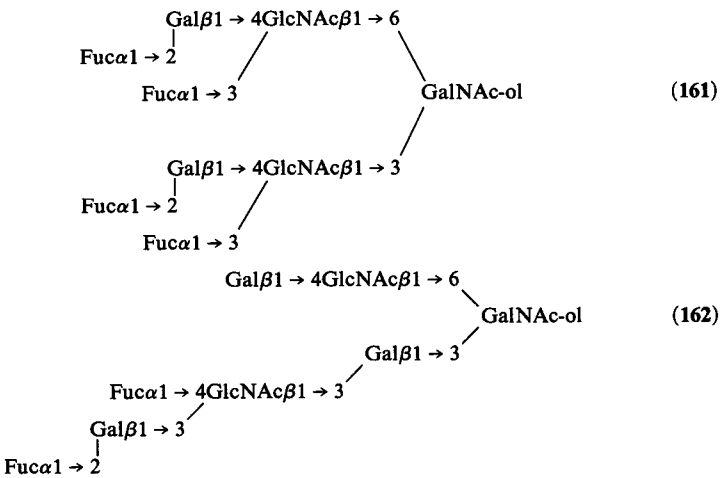

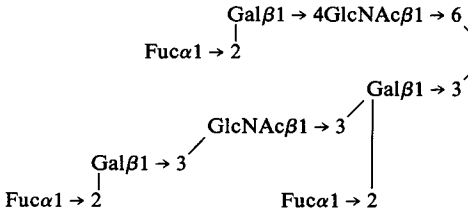

(163)

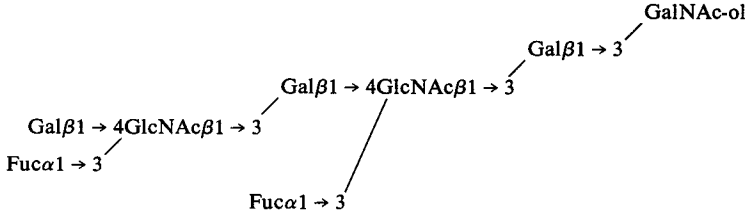

(164)

Table 36. The ^{1}H-NMR spectra of **165–168** are depicted in the respective references.

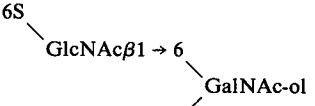

(165)

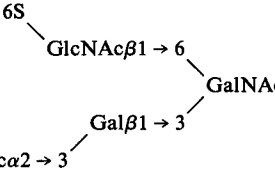

(166)

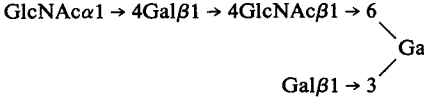

(167)

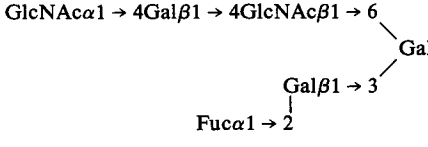

(168)

For ^{1}H-NMR data and ^{1}H-NMR spectra of structures having GlcNAcβ1 → 6(NeuAcα2 → 3Galβ1 → 3)GalNAc-ol in common and extensions of the upper branch with Galβ1 → 3GlcNAcβ1 → 3Galβ1 → 4(Fucα1 → 3), Galβ1 → 4GlcNAcβ1 → 3Galβ1 → 4(Fucα1 → 3), Fucα1 → 2Galβ1 → 3(Fucα1 → 4)GlcNAcβ1 → 3Galβ1 → 4GlcNAcβ1 → 3Galβ1 → 4, Galβ1 → 3(Fucα1 → 4)GlcNAcβ1 → 3Galβ1 → 4GlcNAcβ1 → 3Galβ1 → 4(Fucα1 → 3), Galβ1 → 4(Fucα1 → 3)GlcNAcβ1 → 6[Fucα1 → 2Galβ1 →

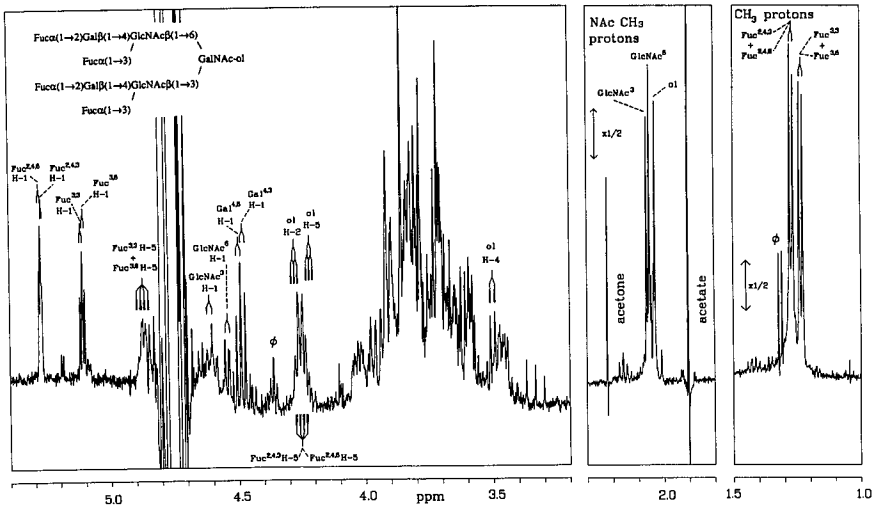

Figure 95. Resolution-enhanced 500-MHz ^{1}H-NMR spectrum of **161**. For comments, see Figure 80.

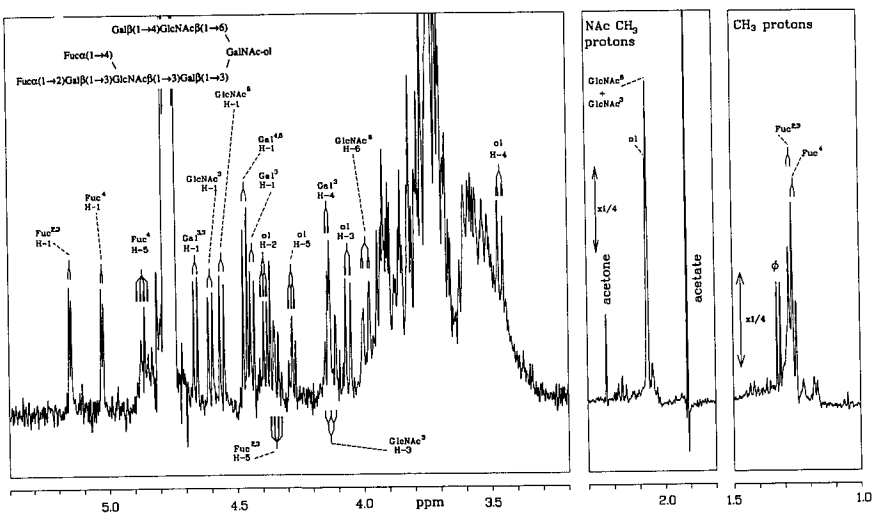

Figure 96. Resolution-enhanced 500-MHz ^{1}H-NMR spectrum of **162**. For comments, see Figure 80.

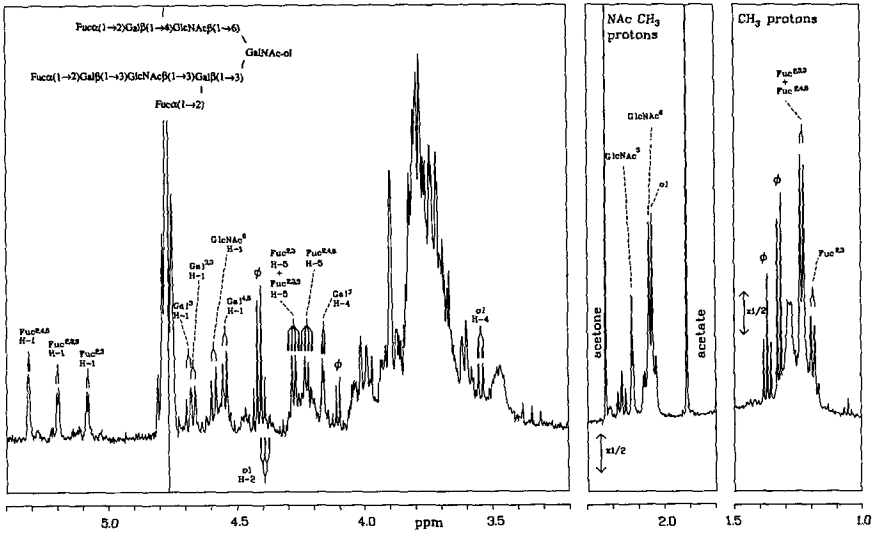

Figure 97. Resolution-enhanced 500-MHz ^{1}H-NMR spectrum of **163**. For comments, see Figure 80.

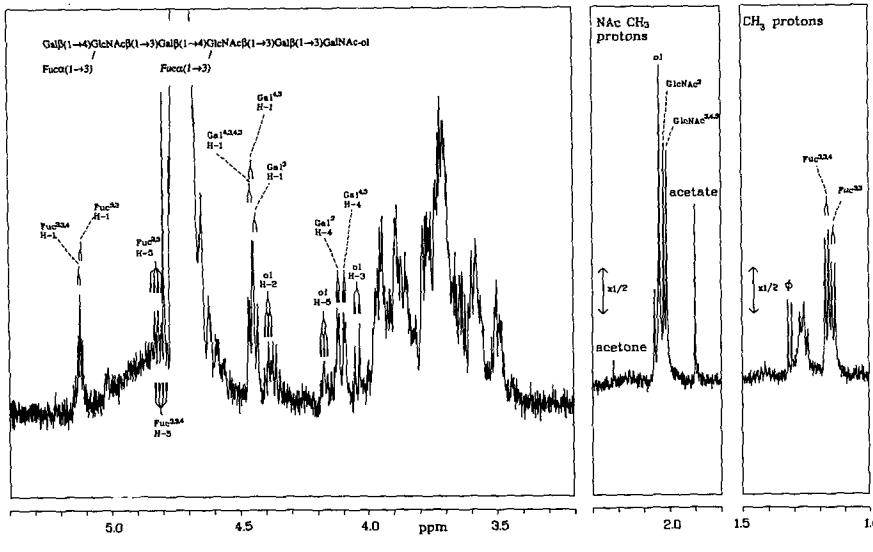

Figure 98. Resolution-enhanced 500-MHz ^{1}H-NMR spectrum of **164**. For comments, see Figure 80.

TABLE 36

^{1}H Chemical Shifts of Structural-Reporter Groups of Constituent Monosaccharides for the Oligosaccharide-Alditols 165–168

Residue	Reporter group	165 	166 	167 	168 
GalNAc-ol	H-2	4.387	4.387	4.401	4.408
	H-3	4.055	4.064	4.065	4.086
	H-4	3.459	3.429	3.460	3.500
	H-5	4.271	4.250	4.291	4.274
	H-6	3.934	3.924	3.94	n.d.
	NAc	2.064	2.066	2.068	2.055
GlcNAc^6	H-1	4.551	4.550	4.564	4.562
	H-6	4.233	4.233	4.017	4.020
	H-6′	4.353	4.349	3.84	n.d.
	NAc	2.064	2.061	2.068	2.059
Gal^4	H-1	—	—	4.523	4.530
	H-4	—	—	3.982	3.983
GlcNAc^4	H-1	—	—	4.852[a]	4.85[a]
	H-5	—	—	4.194	4.195
	NAc	—	—	2.068	2.067
Gal^3	H-1	4.456	4.525	4.466	4.563
	H-2	3.565	3.605	3.562	n.d.
	H-3	3.664	4.111	3.668	n.d.
	H-4	3.891	3.914	n.d.	n.d.
Fuc^2	H-1	—	—	—	5.222
	H-5	—	—	—	4.281
	CH_3	—	—	—	1.244
NeuAc^3	H-3a	—	1.796	—	—
	H-3e	—	2.767	—	—
	NAc	—	2.024	—	—

[a] Spectrum recorded at 285 K.

3(Fucα1 → 4)GlcNAcβ1 → 3]Galβ1 → 4, or Galβ1 → 4GlcNAcβ1 → 6[Fucα1 → 2Galβ1 → 3(Fucα1 → 4)GlcNAcβ1 → 3]Galβ1 → 4(Fucα1 → 3) elements, see Pierce-Cretel *et al.* (1989). The same holds for Fucα1 → 2Galβ1 → 3GlcNAcβ1 → 3Galβ1 → 4GlcNAcβ1 → 6(Galβ1 → 3)GalNAc-ol. Finally, ^{1}H-NMR data have been reported for oligosaccharide-alditols built up of GalNAc-ol substituted at C-3 with β-Gal and at C-6 with Galβ1 → 3/4GlcNAcβ1[→ 6Galβ1 → 4GlcNAcβ1 →]$_{1-2}$ elements (Hanisch *et al.*, 1989).

ACKNOWLEDGMENTS. The authors thank their former co-workers of the Department of Bio-Organic Chemistry (Utrecht University) Dr. L.

Dorland, Dr. J. Haverkamp, Dr. H. Van Halbeek, Dr. J. H. G. M. Mutsaers, Dr. J. Breg, and Dr. P. De Waard, and their present co-worker Dr. J. A. Van Kuik for their enthusiastic contributions to the development of the ^{1}H-NMR concepts for the analysis of mucin-type *O*-linked carbohydrate chains. Most of the data are from the authors' laboratory, in collaboration with several research groups, who made large series of oligosaccharide-alditol samples available. In this context we want to thank especially Prof. Dr. D. Aminoff, Prof. Dr. P. Jollès, Prof. Dr. E. A. Kabat, Prof. Dr. N. K. Kochetkov, Prof. Dr. M. F. Kramer, Prof. Dr. J. Montreuil, Prof. Dr. Nasir-Ud-Din, Prof. Dr. P. Roussel, Prof. Dr. K. Schmid, and their respective involved co-workers. The NMR investigations of the authors' laboratory were supported by the Netherlands Foundation for Chemical Research (SON) with financial aid from the Netherlands Organization for Scientific Research (NWO) and by the Dutch Cancer Society (KWF, grants UUKC-OC 79-13, 83-13, and 88-13).

REFERENCES

Akiyama, F., Stevens, R. L., Hayashi, S., Swann, D. A., Binette, J. P., Caterson, B., Schmid, K., Van Halbeek, H., Mutsaers, J. H. G. M., Gerwig, G. J., and Vliegenthart, J. F. G., 1987, *Arch. Biochem. Biophys.* **252**:574.

Akiyama, K., Simons, E. R., Bernasconi, P., Schmid, K., Van Halbeek, H., Vliegenthart, J. F. G., Haupt, H., and Schwick, H. G., 1984, *J. Biol. Chem.* **259**:7151.

Anderson, D. R., and Grimes, W. J., 1985, *Anal. Biochem.* **146**:13.

Aspinall, G. O. (ed.), 1982, *The Polysaccharides*, Vol. 1, Academic Press, New York.

Aspinall, G. O. (ed.), 1983, *The Polysaccharides*, Vol. 2, Academic Press, New York.

Aspinall, G. O. (ed.), 1985, *The Polysaccharides*, Vol. 3, Academic Press, New York.

Berger, E. G., Buddecke, E., Kamerling, J. P., Kobata, A., Paulson, J. C., and Vliegenthart, J. F. G., 1982, *Experientia* **38**:1129.

Berman, E., 1987, *Magn. Reson. Chem.* **25**:784.

Bernard, N., Engler, R., Strecker, G., Montreuil, J., Van Halbeek, H., and Vliegenthart, J. F. G., 1984, *Glycoconj. J.* **1**:123.

Blanchard, D., Cartron, J.-P., Fournet, B., Montreuil, J., Van Halbeek, H., and Vliegenthart, J. F. G., 1983, *J. Biol. Chem.* **258**:7691.

Bock, K., Meldal, M. D. R., Iversen, T., Pinto, B. M., Garegg, P. J., Kvarnstrom, I., Norberg, T., Lindberg, A. A., and Svenson, S. B., 1984, *Carbohydr. Res.* **130**:35.

Bot, D. S. M., Cleij, P., Van 't Klooster, H. A., Van Halbeek, H., Veldink, G. A., and Vliegenthart, J. F. G., 1988, *J. Chemometrics* **2**:11.

Breg, J., Van Halbeek, H., Vliegenthart, J. F. G., Lamblin, G., Houvenaghel, M.-C., and Roussel, P., 1987, *Eur. J. Biochem.* **168**:57.

Breg, J., Romijn, D., Vliegenthart, J. F. G., Strecker, G., and Montreuil, J., 1988a, *Carbohydr. Res.* **183**:19.

Breg, J., Van Halbeek, H., Vliegenthart, J. F. G., Klein, A., Lamblin, G., and Roussel, P., 1988b, *Eur. J. Biochem.* **171**:643.

Brisson, J.-R. and Carver, J. P., 1983, *J. Biol. Chem.* **258**:1431.

Brockhausen, I., Orr, J., and Schachter, H., 1984, *Can. J. Biochem. Cell Biol.* **62**:1081.

Brockhausen, I., Matta, K. L., Orr, J., and Schachter, H., 1985, *Biochemistry* **24**:1866.
Bush, C. A., Yan, Z.-Y., and Rao, B. N. N., 1986, *J. Am. Chem. Soc.* **108**:6168.
Capon, C., Leroy, Y., Wieruszeski, J.-M., Ricart, G., Strecker, G., Montreuil, J., and Fournet, B., 1989, *Eur. J. Biochem.* **182**:139.
Carver, J. P., and Brisson, J.-R., 1984, in *Biology of Carbohydrates* (Ginsburg, V., and Robbins, P. W., eds.), Vol. 2, p. 289, Wiley, New York.
Carver, J. P., and Cumming, D. A., 1987, *Pure Appl. Chem.* **59**:1465.
Damm, J. B. L., Kamerling, J. P., Van Dedem, G. W. K., and Vliegenthart, J. F. G., 1987, *Glycoconj. J.* **4**:129.
D'Arcy, S. M., Donoghue, C. M., Koeleman, C. A. M., Van Den Eijnden, D. H., and Savage, A. V., 1989, *Biochem. J.* **260**:389.
Dell, A., 1987, *Adv. Carbohydr. Chem. Biochem.* **45**:19.
Dickenson, J. M., Huckerby, T. N., and Nieduszynski, I. A., 1990, *Biochem. J.* **269**:55.
Dill, K., Berman, E., and Pavia, A. A., 1985, *Adv. Carbohydr. Chem. Biochem.* **43**:1.
Dorland, L., Van Halbeek, H., and Vliegenthart, J. F. G., 1984, *Biochem. Biophys. Res. Commun.* **122**:859.
Dorland, L., Van Halbeek, H., Vliegenthart, J. F. G., Schauer, R., and Wiegandt, H., 1986, *Carbohydr. Res.* **151**:233.
Dua, V. K., and Bush, C. A., 1983, *Anal. Biochem.* **133**:1.
Dua, V. K., Dube, V. E., and Bush, C. A., 1984, *Biochim. Biophys. Acta* **802**:29.
Dua, V. K., Dube, V. E., Li, Y.-T., and Bush, C. A., 1985, *Glycoconj. J.* **2**:17.
Dua, V. K., Rao, B. N. N., Wu, S.-S., Dube, V. E., and Bush, C. A., 1986, *J. Biol. Chem.* **261**:1599.
Dwek, R. A., Rademacher, T. W., and Parekh, R. B., 1988, *Annu. Rev. Biochem.* **57**:785.
Egge, H., and Peter-Katalinic, J., 1987, *Mass Spectrom. Rev.* **6**:331.
Feeney, J., Frenkiel, T. A., and Hounsell, E. F., 1986, *Carbohydr. Res.* **152**:63.
Feizi, T., and Childs, R. A., 1987, *Biochem. J.* **245**:1.
Fiat, A.-M., Chevan, J., Jollès, P., De Waard, P., Vliegenthart, J. F. G., Piller, F., and Cartron, J.-P., 1988, *Eur. J. Biochem.* **173**:253.
Finne, J., Breimer, M. E., Hansson, G. C., Karlsson, K.-A., Leffler, H., Vliegenthart, J. F. G., and Van Halbeek, H., 1989, *J. Biol. Chem.* **264**:5720.
Gejyo, F., Chang, J.-L., Bürgi, W., Schmid, K., Offner, G. D., Troxler, R. F., Van Halbeek, H., Dorland, L., Gerwig, G. J., and Vliegenthart, J. F. G., 1983, *J. Biol. Chem.* **258**:4966.
Ginsburg, V. (ed.), 1978, *Methods in Enzymology*, Vol. 50, Academic Press, New York.
Ginsburg, V. (ed.), 1982, *Methods in Enzymology*, Vol. 83, Academic Press, New York.
Ginsburg, V. (ed.), 1987, *Methods in Enzymology*, Vol. 138, Academic Press, New York.
Ginsburg, V., and Robbins, P. W. (eds.), 1981, *Biology of Carbohydrates*, Vol. 1, Wiley, New York.
Ginsburg, V., and Robbins, P. W. (eds.), 1984, *Biology of Carbohydrates*, Vol. 2, Wiley, New York.
Gleeson, P. A., Feeney, J., Mills, G., and Hughes, R. C., 1984, *Eur. J. Biochem.* **144**:143.
Gottschalk, A. (ed.), 1972, *Glycoproteins*, B.B.A. Library, Vol. 5A/B, Elsevier, Amsterdam.
Green, E. D., Adelt, G., Baenziger, J. U., Wilson, S., and Van Halbeek, H., 1988, *J. Biol. Chem.* **263**:18253.
Hanisch, F.-G., Uhlenbruck, G., Peter-Katalinic, J., Egge, H., Dabrowski, J., and Dabrowski, U., 1989, *J. Biol. Chem.* **264**:872.
Hanisch, F.-G., Peter-Katalinic, J., Egge, H., Dabrowski, U., and Uhlenbruck, G., 1990, *Glycoconj. J.* **7**:525.
Herkt, F., Paz Parente, J., Leroy, Y., Fournet, B., Blanchard, D., Cartron, J.-P., Van Halbeek, H., and Vliegenthart, J. F. G., 1985, *Eur. J. Biochem.* **146**:125.
Herlant-Peers, M.-C., Montreuil, J., Strecker, G., Dorland, L., Van Halbeek, H., Veldink, G. A., and Vliegenthart, J. F. G., 1981, *Eur. J. Biochem.* **117**:291.

Hindsgaul, O., Norberg, T., Le Pendu, J., and Lemieux, R. U., 1982, *Carbohydr. Res.* **109**:109.
Hirabayashi, Y., Matsumoto, Y., Matsumoto, M., Toida, T., Iida, N., Matsubara, T., Kanzaki, T., Yokota, M., and Ishizuka, I., 1990, *J. Biol. Chem.* **265**:1693.
Horowitz, M. I. (ed.), 1982a, *The Glycoconjugates*, Vol. III, Academic Press, New York.
Horowitz, M. I. (ed.), 1982b, *The Glycoconjugates*, Vol. IV, Academic Press, New York.
Horowtiz, M. I., and Pigman, W. (eds.), 1977, *The Glycoconjugates*, Vol. I, Academic Press, New York.
Horowitz, M. I., and Pigman, W. (eds.), 1978, *The Glycoconjugates*, Vol. II, Academic Press, New York.
Hounsell, E. F., 1987, *Chem. Soc. Rev.* **16**:161.
Hounsell, E. F., Wright, D. J., Donald, A. S. R., and Feeney, J., 1984, *Biochem. J.* **223**:129.
Hounsell, E. F., Lawson, A. M., Feeney, J., Gooi, H. C., Pickering, N. J., Stoll, M. S., Lui, S. C., and Feizi, T., 1985, *Eur. J. Biochem.* **148**:367.
Hounsell, E. F., Lawson, A. M., Feeney, J., Cashmore, G. C., Kane, D. P., Stoll, M. S., and Feizi, T., 1988, *Biochem. J.* **256**:397.
Hounsell, E. F., Lawson, A. M., Stoll, M. S., Kane, D. P., Cashmore, G. C., Carruthers, R. A., Feeney, J., and Feizi, T., 1989, *Eur. J. Biochem.* **186**:597.
Hounsell, E. F., and Wright, D. J., 1990, *Carbohydr. Res.* **205**:19.
Iwasaki, M., Nomoto, H., Kitajima, K., Inoue, S., and Inoue, Y., 1984, *Biochem. Int.* **8**:573.
Iwasaki, M., Inoue, S., and Inoue, Y., 1987a, *Eur. J. Biochem.* **168**:185.
Iwasaki, M., Inoue, S., Nadano, D., and Inoue, Y., 1987b, *Biochemistry* **26**:1452.
Kamerling, J. P., and Vliegenthart, J. F. G., 1989, in *Clinical Biochemistry: Principles, Methods, Applications*, Vol. 1, *Mass Spectrometry* (Lawson, A. M., ed.), p. 175, de Gruyter, Berlin.
Kitajima, K., Nomoto, H., Inoue, Y., Iwasaki, M., and Inoue, S., 1984, *Biochemistry* **23**:310.
Klein, A., Lamblin, G., Lhermitte, M., Roussel, P., Breg, J., Van Halbeek, H., and Vliegenthart, J. F. G., 1988, *Eur. J. Biochem.* **171**:631.
Klein, A., Carnoy, C., Lamblin, G., Roussel, P., Van Kuik, J. A., De Waard, P., and Vliegenthart, J. F. G., 1991, *Eur. J. Biochem.* **198**:151.
Koerner, T. A. W., Prestegard, J. H., Demou, P. C., and Yu, R. K., 1983, *Biochemistry* **22**:2687.
Koerner, T. A. W., Scarsdale, J. N., Prestegard, J. H., and Yu, R. K., 1984, *J. Carbohydr. Chem.* **3**:565.
Koerner, T. A. W., Prestegard, J. H., and Yu, R. K., 1987, *Methods Enzymol.* **138**:38.
Korrel, S. A. M., Clemetson, K. J., Van Halbeek, H., Kamerling, J. P., Sixma, J. J., and Vliegenthart, J. F. G., 1984, *Eur. J. Biochem.* **140**:571.
Korrel, S. A. M., Clemetson, K. J., Van Halbeek, H., Kamerling, J. P., Sixma, J. J., and Vliegenthart, J. F. G., 1985, *Glycoconj. J.* **2**:229.
Lamblin, G., Boersma, A., Klein, A., Roussel, P., Van Halbeek, H., and Vliegenthart, J. F. G., 1984a, *J. Biol. Chem.* **259**:9051.
Lamblin, G., Boersma, A., Lhermitte, M., Roussel, P., Mutsaers, J. H. G. M., Van Halbeek, H., and Vliegenthart, J. F. G., 1984b, *Eur. J. Biochem.* **143**: 227.
Lecat, D., Lemonnier, M., Derappe, C., Lhermitte, M., Van Halbeek, H., Dorland, L., and Vliegenthart, J. F. G., 1984, *Eur. J. Biochem.* **140**:415.
Lemieux, R. U., 1978, *Chem. Soc. Rev.* **7**:423.
Lemieux, R. U., Bock, K., Delbaere, L. T. J., Koto, S., and Rao, V. S., 1980, *Can. J. Chem.* **58**:631.
Lennarz, W. J. (ed.), 1980, *The Biochemistry of Glycoproteins and Proteoglycans*, Plenum Press, New York.
Linden, H.-U., Klein, R. A., Egge, H., Peter-Katalinic, J., Dabrowski, J., and Schindler, D., 1989, *Biol. Chem. Hoppe-Seyler* **370**:661.
Marti, T., Schaller, J., Rickli, E. E., Schmid, K., Kamerling, J. P., Gerwig, G. J., Van Halbeek, H., and Vliegenthart, J. F. G., 1988, *Eur. J. Biochem.* **173**:57.
Montreuil, J., 1980, *Adv. Carbohydr. Chem. Biochem.* **37**:157.
Montreuil, J., 1982, *Compr. Biochem.* **19B**(II):1.

Mutsaers, J. H. G. M., Van Halbeek, H., Vliegenthart, J. F. G., Wu, A. M., and Kabat, E. A., 1986, *Eur. J. Biochem.* **157**:139.

Nadano, D., Iwasaki, M., Endo, S., Kitajima, K., Inoue, S., and Inoue, Y., 1986, *J. Biol. Chem.* **261**:11550.

Nasir-Ud-Din, Jeanloz, R. W., Lamblin, G., Roussel, P., Van Halbeek, H., Mutsaers, J. H. G. M., and Vliegenthart, J. F. G., 1986, *J. Biol. Chem.* **261**:1992.

Nato, F., Goulut, C., Bourrillon, R., Van Halbeek, H., and Vliegenthart, J. F. G., 1986, *Eur. J. Biochem.* **159**:303.

Nomoto, H., Iwasaki, M., Endo, T., Inoue, S., Inoue, Y., and Matsumura, G., 1982, *Arch. Biochem. Biophys.* **218**:335.

Paulsen, H., and Paal, M., 1984, *Carbohydr. Res.* **135**:71.

Paulsen, H., Schultz, M., Klamann, J.-D., Waller, B., and Paal, M., 1985, *Liebigs Ann. Chem.* 2028.

Paz-Parente, J., Strecker, G., Leroy, Y., Montreuil, J., Fournet, B., Van Halbeek, H., Dorland, L., and Vliegenthart, J. F. G., 1983, *FEBS Lett.* **152**:145.

Pierce-Cretel, A., Decottignies, J.-P., Wieruszeski, J.-M., Strecker, G., Montreuil, J., and Spik, G., 1989, *Eur. J. Biochem.* **182**:457.

Rao, B. N. N., Dua, V. K., and Bush, C. A., 1985, *Biopolymers* **24**:2207.

Santer, U. V., Glick, M. C., Van Halbeek, H., and Vliegenthart, J. F. G., 1983, *Carbohydr. Res.* **120**:197.

Savage, A. V., Koppen, P. L., Schiphorst, W. E. C. M., Trippelvitz, L. A. W., Van Halbeek, H., Vliegenthart, J. F. G., and Van Den Eijnden, D. H., 1986, *Eur. J. Biochem.* **160**:123.

Savage, A. V., D'Arcy, S. M., and Donoghue, C. M., 1987, *Glycoconjugates, Proc. IXth Int. Symp.* (Montreuil, J., Verbert, A., Spik, G., and Fournet, B., eds.), Lerouge, Tourcoing, p. A11.

Savage, A. V., D'Arcy, S. M., Donoghue, C. M., Koeleman, C. A. M., and Van Den Eijnden, D. H., 1988, *Sialic acids, Proc. Japanese-German Symp.* (Schauer, R., and Yamakawa, T., eds.), Kieler Verlag Wissenschaft, p. 90.

Savage, A. V., Donoghue, C. M., D'Arcy, S. M., Koeleman, C. A. M., and Van Den Eijnden, D. H., 1990a, *Eur. J. Biochem.* **192**:427.

Savage, A. V., Donohue, J. J., Koeleman, C. A. M., and Van Den Eijnden, D. H., 1990b, *Eur. J. Biochem.* **193**:837.

Schachter, H., and Brockhausen, I., 1992, in *Handbook of Glycoproteins* (Allen, H. J., and Kisailus, E. C., eds.), Dekker, New York, in press.

Sharon, N., and Lis, H., 1981, *Chem. Eng. News* **59**:21.

Sharon, N., and Lis, H., 1982, *The Proteins* **V**:1.

Shimamura, M., Endo, T., Inoue, Y., and Inoue, S., 1983, *Biochemistry* **22**:959.

Shimamura, M., Endo, T., Inoue, Y., Inoue, S., and Kambara, H., 1984, *Biochemistry* **23**:317.

Strecker, G., Ollier-Hartmann, M.-P., Van Halbeek, H., Vliegenthart, J. F. G., Montreuil, J., and Hartmann, L., 1985, *C. R. Acad. Sci.* **301**:571.

Strecker, G., Wieruszeski, J.-M., Martel, C., and Montreuil, J., 1987, *Glycoconj. J.* **4**:329.

Strecker, G., Wieruszeski, J.-M., Martel, C., and Montreuil, J., 1989a, *Carbohydr. Res.* **185**:1.

Strecker, G., Wieruszeski, J.-M., Michalski, J.-C., and Montreuil, J., 1989b, *Glycoconj. J.* **6**:67.

Strecker, G., Wieruszeski, J.-M., Michalski, J.-C., and Montreuil, J., 1989c, *Glycoconj. J.* **6**:271.

Takahashi, N., Hotta, T., Ishihara, H., Mori, M., Tejima, S., Bligny, R., Akazawa, T., Endo, S., and Arata, Y., 1986, *Biochemistry* **25**:388.

Van Halbeek, H., 1984, *Biochem. Soc. Trans.* **12**:601.

Van Halbeek, H., Dorland, L., Vliegenthart, J. F. G., Fiat, A.-M., and Jollès, P., 1980, *Biochim. Biophys. Acta* **623**:295.

Van Halbeek, H., Dorland, L., Haverkamp, J., Veldink, G. A., Vliegenthart, J. F. G., Fournet, B., Ricart, G., Montreuil, J., Gathmann, W. D., and Aminoff, D., 1981a, *Eur. J. Biochem.* **118**:487.

Van Halbeek, H., Dorland, L., Vliegenthart, J. F. G., Fiat, A.-M., and Jollès, P., 1981b, *FEBS Lett.* **133**:45.

Van Halbeek, H., Dorland, L., Veldink, G. A., Vliegenthart, J. F. G., Garegg, P. J., Norberg, T., and Lindberg, B., 1982a, *Eur. J. Biochem.* **127**:1.

Van Halbeek, H., Dorland, L., Vliegenthart, J. F. G., Hull, W. E., Lamblin, G., Lhermitte, M., Boersma, A., and Roussel, P., 1982b, *Eur. J. Biochem.* **127**:7.

Van Halbeek, H., Dorland, L., Vliegenthart, J. F. G., Kochetkov, N. K., Arbatsky, N. P., and Derevitskaya, V. A., 1982c, *Eur. J. Biochem.* **127**:21.

Van Halbeek, H., Gerwig, G. J., Vliegenthart, J. F. G., Smits, H. L., Van Kerkhof, P. J. M., and Kramer, M. F., 1983a, *Biochim. Biophys. Acta* **747**:107.

Van Halbeek, H., Vliegenthart, J. F. G., Winterwerp, H., Blanken, W. M., and Van den Eijnden, D. H., 1983b, *Biochem. Biophys. Res. Commun.* **110**:124.

Van Halbeek, H., Gerwig, G. J., Vliegenthart, J. F. G., Tsuda, R., Hara, M., Akiyama, K., and Schmid, K., 1985a, *Biochem. Biophys. Res. Commun.* **131**:507.

Van Halbeek, H., Vliegenthart, J. F. G., Fiat, A.-M., and Jollès, P., 1985b, *FEBS Lett.* **187**:81.

Van Halbeek, H., Breg, J., Vliegenthart, J. F. G., Klein, A., Lamblin, G., and Roussel, P., 1988, *Eur. J. Biochem.* **177**:443.

Van Kuik, J. A., Hoffmann, R. A., Mutsaers, J. H. G. M., Van Halbeek, H., Kamerling, J. P., and Vliegenthart, J. F. G., 1986, *Glycoconj. J.* **3**:27.

Van Kuik, J. A., De Waard, P., Vliegenthart, J. F. G., Klein, A., Carnoy, C., Lamblin, G., and Roussel, P., 1991, *Eur. J. Biochem.* **198**:169.

Van Pelt, J., Van Bilsen, D. G. J. L., Kamerling, J. P., and Vliegenthart, J. F. G., 1988, *Eur. J. Biochem.* **174**:183.

Vliegenthart, J. F. G., Van Halbeek, H., and Dorland, L., 1980, in *27th Int. Congress Pure Appl. Chem.* (Varmavuori, A., ed.), Pergamon Press, Elmsford, N.Y., p. 253.

Vliegenthart, J. F. G., Van Halbeek, H., and Dorland, L., 1981, *Pure Appl. Chem.* **53**:45.

Vliegenthart, J. F. G., Dorland, L., Van Halbeek, H., and Haverkamp, J., 1982, *Cell Biol. Monogr.* **10**:127.

Vliegenthart, J. F. G., Dorland, L., and Van Halbeek, H., 1983, *Adv. Carbohydr. Chem. Biochem.* **41**:209.

Weisshaar, G., Baumann, W., Friebolin, H., Brunner, H., Mann, H., Sieberth, H.-C., and Opferkuch, H. J., 1987, *Biol. Chem. Hoppe-Seyler* **368**:1545.

Wieruszeski, J.-M., Michalski, J.-C., Montreuil, J., Strecker, G., Peter-Katalinic, J., Egge, H., Van Halbeek, H., Mutsaers, J. H. G. M., and Vliegenthart, J. F. G., 1987, *J. Biol. Chem.* **262**:6650.

Wieruszeski, J.-M., Michalski, J.-C., Montreuil, J., and Strecker, G., 1990, *Glycoconj. J.* 7:13.